Vers le traitement biologique semi-passif de Drainages Miniers Acides arséniés : dynamique physico-chimique et microbiologique dans des bioréacteurs mis en œuvre in-situ

Camila Diaz Vanegas

THÈSE POUR OBTENIR LE GRADE DE DOCTEUR DE L'UNIVERSITÉ DE MONTPELLIER

En Science de l 'Eau

École doctorale GAIA

Unité de recherche Hydrosciences Montpellier UMR 5569

Vers le traitement biologique semi-passif de Drainages Miniers Acides arséniés : dynamique physico-chimique et microbiologique dans des bioréacteurs mis en œuvre *in situ*.

Présentée par Camila DIAZ VANEGAS

Le 8 décembre 2022

Sous la direction de Corinne CASIOT et Fabienne BATTAGLIA-BRUNET

Devant le jury composé de

Carmen NECULITA, Professeur, Université du Québec en Abitibi-Témiscamingue	Rapportrice
Christophe DAGOT, Professeur, Université de Limoges	Rapporteur
Jean MARTINS, Directeur de Recherche au CNRS, Université de Grenoble Alpes	Examinateur
Robert DURAN, Professeur, Université de Pau et des Pays de l'Adour	Examinateur
Miguel LOPEZ-FERBER, Professeur, IMT Mines Alès, HSM, UMR	Représentant
Corinne CASIOT, Directrice de Recherche au CNRS-Montpellier	Directrice
Fabienne BATTAGLIA-BRUNET, Ingénieure-Chercheuse BRGM Orléans	Co-directrice
Marina HERY, Maîtresse de Conférences à l'Université de Montpellier	Co-encadrante, Invitée
Catherine JOULIAN, Ingénieure-Chercheuse, BRGM Orléans	Co-encadrante, Invitée

UNIVERSITÉ DE MONTPELLIER

Dédié à ma mère

Remerciements

La vérité est que le succès de l'obtention de mon doctorat a été le résultat d'un travail d'équipe, je n'aurais pas atteint ce stade sans toute la force, la patience et l'amour des personnes qui m'ont entouré pendant ces trois années.

Je tiens tout d'abord à remercier mon équipe d'encadrement qui, en plus de me donner l'opportunité de réaliser ce travail, m'a guidée pendant les trois années de thèse, m'a motivée en permanence. Ainsi qu'un grand merci pour toutes les connaissances qu'vous m'avez transmise. C'était très agréable travailler avec vous. En particulier, je te remercie Corinne pour ton investissement, merci pour ton excellent encadrement académique, patience et accompagnent au labo et terrain. A Marina, je te remercie pour ton engagement et ton soutien, merci d'avoir cru en moi depuis le début aussi pour ton empathie et pour avoir veillé à que je dispose des bonnes conditions physiques et mentaux pendant toute ma thèse. Fabienne, Catherine et Jérôme Jacob merci pour votre accueil au BRGM à Orléans, malgré mon court séjour vous l'avez rendu très agréable, merci pour vos réponses rapides à toutes mes questions, des contributions et des discussions très intéressantes.

Je profite également de cette occasion pour remercier toutes les entités qui ont contribué au financement de ce travail de recherche, la Région Occitanie et le BRGM qui ont directement financé mon contrat doctoral, je remercie l'ADEME qui a financé le projet COMPAS, dans lequel mon travail a été encadré. Je remercie donc Patrick Lachassagne directeur du laboratoire HSM, ainsi que Christopher Bryan, responsables de l'unité Bio-géochimie environnementale et qualité de l'eau du BRGM, de m'avoir accueilli au sein de ces structures.
Merci à tous les membres du jury d'avoir accepté de corriger ce manuscrit. Je remercie tout particulièrement Carmen Neculita et Christophe Dagot, pour avoir accepté d'être rapporteurs de cette thèse, ainsi que Jean Martins et Robert Duran pour leur participation au jury en tant qu'examinateurs. Je remercie également Miguel Lopez-Ferber et Jean-Luc Rols pour leur participation aux comités de suivi de thèse.

Grâce à l'équipe du laboratoire d'HydroSciences Montpellier (HSM) et du BRGM d'Orléans, grâce à leur travail, j'ai pu réaliser de nombreuses analyses et interpréter les résultats (Rémi, Eleonor, Léa, Mylène, Mickaël, Odile et Sophie). Un merci particulier à Angélique, merci pour ton engagement et ton soutien, merci pour les longues heures de travail au laboratoire, sur le logiciel R et sur terrain. Ton travail a grandement contribué au succès de ma thèse. J'apprécie le dévouement de tous les stagiaires Amandine, Oumar, Adam et Enzo, leur travail et leur dévouement ont été essentiels pour atteindre les objectifs du projet. Merci pour les rires et les bons moments passés sur le terrain malgré les conditions de chaleur ou pluviosité. Ma reconnaissance à Catherine, Fabienne et Elise qui m'ont aidé et guidé dans tous les problèmes administratifs de la thèse.

Merci à tous les doctorants et postdocs de HSM, les rires, les pauses, les cafés, les croissants, le secret Santa, le biercredi, le jeudrink. Tous ces moments ont rendu ces trois années de thèse beaucoup plus agréables. Un grand merci en particulier à Ben, Vianney, Marie, Coralie et Garance, merci d'être devenus comme ma famille à Montpellier, merci de m'avoir aidé à améliorer mon français, merci de contribuer à mon immersion dans la culture française, merci pour vos mots, votre soutien et vos câlins. Merci à Syrine, Nesrine, Junior, Colin, Pierre, Beshad, Laina et Leila.

Merci aux belles personnes que Montpellier m'a donné Hugo, Manuel, Oscar Santi, Julia, Marion et Brice, merci pour m'avoir encouragé, pour vos mots, merci pour les bons moments et pour votre patience dans mes moments de stress. Merci à mes amis de toujours, Gela, Luchis, Pau et Pipe, pour leur soutien inconditionnel, pour ne jamais me laisser seule et pour m'aider à garder confiance en moi. Gracias infinitas Pipe por tu apoyo, comprensión y paciencia, tu presencia incondional los dos primeros años de la tesis fueron pieza clave en este logro. Merci à mon sensei, Fabio Roldan, je ne pense pas que j'aurais entrepris toute cette aventure sans son soutien, sa motivation et ses conseils. Gracias Fabio por ser mi sensei profesional, gracias por tu apoyo incondicional por créer en mi, gracias por impulsarme a salir de mi zona de confort.

Merci à titi, mon père, Pini, Josue, Yoyo et au reste de ma famille pour avoir cru en moi, pour vos prières et vos mots de soutien. Mais surtout, merci à ma mère, car la vérité est que c'est grâce à ses efforts, son dévouement et son soutien que je suis ici, à plus de 8000 km de mon pays, à me battre pour réaliser mes rêves. Gracias Mami y titi ustedes han sido el equipo más increíble, su amor infinito, su presencia, su apoyo y sus palabras han contribuido a la persona que soy ahora, ha sido gracias a eso que pese a los momentos difíciles de fatiga, de fustración o tristeza logré levantarme y sacar este doctorado adelante.

Résumé

L'exploitation minière des métaux a laissé un lourd héritage environnemental, en particulier des résidus miniers contenant des concentrations élevées d'arsenic (As). L'altération de ces résidus génère du drainage minier acide (DMA) qui favorise le transport de l'As vers le milieu aquatique, avec des effets négatifs sur l'écosystème et la santé humaine. Bien que de nombreuses méthodes aient été utilisées pour traiter le DMA, le développement de stratégies plus durables adaptées aux mines abandonnées et aux DMA riches en As est nécessaire. Une de ces stratégies est la bioremédiation ; elle a montré son efficacité et une production moindre de déchets solides comparée aux traitements chimiques.

Cette thèse se concentre sur l'évaluation de deux approches de bioremédiation pour traiter les DMA riches en As : 1) la bio-oxydation du fer (Fe) et de l'arsenic (As), qui conduit à leur co-précipitation et 2) la réduction biologique des sulfates, qui conduit à la précipitation de l'As, du zinc (Zn) et du Fe sous forme de sulfures. Le traitement par bio-oxydation a été mis en œuvre via deux bioréacteurs de terrain de $1m^3$ à écoulement gravitaire remplis avec des supports de biomasse différents (plastique ou mélange de bois et pouzzolane). Le traitement par réduction biologique du sulfate a été mis en œuvre via un bioréacteur de 25 litres à flux ascendant rempli de pouzzolane et complémenté en glycérol (0.5g/L). Les performances des bioréacteurs ont été suivies sur site pendant un an pour le traitement du DMA riche en As de l'ancienne mine de Carnoulès dans le sud de la France. La géochimie des eaux et des bioprécipités a été caractérisée (analyse élémentaire, spéciation rédox de l'arsenic, minéralogie des précipités). La dynamique des communautés bactériennes (communautés bactériennes totales et actives) au sein de ces systèmes a été décrite à l'aide des outils de génomique environnementale (séquençage de l'ARNr 16S et qPCR ciblant le gène d'oxydation de l'arsenic *aioA*).

Les réacteurs de bio-oxydation alimentés par le DMA contenant jusqu'à 111 mg/L d'As et 1067 mg/L de Fe ont précipité 67 ± 10 % de l'As et 43 ± 11 % du Fe, et abaissé le pH de l'effluent à 2.8, pour un temps de séjour de 9 h. Le bioréacteur de sulfato-réduction a précipité la totalité de l'As et du Zn, augmenté le pH au-delà de 5.5 et a montré une conversion efficace du sulfate en H_2S par l'oxydation complète du glycérol, pour un temps de séjour testé décroissant de 29 à 4 jours. Les facteurs qui ont influencé la structure et la diversité des communautés bactériennes développées dans les bioréacteurs sont le temps de résidence, le pH, la température, la physico-chimie du DMA et le support de biomasse (uniquement pour la bio-oxydation). La résilience et la redondance fonctionnelle des communautés bactériennes apparaissent comme des facteurs de robustesse et stabilité de ces systèmes de traitement. L'ensemble de ces résultats fournit des données utiles pour l'ingénierie de ces systèmes et contribue à dépasser l'approche empirique utilisée jusqu'ici pour le dimensionnement d'installations de traitement biologique de DMA.

Abstract

Metals mining conducted during ages has left an environmental legacy of mine tailings containing high levels of arsenic (As). The weathering of those tailings generates acid mine drainage (AMD), which promotes the spread of As in aquatic ecosystems, resulting in negative impacts on human and environmental health. Despite that numerous methods have been used to treat AMD, there is a need for more sustainable and cost-effective strategies adapted to abandoned mines and As-rich AMD. The bioremediation is one of the strategies that has showed to be affective and produce less solid waste than the chemical treatments. This thesis is focused on the evaluation of two bioremediation approaches to treat As-rich AMD: 1) bio-oxidation of iron (Fe) and arsenic (As), which leads to their co-precipitation and 2) biological reduction of sulfate, which leads to the precipitation of As, Zn and Fe in the form of sulfides. The oxidation approach was evaluated by two bioreactors of $1m^3$ with gravity flow, each one was filled with a different biomass carrier (plastic support or a mix of wood and pozzolana). The sulfate reducing approach was evaluated with a bioreactor of 25L fed up-flow filled with pozzolana and supplemented with glycerol (0.5g/L).The performances of field-scale bioreactors were monitored in-situ during one year for the treatment of the As-rich AMD from the Carnoulès mine in the south of France. The geochemistry of the water and bioprecipitates were characterized (elemental analysis, redox speciation and mineralogical analysis of the bioprecipitates). The dynamics of the bacterial communities (total and active bacterial communities) developed in the bioreactors were described by the use of environmental genomics tools (16S rRNA metabarcoding and qPCR targeting the gene associated with the arsenite oxidation *aioA*).

The bio-oxidation bioreactors were fed by an affluent containing up to 111 mg/L As and 1067 mg/L Fe, they precipitated 67 ± 10 % of As, 43 ± 11 % of Fe and decreased the pH of the effluent to 2.8, using a residence time of 9 h. The sulfate-reduction bioreactor showed total and stable As and Zn precipitation, also contributed to increase the pH of the effluent above 5.5 and showed an efficient conversion of sulfate to H_2S by the complete oxidation of glycerol, those performances were obtained despite the decrease of the residence time from 29 to 4 days. The factors that influenced the structure and diversity of the bacterial communities developed in the bioreactors were residence time, pH, temperature, physico-chemistry of the AMD and biomass carrier (only for the bio-oxidation). Our results suggest that the resilience and functional redundancy of the bacterial communities conferred robustness and stability to the treatment systems. Finally, the present thesis provides fundamental data and knowledge to progress towards up-scaling of AMD bioremediation facilities based on knowledge-based practice rather than empirical practice.

Publications associées à cette recherche

Revue à comité de lecture :

Diaz-Vanegas C, Casiot C, Lin, L, De Windt L, Héry M, Desoeuvre A, Bruneel O, Battaglia-Brunet F, Jacob J (2022). Performance of semi-passive systems for the biological treatment of high-As acid mine drainage: Results from a year of monitoring at the Carnoulès Mine (Southern France). Mine Water Environ. https://doi.org/10.1007/s10230-022-00885-4

Acte de colloques à comité de lecture :

Diaz-Vanegas C, Casiot C, Lin L, De Windt L, Djibrine A, Malcles A, Héry M, Desoeuvre A, Bruneel O, Battaglia-Brunet F, Jacob J (2021). Performances of a semi-passive field-pilot for bioremediation of As-rich Acid Mine Drainage at the Carnoulès mine (France) – In: Stanley P, Wolkersdorfer C, Wolkersdorfer K. Mine Water Management for Future Generations. Cardiff, Wales, United Kingdom (Natural Resources Wales, The Coal Authority, Welsh Government, Cardiff University), pp 122 – 128

Communications à des congrès, symposium :

Diaz-Vanegas C, Hery M, Lin L, Malcles A, Desoeuvre A, Bruneel O, Battaglia-Brunet F, Joulian C, Jacob J, Casiot C (2020). Field testing of two filling materials for the bioremediation of arsenic-rich Acid Mine Drainage. In EcotoxicoMic 2020-Second International Conference on Microbial Ecotoxicology. Flash presentation and Poster

Diaz-Vanegas C, Casiot C, Lin L, De Windt L, Djibrine A, Hery M, Desoeuvre A, Bruneel O, Battaglia-Brunet F, Jacob J (2021) Exploitation of microbial Fe and As oxidation for semi-passive treatment of high-As Acid Mine Drainage (AMD) in a field-pilot. Goldschmidt, 4 - 9 July 2021, Virtual. Flash presentation and Poster

Diaz-Vanegas C, Battaglia-Brunet F, Joulian C, Barry O, Djibrine A, Malcles A, Lin L, Desoeuvre A, Casiot C, Héry M, Jacob J (2021) On-site Treatment of Arsenic-rich Acid Mine Drainage by Sulfate-reducing Bioreactor. EcotoxicoMicYR 2021, 22 novembre - 6 décembre 2021, Virtual. Oral presentation

Diaz-Vanegas C, Casiot C, Desoeuvre A, Lin L, Bruneel O, Battaglia-Brunet F, Joulian, C, Jacob J, Héry M (2022) Dynamics of the total and active bacterial communities in a bioremediation field-trial of As-rich acid mine drainage. 3rd International Conference in Microbial Ecotoxicology. November 15-18, 2022. Montpellier, France. Oral presentation

Sommaire

Liste des abréviations

AMD Acid Mine Drainage

FeOB Iron Oxidizing Bacteria

SRB Sulphate Reducing Bacteria

HRT Hydraulic Retention Time

DAS Dispersed Alkaline Substrate

TOC Total Organic Carbon

DOC Dissolved Organic Carbon

PS Plastic Support

WP Wood and Pozzolana

SS Sludge Samples

XRD X-Ray Diffraction

RDA Redundancy Analysis

NMDS Non-metric Multidimensional Scaling

OTU Operational Taxonomic Unit

Liste des figures

Liste des tableaux

Introduction générale

Problématique

Depuis l'antiquité l'exploitation minière a joué un rôle important dans le développement économique du monde entier (Randive et al. 2021). Aujourd'hui encore, elle joue un rôle essentiel dans la transition énergétique (Eni-ibukun and Ripley 2021). Cependant, l'exploitation minière est aussi une source historique de dommages environnementaux. Au XX^{ème} siècle, des millions de tonnes de rejets riches en minéraux sulfurés (incluant potentiellement l'arsénopyrite) ont été stockés près des sites d'extraction de minerai, dans des conditions inappropriées. L'altération de ces rejets peut libérer des effluents acides (pH < 4,5) appelés Drainages Miniers Acides (DMA) caractérisés par de fortes concentrations en métaux (i.e. Fe(II), Al(III), Mn(II), Zn(II), Pb(II), Cd(II)) et métalloïdes (i.e. arsenic, As) (Nordstrom and Alpers 1991; Johnson and Hallberg 2003; Delgado et al. 2009). Cette pollution peut perdurer des siècles après la fermeture de la mine (Nordstrom and Alpers 199; Ighalo et al. 2022). Les DMA représentent une menace pour les écosystèmes aquatiques et terrestres (Simate and Ndlovu 2014). L'arsenic est un métalloïde souvent présent dans les DMA en raison de son affinité pour les minéraux sulfurés (Cheng et al. 2009; Paikaray 2015). La mobilisation de l'As dans l'environnement aquatique représente une menace pour la santé environnementale et humaine (Anand et al. 2022).

Plusieurs stratégies existent pour traiter ce type de pollution. Les traitements chimiques et physiques ont été largement utilisés, et ont prouvé leur efficacité pour une large gamme de caractéristiques de DMA (Johnson and Hallberg 2005). Cependant, ces stratégies produisent de grandes quantités de boues à stocker ou éliminer, nécessitent une maintenance importante, ont généralement un coût d'exploitation élevé et une importante empreinte carbone. Dans ce contexte, la bioremédiation, basée sur l'exploitation des capacités naturelles de micro-organismes ou/et plantes représente une alternative prometteuse (Atlas et al. 2005), permettant d'utiliser moins de produits chimiques et d'énergie pour la réhabilitation des sites miniers. Ces techniques sont relativement moins coûteuses et produisent moins de déchets que les traitements chimiques (Azubuike et al. 2016). En revanche, l'un des principaux facteurs qui limitent l'utilisation de la bioremédiation est la compréhension incomplète des processus bio(géo)chimiques impliqués dans le traitement et leur régulation (Elekwachi et al. 2014). Il est en effet difficile de prévoir et de contrôler les performances de tels systèmes dépendant de l'activité biologique, surtout *in situ*. La stabilité à long terme des dépôts qui s'y accumulent est également incertaine, car elle n'a été que peu étudiée.

Pour cette raison, la bioremédiation reste peu appliquée aux DMA et en particulier aux DMA arséniés. Les mécanismes biogéochimiques impliqués dans le traitement de cette pollution impliquent des biotransformations de l'As et d'autres éléments. Contrairement aux polluants organiques, les polluants inorganiques (y compris les métaux et les métalloïdes) ne peuvent pas être dégradés, et leur remédiation vise donc à réduire leur mobilité et leur biodisponibilité (Bahar et al. 2013). Les mécanismes biogéochimiques impliqués comprennent les processus d'oxydation-réduction, de coprécipitation et de sorption. Ces trois processus sont à la base de deux approches utilisées dans la bioremédiation de DMA arséniés : 1) une étape aérobie d'oxydation biologique du fer dont l'objectif est la co-précipitation du Fe et de l'As et 2) une étape anaérobie de sulfato-réduction afin de précipiter des cations métalliques et/ou des métalloïdes, en particulier Zn et As sous forme de sulfures métalliques. Les deux approches sont complémentaires (Hedrich and Johnson 2014; Sato et al. 2018).

La compréhension de ces processus complexes et leur régulation par les facteurs environnementaux est un verrou important pour la mise en place de systèmes de traitement biologiques performants. Afin de mieux comprendre ces processus complexes, les deux approches complémentaires sont étudiées respectivement à HydroSciences Montpellier et au laboratoire de microbiologie du BRGM, depuis une dizaine d'années, dans le but d'être appliquées pour le traitement du DMA riche en As provenant de l'ancienne mine de plomb-zinc de Carnoulès (France, département du Gard).

Les études précédentes ont été menées à différentes échelles, dans des réacteurs de laboratoire (oxydation du fer et réduction des sulfates) et dans un pilote de terrain (oxydation du fer) dans le cadre des thèses de Lidia Fernandez-Rojo (2017) et d'Elia Laroche (2019). Leurs travaux ont permis des avancées sur la définition des conditions optimales de traitement et sur la dynamique des communautés bactériennes dans les pilotes, mais des questions scientifiques subsistent à l'issue de ces travaux.

L'étape aérobie basée sur l'oxydation biologique du fer a montré des performances variables au cours des différentes expériences qui ont été menées, en termes d'abattement du fer et de l'arsenic, ainsi qu'une grande variabilité temporelle lors de l'étude en pilote de terrain. La nature minéralogique des précipités formés et l'état d'oxydation de l'arsenic dans ces précipités variaient également en fonction des expériences. L'étude de la dynamique des communautés bactériennes et l'identification des facteurs susceptibles de réguler les performances et l'expression du potentiel génétique d'oxydation de l'As n'a donc pas pu être menée dans des conditions de fonctionnement optimales. Il était donc nécessaire de mieux contrôler les conditions opératoires (utilisation d'un matériau support de haute porosité, aération forcée, alimentation par pompage plutôt que par écoulement gravitaire) pour une nouvelle étude sur site, en pilote de terrain.

En ce qui concerne l'approche basée sur la sulfato-réduction, toutes les expériences précédentes ont été réalisées à petite échelle (300 mL) en laboratoire et la mise en œuvre de ce traitement sur site devait surmonter de nombreux obstacles potentiels, tels que la sensibilité des bactéries à l'oxygène ou au fer ferrique (soluble ou précipité). De plus, la réduction des sulfates n'avait été testée qu'avec des temps de séjour très longs dans des expériences de laboratoire (58, 29 et 14,5 jours).

La présente thèse associe recherche appliquée et recherche fondamentale. Son objectif opérationnel est la mise en place, le suivi à long terme et l'optimisation des performances, dans des conditions de terrain, des deux étapes d'un traitement biologique du DMA riche en arsenic de l'ancienne mine de Carnoulès, France. Les conditions opératoires et l'échelle des bioréacteurs ont été définies en prenant en considération les limitations et les avancées des travaux précédents. D'un point de vue fondamental, il s'agit de contribuer à l'avancée des connaissances sur les processus biogéochimiques se déroulant au sein des systèmes de traitement, la dynamique des communautés bactériennes en lien avec le cycle du fer, de l'arsenic et du soufre, et l'identification des facteurs contrôlant le fonctionnement de ces systèmes.

Questions scientifiques

Les questions générales relatives aux deux approches (oxydation du fer et de l'arsenic, réduction des sulfates) sont les suivantes :

- Quelles sont les limites, en termes de concentration en As, Fe et Zn atteignables dans l'eau traitée par les deux approches avec des bioréacteurs semi-passifs dans des conditions de terrain ?
- Comment la dynamique des communautés bactériennes et l'expression de fonctions clés exploitées dans chacune des approches sont-elles affectées en réponse à des variations des conditions physico-chimiques, opératoires ou environnementales ?
- Ces deux approches semi-passives, mises en oeuvre séparément ou combinées, sont-elles une solution efficace et adaptée pour traiter le DMA riche en As de l'ancienne mine de Carnoulès ?

Les questions fondamentales et appliquées spécifiques à chacune de ces approches sont les suivantes :

<u>Approche par oxydation du fer (traitement aérobie)</u>

- Quelles sont les limites de cette étape en termes de concentrations en As et Fe atteignables dans l'eau traitée dans des conditions opératoires optimisées, y compris l'aération forcée et les supports poreux de biomasse ?
- Quels sont les principaux paramètres qui influencent les performances du bioréacteur en termes de traitement de l'arsenic et du fer (temps de rétention hydraulique, variabilité de la chimie de l'eau au fil des saisons, enrichissement en As des boues, disponibilité de l'oxygène, nature du support de biomasse, structure et dynamique de la communauté microbienne totale et active, communauté microbienne en suspension et fixée) ?
- Quels sont les conditions opératoires et les paramètres géochimiques qui influencent la diversité et l'activité bactérienne dans le bioréacteur d'oxydation

du fer, et en particulier quels sont les facteurs susceptibles de réguler l'expression du potentiel génétique d'oxydation de l'As dans les bioréacteurs ?

Approche par sulfato-réduction bactérienne (traitement anaérobie)

- Quels sont les effets des conditions environnementales liées au traitement sur site (variations saisonnières de la chimie du DMA de Carnoulès, température, pH, présence de Fe(III) dans l'eau d'alimentation) sur le processus de réduction des sulfates ?
- Quel est l'effet de la diminution du temps de résidence sur l'efficacité du bioréacteur de sulfato-réduction et la dynamique de la communauté bacterienne ?

Couplage des deux approches

- Y a-t-il un intérêt à coupler les deux approches (bioréacteur de sulfato-réduction et bioréacteur d'oxydation du fer) ? Le couplage affecte-t-il les performances du bioréacteur d'oxydation du fer installé à la sortie du bioréacteur de réduction des sulfates ?
- Quels sont les principaux facteurs spécifiques à l'effluent de l'étape de sulfato-réduction (carbone organique, bactéries transportées depuis le réacteur SRB, pH) qui pourraient affecter ces performances et la structure de la communauté bactérienne du réacteur d'oxydation en aval ?

Organisation du manuscrit

Le manuscrit comprend quatre chapitres. Le premier chapitre est consacré à une revue bibliographique. L'objectif est de présenter les processus biogéochimiques responsables de la formation de DMA riches en As, les principales stratégies mises en œuvre jusqu'à présent pour traiter ce type de pollution, y compris les traitements physico-chimiques passifs et les alternatives biologiques. Dans ce premier chapitre a été incluse l'analyse des résultats issus des études précédentes portant sur le traitement du DMA de l'ancienne mine de Carnoulès.
Le deuxième chapitre décrit les résultats du suivi *in situ* de deux bioréacteurs d'oxydation biologique, semi-passifs, pour la biorémédiation du DMA de Carnoulès, basée sur l'oxydation du fer et la co-précipitation de l'As. Les deux bioréacteurs ont permis de comparer deux types de supports poreux de biomasse (plastique ou mélange de copeaux de bois et pouzzolane). Ce chapitre est principalement axé sur l'étude du processus biogéochimique contrôlant les performances et sur la détermination des limites de ces systèmes.
Le troisième chapitre est principalement axé sur l'intégration des données microbiologiques et géochimiques pour mieux caractériser le fonctionnement des bioreacteurs d'oxydation. Ce chapitre présente la dynamique des communautés bactériennes totales et actives, en suspension et fixées, qui se sont succédé au cours des différentes étapes de fonctionnement des bioréacteurs. Des liens potentiels sont recherchés entre la dynamique des communautés, les

variations des conditions environnementales ou opératoires (physico-chimie du DMA, nature du support de biomasse, conditions opératoires), et les performances des systèmes.

Le quatrième chapitre est principalement axé sur le bioréacteur de sulfato-réduction fonctionnant seul ou couplé en amont d'un bioréacteur d'oxydation du fer. Ce bioréacteur a été testé pour la première fois sur le terrain et suivi pendant presque un an, en diminuant progressivement le temps de résidence afin de tester les limites du système. Ce chapitre présente les résultats du suivi des paramètres physico-chimiques et de la microbiologie de ce bioréacteur anaérobie.

Enfin, la dernière section du manuscrit comprend une synthèse globale des principaux résultats obtenus au cours de cette thèse et les conclusions générales. En outre, cette dernière section inclut les perspectives et l'applicabilité de ce travail à l'échelle réelle pour traiter la pollution liée au DMA de Carnoules.

Le premier chapitre est présenté sous la forme d'une revue tandis que les trois chapitres suivants sont présentés sous la forme d'articles scientifiques, un article déjà publié et deux en vue de leur publication.

Chapitre 1 : Implication des micro-organismes dans la génération et le traitement du drainage minier acide

Introduction

L'une des conséquences négatives des activités minières est la génération de drainage minier acide (DMA), qui peut être la conséquence d'une gestion négligée des rejets miniers et des stériles (Sheoran et al. 2010). Le DMA est un produit de l'oxydation des minéraux sulfurés présents dans ces rejets zaminiers. Le rejet de DMA a des effets négatifs sur la qualité des eaux de surface et souterraines, en raison de fortes teneurs en métaux, métalloïdes, sulfates et du pH faible (Nordstrom and Alpers 1991; Johnson and Hallberg 2003). En particulier, pendant l'altération des minéraux sulfurés contenant de l'arsenic, ce métalloïde est libéré en concentrations élevées (Paikaray 2015).

La pollution par l'arsenic via les DMA est un problème mondial qui fait l'objet d'une attention particulière en raison de la haute toxicité de ce métalloïde. De nombreuses approches ont été développées pour traiter ces effluents polluants. Certaines de ces approches reposent sur les processus microbiens, qui contrôlent la mobilité et la disponibilité de l'As (Anand et al. 2022). Malgré l'intérêt croissant pour la bioremédiation, son application au traitement du DMA riche en As est encore très limitée.

L'objectif de ce chapitre est de résumer les processus biogéochimiques impliqués dans la formation et la libération des DMA, de décrire la microbiologie de ces effluents acides. En outre, l'objectif est également de fournir une synthèse actualisée des connaissances disponibles sur les principales méthodes de traitement des DMAs riches en arsenic, y compris les traitements chimiques passifs et les traitements biologiques. Un accent particulier est mis sur les bioréacteurs basés sur l'oxydation biologique du fer et les bioréacteurs basés sur la réduction des sulfates. Quelques exemples de mise en œuvre des traitements basés sur ces deux types de bioréacteurs sont présentés, avec un accent particulier sur des expériences menées sur le terrain.

Dans ce chapitre, nous incluons également une brève description des connaissances disponibles sur la géochimie et la microbiologie du ruisseau acide du Reigous, en aval del'ancienne mine de Carnoulès, où l'atténuation naturelle de l'arsenic a été observée et étudiée, notamment dans le cadre de l'observatoire OREME (Observatoire de Recherche Méditerranéen de l'Environnement). Ce DMA correspond au site d'étude du présent travail de thèse.

Les recherches relatives à ce chapitre sont présentées sous forme de synthèse bibliographique.

1 Biological treatment of As-rich Acid Mine Drainage: an overview

1.1 Acid mine drainage origin and formation

1.1.1 Definition and characteristics

Acid mine drainage (AMD) is an undesired and hazardous product of mining operations (Vasquez et al. 2018). The main route of production of this toxic effluent is the biotic and abiotic oxidation of the sulfide minerals present in the orebodies and tailings (Nordstrom and Alpers 1991). The oxidation occurs by the exposure of the minerals to oxygen and water. This phenomenon is extensively promoted during the extraction of raw materials and during weathering of tailings remnant from the recovery process (Johnson and Hallberg 2005). Another term used as synonym of AMD is acid mine water, because it finally represents the waters that drain from the tailings and underground mines into natural water bodies (Nordstrom and Alpers 1991).

The properties and composition of the mine drainage change drastically from one site to another, they depend on the geological composition of the bedrock, the microbial communities present and active, the hydrological conditions and the microclimate of the site (Rambabu et al. 2020). For instance, the pH of the mine drainage depends on the mineralogical materials present in the tailings. It is common to observe the release of neutral mine drainage (NMD) from tailings rich in carbonates, mainly due to the carbonates' capacity to buffer the acidity released during sulfide minerals' oxidation (Nordstrom et al. 2015).

The common properties of AMD include an acid pH range (between 2 and 5), elevated concentrations of sulfates, iron and other metals and metalloids such as As, Zn, Pb, Cd, Cu and Mo (Johnson and Hallberg 2005). These properties make the acid mine waters a threat for the living organisms and contribute to reduce the biodiversity in fresh water ecosystems. The negatives impacts are due to the toxicity of metals and metalloids towards living organisms, as well as to the decrease of the quality of the habitat and modification of the food webs (Hogsden and Harding 2012), linked to the contamination of sediments downstream the AMD discharge point, even at sites where the pH and dissolved metal concentrations are close of those of non-impacted water bodies.

1.1.2 Biogeochemical process for the acid mine drainage formation

The generation of AMD is the result of the weathering of sulfide minerals (Johnson and Hallberg 2003). Pyrite (FeS_2) is the most abundant mineral associated with AMD generation. Chemical and biological processes involved in pyrite oxidation release into solution sulfates, ferrous iron and trace elements associated with this mineral (Neculita et al. 2007). Some of the trace elements often associated with the AMDs are: As, Pb, Zn, Cu, Co, Cd, Sb and Ni. The first step of the pyrite transformation is described mostly as an abiotic oxidation. It mostly starts at neutral pH (~ 7) and the oxygen and ferric iron are the most common oxidizing agents. For instance, the pyrite oxidation by oxygen produces two moles of H^+ per mole of pyrite, the

H^+ released contribute to decrease the effluent pH (**Error! Reference source not found.**). However, this first phase can be also mediated by bacteria, through an enzymatic attack of the pyrite by the bacteria growing at the surface of the minerals (Nordstrom and Alpers 1991; Edwards et al. 1998; Srichandan et al. 2019).

The dissolved ferrous iron released from the first reaction is then oxidized to ferric iron (**Error! Reference source not found.**). This oxidation is catalyzed by bacteria such as *Acidothiobacillus ferrooxidans* (named first *Thiobacillus ferrooxidans*) (Nordstrom and Alpers 1991). Indeed, under pH < 4, bacterial iron oxidation is almost 10^6 times faster than abiotic oxidation (Wang and Zhou 2012). Subsequently, a fraction of the ferric iron precipitates as Fe-oxyhydroxides and this precipitation releases protons contributing to decrease the effluent's pH (**Error! Reference source not found.**The other fraction of the ferric iron continues promoting the pyrite oxidation, which restarts the cycle of AMD generation (Johnson and Hallberg 2003).

$$FeS_{2(s)} + \frac{7}{2}O_2 + H_2O \rightarrow Fe(OH)_{3(s)} + 2\,SO_4^{2-} + 2H^+ \quad \textit{Equation 1}$$

$$Fe^{2+} + \frac{1}{4}O_2 + H^+ \rightarrow Fe^{3+} + \frac{1}{2}H_2O \quad \textit{Equation 2}$$

$$Fe^{3+} + 3H_2O \rightarrow Fe(OH)_{3(s)} + 3H^+ \quad \textit{Equation 3}$$

The overall process of minerals transformation and AMD release can keep going during centuries, which is often the case for the abandoned mines (Johnson and Hallberg 2005). The main concern is that the acidity of the polluted effluent contributes to the metals and metalloids mobility through the water bodies. In general, the streams affected by AMD can be distinguished easily by the orange precipitates, which relies on the presence iron oxyhydroxides and iron hydroxysulfates (Nordstrom and Alpers 1991).

Some of the main iron oxyhydroxides and iron hydroxysulfates identified in AMD streams are schwertmannite ($Fe_8O_8(OH)_6SO_4$), jarosite ($KFe_3(SO_4)_2(OH)_6$, ferrihydrite $Fe_5(OH)_8 \cdot 4H_2O$, goethite (FeOOH) (Nordstrom and Alpers 1991; Bigham et al. 1996). One of the main parameters that control the formation of a particular mineral phase in AMD is the pH. Schwertmannite and jarosite precipitate at pH 2.5-3.5, while the ferrihydrite precipitates at pH >6 (Sánchez España et al. 2007). In AMD containing high concentrations of arsenic, As-rich secondary minerals occur such as tooleite ($Fe_6(AsO_3)_4SO_4(OH)_4 \cdot H_2O$) (Egal et al. 2009) and scorodite ($FeAsO_4$) (Coudert et al. 2020).

1.1.3 The microbiology associated with Acid Mine Drainage

Mine tailings, AMD springs and natural waters acidified by AMD are the habitats of specific groups of microorganisms. A large part of the microorganisms present in these ecosystems are associated with the iron and sulfur biochemical cycles, as these two elements are present in elevated concentrations and are the main sources of energy (Figure 1). Some taxa are capable

to potentially perform nitrogen and carbon fixation such as *Leptospirillum* (Figure 1). A large part of the microorganisms inhabiting under the extreme AMD conditions are acidophilic procaryotes (*Bacteria* and *Archaea* domains), with optimal growth pH between 2 and 4. Organisms from the *Eukarya* domain are also present, but in lower proportions (Méndez-García et al. 2015).
As mentioned in the previous section (1.1.2), during the AMD formation the iron oxidizing bacteria (FeOB) can take part of the pyrite oxidation by two mechanisms: the first one is a "direct oxidation" that implies the bacterial adhesion into the mineral grain surface (**Error! Reference source not found.**). The bacteria release enzymes that promote the biofilm formation and finally cause the pyrite oxidation (Edwards et al. 1998). Particularly, Nordstrom & Alpes (1991) described a proteinaceous cell surface appendage that facilitated the attachment and it was present only in the bacteria cells adhered to the mineral surface. The production of extracellular polymeric substances (EPS) is another feature that facilitates the bacterial attachment to the mineral surface (Srichandan et al. 2019). For instance, *Acidothiobacillus ferrooxidans* is one of the first bacteria reported able to oxidize the pyrite by direct contact (Nordstrom and Alpers 1991).

The second mechanism is the "indirect oxidation", which may or may not involve bacterial contact with the mineral grain (**Error! Reference source not found.**). This "indirect mechanism" includes the oxidation of the dissolved ferrous iron to ferric iron, the ferrous iron was released during the first mechanism of the pyrite oxidation (Nordstrom and Alpers 1991; Edwards et al. 1998). *Leptospirillum* can be attached to the ore particles not because it directly oxidize the minerals, but because the dissolved Fe(II) can be available near the mineral surface (Battaglia-Brunet et al. 2002a). Indeed, strains of *Leptospirillum* and *Acidothiobacillus* are described to be able to growth on soluble ferrous iron or solid pyrite (Vardanyan et al. 2019).

Most of the iron oxidizing bacteria (FeOB) are chemolithotrophic bacteria, which are able to use ferrous iron as source of energy. *Ferrovum myxofaciens*, *Acidothiobacillus ferrivorans*, *Leptospirillum* and *Galionella* are examples of chemolithotrophic FeOB that have been identified in many AMD over the world and also associated to the passive AMD treatments (Méndez-García et al. 2015; Florence et al. 2016). Particularly, as mentioned before, *Acidothiobacillus ferrooxidans* is a chemolithoautotrophic bacteria recognized to have a versatile metabolism; it can oxidize iron and sulfur, fix atmospheric carbon and nitrogen and under anaerobic conditions can reduce ferric iron and elemental sulfur (Valdés et al. 2008; Méndez-García et al. 2015). *Leptospirillum* and *Ferrovum* have a strict metabolism, they are recognized as obligate aerobic bacteria, and they use the ferrous iron as unique acceptor donor. Studies have reported a few heterotrophic FeOB such as *Sulfobacillus* (Afzal Ghauri et al. 2007; Hallberg 2010; Emerson et al. 2013).
Iron reducing bacteria is another group associated with the AMD affected ecosystem, present in less proportion than the FeOB. There are also chemolithotroph and heterotrophic iron reducing bacteria. The first ones are able to use inorganic sources of electrons such as sulfur or hydrogen. The heterotrophic iron reducing bacteria such as *Acidiphilium* and *Acidocella* use organic sources (i.e glycerol and glucose).

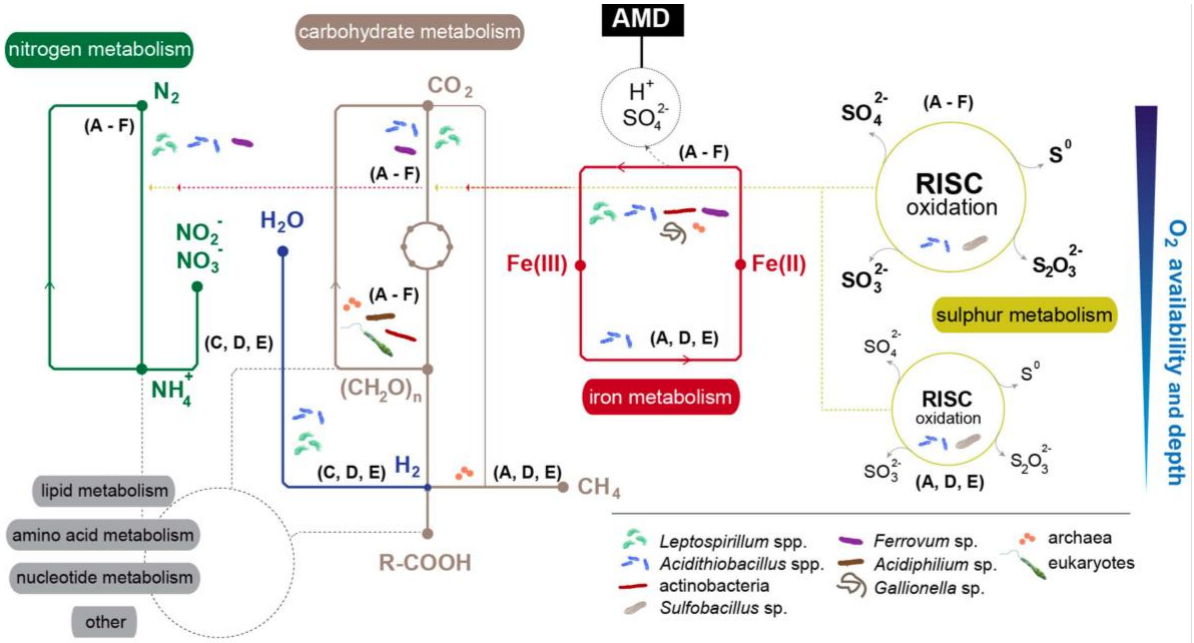

Figure 1. *Overview of the metabolic networks that govern adaptation to extreme conditions in AMD microbial communities by micro-environment (A–F). The main taxa implicated in the AMD release are presented. Modified from Mendes-Garcia et al. 2015. Oxygen availability and depth affect iron, sulfur, carbohydrates and nitrogen metabolisms. A: sediments, B: AMD column, C: pellicle floating biofilm, D: stratified streamer, E: submerged mat and F: snottite.*

Table 1 *Most common bacteria identified in AMD over the world and associated with iron, sulfur or arsenic oxidation.*

Phylum/ Class	Genus/species	Oxidation			Type of metabolism	Type of respiration	Location of AMD or mining site (Reference)
		Fe	S	As			
γ-proteobacteria	*Ferrovum myxofaciens*	+	-	-	Autotrophic	Aerobic	Cae Coch (UK) (Hedrich and Johnson 2013) Lower Reid Eyes (US) (Brown et al. 2011) Tong Shankou (Chine) (Xie et al. 2007)
	Gallionella sp (e.g G. ferruginea)	+	-	-	Mixotrophic	Micro-aerobic	Carnoulès (France) (Volant et al. 2014) Uranium-mining district of Ronneburg (Germany) (Fabisch et al. 2016) Yunfu sulfide mine (China) (He et al. 2007)
	Thiomonas spp.	+	+	+	Mixotrophic	Aerobic	Carnoulès (France) (Bruneel et al. 2003) Storwartz (Norway) Ynysarwed (UK), and Parys Mountain mines (UK) (Méndez-García et al. 2015)
	Sideroxydans sp.	+/-	-	-	Mixotrophic	Microaerophilic	AMD Pilot plant in Tzschell (Germany) (Muehling et al. 2016)
	Sulfuriferula	-	+	-	Heterotrophic	Facultative Anaerobic	AMD treatment pilot at Carnoulès (France) (Laroche et al. 2018) Transbaikalia AMD (Russia) (Gavrilov et al. 2019)
	Acidithiobacillus sp. (e.g Acidithiobacillus ferrooxidans)	+	+	+	Autotrophic	Facultative Anaerobic	Carnoulès (France) (Volant et al. 2014) Tinto river (Spain) (Sánchez-Andrea et al. 2011) Pb/Zn mine (Chine) (Chen et al. 2013) Balya AMD pond (Turkey) (Aytar et al. 2015)
	Metallibacterium (Iron-reducer)	-	+	-	Heterotrophic		Iberian Pyrite belt, (Spain) (Falagán et al. 2017) Harz Mountains mine (Germany) (Gavrilov et al. 2019)
	Acidiphillum sp. (Iron-reducer)	-	+	-	Heterotrophic	Facultative Anaerobic	Çan AMD (Turkey) (Aytar et al. 2015)
Nitrospirae	*Leptospirillum ferriphilum*	+	-	-	Autotrophic	Aerobic	Richmond AMD (USA) (Goltsman et al. 2013) Tinto river (Spain),

							Drei Krorien (Germany) (Méndez-García et al. 2015) Lechang (Chine) (Tan et al. 2007) Carnoulès AMD (France) (Volant et al. 2014) Ça AMD (Turkey) (Aytar et al. 2015)
Acidobacteria	*Acidobacterium sp (Iron-reducer)*	-	-	-	Heterotrophic	Anaerobic	Yanahaya mine (Japon) and Matsuo AMD (Japon) (Falagan et al. 2017)
	Acidocapsa	-	-	-	Heterotrophic	Aerobic	Ça AMD (Turkey) (Aytar et al. 2015), Iberian Pyrite Belt (Spain) (Falagan et al. 2017)
	Granulicella	-	-	-	Heterotrophic	Aerobic	Iberian Pyrite Belt (Spain) (Falagan et al. 2017)
Firmicutes/ Clostridiales	*Sulfobacillus*	+	+	-	Mixotrophic		Richmond mine (USA) (Goltsman et al. 2013) Northern Chile (Travisany et al. 2012)

+ represented a yes for the metabolic feature, - represented an absence of the feature.

1.1.4 Ecological impacts of AMD

The release of AMD into the environment increases greatly when the mines close down and the tailings are abandoned. Without a suitable management, it contributes to the contamination of groundwater, rivers, lakes, and other aquatic systems near the mining sites (Nordstrom and Alpers 1991).
The level of AMD toxicity to organisms depends on its composition in metals and metalloids and their concentration. These polluted effluents can cause the deterioration and destruction of aquatic ecosystems, they can flow out and reach the soil and plants close to those mining areas, causing widespread contamination (Rambabu et al. 2020).

Human communities located near and downstream from mines can be affected by the use and exposure of water contaminated with AMD. Especially, in areas where those waterbodies and groundwater are the main sources for bathing and domestic chores (Morodi and Mpofu 2018; Moeng 2019). The exposure routes include ingestion and/or dermal contact with the AMD-polluted waters. The metals and metalloids present in the AMD are a threat for human health particularly during long-term exposure. However, accurate figures of human exposure and health effects to AMD is still lacking (Moeng 2019).

One of the main concerns of the water contaminated with AMD is arsenic, which is often present in the order of tens of µg/L to tens of g/L (Garcia-Rios et al. 2020; Yuan et al. 2021). Contrary to Fe and other metallic cations, As-oxyanions are soluble in a large range of pH (Weidner and Ciesielczyk 2019) including neutral pH conditions. Particularly, the biggest threat is the occurrence of the reduced species As(III), which are highly mobile in hydrosystems and can migrate far away from the mining sites (Rötting et al. 2008). The toxicity of As(III) is based on its capacity to inactivate some proteins by binding with the cysteine present in these proteins. The toxicity of As(V) relies on its structural analogy with phosphate. For that reason, it can enter easily into the cells and affect the oxidative phosphorylation (García-Sánchez et al. 2010; Sarmiento et al. 2012).

The plants irrigated with AMD-polluted water could have physiological issues in their development; including decrease of the seed germination, limitation growth and total inhibition of the photosynthesis (Rambabu et al. 2020). Arsenic is often found in the mining environments. There are more than 200 minerals containing arsenic, including sulfides, carbonates, silicates and oxides (Alam and Mcphedran 2019). Due to the As particularity of being associated with almost all metals, it has been used as an indicator for mineral exploration, principally for gold mining (Laperche et al. 2003). The highest fluxes of As in the environment are often associated with mining activities, in relation with the oxidation and dissolution of sulfide minerals present in the tailings (Asta et al. 2010b; Majzlan et al. 2014). The most frequent arsenic sulfide minerals are arsenopyrite (FeAsS), realgar (AsS) and orpiment (As_2S_3) (Laperche et al. 2003). Under carbonate-poor conditions, the oxidation of these minerals can lead to the formation of As(III)- and Fe(II)- rich AMD, following the pathway described for the pyrite oxidation (described in the section 1.1.2 Biogeochemical process for the acid mine drainage formation) (Burton et al. 2021). To sum-up, As release is facilitated by abiotic or/and

biotic mechanisms. The oxidation of As-sulfide minerals can occur abiotically with O_2, but the oxidation rate is enhanced by bacteria.

The highest As concentrations reported in AMD or mine waters are in the order of 100 g/L (Majzlan et al. 2014; Migaszewski et al. 2018; Coudert et al. 2020; Zhu et al. 2020) (Table 2). Under oxidizing and acid conditions, As can be present in the form of arsenate As(V) and arsenite As(III), the later species being more mobile, as mentioned above. Under reduced conditions species, of thioarsenic can also be present due to the high affinity between As and sulfur (Stauder et al. 2005). In fact, the formation of thioarsenic is mainly driven by S/As ratio pH and oxygen concentration (Planer-Friedrich et al. 2007; Coudert et al. 2020).

Table 2 *Different As-rich (> 10 mg/L) AMD and mine water worldwide, As concentration and pH ranges*

Localization	As dissolved concentration	pH	Type of mining	Reference
Svornost mine (Czech Republic)	80 -130 g/L	Close to 0	Ag-Co-Ni-Bi-U deposit	(Majzlan et al. 2014)
Wiśniówka mining area (south-central Poland)	Up to 1548 mg/L	2.4 -2.6	quartzites and quartzitic sandstones extraction	(Migaszewski et al. 2019)
Berikul Au mine (Russia)	976 ± 544 mg/L	2.3 ± 0.1	Gold mine	
Carnoulès (France)	50-350 mg/L	2.8 - 4	Pb and Zn mine	
Richmond mine (USA)	Up to 187 mg/L	0.5 -0.9	Au, Ag, Cu, Fe, Zn, and pyrite deposits	(Druschel et al. 2004)
Pezinok (Slovakia)	Up to 81 mg/L	7.1 ± 0.6	Sb deposit	(Majzlan et al. 2007)
Different mines in the Iberian Pyrite Belt (Spain)	Up to 17 mg/L	1.4 - 4.0	IPB comprises more than 80 mines	(España et al. 2016)

Table organized by descending order of As concentration.

The release and spreading of AMD is a major source of As pollution of groundwater and surface water throughout the world (Williams 2001; Paikaray 2015). This is a big challenge due to its high toxicity, which has consequences to all organisms. For instance, regarding human health, arsenic is an important cause of cancer, cardiovascular and neurological diseases (Hedrich and Johnson 2012; Asere et al. 2019; Villegas-Plazas et al. 2019). Regulatory organizations such as World Health Organization (WHO), USEPA and European commission established 0.01 mg/L as the maximum concentration for As in drinking water. The Water Framework Directive in France established environmental quality guideline for As in surface waters at 0.83 µg/L (over the local geochemical background value) (Le Préfet de l'Hérault, Order of July 27, 2015).

Considering the toxicity of arsenic and its widespread character in AMD worldwide, the development of remediation strategies focused on arsenic removal or its immobilization is a priority.

1.2 Arsenic rich acid mine drainage treatment

Distribution of As between solid and aqueous phases is affected by the pH, redox status and availability of complexing agents (Brusseau and Chorover 2019). These factors also control the solubility and charge of the solid minerals that serve as carrier materials for inorganic pollutants (Brusseau and Chorover 2019).

The most common technologies for arsenic remediation include oxidation, precipitation, coagulation and membrane separation (Mohan and Pittman 2007; Coudert et al. 2020). Most of them are based on three key processes: pH neutralization, oxidation/reduction, precipitation or sorption.

1.2.1 Key abiotic and biotic processes of pollutants removal

In this section, the principles of the four key processes (pH neutralization, oxidation/reduction, precipitation or sorption) will be described shortly, but the details are presented further in the description of the remediation technologies. These processes can be biotic or abiotic.

1.2.1.1 pH neutralization

pH has a critical effect on the transport and fate of inorganic pollutants, this parameter affects the chemistry of the solution and the chemistry of the mineral surface (Brusseau and Chorover 2019). The sorption of metals onto the mineral surfaces is generally directly correlated with the pH; with a lower pH, the metal's sorption decreases, while the increase of pH also increases the sorption (Holt et al. 2018).
The pH of AMD is below 6. The total acidity of these effluents originates from the hydrogen ions released during the first stage of the sulfide oxidation and the precipitation of metals (especially Fe), which finally releases additional number of protons (Johnson and Hallberg 2005). Neutralizing AMD by adding alkaline amendments has been the traditional way to overcome the problem during centuries (Park et al. 2019). The neutralization raises the pH and promotes the precipitation of metals, which are no longer available to organisms (Park et al. 2019).

1.2.1.2 Precipitation and co-precipitation

When the As concentration in AMD reaches several mg/L, secondary As minerals can precipitate and limit As mobility. Under oxidative conditions, soluble As can co-precipitate with Fe(III) and form well crystallized minerals such as scorodite (FeAsO4) (Burton et al. 2009) or amorphous phases such as ferric arsenate (Carlson et al. 2002; Maillot et al. 2013). In rare cases, the mineral tooeleite ($Fe_6(AsO_3)_4(SO_4)(OH)_4 \cdot 4H_2O$), that contains As(III), or amorphous Fe(III)-As(III) phases has been evidenced (Morin et al. 2003; Liu et al. 2015). Under reductive conditions, the biogenic precipitation of As(III) into sulfides such as orpiment and realgar has been evidenced in AMD (Newman et al. 1997a).

However, under particular conditions the dissolution of those minerals can occur by biological or abiotic reactions (Brusseau and Chorover 2019) and enhance the remobilization of the metals and metalloids (Desoeuvre et al. 2015). For example, the storage of scorodite under anaerobic conditions would promote its bacterial dissolution, which finally enhances the release of As into solution (Filippi et al. 2015).

1.2.1.3 Sorption

The sorption process refers to the association of the contaminant molecules with a solid phase, often called sorbent. This process influences the fate of contaminant in the environment (Brusseau and Chorover 2019).
Sorption is a widespread natural As immobilization process. It involves the association of As with materials such as mineral oxides, activated carbon or resins (Mohan and Pittman 2007). In general, the main principle of the association of the inorganic pollutants with the sorbent's surface is related to their charge properties (Brusseau and Chorover 2019). For As, there are two principles described in the literature: i) the bonding nature of the As(V) or As(III) on iron (oxyhydr)oxides surface and ii) the substitution of SO_4^{2-} groups by As(V), for example during jarosite formation (Paikaray 2015; Shi et al. 2021).
Incorporation of As into the mineral oxides depends on the available surface and crystallized state of the mineral. The Fe(III)-oxyhydroxy-sulfate minerals widely described for As sorption are jarosite, goethite and schwertmannite (Burton et al. 2009). Schwertmannite is a poorly crystalline mineral that has shown capacity to sorb both As(V) and As(III), while under acid conditions jarosite and goethite show higher affinity for As(V) (Dixit and Hering 2003; Asta et al. 2009).

One concern regarding sorption as a process for As immobilization is the stability of the association between As and the mineral surface. Under reductive conditions, As can be released from iron oxides by reduction of As(V) into As(III) and its subsequent desorption or by reductive dissolution of the Fe mineral (Burton et al. 2009). Therefore, the stability of the mineral association regarding physico-chemical conditions is of prime importance.

1.2.1.4 Oxidative or Reductive process

The oxidation state of the metals and metalloids plays an important role in their mobility and toxicity in the aqueous phase. During the AMD treatment the aim is to reduce the Fe and As mobility by oxidation or reduction processes, involving an electron transport chain where electrons are transferred from the reduced species (donors) to acceptors. The main electron donors available in AMD are: $S^{(-1)}$ in pyrite, $Fe^{(+2)}$, $As^{(+3)}$, H_2 and the acceptors are: O_2, $Fe^{(+3)}$, SO_4^{-2}, $As^{(5+)}$, NO_3.

Under oxidizing conditions and low pH, iron is mainly present as slightly soluble ferric iron Fe(III). Under reducing conditions, highly soluble ferrous iron Fe(II) dominates (Brusseau and Chorover 2019). The oxidation of Fe(II) into Fe(III) promotes the Fe precipitation. The kinetic

and nature of this reaction is linked to the pH; at pH >5 the Fe oxidation is fast and mainly abiotic as shown
Figure 2Figure 2. But under a pH of 5 the kinetic of the abiotic oxidation decrease and it is mainly insignificant (Kirby et al. 1999; España et al. 2005b). At pH less than 5, Fe(II) oxidation is mainly catalyzed by FeOB. FeOB draw energy from this reaction for their growth. Therefore, under acid conditions, bacterial Fe(II) oxidation promotes the precipitation of Fe as oxyhydroxides, which are important sinks of metals and metalloids, such as arsenic.

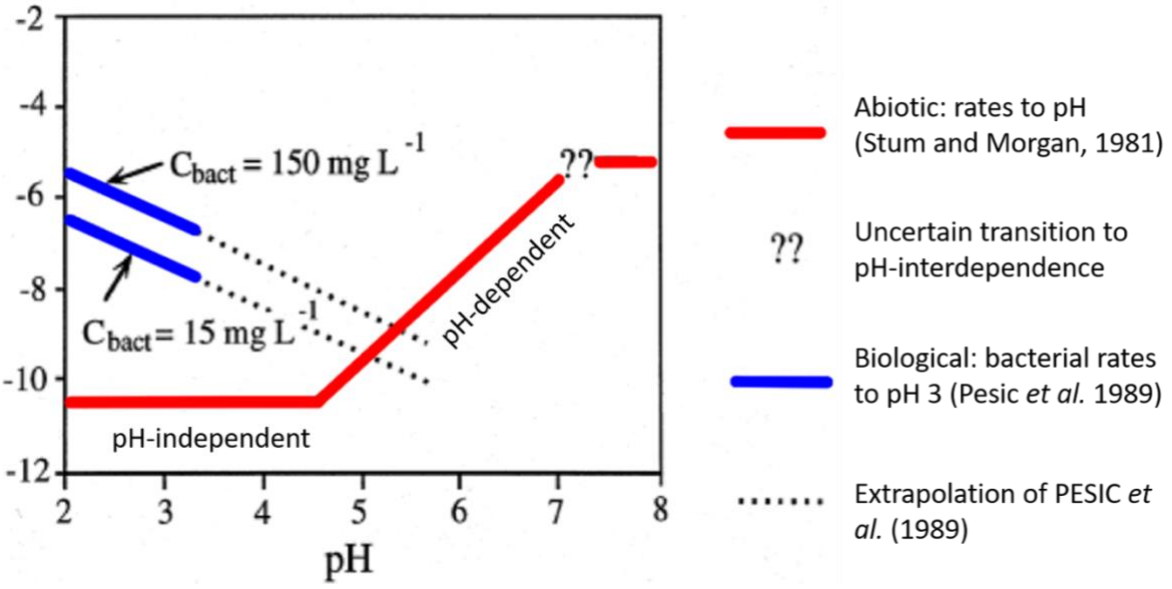

Figure 2. *Biologic and abiotic rates laws of Fe(II) oxidation, based on the biological rates studied by Pesic et al. (1989) and abiotic rates studied by Stumm and Morgan (1981). Cbact is the concentration of T. ferrooxidans in mg/L (dry weight). Modified from Kirby et al. (1999).*

Furthermore, the oxidation state of As has implications on its mobility. The affinity of As(V) with solid phases is higher than As(III) (Casiot et al. 2003b). Therefore, the oxidation of As(III) into As(V) strongly decreases As mobility in the AMD. This process can be catalyzed by microorganisms, which greatly accelerate natural As attenuation in AMD (Wakao et al. 1988; Bruneel et al. 2003). Thus, by oxidizing As(III) into As(V), bacteria promote the immobilization of As into minerals and subsequently decrease the availability and mobility of this inorganic pollutant (Casiot et al. 2003b). In the environment, many reactions are enhanced by microorganisms, but they only proceed when they are thermodynamically favorable, which applies to the oxidation of As(III) by oxygen (Brusseau and Chorover 2019).

Redox sulfur changes also play an important role in the immobilization of As in AMD. The solubility of As-sulfides is low in acid conditions; thus, the reduction of sulfate into sulfide under anaerobic and acid conditions favors As immobilization. Furthermore, the sulfate-reduction reactions consume protons, which increase the pH of the AMD (Newman et al. 1997a). This process will be explained in more detail in the remediation technologies section.

1.3 Approaches of As-rich AMD treatment based on key biotic or abiotic process

There are several classifications for the treatments applied to AMD. Some authors distinguish aerobic and anaerobic treatments. Others prefer the distinction between passive and active treatments, whatever the conditions of aeration (Hallberg & Johnson, 2005). Active treatments require energy, continuous addition of reagents and nutrients, permanent maintenance and monitoring. Conversely, passive treatments aim little or no handling or mechanical equipment, and the supply of nutrients or amendments (e.g sources of carbon) is only provided once, during the installation. Passive treatments need a minimal maintenance and monitoring. Both active and passive treatments include physico-chemical and biological methods (Lottermoser, 2007). In the following sections, we will distinguish abiotic and biological treatments (Hallberg & Johnson, 2005). Both kinds of approaches have one or more drawbacks, limitations and scopes of application.

1.3.1 Abiotic passive treatments of AMD

Most of the abiotic passive treatments used for AMD are focused on pH neutralization, which promotes metals/metalloids precipitation and sorption (Park et al. 2019). The main advantages are their efficiency to reduce most of the iron and increase the pH. However, the main disadvantages are the production of high amounts of bulky sludge, the short durability of the systems due to the reduction of the permeability and reactivity of the buffering materials once coated with Fe precipitates (Fan et al. 2019). Therefore, these passive systems are not recommended to treat AMD with high concentrations of metals, especially Fe, unless regular replacement of the buffering materials is provided. Other disadvantages of abiotic passive treatments are their cost and large land area requirement. These are two important limitations dealing with abandoned mines (Park et al. 2019).

The mode of implementation of an abiotic passive treatment based on pH neutralization depends on different features of the AMD, such as the pH, the flow rate of the effluent, the concentration of Fe(III) and oxygen. Neculita et al. (2021) has proposed some criteria for choosing the most adapted solution among anoxic limestone drains, open limestone channel and oxic limestone drain. The criteria are based on two principles: the available dissolved oxygen and the proportion of Fe(III).

1.3.1.1 Anoxic limestone drains (ALD)

The anoxic limestone drain is a neutralizing method adapted to AMD containing Fe and/or Mn under the reduced form ($Fe(III)/Fe_{total} < 10\%$). Also they exclusively treat AMD with a dissolved oxygen concentration (DO) lower than 2 mg/L (Neculita et al. 2021). Skousen et al. (2017) mentioned that this ALD is optimal for AMD containing less than 1 mg/L of dissolved Fe^{+3}, Al, and O_2. This method consists of using an alkaline material to increase the pH. The main purpose is to reduce the clogging of the drains due to formation of ferric precipitates. Instead, the anoxic conditions accelerate the dissolution of the limestone by the increase of the

CO_2 pressure (Skousen et al. 2017). At the drain outlet, aeration of the neutralized effluent promotes rapid abiotic Fe(II) oxidation and precipitation.

1.3.1.2 Open limestone channels

In the open limestone channels, the principle is the use of lime to promote iron oxidation under aerobic conditions and the precipitation of ferric-hydroxides (this method is also based on neutralization and precipitation) (Fan et al. 2019). This strategy is well adapted to an oxygenated AMD, with DO concentration higher than 5 mg/L and Fe(III)/Fe total > 25% (Ziemkiewicz et al. 1994; Neculita et al. 2021).

1.3.1.3 DAS (Dispersed alkaline substrate)

The dispersed alkaline material consists in a mix of fine-grain alkaline reagent and inert high surface material (Rötting et al. 2008). The inert material should be a coarse material with high porosity and permeability. Its main aim in the system is to improve the efficiency of the alkaline material by separating the alkaline grains among its large pores. This separation reduces or at least retards the clogging during the metal's precipitation. Wood chips are the most common inert high surface materials used; while the limestone sand is a cheapest and efficient alkaline amendment.

DAS has showed better results than the anoxic and open limestone channel in the removal of metals from AMD, particularly for AMD containing high concentrations of Fe, Cu and Pb.

However, this passive system is not efficient to remove divalent metals such Zn, Mn, Cd and Co (Rötting et al. 2008). Nowadays, this system is often used in combination with biological treatments (Quiceno-Vallejo et al. 2020). Particularly, for As removal, the DAS showed efficient results in combination with an Fe-oxidizing lagoon, but it has not been tested in concentration above 1 mg/L As (Macías et al. 2012a).

1.3.1.4 Permeable reactive barriers

The principle is also the neutralization and subsequent precipitation and/or adsorption of metals, but the reactive barrier is installed underground, perpendicular to the AMD flow (Rambabu et al. 2020). Hence, the AMD passes through the material, where the remediation occurs. For As removal, zero valent iron, manganese oxide and iron oxides are the most common reactive barrier materials used (Kanel et al. 2006; Wang et al. 2019b; Rambabu et al. 2020). Some of the biggest disadvantages of this treatment are large amounts of material needed that imply significant costs (Gibert et al. 2002).

1.3.2 Biological treatments of AMD containing As

Autochthonous microorganisms present in polluted environments hold a key to clean-up the human pollution by their metabolism (Azubuike et al. 2016). Particularly, for the biological treatment of As-rich AMD the aim is to use the capacities of the microorganisms to reduce the transport and availability of metals and metalloids, especially As. These capacities include the oxidation, reduction, biosorption and bioaccumulation of those toxic elements (Villegas-Plazas et al. 2019). Basically, the aim of this bioremediation approach is to reverse the reactions of

the AMD generation by the immobilization of the metals and metalloids in stable precipitates (Johnson and Hallberg 2005).

The biological treatments show advantages over the active abiotic treatments such as less energy consumption, lower operational cost in long-term, formation of less and more stable sludge (Neculita et al. 2007; Azubuike et al. 2016). However, there are still many gaps and limitations to make the bioremediation a suitable and efficient alternative to chemical treatment at large scale and under different environmental conditions.

Two of the most common processes used in the biological treatment of As-rich AMD to remove As and Fe from the aqueous fraction are: i) biological Fe and As oxidation, followed by their co-precipitation and ii) As and Fe precipitation in the form of sulfides mediated by biological sulfate reduction. These two biogeochemical process are applied within different technologies, the most common are wetlands and bioreactors (Johnson and Hallberg 2005).

1.3.2.1 Iron and As oxidation and co-precipitation

AMD streams undergo biogeochemical processes that decrease Fe and As mobility. Some of these natural attenuation processes are based on Fe(II) oxidation catalyzed by FeOB. Thus, the biological oxidation of ferrous iron is the base of this bioremediation approach.

Once the ferrous iron is oxidized to ferric iron, Fe(III) precipitates into ferric-hydroxides and -hydroxysulfate minerals (i.e schwertmannite, jarosite, goethite). The formation of Fe(III) minerals contribute to limit As mobility by co-precipitation and/or sorption. Arsenic can be removed in its reduced As(III) and/or oxidized As(V) form (Ahoranta et al. 2016). However, it is well described that As(V) has a stronger affinity for the Fe(III) minerals than As(III) in AMD (Casiot et al. 2003b). Thus, the sorption and sludge stability are enhanced by As(III) oxidation (Coudert et al. 2020). The microbial catalyzed As(III) oxidation shows more efficient rates than the abiotic As oxidation (more details about the As oxidation in a section below).

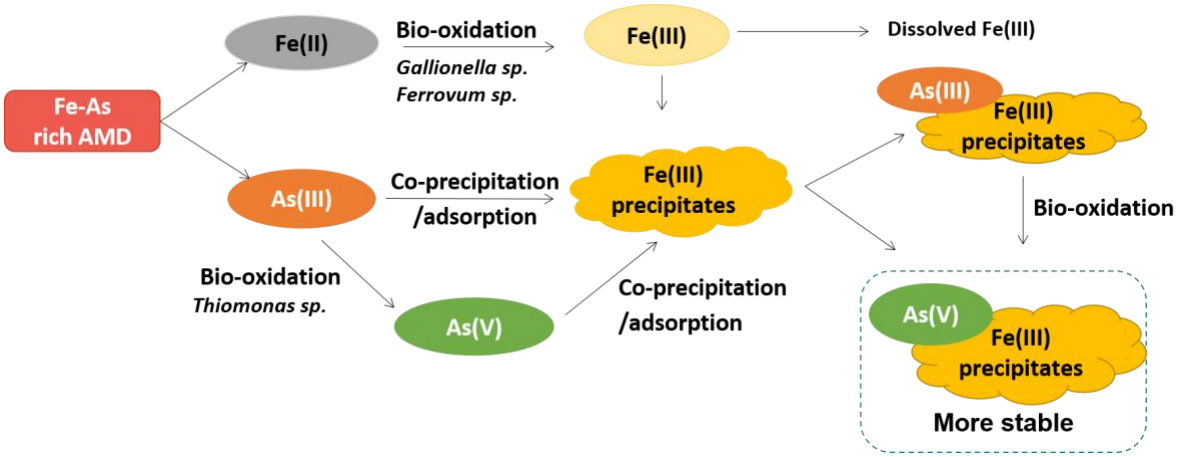

Figure 3. *Schematic representation of the fundamental of the biological treatment of an As rich AMD based on Fe(II) oxidation. This treatment includes the biological Iron and As oxidation followed by their co-precipitation.*

This natural attenuation process was observed in the Reigous creek (southern France), which is a permanent AMD at the ancient Pb-Zn Carnoulès mine (Leblanc et al. 2002). Thirty percent of As present at the spring of the AMD precipitated within thirty meters along the AMD stream (Casiot et al. 2003a; Egal et al. 2010). Similar natural attenuation processes were described worldwide, including the AMD from the Iberian Pyrite Belt (Spain) (Asta et al. 2010), Ilkwang mine in Korea (Park et al. 2016), Nishinomaki mine in Japan (Fukushi et al. 2003) and Santa Lucia mine in Cuba (Romero et al. 2010). Sanchez-España et al. (2005; 2007) reported a removal of 70% of the total dissolved Fe and up to 95% of the initial As content from the AMD that contained 700 mg/L Fe and 0.1 mg/L As. The observation of this natural attenuation process in several AMD worldwide suggests that it might be exploited and optimized in a treatment device for the treatment of As-rich AMD. The advantage of this process is that it requires a low maintenance and there is no need to add any carbon source or other substrates during its functioning (Xu et al. 2021)

1.3.2.1.1 Fe(III) minerals that contribute to As removal

The co-precipitation and/or sorption of As at acid pH can be performed by the formation of different Fe(III) minerals briefly mentioned in the previous section 1.2.1. The most studied minerals associated with this bioremediation process are:

- Schwertmannite

Schwertmannite is one of the minerals most described in the AMD in the pH range 2.8 - 4.5 (Bigham et al. 1996). The precipitation reaction can be written as follows (Bigham et al. 1996; Wang et al. 2019a) :

$$\mathbf{8}\,Fe^{+3} + SO_4^{2-} + \mathbf{14}H_2O \leftrightarrow \mathbf{21}H^+ + Fe_8O_8(OH)_6SO_4 + \mathbf{22}H^+ \quad \textit{Equation 4}$$

Schwertmannite is an iron-hydroxysulfate mineral considered a strong As scavenger, mainly due to its high surface area (> 320 m^2 /g) and exchangeable sulfate fraction (Paikaray 2020). This poorly crystalline mineral is able to co-precipitate and sorb arsenite As(III) and arsenate As(V), with a higher affinity for As(V) (Maillot et al. 2013). Maillot et al. (2013) observed that dissolved As(V) concentration in equilibrium with As-schwertmannite was ten times lower than for As(III), for similar As/Fe molar ratio in the solid phase.
Schwertmannite is metastable and is transformed to other minerals such as jarosite or goethite during aging under environmental conditions (Asta et al. 2009). The presence of high concentration of As(V) into schwertmannite accelerates its transformation into jarosite (Burton, 2021). During this transformation, As is partly remobilized into the aqueous fraction (Asta et al. 2009).

- Jarosite

Jarosite is another ferric hydroxysulfate mineral found in AMD. Its main formula is presented in **Error! Reference source not found.**, where X is usually K^+ (potassium jarosite) , Na^+(natrojarosite), NH_4^+ (ammoniojarosite) or H_3O^+ (hydronium jarosite) (Grishin et al. 1988; Johnston et al. 2012). The formation of jarosite and schwertmannite under acid conditions increases in presence of FeOB. Whereas the jarosite formation is favorised when there is a high

concentration of monovalent cations in the aqueous phase (Wang et al. 2006; Nazari et al. 2014).

$$3Fe^{3+} + X^{+} + 2HSO_4^{-} + 6H_2O \rightarrow XFe_3(SO_4)_2(OH)_6 \quad \textit{Equation 5}$$

Jarosite removes As(V) by sulphate-arsenate anion exchange; this mechanism makes jarosite more stable regarding As retention under anoxic conditions compared to schwertmannite (Asta et al. 2009). Generally, schwertmannite and jarosite can coexist but jarosite is formed at lower pH (<2.8, (Wang et al. 2006).

- Tooeleite

Tooleite is an arsenite-sulfate mineral; its formation reaction is presented in Equation 3 (Li et al. 2020). Tooeleite can be formed by the action of microorganisms such as *Aciditiohiobaillus ferrooxidans* (Morin et al. 2003; Majzlan et al. 2016). This mineral has a Fe/As molar ratio of 1.5 and an arsenic content of 25 wt% (Li et al. 2020). It is one of the main poorly crystallized minerals identified in the As(III) rich Carnoulès AMD (France) and it is involved in the As(III) removal from the aqueous fraction (Egal et al. 2009). The mechanism of tooeleite formation requires the selective Fe(II) oxidation without As(III) oxidation (Majzlan et al 2016). In fact, the presence of As(V) might inhibit tooeleite formation as the As(V)/Astotal ratio is higher than 43% (Liu et al. 2015).

$$6Fe^{3+} + 4AsO_3^{3-} + SO_4^{-} + 8H_2O \rightarrow Fe_6(AsSO_4)(OH)_4 \cdot 4H_2O + 4H^{+} \quad \textit{Equation 6}$$

Li et al (2020) studied As removal by biogenic tooeleite under laboratory conditions; they observed up to 95% of As removal from an synthetic Fe(II)-As(III)-rich AMD water containing Fe(II) concentration of 10 g/L and initial pH of 2-3. However, under acid conditions (pH between 1.8 and 4.6), tooeleite was unstable and remobilized more than 10 mg/L of As (Chai et al. 2016b). Probably this remobilization was due to the transformation of tooeleite to amorphous ferric compound. This behavior showed that this biomineral is not the most appropriate for As immobilization and storage (Chai et al. 2016b).

- Scorodite

The chemical formula of scorodite is $FeAsO_4 \cdot 2H_2O$. Scorodite is an arsenate mineral found in nature associated with the weathering of As-bearing sulfide ore deposits as shown Equation 4 (Gonzalez-Contreras et al. 2010). Its formation includes chemical and biological mechanisms under specific conditions, including high temperature (≥ 60°C) and extreme acid pH (pH below 1.3) (Paktunc and Bruggeman 2010; Gonzalez Contreras 2012). Because of its high As/Fe molar ratio (As/Fe = 1) and its high crystallinity, this solid phase is interesting regarding arsenate trapping. It promotes strong As immobilization into a low volume of solid (Paktunc and Bruggeman 2010).

$$FeAsS + 14Fe^{3+} + 10H_2O \rightarrow 14Fe^{2+} + FeAsO_4 \cdot 2H_2O + SO_4^{2-} + 16H^+$$ *Equation 7*

- Amorphous ferric arsenate (AFA)

Amorphous ferric arsenate also commonly called amorphous scorodite and hydrous ferric arsenate (Burton et al. 2021) is a group of solid phases with variable Fe and As concentrations, represented by the chemical formula $Fe_x(AsO_4)_y(SO_4)_z \cdot nH_2O$ (x, y and z variables) (Drahota and Filippi 2009). AFA and well-crystallized scorodite are the least soluble ferric arsenate mineral phases (Langmuir, 2006). Maillot et al (2013) observed the presence of AFA in the Carnoulès AMD; this amorphous phase was formed upon As(III) oxidation for As(V)/Fe(III) molar ratio higher than 0.2. On the contrary, when the As(V)/Fe(III) molar ratio was lower than 0.2, the dominant mineral phase involved into As removal was schwertmannite. Thus, the kinetics of As(III) and Fe(II) oxidation play a role in the AFA formation. Burton et (2021) observed that AFA formation was promoted at pH 2.4-2.8 and aqueous As(V) concentration over 2.4 mg/L. Under these conditions, AFA was thermodynamically favored over schwertmannite and the transformation of schwertmannite to AFA in presence of high As(V) concentration involved jarosite as an intermediate phase. Altogether, these observations suggest that AFA is the mineral phase most adapted to As sequestration in bioremediation systems exploiting biological Fe and As oxidation.

1.3.2.1.2 Microbiology associated with the iron oxidation treatment

Hedrich et al (2011) subdivided the iron oxidizing bacteria (FeOB) in four main physiological groups (i) acidophilic, aerobic iron oxidizers, (ii) neutrophilic, aerobic iron oxidizers, (iii) neutrophilic anaerobic (nitrate-dependent) iron oxidizers and (iv) anaerobic photosynthetic iron oxidizers.
Acidophilic FeOB are involved in the first stage of the remediation process which is the oxidation of ferrous iron present in the AMD into ferric iron (Equation 1). Some of the main FeOB identified in the AMD are listed in Table 1; they belong to different phyla such as Proteobacteria (i.e *Acidithiobacillus*, *Ferrovum*, *Gallionella*), Nitrospirae (i.e *Leptospirillum*) and Firmicutes (i.e *Sulfobacillus*) (Hedrich et al. 2011).

Under acid conditions, most of the FeOB are able to obtain energy from the oxidation of ferrous iron when this process is coupled to the oxygen reduction. This reaction is competitive compared to abiotic Fe(II) oxidation because the latter is slower at acid pH (Johnson et al. 2014).

Besides their role in Fe(II) oxidation, bacteria can promote the biomineralization by influencing parameters such pH or iron concentration that facilitate Fe precipitation or by providing nucleation sites for crystal formation (Hoffmann et al. 2021). Some examples are the biosynthesis of schwertmannite and tooletite by *Acidithiobacillus ferrooxidans* (Chai et al. 2016a; Li et al. 2020). This nucleation capacity is also observed among the archaea. For

instance, *Acidianus sulfidivorans* is a specie of archaea able to oxidize ferrous iron and induce scorodite crystallization (Gonzalez-Contreras et al. 2010).

- Arsenic oxidation

Bacteria have developed various strategies to tolerate or detoxify arsenic, some can even use arsenic as a source of energy for their metabolism These strategies often rely on As biotransformation such as oxidation, reduction and methylation (Kabiraj et al. 2022). Because theses biotransformations influence As speciation, the bacteria involved in arsenic cycling play an important role in the behavior of this metalloid in contaminated environments.
In particular, bacterially mediated arsenite oxidation contributes to reduce arsenic mobility in the environment and thus, play an important role in the remediation of As contaminated environments.
Several heterotrophic arsenite oxidizers (HAOs) and chemolithoautotrophic arsenite oxidizers (CAOs) are able to oxidize arsenite. Most of the HAOs and CAOs use arsenite oxidation as a detoxification mechanism. Some CAOs are able to use As(III) as source of energy for their growth; in this case, arsenite oxidation is coupled with the respiratory electron chain, connected with the assimilation of CO_2 (Drewniak and Sklodowska 2013).

The oxidation of As(III) can be catalyzed by three kinds of oxidases (i.e Aio, Arx and Ano), Aio and Arx belongs to the dimethyl sulfoxide reductase (DMSO) family of molybdoenzymes. The arsenite oxidase (Aio) enzyme is composed by two subunits. The large subunit is encoded by *aio*A gene and the small subunit by *aio*B gene (Li et al. 2016a; Kabiraj et al. 2022).. The *aio*A has been used as a marker to track the As(III) oxidizing microbial communities (Quéméneur et al. 2010).

The arsenate respiratory reductase (Arx) was identified most recently than the Aio, this Arx enzyme was identified in an isolate of *Alkalilimnicola ehrlichii* MLHE-1 in the genoma sequences of the Mono Lake (USA), this bacteria is an arsenite-oxidizing nitrate reducer. The Arx enzyme catalyze the anaerobic arsenite oxidation using nitrate as terminal electron acceptor (Oremland et al. 2002; Zargar et al. 2010; Hudson-Edwards and Santini 2013). The oxidoreductasa Ano is able to oxidase the As(III) in vitro but this enzyme tends to catalyze more efficiently the Sb(III) (Li et al. 2016b).

The abiotic oxidation of As by oxygen in absence of catalysis (such as illumination with near UV light (Emett and Khoe 2001) is many orders of magnitude slower than the microbial mediated oxidation (Asta et al. 2012). Therefore, arsenic oxidation in acid mine water has for a long time been attributed to microbial activity (Wakao et al. 1988). Wakao et al (1988) isolated the first acidophilic As(III) oxidizing bacteria from streams of acid mine water in northern Japan. Since then, many As(III) oxidizing bacteria have been identified in AMD-affected ecosystems, including *Thiomonas* which is one of the most studied. Bacteria belonging to the genus *Thiomonas* are described as facultative chemolithoautotrophs, they can growth on mixtures of inorganic and organic substrates (Battaglia-Brunet et al. 2006). Some species of

Thiomonas only use As oxidation as a detoxification mechanism (Bruneel et al. 2003), while others are able to use this metalloid as energy source (i.e *Thimonas arsenivorans*) (Battaglia-Brunet et al. 2006).

These bacteria are able to catalyze the oxidation of As(III) present in the aqueous fractions but also in the sediments as shown Figure 3 (Anand et al. 2022). This process could increase the stability of the precipitates formed in an iron oxidation treatment unit.

1.3.2.1.3 Parameters that can influence treatment performances

Several abiotic and biotic parameters affect the rates and yields of AMD bioremediation based on Fe and As oxidation and co-precipitation. Some of these parameters have been studied during natural attenuation occurring in AMD streams, others have been studied under controlled conditions in designed bioremediation units, in laboratory or field conditions. The most studied parameters are:

- pH

pH is one of the most important parameters controlling the rates of biological iron and arsenic oxidation (Pesic et al. 1989). Under acid conditions, biological iron oxidation can be up to 10^6 faster than abiotic oxidation (España et al. 2005b). However, some variations exist even at low pH (pH < 5). According to Larson et al. (2014), the biological Fe(II) oxidation is faster at pH 2.1 than at pH 4.2 due to thermodynamic control, in relation with the higher solubility of Fe(III). However, under field conditions Sánchez España et al. (2007) observed slower Fe(II) oxidation in AMD at pH 2 than at pH 3, suggesting that other parameters control biological Fe oxidation rate. pH is also an important factor controlling the distribution of FeOB populations (Jones et al. 2015). For instance, the presence of *Ferrovum* and *Acidithiobacillus* is favored at pH < 3, compared with *Gallionella* that is favored at pH > 3 (Jones et al. 2015).Under acid conditions, the structure of the bacterial community is one of the main factors driving the rates of iron oxidation in a bioremediation system (Jones et al. 2015).

Regarding As(III) oxidation, Battaglia-Brunet et al. (2002) showed that biological oxidation by a bacterial consortium originating from a mining site was maintained over a large pH range, between 2 and 10; As(III) oxidation was thermodynamically favored at pH 5 compared to pH 2, which provided a higher energy release for the microorganisms at a higher pH.
In a laboratory bioreactor treating As-rich AMD, Ahoranta et al. (2016) observed the highest iron oxidation and precipitation rates at pH 3; arsenic removal was inefficient below pH 2.4 due to the higher solubility of Fe–As co-precipitates.

- Temperature

Temperature is an important parameter controlling biological processes (Méndez-García et al. 2015). It has an effect on microbial metabolism and diversity in acid mine waters (Sánchez España et al. 2007; Volant et al. 2014; Tardy et al. 2018). Kirby (1990) mentioned the

temperature as the second parameter that controls biological iron oxidation rates after the pH. Sanchez España (2007) showed daily variation of iron oxidation rates in acid mine effluents, with the lowest rates measured in the morning and night, while the highest rates were observed at noon. They ascribed this variation to daily water temperature cycle, ranging between 15 and 35°C. These observations agree with other microbiological studies that showed that the optimal temperature for iron oxidation is between 25-35 °C (Johnson and Hallberg 2005; Sánchez España et al. 2007; Hedrich and Johnson 2014; Falagán et al. 2017).
Regarding arsenic, most of the bacteria associated with natural As attenuation and oxidation in AMD are mesophilic (growth between 10 to 40 °C) (Johnson and Hallberg 2003).

Tardy et al. (2018) showed that an increase of temperature from 20°C to 35°C induced an increase of As(III) oxidation rate in bioassays carried out with the AMD from the Carnoulès mine; they associated the increase of the As(III) oxidation rates with the dominance of the genus *Thiomonas* in the bacterial community at 35°C while iron oxidizing genera predominate at 20°C. Despite the stimulating effect of high temperature on biological arsenic oxidation, As(III) oxidizing bacteria seem to thrive with large temperature ranges; some representatives have been isolated from extreme conditions including psychrophilic and thermophilic conditions (Osborne et al. 2010; Yang et al. 2017).

- Oxygen

Under the acid conditions provided by the AMD, oxygen is the only thermodynamically viable electron acceptor for the ferrous iron oxidation. The effect of dissolved oxygen concentration on biological Fe(II) oxidation rates has been validated decades ago (Pesic et al. 1989). Oxygen concentration is a key factor that controls the structure of the microbial communities in AMD (Ziegler et al. 2013; Volant et al. 2014; Méndez-García et al. 2015). For instance, *Gallionella* and *Sideroxydans* are examples of microaerophilic FeOB found in AMD (Hedrich et al. 2011) while *Ferrovum* and *Leptospirillum* are strictly aerobic bacteria (Hanert, 2006; Johnson, 2014). The abundance of *Ferrovum* could be correlated to oxygen concentration increase (Fabisch et al. 2016; Fernandez-Rojo et al. 2018; Laroche et al. 2018).
In fact, oxygen drives the kinetic of the Fe oxidation and consequently bioremediation processes, the structure and diversity of the bacterial communities responsible for either the (Garcia-Ochoa et al. 2010; Quemeneur et al. 2010; Fernandez-Rojo et al. 2018; Garcia-Rios et al. 2020).
Regarding biological As(III) oxidation, some As(III)-oxidizing bacteria are able to use other electron acceptor such as nitrate; however, it is not often available in AMD. Debiec et al. (2017) showed that aeration accelerates As(III) oxidation in cultures of *Sinorhizobium*, when the necessary substrates were provided.

- Bacterial community

Fe(II) oxidation rate at acid pH is directly dependent on the biological performance of FeOB (Pesic et al. 1989). This performance depends on the density and composition of the iron

oxidizing bacterial community (Jones et al. 2015). Different FeOB genera exhibit different specific rates of ferrous iron oxidation (Johnson et al. 2012).
Pessic et al (1989) proposed a rate formula for the biologically catalyzed Fe(II) oxidation that considers that the rate is directly proportional to the concentration of bacteria, ferrous iron, oxygen and hydronium ion for a pH above 2.2 (Equation 8).

$$\boldsymbol{Rate}_{\boldsymbol{Fe(II)}}\ (\boldsymbol{mol\ Fe(II)\cdot L^{-1}}) = -\frac{\boldsymbol{d[Fe(II)}}{\boldsymbol{dt}} = \boldsymbol{k\cdot C_{bact}\cdot [O_2]\cdot [Fe(II)]\cdot [H^+]}\quad \textbf{Equation 8}$$

In this formula, k is the rate constant ($L^3 \cdot mg^{-1}\ mol^{-2}\ s^{-1}$), C_{bac} is the concentration of Fe(II)-oxidizing bacteria ($mg \cdot L^{-1}$, dwt), [O_2], [Fe(II)] and [H^+] are the concentrations of dissolved oxygen, ferrous iron and hydronium ion, all in $mol \cdot L^{-1}$. This approach works mainly under laboratory conditions, using only a single type of bacteria; it may be not adapted to field conditions, in presence of diverse groups of bacteria.

1.3.2.2 Sulfate reduction followed by As and S precipitation

Another widely used bioremediation strategy to deal with AMD has been the use of sulfate-reducing process. The microbial reduction of sulfate (SO_4^{2-}) to sulfide (S^{2-}) with organic electron donor or H_2 is coupled to microbial growth. The sulfate reduction consumes protons that leads to an increase in the pH (**Error! Reference source not found.**). Then the biogenic H_2S reacts with the soluble metals present in the AMD and precipitates with them in the form of metal sulfides (**Error! Reference source not found.**). H_2S can also react with metalloids such as arsenic (**Error! Reference source not found.**). This process is widely recognized as an important mechanism of metals and metalloids removal (Johnson and Hallberg 2005; Sánchez-Andrea et al. 2014). The sulfate reduction process is catalyzed only by anaerobic archaea and bacteria, the latter being termed Sulfate-Reducing Bacteria (SRB).

$$\boldsymbol{SO_4^{2-} + organic\ matter \rightarrow H_2S + HCO_3^-}\quad \textbf{Equation 9}$$

$$\boldsymbol{M^{2+} + H_2S \rightarrow 2H^+ + M^{2+}S}\quad \textbf{Equation 10}$$

$$\boldsymbol{H_3AsO_3 + 1.5H_2S \rightarrow 0.5As_2S_3\downarrow + 3H_2O}\quad \textbf{Equation 11}$$

$$\boldsymbol{As_2S_3 + 1.5H_2S \rightarrow 2AsS + H_2S_2}\quad \textbf{Equation 12}$$

In Equation 10, M^{2+} represents metallic cations, while Equation 11 and Equation 12 represent the paths of As removal. Equation 11 shows As(III) precipitated as arsenic sulfide with hydrogen sulfide forming an orpiment phase (As_2S_3) (Alam and Mcphedran 2019). Equation 12 shows the possible transformation of As2S3 into a crystalline realgar-like phase (AsS) (Le Pape et al. 2017).

The main advantages to use sulfate reduction followed by metals and metalloids precipitation to treat AMD are: (1) Selective precipitation due to different solubility of metal sulfides at different pH, (2) the formation biogenic precipitates with low solubility, good dewatering and good settling properties (Ňancucheo and Johnson 2012; Xu and Chen 2020). The selective

precipitation allows to reduce the volume of precipitates that contain toxic elements for disposal and also to reduce the clogging of the bioreactor with the Fe precipitates (Battaglia-Brunet et al. 2021).

One of the most critical factors in the treatment of AMD by biological sulfate reduction is the availability of organic substrates, mainly due to the relatively low concentration of organic carbon available in AMD (< 10 mg/L) (Neculita et al. 2007). Sulfate-reducing bacteria (SRB) use simple organic compounds as electron donors, source of energy and source of carbon. (i.e methanol, ethanol and lactate). The easily degradable compounds can come from degradation of organic matter or the products of photosynthesis carried out by plants. Passive sulfate-reducing anaerobic bioreactors are generally filled with raw organic materials (i.e rice bran, animal manure, saw dust, wood chips) or reactive mixture of those materials; those materials allow to reduce the cost, they are available locally and have long-term biodegradability (Neculita et al. 2007). However, these complex organic materials require periodic replacements and the disposal of these polluted organic wastes generate an additional problem (Ňancucheo and Johnson 2012).

Furthermore, when the selective precipitation of some metals or metalloids is expected, bioreactors fed with more simple substrates are generally preferred (Battaglia-Brunet et al. 2021). Energy and carbon sources used by SRB include hydrogen, acetate, lactate, ethanol, and glycerol. Ňancucheo and Johnson (2012) proved that glycerol was a suitable electron donor because it is less toxic than organic acids in acid conditions, so it provide a better control of reduction rates in a sulfidogenic bioreactor. These authors showed for the first time that it was possible to selectively precipitate metals (Cu and Zn) in acid mine waters within pH 2.8 – 4 by modifying the glycerol concentration. When the biological sulfate reduction is coupled to the oxidation of glycerol, the products are either acetate or CO_2 (Figure 4), depending on the SRB strains (Nancucheo et al. 2017; Zhou et al. 2022). In fact, the accumulation of acetate could be toxic for the SRB at acid pH (Sánchez-Andrea et al. 2014). For that reason and for the efficiency of the treatment, it is thus desired to promote the total oxidation that is not always achievable at acid pH (Campos-Quevedo et al. 2021b). However, fermentative bacteria such as *Clostridium* spp. are able to degrade acetate and then promotes indirectly SRB activity (Hernández et al. 2022). Likewise, SRB such *Desulfotomaculum* and *Desulfatirhabdium* are able to use directly acetate during the sulfate reduction (Campos-Quevedo et al. 2021b). Recent studies showed that the use of biomass carrier such as the zeolite in the bioreactors can promote the growth of SRB able to degrade acetate (Campos-Quevedo et al. 2021a).

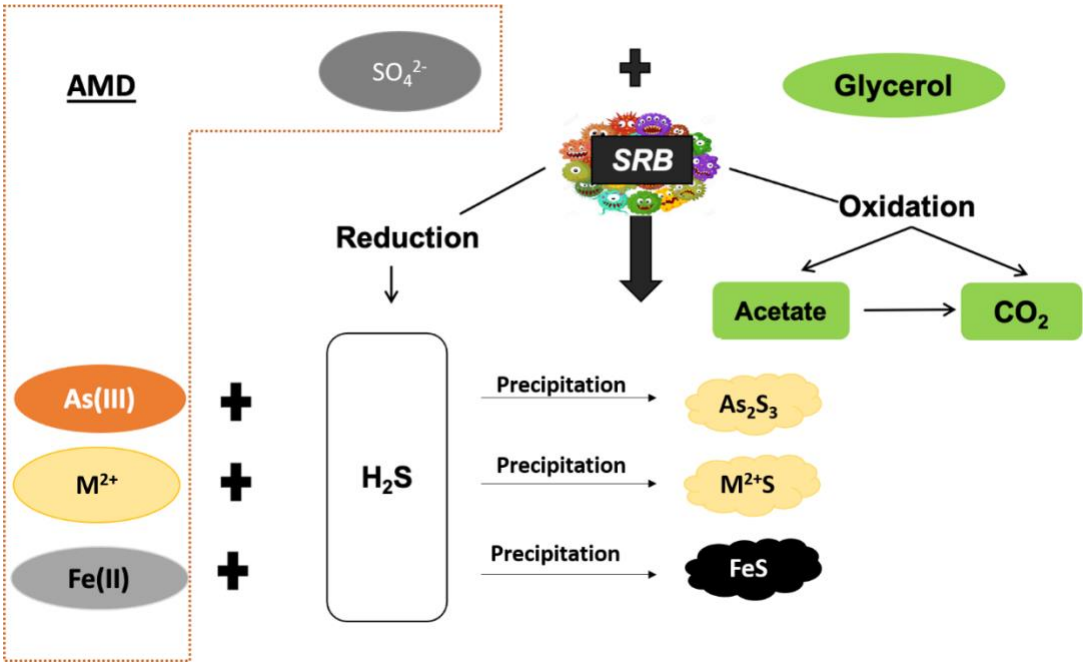

Figure 4. *Schematic representation of the principle of the sulfate reduction treatment of an As rich AMD. The dotted lines represent the principal composition of the AMD, which contains metals, metalloids and sulfate (SO_4^{-2}). The treatment couples the reduction of sulfate to the oxidation of glycerol, which is the substrate used as main carbon source for the sulfate-reducing bacteria. M^{2+} represents the metal cations*

Realgar (AsS) and orpiment (As_2S_3) are the main minerals responsible for As removal during sulfate reduction (Le Pape et al. 2017). Newman et al. (1997) showed for the first time the formation of amorphous orpiment in the presence of SRB. This precipitation is favored at low pH (Battaglia-brunet et al. 2012) .

1.3.2.2.1 Microbiology

The detailed metabolism of SRB for sulfate reduction is presented in the Equations 13 to 15 (Rambabu et al. 2020; Xu and Chen 2020). The first step in the sulfate reduction is the conversion of sulfate to adenosine-phosphosulfate (APS). For this process, the sulfate is actively transported across the cytoplasmic membrane of SRB, then it is activated by the adenosinemonophosphate (AMP) and the adenosinetriphosphate (ATP). The obtained APS is reduced to biogenic sulfite and then to biogenic sulfide by intracellular electron mediators, finally the sulfide binds and precipitates with the metals or metalloids present in the AMD.

$$AMP^{4-} + SO_4^{2-} + H^+ \rightarrow APS^{2-} + HP_2O_7^{3-} \quad \textit{Equation 13}$$

$$APS^{2-} + 2e^{2-} + H^+ \rightarrow HSO_3^- + AMP^{2-} + \quad \textit{Equation 14}$$

$$HSO_3^{-2-} + 6e^+ + 6H^- \rightarrow HS^- + H_2O\ (Metal\ cation) \quad \textit{Equation 15}$$

The sulfate reduction can be either assimilatory or dissimilatory. The assimilatory pathway produces sulfur which is used for the bacteria biomass, for the synthesis of proteins and amino-acids. The dissimilatory is coupled to energy conservation and bacterial growth; it results in the release of sulfides out of the cell (Sánchez-Andrea et al. 2014).

SRB are ubiquitous organisms; their function is vital within the sulfur cycle and they have an important role in generating alkalinity within wetlands. This group of bacteria belongs to different taxa: *Delproteobacteria*, *Firmicutes*, *Nitrospira* and *Thermodesulfobacteria*. Some of the most common genera identified as sulfate-reducing bacteria include: *Desulfosporosinus, Desulfobacter, Desulfobulbus, Dessulfococcus, Desulfonema, Desulfosarcina, Dessulfotomaculum* and *Desulfovibrio* (Sánchez-Andrea et al. 2014). However, their presence in AMD is restricted to *Deltaproteobacteria* and *Firmicutes* (Méndez-García et al. 2015).

As reviewed by Sánchez-Andrea et al. (2014), in sulfidogenic systems, SRB is not the only metabolic group present. Other groups such as fermentative bacteria, acetogenic bacteria and methanogenic archaea also play a key role in the AMD treatment. For instance, fermentative and hydrolytic bacteria break-down complex organic substrates and provide small molecules to the SRB community. When cellulose is provided, the most common genera associated are *Clostridum, Acetivibrio, Sprichaeta* and *Celullomonas.*

Acetogenic bacteria reduce CO_2 by assimilating carbon into the cell trough the acetyl-coA pathway. Some of the most common acetogenic genera found in AMD are *Acetobacterium* and *Clostridum*, in lower extent *Ruminococcus* and *Oxobacter*. In general, methanogens are sensitive to acid pH but there are particular groups that have been identified in AMD systems, especially in AMDs with excess of sulfate. Examples of methanogens detected in bioreactors treating AMD are *Mehanosaeta*, *Methanosarcina* and *Methanobrevibacter*.

Reverse dissimilatory sulfite reductase (DsrAB) is a key enzyme in the biochemical sulfur cycle. It catalyzes the reduction of sulfite to sulfide in anaerobic conditions. The DsrAB enzyme is composed by two subunits α and β encoded by *dsr*A and *dsr*B, respectively (Müller et al. 2015). *dsr g*enes are the most common biomarkers used to detect the presence of SRB (Geets et al. 2006).

1.3.2.2.2 Parameters that can influence the treatment performance

- Organic electron donor

There are different criteria to consider for choosing a source of carbon and electron donors to treat an As-rich AMD with biological sulfate reduction. Ayangbenro et al. (2018) summarized them as follows: 1) suitability of the substrate with the AMD composition, 2) amount of sulfate to reduce, 3) substrate cost and 4) toxicity of the by-products.

It is well known that SRB are not able to use directly complex compounds such as cellulose, fats, polymeric compounds, starch and proteins. However, as mentioned before, SRB can benefit from the metabolism of anaerobic fermentative bacteria (such as *Clostridium*) that release more simple compounds such as low-molecular weight acids.

The selectivity of the metals or metalloids precipitation is an additional criterion to consider for the selection of organic electron donor. If the purpose of the AMD treatment is to selectively precipitate and separate specific elements, the substrate would preferably be simple such as hydrogen or glycerol (Ňancucheo and Johnson 2012).

- pH

Xu and Chen (2020) summarized how the pH influence the SRB remediation performances: 1) pH affects the competition between SRB species and other metabolic groups, 2) pH affects the microbial metabolic mechanisms, 3) pH affects the recovery of metals and 4) pH affects the sulfide speciation.

At low pH, H_2S and organic acids are toxic for SRB. These compounds can cross the cell membrane and acidify the cytoplasm, affecting SRB growth. For that reason, the potential toxicity of the electron donor should be taken into consideration. Particularly the glycerol, H_2 and alcohols are not toxic at acid pH because they do not get ionized at low pH (Sánchez-Andrea et al. 2014).

A low pH can also be beneficial to biological sulfate reduction treatment. Considering the thermodynamic properties of metal sulfides, sulfate reduction becomes more energetically favorable in presence of higher concentration of hydronium ions (Alam and Mcphedran 2019).

Furthermore, the solubility of metals and metalloids sulfides depends on pH. Consequently, pH is a factor that controls metals and metalloids removal. The increase of pH during sulfate reduction will result in the consecutive precipitation of arsenic (under acid conditions), followed by Zn, Ni, Fe and finally Mn (pH around 8) (Le Pape et al. 2017; Xu and Chen 2020). Regarding arsenic, high pH is detrimental to As removal due to the formation of thioarsenate species, which enhances the As mobility (Battaglia-Brunet et al. 2012).

- Temperature

Temperature is another important parameter that affects the structure and activity of the microorganisms during sulfate reduction. SRB thrive in a wide range of temperatures, from < 5°C to 80°C (Ben Ali et al. 2019a). However, the efficiency of the treatment is affected by extreme conditions, especially for the passive treatments that utilize complex organic mixtures. When the temperature decreases from 22°C to 2°C, the efficiency of the SRB systems can decrease by more than 50%. Strategies have been implemented to control SRB bioreactors efficiency during winter in temperate countries; one is to install the SRB bioreactors at a depth

below the freezing point in the soil and to cover them with insulating materials. Another alternative is to use easily degradable electron donors such as methanol, lactate, acetate or glucose; these sources provided higher treatment performances at temperatures under 4 - 5°C.

Tsukamoto et al. (2004) showed that a period of acclimation could help to maintain the performance of a semi-passive SRB bioreactor for temperatures as low as 6°C.

- Metals or metalloids speciation and concentration

Some metals can be toxic for SRB at high concentration. Toxic effects include the denaturation of proteins or inactivation of some enzymes. For instance, Labastida et al. (2013) correlated the decrease of the sulfate-reducing rate under batch conditions with the high concentration of Pb.
For the treatment of AMD containing high concentrations of arsenic, the tolerance of SRB to this toxic metalloid is one important point to considerer. High concentration of arsenic can affect the SRB growth and metabolism, finally affecting the efficiently of the treatment of As-rich AMD. Newman et al. (1997b) observed a decrease of sulfate reduction efficiency by the presence of As(V). They explained it by a toxic effect or sulfate reduction inhibition (Newman et al. 1997b).

One strategy for high-As AMD treatment is to use native microorganisms already adapted to high As concentrations. Many SRB have shown to tolerate As and to be able to reduce As(V) to As(III). For instance, *Desulfotomaculum auripigmentum* described by Newman et al. (1997b) can use either arsenate or sulfate as electron acceptor, but the arsenate reduction is faster, because the As reduction is more energetically favorable than the sulfate reduction. In the case, the community present in the treatment unit has the capacity to reduce As probably start with this reduction and then, if there are electron donors available the community will reduce the sulfate. Therefore, the composition of the bacterial community present in the treatment unit is so important in the performances of the treatment.

It is noteworthy that the presence of metals such as Fe could enhance the removal of other elements such as As by co-precipitation or sorption onto FeS (Alam and Mcphedran 2019).

1.4 Implementation of high-As AMD bioremediation

Biological treatments are an interesting strategy to deal with AMD pollution, especially to overcome the drawbacks of the chemical and physical methods. Those drawbacks include the high cost, the maintenance, the elevated volumes of toxic solid wastes and the space needed. The most common implementation methods for the two bioremediation approaches described in the sections 1.3.2.1 and 1.3.2.2 include wetlands and bioreactors.

1.4.1 Wetlands

Natural and constructed wetlands have been used to clean water over centuries. The wetlands work as biological filters to remove different kinds of pollutants. Processes such as bacterial degradation, plant uptake, neutralization, precipitation and sorption are some of the mechanisms involved in pollutants removal in the wetlands (Sheoran and Sheoran 2006). Specifically, the wetlands have been widely applied to treat AMD from coal and metal mining. However, as far as we know, arsenic has not been a targeted pollutant in the use of wetlands in the treatment of AMD. For that reason, there are gaps in the understanding of the mechanisms and processes controlling the As removal in wetlands and their As removal efficiency is uncertain (Lizama et al. 2011).

Sorption on suspended particles and sediments and co-precipitation are among the main mechanisms involved in As removal in wetlands. Plants also play a role. For instance, the wetland plants release oxidants (including oxygen) that promote iron oxidation at the roots surface; this oxidation is followed by the precipitation and the formation of iron plaques. These plaques can work as reactive sink for metal(loid) sequestration (e.g As and Zn) (Sheoran and Sheoran 2006).

These complex ecosystems are able to sustain different groups of microorganisms including SRB. Therefore, the precipitation of metals and metalloids to form stable and insoluble biogenic sediments also occurs at the bottom of the wetlands (Johnson and Hallberg 2005).

1.4.2 Bioreactors

Bioreactors are engineered systems designed to optimize biogeochemical processes involved in the treatment of water, soil, sediment or sludge. These systems draw on knowledge and experience from different fields, including thermodynamics, chemical kinetics, fluids mechanics and mass transfer.

For a single fluid reaction, the types of ideal reactors are divided in: a) perfectly mixed batch reactors, b) plug flow reactors and c) mixed flow reactors. In batch reactors inlet flow is initially charged into the reactor, then it is left inside the reactor for a certain period and then the treated water is discharged (Levenspiel 1999; Fogler 2004). In the plug flow reactor, the inlet flow is not intentionally mixed along the flow, there is a gradient or lateral mixing; this kind of reactor include vertical and horizontal reactor. The basic principle of this type of reactor is that the residence time must be the same for all fluids. In the steady-state flow reactor, also called stirred flow reactor, the main principle is to mix the effluent constantly to guaranty that the treated water will have the same composition than the liquid within the reactor (Levenspiel 1999).
Several versions of these three kinds of ideal bioreactor exits, depending on the aim of the process, substrates and conditions the main principle can be adapted. Particularly, dealing with AMD bioremediation the bioreactors are grouped (Figure 5): based on flow modes (batch, continuous mode or semi continuous mode), based on solid catalysts (fixed bed, fluidized beds

or slurry), based on microbial growth type (suspended growth or biofilm), number of stages (one stage or two stages) and injection mode (up-flow or down flow) (Sánchez-Andrea et al. 2014).

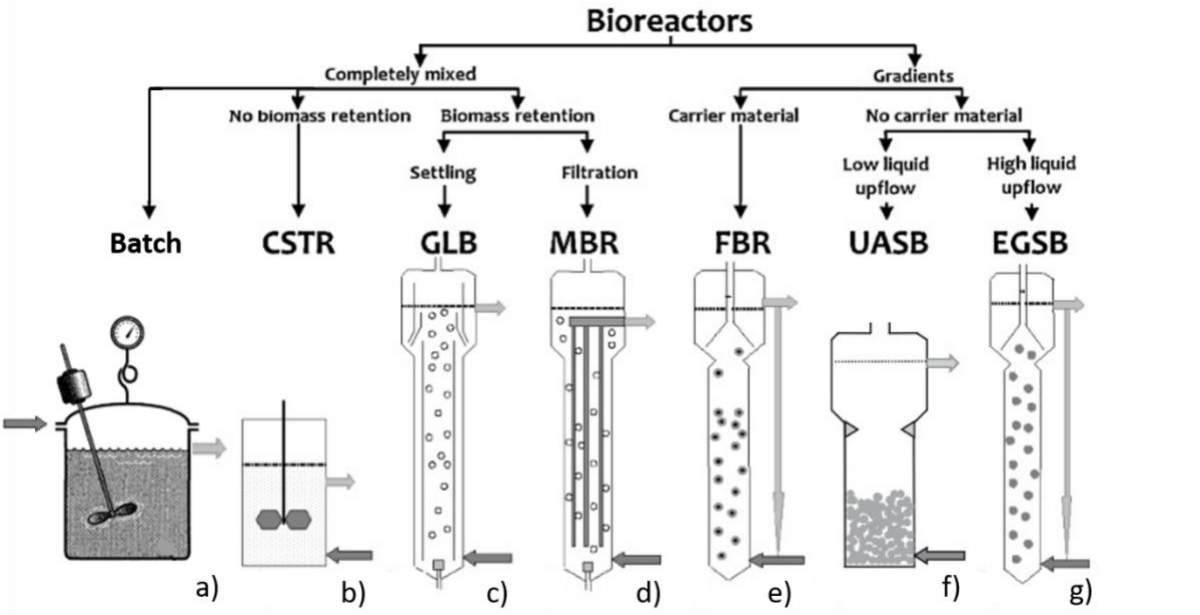

Figure 5. *Types of bioreactors A) Perfectly mixed batch reactor, B) continuous stirred-tank reactor ; liquor is mixed by a mechanical stirrer (CTSR), C) gas-lift bioreactor is used with gaseous electrons donors (GLB), D) membrane reactor is used to retain the biomass in slow growing process, E) fluidized bed reactor use a carrier material to promote the biomass growth and biofilm formation; the biofilm is attached to the carrier material (FBR), F) up-flow granular sludge bed (UASB) and G) expanded granular sludge bed reactor, which use liquid recirculation (EGSB). Modified from Sanchez-Andrea et al. 2014.*

1.4.3 Examples of biological treatments of high-As AMD

Examples of bioreactors applying sulfate reduction or iron oxidation to As-rich AMD are listed in Table 3 and Table 4. Some of them were fed with synthetic AMD that allowed to control most of the variables, which is a primarily phase to understand part of the biogeochemical process and evaluate the efficiency of the treatment (Ahoranta et al. 2016, 2020; Xu et al. 2021). Semi passive bioreactors for the treatment of high-As AMD have been rarely implemented under field conditions (Fernandez-Rojo et al. 2019; Diaz-Vanegas et al. 2022). The active bioreactors show high yields, stability in its performance and achieve to treat elevated concentration of As (Gonzalez-Contreras et al. 2012b). However, it is not a viable strategy for abandoned mines, which is the main sources of As-rich AMD.

The anaerobic treatment with sulfate-reducing bacteria show excellent potential to deal with the As rich AMD, most of the studies present in the table 2 reach As removal yields among 65 to 100%. But until now most of those studies are still at laboratory phases, which are “ideal conditions” but still far for real conditions. Under real conditions, there many factors such as HRT, geochemical and operational perturbations that cannot be always controlled. Hence the importance of moving to field conditions.

For the aerobic treatment using iron oxidation bioreactors the only experience that achieved 100% of As removal was applied to an synthetic AMD with 20mg/L of As (Xu et al. 2021), which is a relative low concentration of As compared with the AMD from the ancient mine the Carnoulès (50-100 mg/L) or other mine waters such as Svornost mine in the *Czech* Republic, which reach up to 130 g/L of As (as shown Table 2). Until now most of the studies dealing with As-rich AMD reach to release treated water below the regulations, which is still a threat for the environmental and human health. For consequence the combination of both methods of bioremediation (iron oxidation and sulfate reduction) showed promising results as shown Table 5 (Hedrich and Johnson 2014; Sato et al. 2018; Battaglia-Brunet et al. 2021).

The hydraulic retention time (HRT) applied in average for passive or semi-passive Fe oxidizing bioreactors is 7 ± 2 h, which is faster than the HRT in average applied in the sulfate-reducing bioreactor (50 ± 43h). The long HRT in the anaerobic treatment is required due to a short HRT can promote the input of dissolved oxygen in the reactors and the wash out of the microbial biomass.

Table 3 *Biological iron and arsenic oxidation followed by co-precipitation to treat As rich AMD.*

Reference	**Site**	**Whole design**	**Influent As, Fe and pH**	**Microbial community**	**% Fe and As oxidation**	**Fe removal % (rate)**	**As removal % (rate)**	**HRT (h)**	**Mineralogy**
Ahoranta et al. (2016; 2020)	Lab	Fluidized bed bioreactor (FBR)	Synthetic AMD Fe: 10 g/L pH 1.3 ± 0.1	FeOB inoculum	FeO: 99% (1070 mg/L·h)	99% (28 $mgL^{-1}h^{-1}$)	7 -99.5%	5.7h	Jarosite
Xu et al. (2021)	Lab	Biofilm reactor Perlite particles as the biofilm carrier (As oxidation)	Synthetic AMD pH:3-4 As: 20 mg/L	Consortium by enrichment of AMD	AsO:93-100% (0.3 -4.4 mg/L·h)	NA	93-100%	4-3h	NA
Gonzalez-Contreras et al. (2012)	Lab	Arsenoteq, Airlift Reactor inoculated with Sulfolobales (Archaea)	As: 2 g/L Fe: 1.8 -6 g/L pH 1.2	*Sulfolobales* (Archaea)	FeO: 30-80% AsO:	30% (0.4 $gL^{-1}d^{-1}$)	40 -90% (0.40-0.5 $gL^{-1}d^{-1}$)	40h	Bioscorodite
Fernandez-Rojo et al. (2017)	Lab	Continuous flow bioreactor	As: 84-118mg/L Fe: 50-250mg/L pH: 3.2	AMD native community	FeO: 80%	40% (1.2-2.4 x $10^{-7}molL^{-1}s^{-1}$)	65% (10^{-8} $molL^{-1}s^{-1}$)	8h	Tooleite Amorphous ferric arsenate
Fernandez-Rojo et al. (2019)	*In situ* pilot scale	Aerobic ponds stacked on top of each other connected by cascades	As: 84-118mg/L Fe: 50-250mg/L pH: 3.2	AMD native community	< 10%	<10%	3-97% (10^{-8} $molL^{-1}s^{-1}$)		Tooleite Amorphous ferric arsenate
This study Diaz-Vanegas et al. (2022)	*In situ* pilot scale	Two semi-passive units of 1 m^3 with plastic carrier or wood/pozzolana carrier. Forced aeration.	As: 50-100mg/L Fe: 500-1000mg/L pH: 3.	AMD native community	FeO 86 to 98%	50 – 80% (2 x $10^{-7}molL^{-1}s^{-1}$)	50 – 80% (10^{-8} $molL^{-1}s^{-1}$)	9h	Jarosite and amorphous ferric arsenate

FeO: ferrous iron oxidation

AsO: arsenic oxidation NA: not information available

Table 4 *Sulfate reduction bioreactors to treat As-rich AMD, modified from Alam et al. (2019)*

Reference	Site	Influent	Carbon source	Origin of SRB	As removal %	HRT (h)	Sulfide minerals formed
Costa and Duarte. (2005)	(Packed bed)	As: 0.14 mg/L pH: ~2	Lactose	Sediments mining area	65%	NA	NA
Luo et al. (2008)	Laboratory (Colum packed)	Synthetic mine water As: 1mL/L pH: 8	Ethanol	Dry horse manure	95% in presence of iron	48h	FeS
Castro et al. (1999)	Laboratory (Batch)	As: 1-3mg/L	Compost and potate peel	Compost potato peel	~ 100%	NA	As2S3
Jackson et al. (2013)	Bench and field-scale (BCRs)	Mine waste landfills As: 8.5 mg/L Zn: 23 mg/L	Biosolid matrix	Biosolid matrix	76 – 94%	NA	As2S3, As(II)-O and amorphous phases
Sahinkaya et al. (2015)	Up flow anaerobic sludge blanket (UASB)	Synthetic AMD As: 8.5 mg/L pH: 4	Ethanol	Filled with biomass granules from wastewater reactor	98- 100%	24 to 12h	FeAsS
Le Pape et al. (2018)	Laboratory (Batch)	As:10 mg/L	Glycerol	Sediments AMD spring	80%	NA	As2S3 and AsS
Altun et al. (2014)	Fixed bed up-flow bioreactor (sand as carrier)	Synthetic AMD As: 0.5 – 20 mg/L Fe: 10 -200mg/L pH: 4	Ethanol	Sludge from a sulfate-reducing anaerobic reactor	85%	9.6h	As2S3, FeS, FeS2 and FeAsS
Battaglia-Brunet et al. (2012)	Laboratory (Fixed-film)	As: 100 mg/L pH:	Glycerol and/or Hydrogen	Previous SRB bioreactor (sediments AMD spring)	75-100%	61 to 44h	As2S3
Battaglia-Brunet et al. (2021)	Laboratory (down flow filled with pozzolana)	As: 18-174 mg/L Zn: 4.4 -174 mg/L pH 3.3 -4.0	Glycerol	Previous SRB bioreactor Sediments AMD spring	Up to 99%	5.4 ± 0.5 min	As2S3
Patented by Paques B.V.	Thioteq	< 5000 mg/L of arsenic	H_2 and alcohol	Lab consortium	Up to 99%	NA	As2S3, orpiment
This study	Field scale, ancient Carnoulès mine (France)	Vertical continuously fed SRB	Glycerol	Previous SRB bioreactor (sediments AMD spring)	Up to 99%	29 to 5d	NA

BCRs: biochemical reactors
NA information not available, Thioteq includes two stages: one chemical and the other biological.

Table 5 *Coupled Aerobic and anaerobic treatments*

Reference	Site	Whole design	Influent	Phases [1]	% Removal	Microbiology	Mineralogy
Kalin and Caetano (2003)	Nova Limina mining district (Brazil)	four oxidation–precipitation–settling ponds and three microbial treatments ponds in serie	Mine water pH: 2-4 Zn: 460 mg/L Fe: 20 - 300mg/L	-First oxidation ponds	15-38% Fe removal	NA	NA
				-Anaerobic ponds raw potatoes and whole sugar cane.	95% remaining Fe, remove Ni, Al and Cu	NA	NA
Hedrich and Johnson (2014)	Laboratory scale	Modular bioreactors	Synthetic mine water pH: 2.3 Zn: 460 mg/L Fe: 400mg/L As: 49 mg/L	-Iron oxidation and precipitation	99% Fe removal 99% As (2h by adding 80 mg of the mineral for 1L AMD	*Ferrovum myxofaciens* *Acidithiobacillus ferroxidans* *Acidiphilium sp*	Schwertmannite
				-Sulfidogenic bioreactor	Treat 3% Zn, 100% Cd, 100% Co and 50% Ni	*Desulfosporosinus* (incomplete oxidizer)	ZnS
Sato et al. (2018) JoGMEC	Japan *In situ*	Compact passive treatment	Raw AMD pH: 2.5 Zn: 15 mg/L Fe: 40 mg/L Cu: 5 mg/L	-Iron oxidation	88% Fe removal	NA	NA
				-Sulfate-reducing bioreactor (rice bran and husk)	Treat 99%-100% Cu and 93-100% Cd	*Desulfatirhabdium butyrativorans* was dominant	NA
Battaglia-Brunet et al. (2021)	Laboratory scale	Combining continuously fed SRB with downstream iron oxidation	AMD As: 18-174 mg/L Zn: 4.4 -174 mg/L pH: 3.3 -4.0	-Sulfate-reducing bioreactor (glycerol)	70 to 95% of As	Consortium, with SRB as *Desulfosporosinus* genus.	amorphous orpiment
				-Iron oxidation	NA	AMD native community	NA
This study	Field scale, ancient Carnoulès mine (France)	Combining continuously fed SRB with downstream iron oxidation	AMD As: 18-174 mg/L Zn: 4.4 -174 mg/L pH: 3.3 -4.0	-Sulfate-reducing bioreactor (glycerol)	99% As removal (outlet; 170 µl/L)	SRB Consortium from Carnoulès mine (enriched)	Amorphous phases
				-Iron oxidation	99% Zn removal, As concentration outlet 10 µl/L Up to 100% Fe removal	AMD native community	NA

[1] **Include the different stages of the complete treatment**

1.4.4 Bioreactors' features that contribute to the efficiency of the treatment of high-As AMD

Different features can contribute to the optimization of the treatment performance. Some of them (oxygen, temperature, pH) control the biogeochemical process inside of the bioreactors; their role has been detailed in sections 1.3.2.1.3 and 1.3.2.2.2. Other features (biomass carrier, HRT) are linked to the bioreactor's operation; their role is described below.

1.4.4.1 Biomass carriers

Biomass carriers are support materials that promote the bacterial attachment; they provide a surface for bacterial growth and biofilm development. The carriers decrease the wash out of the bacterial biomass and contribute to minimize the clogging in the reactor (Ahoranta et al. 2020; Mahto and Das 2022).

Different types of biomass carrier have been used in bioremediation of AMD; they are classified in natural organic carriers and inorganic/synthetic carriers. The natural organic carriers include activated carbon, chitosan beads, sawdust, wood chips, pozzolana, rice, alginate, bagasse and diatomite, while the synthetic carriers include polyethylene, porous glass beads, polystyrene and polyurethane foam (Dzionek et al. 2016). The selection of a suitable and durable biomass carrier has important consequences on the rates, the cost of the treatment, the delay before replacement, the risk of clogging and can influence the structure of the microbial community (Zhao et al. 2019; Campos-Quevedo et al. 2021a). One of the materials most described in the literature is pozzolana, which is a volcanic basaltic rock. This material has high porosity and roughness that promote a great surface available for bacterial attachment and development (Challan Belval et al. 2009).

Recent studies have shown that biogenic minerals formed inside the iron oxidation bioreactors can work as biomass carriers. These minerals can be used as a biofilm support maintaining a stable bacterial density, which enhance the efficiency of the iron oxidation. But also can enhance the precipitation acting as a seed of minerals (Wang and Zhou 2012). In fact, along the remediation the biogenic precipitates accumulated inside the bioreactors can start replacing the biomass carriers initially supplied (Kinnunen and Puhakka 2004; Ebrahimi et al. 2005). For instance, Ahoranta et al. (2020) demonstrated that biogenic jarosite can be used for maintenance and recycling of Fe-oxidizing biofilm which provided high rates of Fe oxidation.

1.4.4.2 Hydraulic retention time (HRT)

The HRT is one of the most important parameters to considerer for the optimal performances of a bioreactor; it controls the extent of the reaction but it is also a key hydrodynamic parameter that influences the contact between the AMD water and the bacterial community involved in the treatment (Vasquez et al. 2018; Xu and Chen 2020). In different studies, the decrease of the HRT implied a decrease of the treatment performance due to inefficient contact between the reactants and biofilm (Sahinkaya et al. 2011; Fan et al. 2019). HRT is also an important driver of the structure of the bacterial community, probably because the HRT apply important

variations in the concentration of the reaction products and consequently the pH, which modify the composition of the bacterial community initial established (Fernandez-Rojo et al. 2018).

The choice of a suitable HRT will be driven by performance efficiency/stability and space availability under field conditions. The most common ranges of HRT for biological iron oxidation AMD treatment are between 3h and 7h (Sheng et al. 2017; Fan et al. 2019; Garcia-Rios et al. 2020). Regarding SRB bioreactors, longer HRT ranging from 2 to 7 days have been used; such long HRT favored SRB growth and enhanced degradation of organic carbon (Sato et al. 2018; Vasquez et al. 2018).

1.5 Study case of the ancient Carnoulès mine

In the European context, the ancient Carnoulès mine is the second most studied sites with AMD containing arsenic, after the Iberian Pyrite Belt (Spain). The Carnoulès mine is located in the town of Saint Sébastien d'Aigrefeuille, in the Gard department in southern France, between the cities of Montpellier (60 km) and Ales (12 km). The mine quarry and tailings remnant from the recovery process are located on the Amous river watershed, which is tributary of the Gardon River. This also flows into Rhône River (Figure 6). The site is characterized by a Mediterranean climate, which is composed of dry summer periods and strong rainy events in autumn and spring (Ben Ali et al. 2019b). The mineralization in the area is mainly composed of pyrite, marcasite, galena, and in less proportion sphalerite, silver arsenides such as proustite, copper sulfosalts; with also presence of quartz and barite (Geoderis 2019).

The history of the management of the mining site is documented in detail in Elbaz-Poulichet et al. (2006). Briefly, the Zn and Pb extraction at the site started in 1730 and lasted for centuries. During all the mining activity period, the mine wastes were stored in tailings, which were exposed to rain water, promoting AMD release. During the last exploitation period (1958-1962), the residues from the flotation process, composed of fine sands with 2-3% As-rich pyrite were stored behind a dam, upon the sources of the small Reigous creek, which converted this creek into a permanent AMD (pH 3.3-4.8, 750-2700 mg/L Fe and 2000-7500 mg/L SO_4). This AMD is particularly rich in arsenic (80-350 mg/L As), mainly in the reduced form As(III). The Reigous creek pollutes the Amous River (pH 8.4), located 1.5 km away (Figure 6). In 1961, the barrier of the dam broke of and tailings were disseminated along the hydrosystem downstream. The mining company's owners cleaned up the site and reinforced the dam. A Department decree closed the mine in 1962. However, it left around 1 million tons of tailings rich in Pb, Fe, S and As stored behind a 35-meter-high dam. The tailings were composed mainly of quartz and arsenic-rich pyrite (5-10%). After another dam failure in 1976, the site was rehabilitated in the 1980s and a 30-cm-thick clay cover was disposed upon the tailings to prevent water infiltration. However, it did not avoid the AMD release. The runoff waters were collected by concrete ditches installed along the borders of the tailings pile.

Since the 1970s, the Carnoulès site has been the focus of numerous studies, particularly with more than 20 years of monitoring by HydroSciences Montpellier and the Observatory of Mediterranean Research of the Environment (OSU OREME / https://oreme.org/). This monitoring allowed to understand the biogeochemical processes controlling the AMD formation, the variation of the AMD physico-chemistry across seasons, the natural mechanisms responsible for the As attenuation in the Reigous creek and also the spatio-temporal dynamics of the microbial communities. Leblanc et al. (2002) and Casiot et al. (2003) described the seasonal variation of pH, dissolved oxygen concentration, As and Fe concentrations in the Reigous creek. They evidenced natural attenuation of arsenic and iron in the AMD (Figure 6) and clarified the biological oxidation and precipitation processes, as described in the section 1.2.3.1.

The precipitates formed naturally in the Reigous creek were composed of As(V) and Fe(III) (Morin et al. 2003), whereas the aqueous phase contained As(III) and Fe(II), which confirmed the role of As(III) oxidation into the natural attenuation process (Casiot et al. 2003). The highest Fe and As precipitation rates were observed during the winter (up to 50% for As and 40% for Fe), while the lowest rates were observed during the summer (less than 25% of As and Fe removal) (Leblanc et al. 2002). Morin et al. (2003a) described the variation in the composition of the precipitates formed in the Reigous creek across seasons. They revealed that in winter they were mainly composed of tooleite [$Fe_6(AsO_3)_4(SO_4)(OH)_4 \cdot 4H_2O$], a ferric arsenite sulfate phase, and an amorphous Fe(III)-As(III) phase. In spring and summer, the precipitates were mainly composed of Fe(III)-As(V).

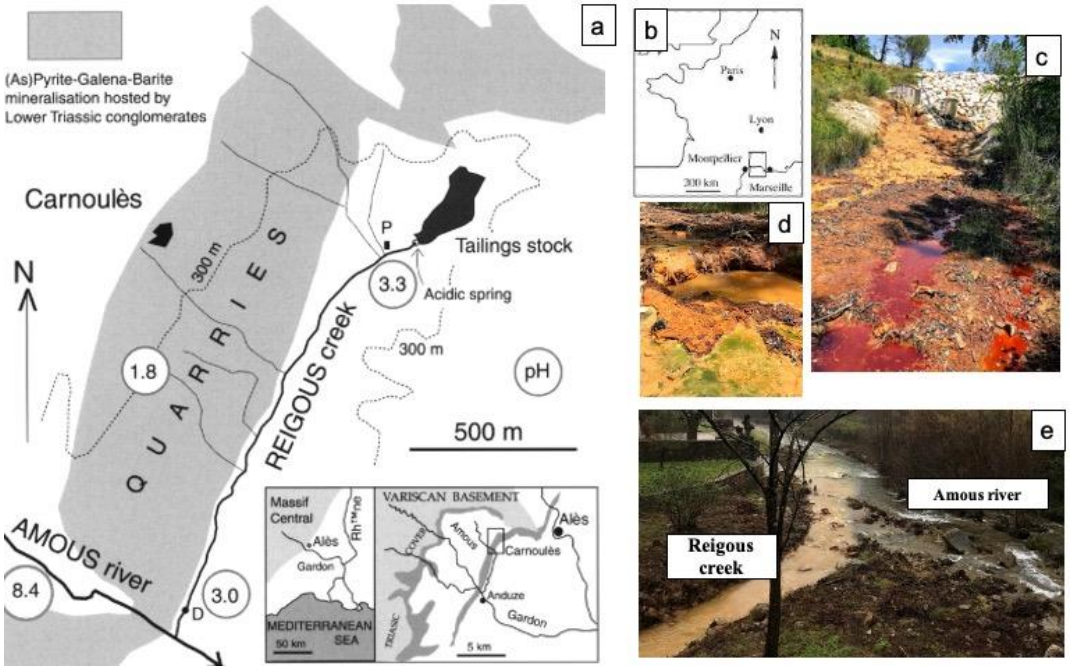

Figure 6. *Location and map of the Carnoulès` mining site (a and b), modified from Leblanc et al. (2002). Recent photos of AMD (c and d) and the junction between the Reigous creek and the Amous river (e).*

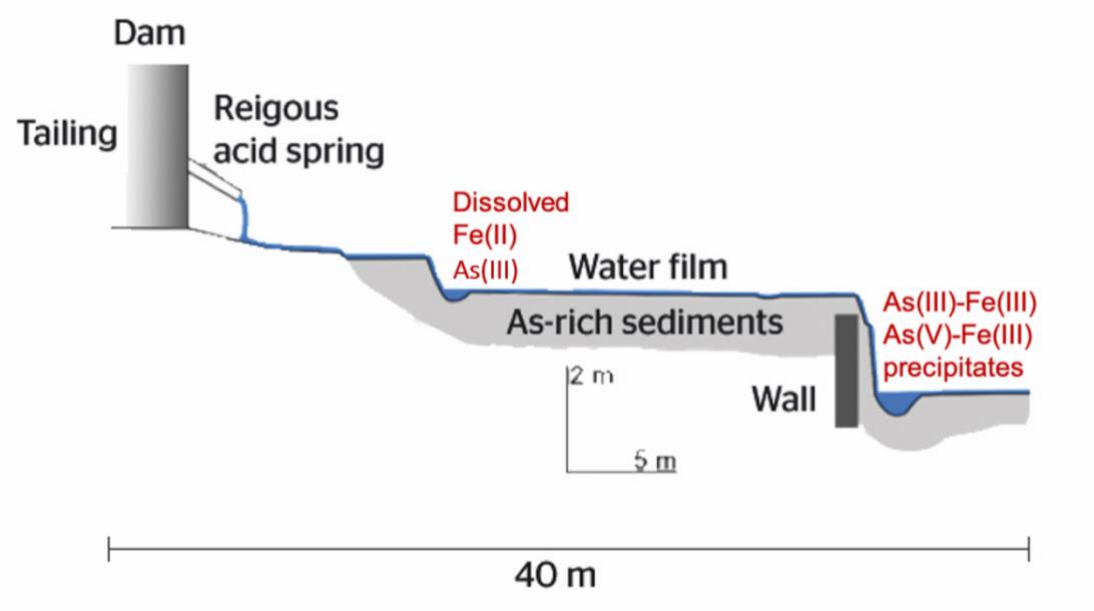

Figure 7. *Cross-section showing the 40 first meters of the Reigous creek. Modified from Casiot et al. (2003b)*

The role of the microorganisms on this natural attenuation process was investigated in the laboratory. The comparison of the rates of Fe and As oxidation in unsterilized - and sterilized - Reigous creek water showed that the oxidation was catalyzed by autochthonous bacterial community (Casiot et al. 2003a). Different strains of *A. ferrooxidans* from the Reigous were able to catalyze Fe(II) oxidation but the precipitates were mainly composed of jarosite and a poorly ordered phase (Duquesne et al. 2003). One bacterial strain of the genus *Thiomonas,* that includes some As-oxidizing representatives (Battaglia-Brunet et al. 2002b), was isolated from the Reigous Creek and was shown to oxidize As(III) into As(V) in the Reigous Creek water (Bruneel et al. 2003). Those arguments supported the major role of *Thiomonas* in the natural As attenuation in the Reigous creek (Bruneel et al. 2003).

The characterization of the microbial community of the Reigous was performed by different techniques such as cloning and sequencing of 16S rRNA gene fragments (Bruneel et al. 2006), metagenomics and metaproteomics (Bertin et al. 2011) and by high-throughput sequencing (Volant et al. 2014). The overall microbial diversity was relatively low compared with unpolluted environments. The most abundant metabolic group present in the AMD is FeOB, particularly OTUs affiliated to *Gallionella ferruginea* and *Acidithiobacillus ferroxidans*.

Volant et al. (2014) also evaluated the spatial dynamics of the bacterial communities along the Reigous creek; arsenic concentration, temperature and sulfate concentration were the main physiochemical drivers of bacterial dynamics. SRB were also present in the Reigous creek; adaptation to acid conditions and high As concentration is not a common feature within the SRB (Giloteaux et al. 2013). This was a prerequisite for subsequent developments of a treatment based on autochthonous SRB consortium, as reported elsewhere (Le Pape et al. 2017; Battaglia-Brunet et al. 2021). The eukaryotic community of the Reigous creek was also described; its structure was mainly driven by the As concentration in the sediment (Volant et

al. 2016). Eucaryotes released small organic molecules that may be used by the heterotrophic bacteria (Halter et al. 2012).

A prefectural decree in 2014 initiated several remediation actions by ADEME (The French Environment and Energy Management Agency) in 2016. They performed reclamation work on the tailings, rehabilitated the storm water collection system, reinforced the retaining wall, and installed a remote system to monitor dam stability.

Nowadays, the Reigous still transports permanently 50-100 mg/l As, 20 mg/l Zn and other metals (Pb, Tl, etc); its flow rate ranges between ~ 1 m^3/h and 5 m^3/h. In the sediments, there is still almost 3% As and high levels of Pb (2330 mg/kg) (Geoderis, 2019).

1.6 Previous treatment trials of Carnoulès AMD

Different trials were carrying out by HydroSciences Montpellier to treat the Carnoulès AMD based on biological Fe and As oxidation. These trials were conducted at different scales, under laboratory and field conditions.

1.6.1 Biological iron oxidation approach

1.6.1.1 Continuous flow laboratory bioreactor

A bench-scale continuous flow reactor fed with water from the Reigous creek (Carnoulès AMD) was used to determine the influence of operating conditions (HRT, water height) on the performance of the treatment based on biological iron oxidation (Fernandez-Rojo et al. 2017, 2018).
The bioreactor reached up to 65% of As removal and more than 80% of Fe(II) oxidation within 8h (Fernandez-Rojo et al. 2017). The water height affected the Fe(II) oxidation rate, in relation with variable oxygen transfer to the biofilm (Fernandez-Rojo et al. 2017). The formation of a floating film at low flow also decreased oxygen transfer and subsequent Fe(II) oxidation rate (Fernandez-Rojo et al. 2017). However, in conditions of low Fe(II) oxidation rate, arsenic was removed from the water by the precipitation of amorphous arsenate phase (AFA).

The HRT influenced Fe and As removal efficiency and the mineralogy of the biogenic precipitates, as expected, but also the structure of the bacterial community that settled in the bioreactor, especially the proportion of FeOB *Gallionella* and *Ferrovum* (Fernandez-Rojo et al. 2018). The highest removal rate obtained in the second series of experiments (Fernandez-Rojo et al. 2018) was lower than in the first series (Fernandez-Rojo et al. 2017). Such variable performances might be ascribed to the different solubility of the mineral phases that precipitate, As(III)-schwertmannite formed in the second series of experiments being more soluble than amorphous ferric arsenate formed in the first series.
The mineralogy of the precipitate was probably driven by the relative rates of As(III) and Fe(II) oxidation, as seen in batch experiments (Morin et al. 2003; Egal et al. 2009; Tardy et al. 2018; Garcia-Rios et al. 2020).

A geochemical model involving slow As(III) oxidation and fast Fe(II) oxidation allowed to correctly reproduce the evolution of aqueous and particulate As and Fe concentrations, identifying that the fast rates of Fe(II) oxidation favors the formation of As(III)-schwertmannite compared to low amount of AFA due to a slow microbial As(III) oxidation in the batch and continuous flow reactors treating AMD from the Carnoulès mine (Garcia-Rios et al. 2020).

1.6.1.2 Field-pilot

The first passive system that exploited biological Fe oxidation was installed *in situ* at the Carnoulès site between 1999 and 2002. However, its performances were not fully evaluated due to its destruction after a flooding event in 2002 (Elbaz-Poulichet et al. 2006). A second passive bioreactor was installed in 2017, it was based on five trays (1.5 m^2) connected in series and continuously fed with the Reigous creek water by gravitational flow. It was monitored during six months (Fernandez-Rojo et al. 2019).

This bioreactor provided highly variable As removal rates, from 4% to 97%, in relation to poorly controlled inlet flow. A low Fe removal rate ~ 11% was obtained, leading to the production of precipitates that contained up to 20% As (dry weight). The mineralogy of the precipitate varied throughout the experiment duration, with tooeleite formed during the first 48 days and then AFA. The increase of As(V) / total As ratio from 16 to 99% in the precipitate throughout time was interpreted as a probable increase of As(III) oxidation efficiency. The ecosystem established in this biological system was comparable to the one developed in the Reigous creek and in the laboratory, in terms of bacterial diversity and dominant taxa (Laroche et al. 2018). The main drivers of the bacterial community structure in the biogenic precipitates were temperature, pH, DO, Eh, total As concentration and Fe(II) concentration (Laroche et al. 2018).
In fact, the deficiency of inlet flow control, the clogging of the sand bed and insufficient oxygen supply using simple diffusion at the air/water interface limited the scope of the study. Indeed, the bioreactor design and operational conditions were not optimal to establish the limit of the treatment in this kind of bioreactor.

Altogether, the results obtained from these laboratory and field trials confirmed the potential of the iron oxidation bioreactor in the remediation of the As rich AMD. These trials showed that FeOB were the dominant groups in the microbial communities developed in the biogenic precipitates inside the bioreactors. Operational parameters such as the aeration, HRT and water height have an important impact in the structure of the bacterial communities and for consequence in the kinetic of the biological Fe oxidation and As removal. For instance, the increase in the relative abundance of the bacteria affiliated with the *Ferrovum* genus was associated with an increase in the remediation efficiency.
*Thiomona*s (2-3%) and the arsenite-oxidizing (*aioA*) gene were present in the biogenic precipitates, showing that arsenite-oxidizing genetic potential was present in the treatment system. However, there was no evidence of arsenite oxidation activity. The mineral phases identified to immobilize As from the AMD under the different conditions evaluated were either the As(III) schwertmannite, As(V) schwertmannite or amorphous ferric arsenate (AFA).

Furthermore, at the operational level, the results suggested that aeration and biofilm surface area were limiting factors for Fe and As removal yields (Fernandez-Rojo et al. 2017, 2019; Garcia-Rios et al. 2020).

1.6.2 Sulfate reduction bioreactor

Treatment based on Fe oxidation does not remove metals such as lead (Pb) and zinc (Zn), which are not adsorbed onto iron oxyhydroxides under acidic conditions. In this context, sulfate reduction appears to be a complementary solution to remove metals and As remaining in the Carnoulès AMD. Trials were carrying out to understand and optimize the operation of a sulfate-reducing bioreactor to treat the Carnoulès As-rich AMD. This complementary treatment is based on the sulfate reduction capacity of the microbial community and the consequent As and metals precipitation with the sulfurs, this principle is described in detail in the section 2.3.2. Particularly, for the treatment of the Carnoulès AMD Giloteaux et al. (2013) studied and described the sulfate reduction potential of the microbial community present in the sediments of the Reigous creek. Thus, the potential of the autochthonous microbial community coupled with the French geological survey (BRGM)'s experience allowed us to developed a prototype of treatment unit.

1.6.2.1 Bioreactor with synthetic AMD

The evaluation of a 300 mL bioreactor fed continuously with a synthetic solution was the first phase in the development of an efficient SRB bioreactor for high-As AMD (Battaglia-brunet et al. 2012). In this trial, a fixed-film column bioreactor was used and inoculated with a consortium of SRB sampled from mining sites and enriched in the laboratory; the treatment was evaluated for a synthetic solution at pH between 2.75 and 5.00 containing 100 mg/L As(V) and hydrogen and/or glycerol as electron donor. The highest sulfate reduction yields (from 1900 mg/L to 400 mg/L, i.e. 78%) were obtained with hydrogen as electron donor (Battaglia-brunet et al. 2012). Orpiment was the main mineral identified. The increase of the sulfate-reducing activity promoted the formation of thioarsenic species, which caused As remobilization. For that reason, the idea is to limit and have a better control of the rates of the SRB activity in future trials using simple electron donor such as the glycerol.

1.6.2.2 Batch experiments with Carnoulès AMD

A consortium of SRB enriched from the Reigous creek sediments was used in batch experiments to evaluate its potential to immobilize the As in the form of biogenic sulfide (Le Pape et al. 2017). This study showed for the first time complete As removal from the Carnoulès AMD by biological sulfate reduction. Arsenic was immobilized into amorphous orpiment, which transformed to AsIIS nanowires.

1.6.2.3 Continuous flow bioreactor

A fixed-film column bioreactors (300 mL) was monitored during 167 days under laboratory conditions to evaluate the As and Zn removal from the Carnoulès AMD by biological sulfate reduction (Battaglia-Brunet et al. 2021). Different operational phases were scheduled in order to test them in the treatment performances: i) feed the bioreactor with synthetic or real AMD, with or without pH adjustment, ii) HRT, and ii) two types of real AMD from Carnoulès, the

typical very acid one (pH 3.3) and another less acidic (pH 4) and less concentrated in As and metals. The selective precipitation of Fe, As and Zn into the corresponding sulfides was also evaluated.

pH influenced the microbial community structure, which has an impact on the glycerol degradation reactional path, leading to total or partial oxidation. However, there was not a direct link between the pH and the glycerol degradation path. Particularly in this laboratory trial the sulfide production was coupled to an incomplete degradation of glycerol that in consequence produced 2.3 times less H_2S than a complete oxidation (Battaglia-Brunet et al. 2021). This difference of the microbial community and finally the type of complete or incomplete glycerol oxidation have to be consider to adapt the concentration of glycerol, in order to avoid a decrease of the efficiency of the bioreactor. Using this bioreactor, the control of the concentration of the substrates (glycerol) resulted in a better control of the sulfate-reducing rate which in turn provided the selective precipitation of As and Zn while avoiding the precipitation of Fe. The pH of the treated water remained acid contrary to the previous test (Battaglia-brunet et al. 2012), in relation with the limited supply of electron donor.
Finally, a coupling test of the two bioremediation approaches was carried out under laboratory conditions.

1.6.2.4 Up-scaling under laboratory conditions.

The 0.3 L bioreactor was used as inoculum for up-scaling to 5 L. This new bioreactor was fed with Carnoulès AMD (Reigous water) and enriched with 0.5 g/L of glycerol and 1g/L yeast extract. It worked with HRT of 38 days during three months. The up-scaling was successfully achieved with complete As, Zn and Fe removal. Ninety percent less nutrient agar was used in the filling material compared to the previous tests.
Further up-scaling was done with a 25 L bioreactor. It worked during 4 months under laboratory conditions at different HRT (58, 29 and 14.5 days). The performance reached up to 99.9 % of As, Zn and Fe removal. The efficiency and robustness of this bioreactor under decreasing HRT values was further evaluated in field conditions, which is part of the present study (results section, Chapter 4).

1.6.3 Synoptic view of advances and locks

1.6.3.1 Biological iron oxidation approach

Study of the Reigous creek

+ Better comprehension of the natural attenuation process
+ Identify some key microorganisms in the Fe and As attenuation
- Identify the maximum As removal performance achievable
- Study how the seasonal variations in the mineralogy of precipitates can influence the efficiency/robustness of As attenuation

Batch test

+ Biological Fe/As oxidation kinetics influences the mineralogy of the precipitates (As(III)-schwertmannite/AFA)
+ Temperature and/or nutrients supply increase the As oxidation kinetics; organic matter supply could inhibit the Fe oxidation
- A floating biofilm formed lowered the oxygen concentration in the water column and had a negative effect on the FeOB activity
- Evaluate if the performances is achievable under continuous flow conditions

Lab. pilot-trial

+ Contributes to better understand the influence of operating conditions on Fe and As oxidation and precipitation
+ Optimized HRT/water height values to maximize As removal efficiency under continuous flow conditions and natural air diffusion (without forced aeration)
+ Stability of the key taxa (FeOB) responsible for biological Fe/ oxidation despite the changes in operating conditions

+ Under conditions of natural air diffusion (without forced aeration), water height above the precipitate is a limiting factor for the Fe oxidation and subsequent As removal

- Longer monitoring is required to evaluate the robustness toward physico-chemical variations

First Field-pilot trial

+ Scale-up of previous trial and robustness toward real physico-chemical variations of AMD chemistry throughout time
+ Feasibility of a passive Fe oxidation bioreactor to remove As
- Low Fe oxidation and precipitation performances
- Highly variable range for As removal
- Rapid clogging using sand as biomass carrier
- Reduced surface area for biofilm formation
- Additional steps are needed to precipitate more Fe and remove other cations Al, Pb, Cd and Zn

1.6.3.2 As removal by sulfate-reducing bacteria (SRB) approach

First step

Bioreactor fed with synthetic solution (fixed-film column)

+ Feasibility to remove As using sulfate-reducing bioreactor
+ Glycerol the most adapted electron donor to control reducing activity
+ Orpiment as main As scavenger formed in the bioreactor
- Verify feasibility with a real acid mine water

Second step

Bioreactor fed with Carnoulès AMD (Batch)

+ A consortium of SRB autochthonous already adapted to the conditions
+ Achievability to remove totally the dissolved As present in the Carnoulès AMD by a sulfate-reducing bioreactor.

Third step

Bioreactor fed with Carnoulès AMD (fixed-film column, evaluation of different combinations)

+ Semi-passive operation was identified as a most suitable option for a highly contaminated AMD
+ Comprehension of the removal dynamics between As and Zn
+ Identified the pH as an important driver in the microbial structure, or consequence in the glycerol oxidation
+ Selective precipitation avoiding the Fe precipitation
- Passive performance was not suitable at long-term
- The acid pH might reduce the efficiency of the Zn removal
- Lack of control in the total or partial glycerol oxidation
- pH of the treated water remained acid

Forth step

Up-scaling under laboratory conditions

+ Successful scaling, keeping total As and Zn removal
+ Reduced 90% of the nutrient agar
+ Stability of the treatment
- Long HRT (14.5 days)
- Verify feasibility and robustness at field conditions

Chapitre 2 : Performances des bioréacteurs semi-passifs à l'échelle des pilotes de terrain pour le traitement d'un DMA arsénié par oxydation

Introduction

La neutralisation par des produits chimiques est la méthode la plus couramment utilisée pour traiter du DMA (Sheoran and Sheoran 2006). Mais cette méthode a été identifiée comme une stratégie non durable à long terme (Igarashi et al. 2020). Ainsi, le développement de processus efficaces, peu coûteux et durables pour traiter ces effluents acides est nécessaire, notamment pour les mines abandonnées où l'utilisation de technologies coûteuses n'est pas possible. Les biotechnologies basées sur les processus biogéochimiques observés dans la nature peuvent être plus durables et rentables, notamment les processus intervenant dans des conditions passives ou semi-passives (Sato et al. 2018).

Un des processus d'atténuation naturelle observé dans les systèmes affectés par les DMA est l'oxydation biologique du fer et l'arsenic par une communauté bactérienne native, et l'incorporation de l'As dans les phases solides Fe-As (Leblanc et al. 2002; España et al. 2005a; Asta et al. 2010b; Park et al. 2016). Ces processus ont été observés dans différentes mines à travers le monde et sont désormais considérés comme la base d'une stratégie de biorémédiation (Gonzalez-Contreras et al. 2010; Ahoranta et al. 2016, 2020; Fernandez-Rojo et al. 2017; Xu et al. 2021). Cette stratégie de bioremédiation a fait l'objet de nombreuses études en laboratoire, mais il existe peu d'exemples d'application de ce processus à l'échelle du pilote de terrain pour traiter du DMA riche en arsenic.

L'objectif de ce chapitre est d'évaluer les performances de deux bioréacteurs installés *in situ* pour le traitement du DMA de Carnoulès. Ces bioréacteurs sont basés sur le processus d'atténuation naturelle décrit ci-dessus qui comprend la bio-oxydation induisant une co-précipitation du fer (Fe) et de l'arsenic (As). Ces bioréacteurs ont été conçus dans des conditions de fonctionnement optimisées (aération forcée, flux contrôlé et support bactérien poreux à grande surface spécifique) sur la base des expériences précédentes en laboratoire et sur le terrain (Fernandez-Rojo et al. 2017, 2018, 2019). Deux bioréacteurs ont été installés dans le but de comparer deux supports de biomasse (copeaux de bois/pouzzolane et plastique). Les bioréacteurs ont été surveillés pendant une période d'un an pour évaluer la robustesse du système par rapport aux variations temporelles de la physicochimie du DMA, du débit et des variations environnementales comme la température.

Afin d'évaluer l'efficacité du traitement pour le traitement de Fe et As, la caractérisation de l'influent et de l'effluent de chacun des bioréacteurs a été réalisée tout au long de l'opération, ainsi que la caractérisation des précipités biogéniques. La caractérisation comprend des mesures physico-chimiques, ainsi que des analyses minéralogiques et microbiologiques. L'interprétation de la chimie des eaux en entrée (DMA) et en sortie des deux bioréacteurs a été réalisée par modélisation géochimique CHESS (van der Lee et al. 2003).

Les recherches relatives à ce chapitre sont présentées sous forme d'un article publié dans la revue « Mine Water and the Environment ».

2 Article : Performance of Semi-passive Systems for the Biological Treatment of High-As Acid Mine Drainage: Results from a Year of Monitoring at the Carnoulès Mine (Southern France)

Mine Water and the Environment
https://doi.org/10.1007/s10230-022-00885-4

TECHNICAL ARTICLE

Performance of Semi-passive Systems for the Biological Treatment of High-As Acid Mine Drainage: Results from a Year of Monitoring at the Carnoulès Mine (Southern France)

C. Diaz-Vanegas[1,2] · C. Casiot[1] · L. Lin[3] · L. De Windt[4] · M. Héry[1] · A. Desoeuvre[1] · O. Bruneel[1] · F. Battaglia-Brunet[2] · J. Jacob[2]

Received: 2 August 2021 / Accepted: 10 June 2022

2.1 Abstract

Two semi-passive treatment systems for iron (Fe) and arsenic (As) removal in acid mine drainage (AMD) were installed and monitored *in situ* for more than a year. These technologies were designed to treat the As-enriched AMD (~ 1g/L Fe(II) and 100 mg/L As(III)) of the ancient Carnoulès mine. The treatment was based on biological Fe and As oxidation by indigenous bacteria, and subsequent immobilization of As by ferric hydroxysulfates. Forced aeration was used and wood/pozzolana or plastic support for biofilm attachment. The system performance ranged from 86 to 98% for Fe oxidation, 30 to 60% for Fe removal, and 50 to 80% for As removal at a hydraulic retention time of 9 h. No significant difference between the two biofilm supports were measured. The wood/pozzolana support had a shorter delay for performance recovery after interruptions. Iron oxidation rates were similar to those obtained in the Carnoulès AMD stream and laboratory bioreactor, while As oxidation seemed to be enhanced. The sludge accumulated between 39 and 91 mg/g of As, mainly in the As(V) oxidation state; jarosite and amorphous ferric hydroxysulfate phases were the main Fe and As scavengers. Challenging environmental conditions during the long period of monitoring confirm the robustness of the treatment units. The data will be useful in the future design of full-scale treatment systems adapted to As-rich AMD.

Keywords Mine waste water, biological arsenic oxidation, biological iron oxidation, bioremediation, field-pilot

2.2 Introduction

Mining activities can adversely affect water resources for decades after mine closure and decommissioning (Neculita et al. 2007; Neiva et al. 2016). The associated oxidation of sulfide minerals and release of acid mine drainage (AMD) into the environment may cause the remobilization of toxic elements such as arsenic (As), contaminating water resources and strongly affecting aquatic ecosystems (Nordstrom and Alpers 1991; Paikaray 2015). In AMD, the two predominant inorganic As species are arsenite As(III) and arsenate As(V); the reduced As(III) form is more mobile than oxidized As(V) due to lower retention on solid phases (Tsai et al. 2009). Thus, the predominance of As(III) upon As(V) in some AMD streams further complicates their treatment (Mondal et al. 2006). Despite the threat represented by As-rich AMD to ecosystems and human health, the treatment of these waters remains challenging, especially at high As concentrations (Whitehead et al. 2005).

Nowadays, active chemical treatments such as lime neutralization are the most common strategies implemented *in situ* to treat AMD (Wang et al. 2018). The main disadvantages of these chemical neutralizations are their cost, the accumulation of large quantities of polluted sludge, and a labor-intensive maintenance (Habe et al. 2020). In general, chemical neutralization alone has been identified as unsustainable strategy in the long term (Igarashi et al. 2020). Thus, the development of affordable, effective, and ecological processes to handle these acid effluents is particularly needed, especially for abandoned mines where the use of expensive technologies is not possible. Passive and semi-passive biotechnology based on biogeochemical processes observed in nature can be more sustainable and cost-effective (Sato et al. 2018).

Iron and arsenic bio-oxidation and subsequent mineral precipitation catalyzed by native microorganisms has been reported as potentially suitable strategy to remove As and Fe from AMD for abandoned mines (Ahoranta et al. 2016; Chen and Jiang 2012; Elbaz-Poulichet et al. 2006; Fernandez-Rojo et al. 2017; Leblanc et al. 2002; Majzlan et al. 2007; Paikaray 2015). The iron bio-oxidation process induces the precipitation of ferric hydroxysulfate minerals that can adsorb or co-precipitate the dissolved As (Majzlan et al. 2016). This process promotes As immobilization by formation of poorly crystalline and/or amorphous phases such as schwertmannite, ferrihydrite, goethite, tooeleite, and amorphous ferric arsenate (Asta et al. 2010a; Carlson et al. 2002). This strategy is based on a natural attenuation process observed and studied in different AMD streams around the world, such as the Iberian pyrite belt in Spain (Asta et al. 2010b) and Reigous Creek (Carnoulès mine) in France (Egal et al. 2010; Morin et al. 2003).

The Carnoulès arsenic-rich AMD gave rise to the Reigous Creek and has been the target of several studies that aimed to develop an *in situ* bioreactor to optimize the natural As attenuation process (Bruneel et al. 2003; Casiot et al. 2003; Elbaz-Poulichet et al. 2006; Fernandez-Rojo et al. 2019; Laroche et al. 2018; Tardy et al. 2018). The relevance of this case study is based on the site's challenging conditions, with high and variable As concentration between 50 and 100 mg/L, mainly in the reduced As(III) form, acid pH (3.2-5), and Fe concentration ranging from 500 to 1000 mg/L. The site, which is located in a small valley, and the climate conditions

with periodic heavy rainfall, makes it difficult to install and operate treatment facilities (Elbaz-Poulichet et al. 2006).

Experimental and modelling results of batch and flow-through experiments have shown that aeration and biofilm surface area were factors limiting Fe and As removal yields in the treatment of high-As AMD by biological oxidation in our previous laboratory and field pilots (Fernandez-Rojo et al. 2017, 2019; Garcia-Rios et al. 2021). Attempts to increase the surface area of the biofilm using river sand as bacteria growth support in a fully passive field-pilot resulted in rapid clogging. Moreover, the supply of oxygen by simple diffusion at the surface of the thin water film was not sufficient, which dramatically decreased Fe(II) oxidation and provided irregular As removal (Fernandez-Rojo et al. 2019). The use of active aeration and a bacteria growth support with a larger porosity were identified as key elements in the design of future field pilot experiments.

In continuity with these previous laboratory and field pilot experiments, the present study was aimed at: (i) evaluating the on-site performance of a scaled up pilot for biological treatment of high-As AMD (> 50 mg/L of As(III)), under optimized operating conditions (forced aeration, suitable bacterial support, controlled flow rate), and during one-year monitoring period; the treatment was based on biological Fe oxidation mediated by a native microbial community, and As incorporation into Fe-As solid phases, (ii) comparing two bacterial growth support media, and (iii) evaluating the robustness of the system with respect to temporal variations of AMD physicochemistry, flow, and different environmental conditions.

2.3 Methods

2.3.1 Set-up and Operation

Two field-scale systems for the biological oxidation were installed downstream of the Carnoulès tailings dam (southern France) in July 2019. Each system consisted of a 1 m^3 plastic tank filled with different substrate materials (Figure 8). At the bottom of each tank, a grid with a mesh size of 19 mm was installed that retains the bacteria substrate in the upper part of the tank to reduce the risk of potential clogging of the outlet pipe. Two air diffusers providing aeration at around 300 L/h were installed beneath the grid for each tank. The devices were supplied with the same AMD from Reigous Creek by a continuous flow mechanism controlled by peristaltic pumps.

One device was filled with 6.5 kg of plastic support (Biofill®, Type A) and the other was filled with 174 kg of 80 wt% pozzolana (pozzolanic ash) and 20 wt% wood chips (pine bark sized 20–40 mm, Jardiland®) mixture. The plastic support has been used as a standard in biological water treatments, due to its high porosity (96%), specific surface area (> 160 m^2/m^3), and irregular shape, which allows an optimal biofilm development without clogging problems. The wood/pozzolana mixture has a larger specific surface area (333 m^2/m^3), but a lower porosity (64%). This mixture has been used previously in passive AMD treatments and has demonstrated good hydraulic properties at low-cost (Rötting et al. 2008b).

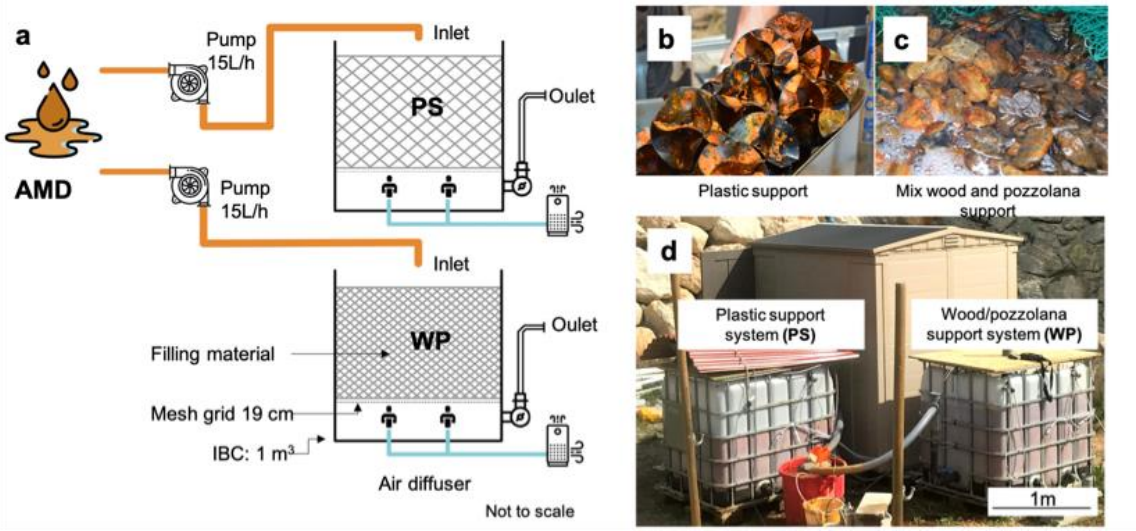

Figure 8. *Schematic representations of the biological oxidative devices, one device filled with a plastic support (PS) and the second device filled with pozzolana and wood mixture (WP (a), plastic support (b), wood and pozzolana mixture support (c) and in situ devices (d).*

The two units were supplied with AMD during seven periods (Figure. 9): A, B, C, D, E, F, and G from July 2019 to September 2020. The flow rates were set to 15 or 30 L/h, which corresponds to hydraulic retention times of 17.5 and 8.7 h for the unit with the plastic support (PS) and 19.3 and 9.7 h for the unit with the wood/pozzolana support (WP). The operational phases were determined by changes in flow rate and flow interruptions as well as operational and technical issues. Power supply for the units was changed from a generator to an electrical connection, while pump maintenance and a Covid-19 lockdown period interrupted the intervals.

In July 2020 (Period F), clogging of the air diffusers occurred in both units due to the accumulation of a yellowish precipitate in the bottom of the tanks. The air diffusers started working properly again after maintenance in September (Period G).

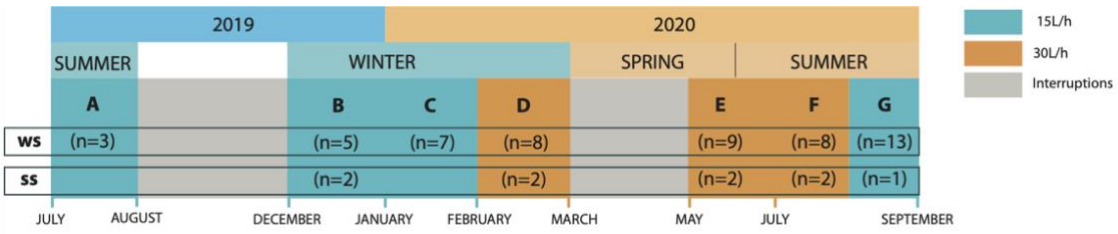

Figure 9.*Timeline of the operation and monitoring of PS and WP treatment devices including, seven periods distributed across seasons, undesired interruptions. The number (n) of water samples (WS) and sludge samples (SS) taken in each period are also indicated.*

2.3.2 Water Sampling and Characterization

Water samples were collected two to three times per week at three sampling points: 1) device inlet with the wood/pozzolana support (which was also representative of the inlet water feeding the device with plastic support), 2) device outlet with wood/pozzolana support, 3) device outlet

with plastic support. Sludge samples were taken every two weeks on the first ten centimeters inside each unit. The number of sampling campaigns are indicated in Fig.2: 3 times during period A, 5 times during period B, 7 times during period C, 8 times during period D, 9 times during period E, 8 times during period F and 13 times during period G.

The water samples were preserved and characterized according to the routine procedures described in Fernandez-Rojo et al. (2017). They were split in two sub samples for *in situ* and lab measurements. The *in situ* physicochemical measurements were conducted using a Hach HQ40D portable multi-meter (i.e. temperature, pH, redox potential, electrical conductivity, and dissolved oxygen concentration). 500 mL of the second subsample was filtered using 0.22 µm cellulose filters. Then the sample was immediately distributed in different aliquots; one aliquot was diluted in 1% HNO_3 solution (Suprapur quality) for major and trace element analysis, another one was diluted in acetate/acetic acid buffer (pH 4.5) and 0.05% (w:w) phenanthrolinium chloride solution for ferrous iron concentration determination and a third one was added acetic acid (0.087 M) and EDTA (0.5 g/L) for redox As speciation analysis. The samples were temperature stabilized at 4°C and treated according to the appropriate protocols for specific chemical analysis.

The ferrous iron Fe(II) concentration was quantified by colorimetry using the ortho-phenanthroline method by absorbance at 510 nm with a JENWAY 6320D spectrophotometer (detection limit = 88 µg/L, accuracy = ± 5%). For the major and trace elements determination including total Fe and As concentrations, the samples were analyzed by inductively coupled plasma-mass spectrometry (ICP-MS; Thermo X7 Series) at the AETE-ISO platform, University of Montpellier (France). An external calibration with internal standard correction procedure and international certified reference waters (CNRC SLRS-5, NIST SRM 1643e) were used for quality control.

Samples for arsenic speciation (As(III) and As(V) proportions) were analyzed by anion-exchange chromatography (25 cm, 4.1 mm inner diameter Hamilton PRP-X100 column) using a Spectra Device SCM1000 solvent delivery pump coupled to an ICP-MS.

2.3.3 Sludge and Suspended Particulate Matter (SPM) Characterization

The precipitate formed during the treatment periods accumulated as sludge onto the filling material, while a small amount was transported with the treated water flow as suspended particulate matter (SPM) in the effluent. Both kinds of solids were analyzed, leading to a total of 9 sludge samples and 11 SPM samples collected at the three monitoring points (influent, PS effluent and WP effluent) at least once for each period of operation.

The SPM fraction was recovered by filtration on cellulose filters (0.22 µm) at the outlet drain of each reactor. After each sampling campaign, the filters were dried under vacuum and stored for further analysis. Sludge sub-samples were centrifuged and dried in a glove box under nitrogen atmosphere for subsequent As speciation analysis and mineralogical characterizations. Total Fe and As concentrations in the sludge were determined by ICP-MS after acid digestion, while As speciation in the sludge and SPM was determined by HPLC-ICP-MS after an extraction using orthophosphoric acid (1M, 85%; Resongles et al. 2016).

Mineral characterization was performed by X-ray powder diffraction (XRD) analyses, using the Co K-α radiation of a Malvern-Panalytical Empyrean diffractometer. Data were collected in continuous mode between 5 and 100°2θ with a 0.026°2θ step, counting around 4 h per sample.

2.3.4 As and Fe Distribution in the Colloidal Fraction

Two water samples in period B and one sample in period E were collected from each of the three sampling points and filtered on-site using 0.22 µm cellulose filters. The filtrates were transported in a cool box to the laboratory within 4 h after collection and then filtered using Vivaspin® 20 Ultrafiltration units. A 100 KDa cutting diameter was used for samples in period B. A 10 KDa cutting diameter was used for samples in period E. The ultrafiltration was done in duplicate; the protocol included centrifugation for 5 minutes at 5000 g. Afterwards the filtrated water was analyzed according to the following speciation: Fe(II), total Fe, As(V), As(III), total As.

2.3.5 Relevant Calculations

The HRT was calculated based on the waterbed volume (L) divided by the input flow rate (L/h). The waterbed volumes of the PS and WP units were 260 and 290 L, respectively. These theoretical HRTs were used to calculate the Fe(II) oxidation rates as well as Fe and As precipitation rates (in mol L^{-1} s^{-1}). Fe(II) was present only in the dissolved phase while Fe(III) was present both in dissolved and particulate phases. Thus, the rate of Fe(II) oxidation was calculated for each device from the decrease of Fe(II) concentration between influent and effluent, according to the following equation:

$$\boldsymbol{rFe(II) = \frac{[Fe(II)]_{inlet} - [Fe(II)]_{outlet}}{(HRT)}} \quad \textbf{Equation 16}$$

where $[Fe(II)]_{inlet}$ was the dissolved Fe(II) concentration measured at the inlet of the units. $[Fe(II)]_{outlet}$ was measured at the outlet of the PS or WP units. The rate of Fe and As precipitation was calculated accordingly, by using the total dissolved (<0.22 µm) Fe and total dissolved As concentrations measured by ICP-MS. The rates were calculated using the concentration values from the stationary phase for periods A, B, C, D, E, and G (except for period F, all data were used). The stationary phase for each period was defined when the performance did not change by more than 10%. For instance, the PS system needed between 5 to 10 days to reach it, while the WP system reached this stationary phase in the first five days.

As(III) and As(V) co-exist both in dissolved and particulate phases. Calculation of the rate of As(III) oxidation was carried out using a mass balance calculation for each unit (see Supplemental Calculation S-1). The mass balance used the concentration of dissolved and particulate As(III) and As(V) species in the inlet and outlet water samples, together with the amount of As(III) and As(V) retained in the sludge and SPM.

For biological Fe(II) oxidation, a first-order kinetic constant $k_{Fe(II)Field}$ (Larson et al. 2014) was also calculated to compare the unit performances with other studies. The general reaction for biological iron oxidation considered in the present study was:

$$Fe^{2+} + 0.25O_2(aq) + H^+ \rightarrow Fe^{3+} + 0.5H_2O \qquad \textit{Equation 17}$$

This first order kinetic law assumes that the Fe(II) oxidation rate is dependent on the dissolved Fe(II) concentration:

$$kFe(II)_{field}\ (min^{-1}) = \frac{-Ln(\frac{[Fe(II)]_{diss.Outlet}}{[Fe(II)]_{diss.Inlet}})}{HRT*60} \qquad \textit{Equation 18}$$

$[Fe(II)]_{diss.Inlet}]$ corresponds to the dissolved Fe(II) concentration at the inlet of the devices, $[Fe(II)]_{diss.Outlet}]$ is expressed as the dissolved Fe(II) concentration of the PS and WP effluents, and HRT (h) defines the hydraulic retention time calculated for each unit in each period. This simple rate law was preferred to the fourth order kinetic rate law used by Pesic et al. (1989) and Sheng et al. (2017) in controlled laboratory experiments; those authors considered the parameters Fe(II) concentration, oxygen concentration, pH, and bacterial cell concentrations. Here, it was not possible to establish a fourth order kinetic rate law in the field conditions of the present study. The range of variation of inlet water pH was relatively narrow, aeration promoted fully oxygenated conditions, and it was not possible to quantify Fe-oxidizing bacterial cell counts among the whole autochthonous bacterial community.

2.3.6 Statistical Analysis

Data were analyzed by the non-parametric Mann-Whitney test for significant performance differences in the two support substrates. The Pearson test was used to evaluate the correlation between independent variables; the p-values were obtained at the level of $p < 0.05$. The statistical analyses and graphs were performed with the free R software (http://www.r-project.org/), version 1.2, using the tidyverse and vegan packages and XLSTAT.

2.3.7 Geochemical Model and Thermodynamic Data

The saturation indices (SI) of As and Fe solid phases with respect to the inlet/outlet water chemistry were calculated with the geochemical module CHESS of the HYTEC code (van der Lee et al. 2003) using the truncated-Davies activity correction model and the thermodynamic database (Blanc et al. 2012) version of 2017. The Fe(III)/Fe(II) and As(V)/As(III) oxidation state couples were decoupled from the calculations. Two additional data sets were considered for the sake of consistency with a previous modeling study of lab experiments on Carnoulès AMD microbial treatment (Garcia-Rios et al. 2021). The thermodynamic constants of an amorphous Fe(III)-arsenate (AFA) was adjusted on the batch and flow-through data. The thermodynamic constant of a more soluble and hydrated form of schwertmannite (Sánchez-España et al. 2011) was found to better fit the same experimental data than the original Thermoddem equilibrium constant.

SI values are good indicators for estimating the saturation state of complex aqueous solution such as the present AMD waters vs. mineral reactivity. SI values between -0.5 and 0.5 mean that the solid phase is close to thermodynamic equilibrium. A positive SI value indicates that the solution is oversaturated and that the solid phase can precipitate from the solution. A

negative SI means that the solid phase cannot precipitate but can possibly dissolve if in contact with water.

2.4 Results

2.4.1 Aqueous Chemistry

Variations of the main physicochemical parameters of the water at the inlet and outlets of the treatment units are presented in Figure 10. and supplemental Table S-1. The inlet revealed a pH range from 3.2 to 5.1 along one year of operation (Figure 10.a). Those values systematically decreased to 2.8 ± 0.3 on average through the PS and WP units (Figure. 10.a). The temperature of the inlet water showed some variability across seasons. Recorded temperatures during summer obtained an average value of 24 ± 4°C and a maximum of 27°C in periods A, F and G, whereas recorded temperatures during winter times were obtained with an average around 12 ± 3°C, and a minimum temperature of 5°C in periods B and C (Figure 10.b). The variation between the inlet and outlets was no more than 6°C (Figure 10.b, supplemental Table S-1). The conductivity at the inlet ranged from 2300 to 4270 µS/cm, with the highest values during summer (periods A, F and G) and the lowest during winter (B and C). It decreased by no more than 20% between inlet and outlets (Figure S-1). The average dissolved oxygen (DO) concentration at the inlet ranged between 6 ± 2 mg/L, and showed high variability (high SD values) within each period (Figure 10.c). It increased between inlet and outlets in periods B, C, and D while it did not significantly change in periods A, E, F, and G. Discrete DO measurements were made in the middle of the reactor bed. These DO values were similar to those in outlet water in periods B and C, but were lower in periods D and F in both WP and PS units. This lower DO levels marked a time period when consumption exceeded oxygen supply in the reactor bed.

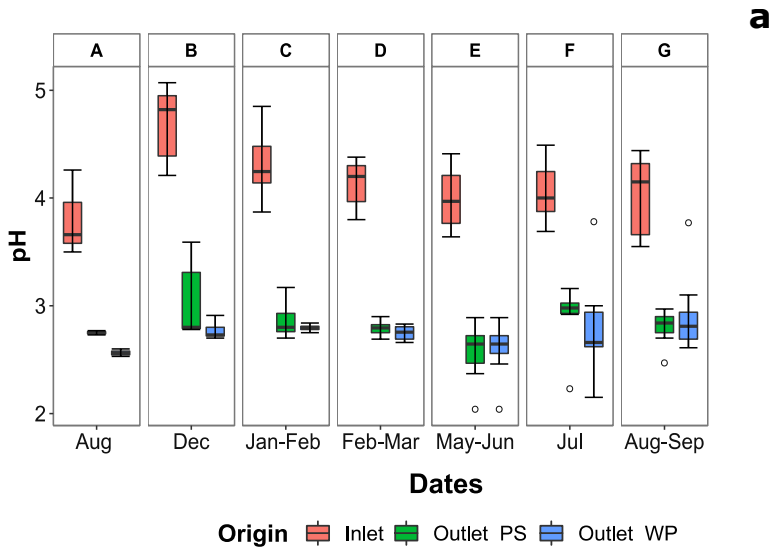

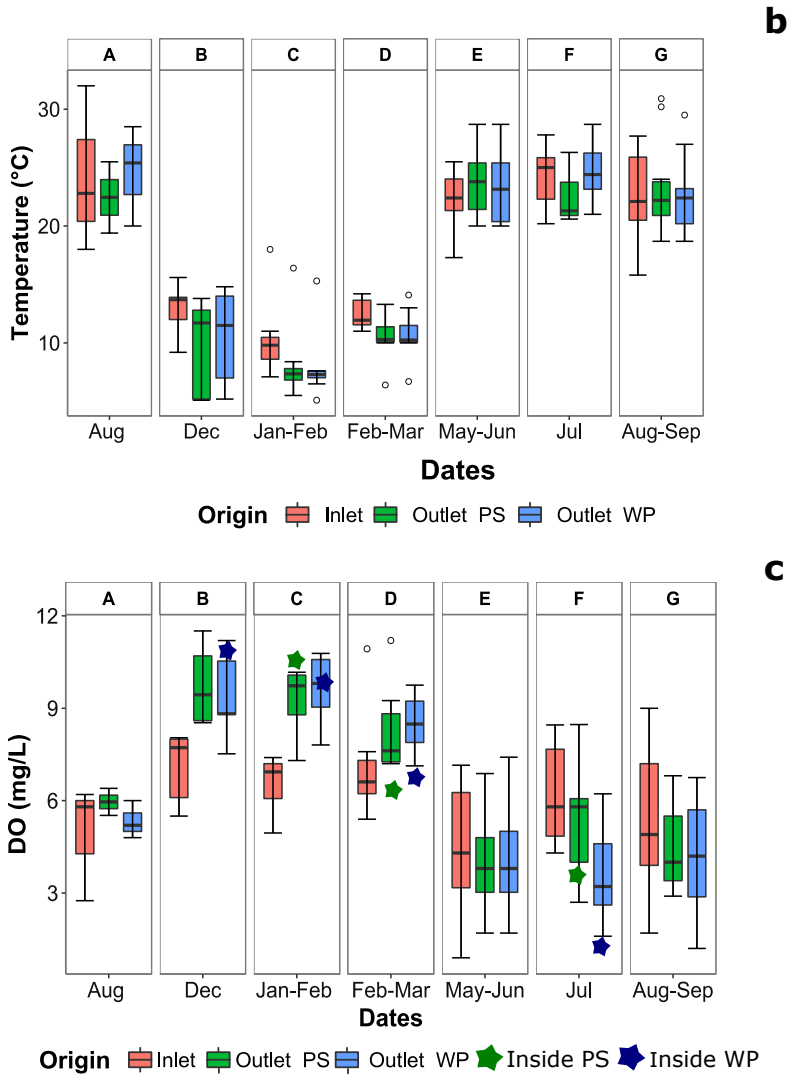

Figure 10. *Boxplot representation of the main physicochemical parameters measured in the inlet water and in the outlet water from the PS and WP devices during seven periods of monitoring, pH (a), temperature (b) and dissolved oxygen concentration (DO) (c). The dot (.) represents the outliers. The inlet flow used for the different periods were 15L/h for A, B, C and G while 30L/h for D, E and F.*

2.4.2 Dissolved Iron Concentrations (Total Fe and Redox Species)

Total dissolved Fe concentration, i.e. the sum of dissolved Fe(II) and dissolved Fe(III) in the inlet water, ranged from 300 to 1000 mg/L. The highest concentrations correlate with droughts during summer time (A, E, F and G periods, Figure 11.a). The total dissolved Fe concentration decreased by 20% to 70% between inlet and outlets for most periods (A–E), except period F and early period G.

Ferrous iron concentrations dominated compared to Fe(III) in the inlet water, representing about 90% of the total dissolved Fe (Figure 11.a and 11.b). As indicated in Figure 11.b, the Fe(II) concentration at the inlet decreased from period A (Jul. 19) to period B (Dec. 19) and then gradually increased until period F (Jul. 20). The Fe(II) concentration then decreased between inlet and outlets (Figure 11.b) while the Fe(III) concentration increased (Figure 11.c), indicating the oxidation of Fe(II) in both units. For the PS unit, the Fe oxidation efficiency

varied from 60% to 98% in periods A–E, while it always exceeded 90% in these periods in the WP unit. Interruptions of operability occurred in both units between periods A and B and between periods B and C, which led to a temporary decrease of Fe oxidation rate down to 50% in PS unit during the first ten days after restart (Figure 11.b and 11.c) while the WP unit recovered its efficiency shortly (in 3 to 5 days). In period F, outlet Fe(II) concentrations increased substantially in both units, and outlet Fe(III) concentration decreased (Figure 11.b), confirming a decreased Fe oxidation efficiency during the time period when the air diffusers were clogged. After maintenance of the aeration system in late period G, outlet Fe(II) concentrations steeply declined, reflecting a recovery of unit performances.

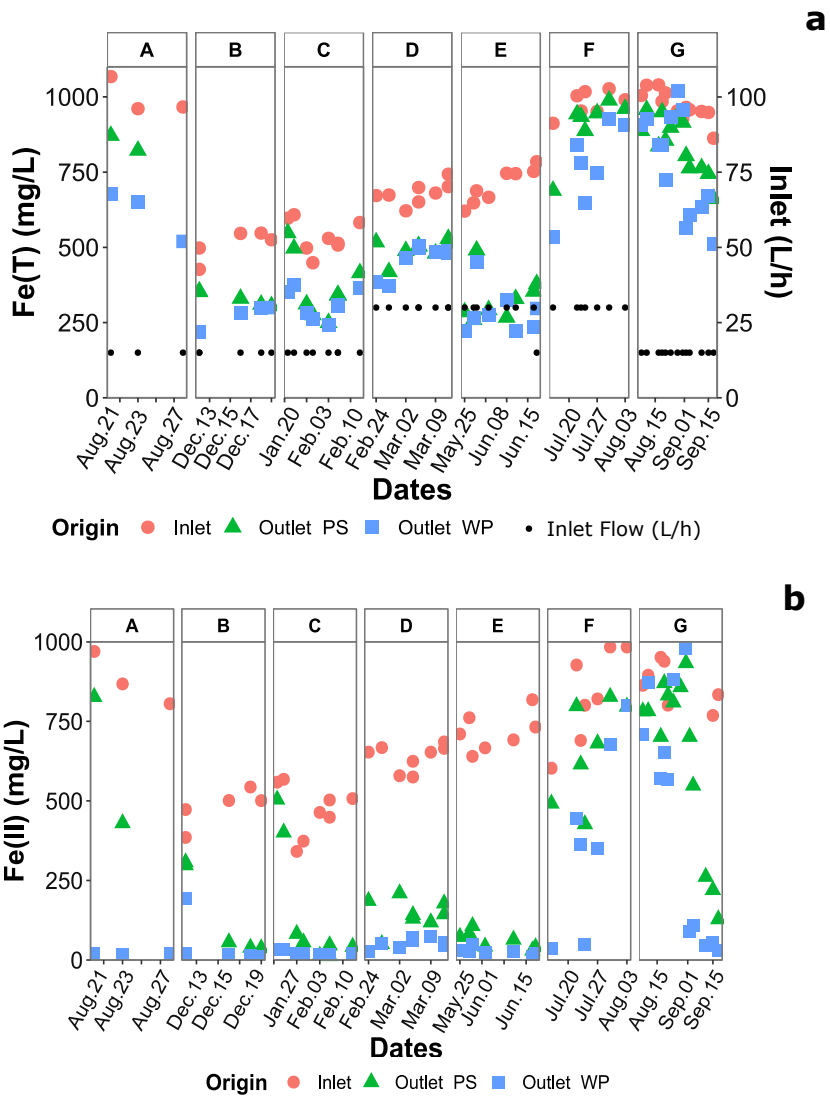

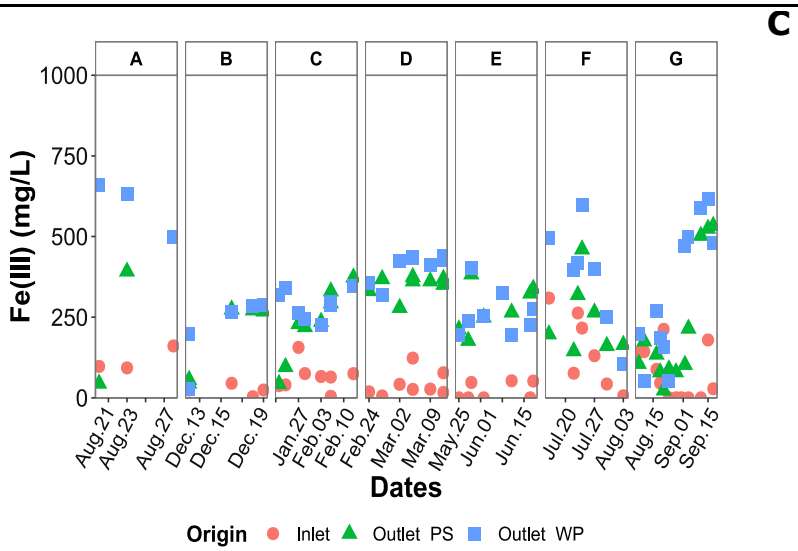

Figure 11.*Variations of the dissolved iron concentration at the inlet and outlet sampling points, for the device with plastic support (PS) and wood/pozzolana support (WP). Total dissolved iron (Fe Total) (a), ferrous iron (Fe(II)) (b) and ferric iron (Fe(III)) (c). Data collected during seven periods of monitoring: A* (Jul.–Aug.19), *B (Dec.19), C (Jan.–Feb.20), D (Feb.–Mar.20), E (May–Jun.20), F (Jul.–Aug.20) and G (Aug.–Sep.20). The inlet flow used for the different periods were 15L/h for A, B, C and G while 30L/h for D, E and F represented with black dots in Figure 11a.*

2.4.3 Dissolved Arsenic Concentrations (Total As and Redox Species)

Total dissolved As concentration at the inlet varied across the seasons concomitantly to total dissolved Fe concentration (Figure 12.a). It increased from 40–70 mg/L during the colder and rainy periods (B, C and D) to 80–100 mg/L during hot periods accompanied by draughts (A, E, F and G). As(III) represented 75±5% of total dissolved As at the inlet (Figure 12.b).

Total dissolved As concentration decreased to a minimum of 10 mg/L at the outlets *sampling points* for both PS and WP units during periods B, C, E, G, which corresponded to a 50–80% As removal (Figure 12.a). Both As(III) and As(V) concentrations exhibited a decrease between inlet and outlets (Figure 12.b and 12.c). Outlet As(V) concentration punctually exceeded its inlet value in periods A, E and G (Figure 12.c).

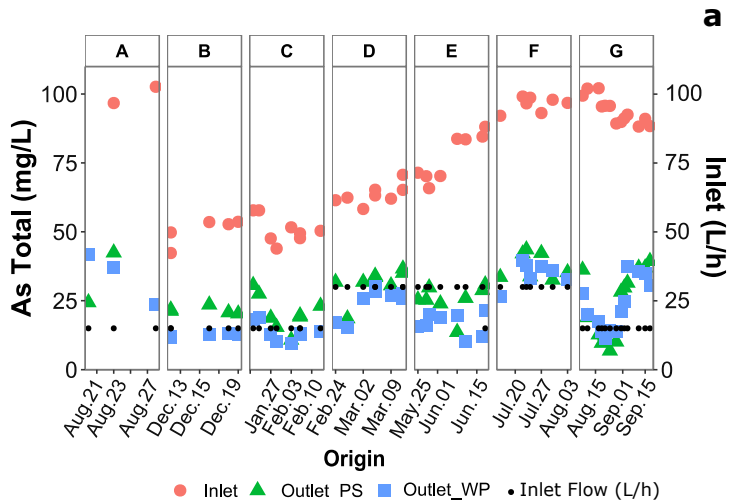

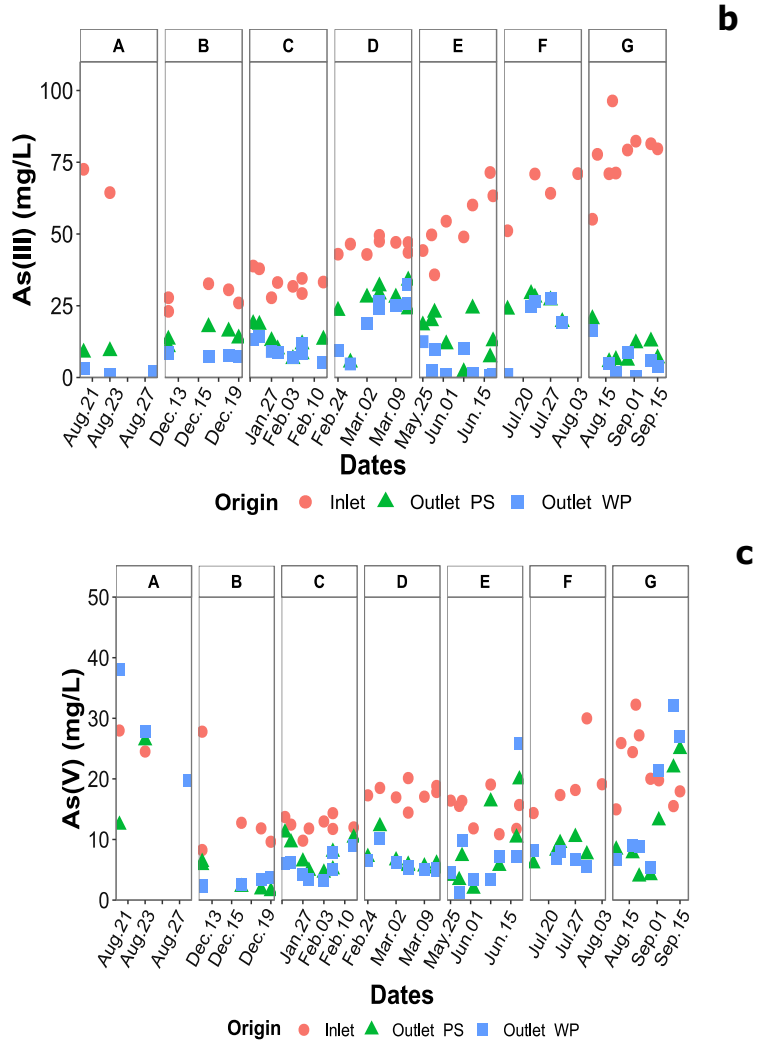

Figure 12. *Variation of the concentration of a) total dissolved (As Total), b) arsenite (As(III)) and c) arsenate (As(V)) at the inlet and outlet sampling points for the device with plastic support (PS) and wood/pozzolana support (WP) during the different periods of operation. The inlet flow used for the different periods were 15L/h for A, B, C and G while 30L/h for D, E and F represented with black dots in Figure 12.a.*

2.4.4 Rates of Fe and As Oxidation and Precipitation

The rates of Fe and As oxidation and precipitation in each period (Table 6, supplemental Figures S-2, S-3, and S-4) were calculated under stationary phases (~ 10 days after restart) for each unit. The rate of Fe (II) oxidation ranged from 0.8 $\times 10^{-7}$ to 3.3 $\times 10^{-7}$ mol L^{-1} s^{-1} (Table 6, supplemental Figure S-2); it was nearly two times lower for Fe (III) precipitation, from 0.4 $\times 10^{-7}$ to 2.1 $\times 10^{-7}$ mol L^{-1} s^{-1} (Table 6, supplemental Figure S-3) and one order of magnitude lower for As precipitation, from 0.7 $\times 10^{-8}$ to 2.6 $\times 10^{-8}$ mol L^{-1} s^{-1} (Table 6, supplemental Figure S-4). The highest rate values for Fe oxidation and precipitation were observed in period E, compared to the highest rate values of As precipitation that were reached in periods E and F (Table 6, supplemental Figure S-2 and S-4). In periods B to E, As removal rate correlated well to the rate of Fe precipitation (r^2 =0.98; Fig. S-5) and also to inlet water As concentration (r^2 =0.89; supplemental Fig. S-6). The As/Fe molar ratio in the precipitate, calculated from As and

Fe removal, averaged 0.13. Such dependency implies a control by As sorption or incorporation into Fe minerals. A similar kinetic dependency was reported by Asta et al. (2010) in AMD from the Iberian Pyrite Belt. In periods F and G, the As removal rate was not correlated to the rate of Fe precipitation; the As/Fe molar ratio exceeded 0.2 due to slower Fe removal (Figure S-7).

Mass balance calculations using dissolved and particulate As speciation data (Figure 12b, 5c; Table 2) provided an estimation of As oxidation rate in each unit (Table 6). This calculation was based on the assumption that SPM in outlet water reflected the composition of the precipitate that forms at the time of outlet water sampling. The estimation of As oxidation reached its maximum rate (10^{-8} mol L^{-1} s^{-1}) during periods F and G for both units, while during periods B and D, the As oxidation rates were both below the detection limit (< 0.5 ×10^{-8} mol L^{-1} s^{-1}). Thus, depleted aeration conditions in periods F and G were not a limiting factor for As oxidation in the units.

Under steady state conditions and optimal performances of the aeration system (periods A-E), the average rates of Fe oxidation and precipitation, and arsenic precipitation were statistically similar for the WP and PS units (p-value > 0.05, Mann-Whitney); however, if the surface area is considered for each support substrate (28 m^2 for the PS unit, 54 m^2 for the WP unit), the maximum precipitation rates in grams of Fe and As precipitated per m^2 of support substrate and per day were twice as high for the PS unit (20.2 g m^{-2} d^{-1} for Fe oxidation, 12.4 g m^{-2} d^{-1} for Fe precipitation and 2.1 g m^{-2} d^{-1} for As precipitation) than for the WP unit (10.8 g m^{-2} d^{-1} for Fe oxidation, 6.99 g m^{-2} d^{-1} for Fe precipitation and 1.09 g m^{-2} d^{-1} for As precipitation).

Table 6 *Rates of Fe oxidation, Fe precipitation, As oxidation and As precipitation (x10^{-7} mol $L^{-1}s^{-1}$) for the PS and WP treatment devices under stationary phases in each period. Average (standard deviation, STD).*

	Fe oxidation		**Fe precipitation**		**As oxidation**		**As precipitation**	
	PS	WP	PS	WP	PS	WP	PS	WP
A	0.8 (0.6)	2.2 (0.2)	0.5 (0.1)	1.0 (0.2)	NA	NA	0.15 (0.05)	0.13 (0.02)
B	1.3 (0.1)	1.3 (0.1)	0.64 (0.03)	0.63 (0.05)	< 0.05	< 0.05	0.070 (0.004)	0.080 (0.001)
C	1.3 (0.1)	1.1 (0.2)	0.6 (0.2)	0.56 (0.09)	NA	NA	0.07 (0.01)	0.07 (0.01)
D	2.8 (0.2)	3.0 (0.2)	1.0 (0.2)	1.1 (0.3)	< 0.05	< 0.05	0.13 (0.01)	0.15 (0.02)
E	3.3 (0.1)	3.3 (0.7)	2.1 (0.7)	2.1 (0.6)	< 0.05	0.1	0.22 (0.01)	0.22 (0.05)
F	0.9 (0.5)	2 (1)	0.4 (0.4)	0.9 (0.5)	0.08 (0.02)	0.1 (0.06)	0.26 (0.04)	0.24 (0.05)
G	1.8 (0.4)	2.2 (0.3)	0.56 (0.02)	0.83 (0.09)	0.1	0.1	0.11 (0.01)	0.100 (0.004)

NA: not available data, <0.05 x10-9 defined as quantification limit for the As oxidation estimation. The inlet flow used for the different periods were 15L/h for A, B, C and G while 30L/h for D, E and F

2.4.5 Suspended Particulate Matter in Outlet Water

The amount and composition of the particulate phase in outflow effluents were determined (Table 7). The concentration of SPM ranged from 2 to 124 mg/L. Particulate Fe represented a maximum of 4 wt.% of total (dissolved + particulate) Fe concentration and particulate As

represented a maximum of 8% of total (dissolved + particulate) As concentration (Table 7). Thus, this amount of particulate As flowing out of the unit is substantial. In the fraction below 0.22 µm, the colloidal Fe and As fractions (> 100 kDa, measured in period B) represented a maximum of 2% of total (dissolved + particulate) Fe concentration and 9% of total As concentration (Table S-1). Ultrafiltration at 10 kDa (measured in period E) indicated the presence of fine colloids that accounted for up to 32% of total (dissolved + particulate) Fe and 68% of total As. The occasional presence of colloidal Fe and As in the outflow fluid may reflect a rapid formation process. Colloid formation might have occurred directly in the fluid phase rather than at the surface of the biofilm due to specific gradients and oversaturation.

The As/Fe molar ratio in SPM (> 0.22 µm) varied from 0.02 to 0.3 in periods B to E; it increased up to 0.9 in the WP unit in period G. As(V) represented 23 to 92% of particulate As concentration; the ratio was generally higher in the SPM from the WP system than those from the PS system, except in period G, where both exhibited high As(V) percentage (≥ 88%).

Table 7 *Concentration of SPM (SPM > 0.22 µm), concentration of particulate Fe and As in outlet water (expressed in mg/L and in proportion of total (dissolved + particulate) Fe and As, and composition of SPM (As/Fe molar ratio, proportion of particulate As(III) and As(V) to total particulate As).*

	Dates (d/m/y)	**Device**	**SPM (mg/L)**	**Fe (mg/L) (wt% Tot. Fe)**	**As (mg/L) (wt% Tot. As)**	**As/Fe (mol/mol)**	**As(III)/As wt%**	**As(V)/As wt%**
B	12/12/2019	PS	NA	NA	NA	NA	NA	NA
		WP	NA	NA	NA	NA	NA	NA
	19/12/2019	PS	6	2 (0.5 %)	0.3 (2 %)	0.1	70	30
		WP	2	0.1 (0.04 %)	0.01 (0.1 %)	0.1	-	100
C	06/02/2020	PS	15	2 (1 %)	0.4 (2 %)	0.1	41	59
		WP	3	0.2 (0.1 %)	0.04 (0.3 %)	0.1	26	74
D	05/03/2020	PS	28	8 (1 %)	1 (3 %)	0.1	76	24
		WP	59	13 (3 %)	2 (8 %	0.1	69	31
	12/03/2020	PS	43	14 (3 %)	1 (1 %)	0.03	77	23
		WP	7	3 (0.6 %)	0.1 (0.3 %)	0.02	47	53
E	29/05/2020	PS	49	11 (2 %)	2 (5 %)	0.1	58	42
		WP	2	0.2 (0.03 %)	0.02 (0.1 %)	0.1	3	97
	18/06/2020	PS	28	3 (0.7 %)	1 (4 %)	0.3	26	74
		WP	9	3 (0.8 %)	0.4 (2 %)	0.1	9	91
F	23/07/2020	PS	124	35 (4 %)	2 (5 %)	0.04	58	42
		WP	14	4 (0.5 %)	1 (3 %)	0.2	22	78
	27/07/2020	PS	NA	NA	NA	NA	NA	NA
		WP	NA	NA	NA	NA	NA	NA
G	15/09/2020	PS	5	0.7 (0.1 %)	0.1 (0.3 %)	0.1	8	92
		WP	57	0.2 (0.03 %)	0.2 (1 %)	0.9	12	88

NA: not available data, the inlet flow used for the different periods were 15L/h for B, C and G while 30L/h for D, E and F.

2.4.6 Sludge Composition

Table 3 lists the measured concentrations of total Fe, total As, As(III), As(V), and total Sulphur (S) in the sludge at different periods of operation. The sludge contained 19wt.% to 31wt.% Fe, 4wt.% to 11wt.% As and 3.5wt.% to 5.4 wt.% S (dry wt.). In each period, the WP sludge contained slightly lower As and Fe contents (5 ± 1wt.% As and 21 ± 7wt.% Fe) compared to the PS sludge (8 ± 1wt.% As and 27 ± 4wt.% Fe). The As/Fe molar ratio varied from 0.24 to 0.5 in both units, with the highest ratio obtained in period G. Arsenate systematically predominated in the sludge; it represented in average 84 ± 5wt.% of the total As concentration among periods B, E, F and G; it did not exceed 64 ± 7wt.% of the total As concentration during period D. XRD analysis revealed the presence of jarosite, gypsum and quartz, but did not present other well crystallized Fe(III)-As phases (Table 8, supplemental Fig. S-8). The morphology of the sludge differed between the two systems: the sludge from the PS system was more compact and attached to the bacteria growth support, it was more homogenously distributed inside the unit. Conversely, the sludge from the WP system contained more fluid (watery) and was easily transported to the bottom of the pilot where it settled.

Table 8 *Average concentration (% dry wt.) of total Fe, total As, As(III), As(V), total S, their ratios, and the minerals identified by XRD in the sludge sampled in each period.*

Period	Device	n	Total As (%)	Total Fe (%)	To. S (%)	As/Fe molar ratio	Fe/S molar ratio	As (III) (%)	As(V) (%)	pH	Crysta-llyzed phases
B	PS	2	9 ± 3	31 ± 6	5.2	0.4 ± 0.2	12.4	17 ± 4	83 ± 4	2.8	Jarosite
	WP	2	4 ± 0.3	19 ± 4	3.5	0.3 ± 0.3	10.9	9 ± 4	91 ± 4	2.7	Jarosite
D	PS	2	7 ± 2	31 ± 5	5.3	0.28 ±0.1	11.8	36 ± 7	64 ± 7	2.7	Jarosite/ Quartz
	WP	2	4 ± 1	24 ± 6	4.7	0.24 ±0.03	10.4	40 ± 10	60 ± 10	2.7	Jarosite/ Quartz
E	PS	2	8 ± 1	31 ± 5	5.3	0.34 ±0.03	12	23	77	2.5	Jarosite/ Gypsum/*
	WP	2	6 ± 2	29 ± 3	5.4	0.29 ± 0.1	10.3	20 ± 2	80 ± 2	2.6	Jarosite
F	PS	2	7 ± 1	27 ± 3	4.3	0.36 ±0.02	12	18 ± 1	82 ± 1	2.9	NA
	WP	2	6 ± 1	29 ± 2	5.0	0.26 ± 0.1	9.9	18 ± 1	82 ± 1	2.7	NA
G	PS	1	11	27	4.6	0.5	12.7	8	92	2.7	Jarosite
	WP	1	7	19	4.6	0.5	9.5	6	94	2.6	Jarosite

NA: not available data
*: quartz, the inlet flow used for the different periods were 15L/h for B, C and G while 30L/h for D, E and F.

2.4.7 Calculated Saturation Indices of Fe-As Phases

Table 4 plots the saturation indices (SI) of the main representative ferric hydroxysulphate and Fe-As phases in the inlet and outlet PS and WP effluents during four periods (B, C, E and F). They generally exhibited values indicating oversaturation with regards to schwertmannite, jarosite, and scorodite in both inlet and outlet effluents. The substantial decrease in pH during the treatment lowered the SI of all Fe(III)-containing phases due to their high solubility dependency with pH. The pH decrease was caused by the precipitation of potassic jarosite (K-jarosite) and/or schwertmannite due to the oxidation of Fe(II) to Fe(III) by bacteria. The SI values are, however, still positive, which demonstrates that their precipitation is under kinetic

control (i.e. thermodynamic equilibrium has not been achieved yet) with respect to the characteristic HRT. Fig. 6 plots the evolution of the SI of K-jarosite and schwertmannite vs. pH of the outlet effluents. The observed trend clearly sustains the fact that jarosite and schwertmannite could co-precipitate, but also that the precipitation of jarosite will be promoted at pH around 2.7–2.8.

The concentration of K^+ is derived from the Carnoules' AMD (inlet concentration: 19 ± 3 mg/L), 39 ± 29% of the potassium entering the units was removed in the treated water and contributed to the K-jarosite formation. However, this phase was not dominant in our units, since the Fe/K molar ratio in the precipitate was 51±33, whereas Fe(mol)/K(mol) = 3 in K-jarosite.

As(V) solubility in the outlet waters was likely controlled by an amorphous ferric arsenate (AFA), as indicated in Table 9. The SI values of amorphous scorodite (from Thermoddem) and AFA (from Garcia-Rios et al. 2021) were within the range -0.5–0.5 (i.e.at equilibrium).

Table 9 Saturation indices calculated from water samples at inlet and outlets with wood/pozzolana support (WP) and plastic support (PS); Thermoddem database, with some additional data (see Methods).

	19 Dec (period B)	**12 March (period C)**	**18 June (period E)**	**23 July (period F)**
	Inlet / PS / WP	**Inlet / PS / WP**	**Inlet / PS / WP**	**Inlet / PS / WP**
K-Jarosite(cr)	9.8 / 6.2 / 5.7	10.1 / 6.4 / 6.3	8.9 / 4.8/ 4.5	12.5 / 7.2 /6.1
Schwertmannite [(1)]	27.3 / 6.4 / 4.2	21.8/ 5.8 / 5.7	17.2 / -0.6 / 0.8	29.7 / 7.1 / 3.7
Scorodite(cr)	4.6 / 1.9 / 2.3	4.1 / 2.5 / 2.4	4.1 / 0.1 / 3.1	4.8 / 3.1 / 2.8
Scorodite(am)	1.9 /-0.7 / -0.4	1.5 / -0.2 / -0.3	1.3 / 0.1 / 0.3	2.0 / 0.3 /-0.04
AFA[(2)]	2.7 / 0.0 / 0.3	2.2 / 0.6 / 0.5	2.1/ 0.9 / 1.1	2.8 /1.0 / 0.7

(1) Sánchez-España et al. (2012); (2) Amorphous Ferric Arsenate, Garcia-Rios et al. (2021).

2.5 Discussion

2.5.1 General System Performance Compared with Previous Systems

The physico-chemistry of the AMD during the monitoring (pH of 3.2–5, As(III) concentrations of 42–102 mg/L and Fe(II) concentrations of 430–1000 mg/L) was similar to long-term observation data at the Carnoulès site (OREME Observatory, https://oreme.org/). Under steady-state conditions, the treatment units oxidized on average 92±6% of the Fe(II) and removed 43±11% Fe and 67±10% As at a HRT of 9 h. These performances were higher and more stable than those obtained with our previous field bioreactor (Fernandez-Rojo et al. 2019). This previous system functioned entirely under passive conditions, i.e aeration was provided by simple oxygen diffusion through a thin water film. As a result, Fe oxidation and removal did not exceed 20% while As removal varied widely between 3% and 97%. For comparison, this previous system reached 40% As removal at a similar HRT (10 ± 1h). The present systems showed similar performance than those obtained in our lab-scale bioreactor that did not use bacterial growth support neither active aeration but a thin water film (4 mm) flowing at the

surface of the Fe(II)-oxidizing biofilm. In that passive lab-scale bioreactor, we obtained a maximum of 80% Fe(II) oxidation, 50% Fe removal, and 65% As removal at a HRT ~ 8h (Fernandez-Rojo et al. 2017). Thus, the thin water film configuration in the lab-scale bioreactor was efficiently compensated by the use of a bacterial growth support (promoting mass transfers between the solution and the biofilm) and active aeration (promoting oxygen supply to the biofilm) in the present units. Considering the capacity of the lab-scale pilot (0.24 L) and field units (263 or 290 L), a scale-up by a factor of more than a thousand was successfully achieved in the present study, while maintaining the performances of the treatment process.

The rates of Fe oxidation in the present units (1×10^{-7}– 4×10^{-7} mol L^{-1} s^{-1}) were in the low range of literature values (1.5×10^{-7} – 40×10^{-7} mol L^{-1} s^{-1}) for laboratory Fe oxidation bioreactors treating As- and Fe-rich AMD at pH 3.2–5 (Ahoranta et al. 2016; Sheng et al. 2017). The kinetic constant k-value was determined considering a first order kinetics approach toward Fe(II) concentration (Eq. 2) We obtained a kinetic constant k-value of k= 0.003 ± 0.0009 min^{-1} under steady-state conditions in operation periods A–E (Fig. S-9), which corresponds to half-life of 3.7h. This k-value fitted with those obtained in AMD streams at pH 3.5–4.2 reported for several AMD in the US and Spain (Larson et al. 2014). This suggests that biological Fe(II) oxidation by the autochthonous microbial community of the Carnoulès AMD was well reproduced in the present treatment units but not enhanced compared to AMD stream conditions. Regarding As removal rates, the present study observed 0.5×10^{-8} to 3×10^{-8} mol L^{-1} s^{-1}, which was similar to our previous field-pilot rates (1×10^{-8} to 2×10^{-8} mol L^{-1} s^{-1}; Fernandez-Rojo et al. 2019) and lab-scale experiments rates (2×10^{-8} to 5×10^{-8} mol L^{-1} s^{-1}; Fernandez-Rojo et al. 2017). The reproducibility of these rates from one pilot to another suggests their ability for future upscaling to full-scale treatment facilities. Regarding As oxidation, 60 to 95% of the As was present as As(V) in the sludge, showing a higher As(III) oxidation yield in the field pilot than in our previous lab-scale experiment in which As(V) reached 48–84% (Fernandez-Rojo et al. 2017, 2018). High oxidation yields were also observed in our previous field pilot where As(V) ranged from 19 to 99% (Fernandez-Rojo et al. 2019)(Fernandez-Rojo et al. 2019)(Fernandez-Rojo et al. 2019)(Fernandez-Rojo et al. 2019). The reason for such differences in As oxidation efficiency between laboratory and field conditions deserves further research.

2.5.2 Effect of the Biofilm Support

The two materials used as biofilm support did not show major differences in term of outlet water hydrochemistry, sludge mineralogy and overall performances. The main difference was the duration of the lag phase regarding Fe(II) oxidation in the early days after restart. The WP system had a shorter lag period than the PS system. This might be associated with the porosity of the wood material providing micro-niches favorable for maintaining an active microbial community (Rötting et al. 2008a). The WP unit showed higher robustness at shutdowns than the PS unit. The lower SPM concentration found in the WP effluent than in the PS effluent might be due to a better SPM settling in the unit containing a mixture of mineral and wood. The relatively high SPM concentration in the PS effluent (up to 0.13 g/L) would require the use of a settling pond downstream of the treatment unit. The WP sludge contained slightly lower As and Fe concentrations compared to the PS sludge, which suggests a dilution by wood

debris from the bacteria growth support in the WP unit. The disaggregation of the wood support may be an important issue in the perspective of long-term treatment and sludge disposal.

The As(V) to total As ratio in SPM was higher in the WP unit than in the PS unit. This may suggest faster As(III) oxidation in the WP unit. The difference did not persist in the sludge due to an aging effect. The wood material provided organic matter that could favor As-oxidizing bacterial populations. An input of nutrients stimulated As(III)-oxidizing bacteria in a batch experiment performed with Carnoulès AMD (Tardy et al. 2018). Occasional measurements of total organic carbon in the PS and WP systems indicated higher concentrations in the WP sludge (71 ± 47 g/kg) than in the PS sludge (3 ± 0.7 g/kg (dry wt.)), although the difference was minor in the treated water (effluent water WP: 5 ± 2 mg/L; PS: 3 ± 1 mg/L). Further research on bacterial As-oxidizing gene expression will be necessary to find a possible role of bacterial growth support on As oxidation rate in the units.

2.5.3 Robustness of the System Towards Variations of Operating Conditions:

An important factor regarding pilot performance was related to air injection. Dissolved oxygen concentration plays both a direct and indirect role on biological Fe(II) oxidation. First, it is one of the factors that directly controls the rate of Fe(II) oxidation. Second, the DO concentration strongly influences the structure of the Fe-oxidizing bacterial community (FeOB), which consists of species exhibiting different specific Fe-oxidation rates (Fernandez-Rojo et al. 2018; Johnson et al. 2012). Optimal DO concentration varies depending on the identity of the FeOB. For example, the microaerophilic *Gallionella* thrive at lower oxygen conditions than other FeOB such as *Ferrovum* and *Leptospirillum* spp. (Hanert 2006; Johnson et al. 2012). Previous studies suggested that increasing oxygen concentrations may favor the development or activity of FeOB belonging to the *Ferrovum* genus (Fabisch et al. 2016; Fernandez-Rojo et al. 2018; Jwair et al. 2016). *Ferrovum* is often associated with the high Fe(II) concentration and high Fe oxidation rates, which explains its importance in AMD treatment (Chen et al. 2020; Johnson et al. 2014). The lower Fe(II) oxidation rate in period F and early period G had a negative impact on Fe precipitation, which decreased to less than 10%, but it did not significantly affect As removal, which remained similar (~ 70%) in period F (partial Fe(II) oxidation) and in period E (complete Fe(II) oxidation). This was attributed to the high As sorption and incorporation capacity of the Fe minerals that formed in the units; the sludge that formed under low DO supply in periods F and G exhibited an As/Fe molar ratio greater than 0.3. A high retention capacity was also observed in our previous field pilot that exhibited Fe oxidation yields below 20% (Fernandez-Rojo et al. 2019). This high As retention and As removal efficiency was probably promoted by the activity of As-oxidizing bacteria; it has been shown that some strains maintain the As oxidation activity at DO value around 1 mg/L (Gonzalez-Contreras et al. 2012; Hambsch et al. 1995)

Interruptions in operation affected Fe(II) oxidation efficiency in the early days after restart. This was indicative of a lag phase typical of biological processes and had been previously observed in biological Fe oxidation in batch and continuous flow experiments with AMD (Egal et al. 2009). Units shut down for several weeks converted the system into a batch reactor. Under these conditions, when the substrate Fe(II) was no longer available, the FeOB probably stopped

growing and became dormant. During system restart, the bacteria need to recover their metabolism. Thus, shutoff periods had a negative effect for a short period of time (≤ 10 days) on pilot performance in terms of Fe(II) oxidation and subsequent As removal.

The flow rate increase from 15 L/h to 30 L/h (HRT decrease from 18 h to 9 h) between periods C and D decreased Fe(II) oxidation yield and Fe and As removal yields by ~ 10%. This suggests that most of the reactions occurred within less than 9 h. Such relatively short HRT fit with the ones reported in other studies for As-rich AMD treatment (Ahoranta et al. 2016). This suggests that the HRT determined in the present study might be used to design a full-scale treatment.

Water temperature may affect the rate of biologically mediated reactions. Previous studies on bacterial strains oxidizing Fe or As isolated from polluted environments showed that their growth and oxidation activities were temperature dependent between 5°C to 30° (Battaglia-Brunet et al. 2002; Dopson et al. 2006; Ito et al. 2012; Kim et al. 2008). Tardy et al. (2018) reported that water temperature greater than 20°C stimulate As oxidation mediated by autochthonous bacterial communities in the Carnoulès AMD water. In our experiments, water temperature ranged from 5°C to 27°C; however, the variation did not correlate directly with Fe or As removal yields. More data would be required to confirm a possible temperature dependency for biological As and Fe oxidation in the systems.

2.5.4 Sludge Composition and Control of Outlet Water Physico-chemistry

Jarosite, gypsum and quartz were identified by XRD in the sludge under routine operation (periods A–E). Quartz originated from the tailings (Fernandez-Rojo et al. 2019). The presence of jarosite at pH ≤ 2.8-3.0 is in agreement with the stability domain of this mineral (Bigham et al. 1996; Sánchez-España et al. 2011). Jarosite has been described as an As scavenger under acidic and sulfate-rich conditions (Asta et al. 2009; Johnston et al. 2012; Kendall et al. 2013). This retention is associated with an initial co-precipitation of As(V) with Fe(III), which is often completed by the replacement of the sulfate groups of jarosite with the As(V) present in solution (Shi et al. 2021). However, jarosite is often considered to have formed by recrystallization of schwertmannite (Asta et al. 2010a)). Wang et al. (2006) reported the transformation of schwertmannite to jarosite with aging. Burton et al. (2021) recently found that increasing levels of As(V) incorporation within schwertmannite enhanced also the transformation of schwertmannite to jarosite. In our previous studies, the formation of As-poor jarosite from the Carnoulès AMD occurred after a first precipitation step of tooeleite ($Fe_6(AsO_3)_4SO_4(OH)_4{\cdot}4H_2O$) or As(III)-schwertmannite (Duquesne et al. 2003). Tooeleite was not evidenced in the present study, probably due to the rapid Fe(II) oxidation and subsequent achievement of lower As(III)/Fe(III) molar ratios in the solid. The reported As/Fe ≤ 0.5 ratio in the sludge of the present field pilot test did not fit the stoichiometric formula of tooeleite (As/Fe = 0.67).

In general, the sorption capacity reported for jarosite is considerably less than that reported for schwertmannite or amorphous phases. Asta et al. (2009) reported that at initial As concentration of 100 mg/L in water, As(V) sorption capacity of synthetic jarosite of 21 mg/g at pH 1.5–2.5. Ahoranta et al. (2016) estimated that the highest As(III) and As(V) sorption capacities of biogenic jarosite at pH 3.0 were 1.24 and 2.07 mg/g, respectively. For comparison, the sorption capacity of schwertmannite at pH 3 has been estimated at 0.31-0.33 mol As(V)/mol Fe,

corresponding to more than 200 mg As(V)/g (Burton et al. 2009; Carlson et al. 2002). In the present study, the As content in the sludge ranged between 39 and 91 mg/g, corresponding to As/Fe molar ratio of 0.3 ± 0.08 (Table 1), which implies the contribution of an amorphous phase for As retention.

The calculated SI indicated that As(V) solubility in most of the outlet water samples was likely to be controlled by amorphous scorodite or AFA (Table 4). This confirms the findings of Langmuir et al. (2006), who highlighted the role of AFA in the control of As mobility in mine tailings. Occurrence of this phase is also a common observation under microbially-active AMD conditions (Maillot et al. 2013; Fernandez-Rojo et al. 2018). Therefore, amorphous schwertmannite and amorphous ferric arsenate were probably the dominant phases responsible for As removal in our field units. The As removal performance was probably limited by the solubility of amorphous ferric arsenate at pH 2.8 ± 0.3. Slightly positive SI values and occurrence of As(V) colloids suggest that kinetics play a role in the precipitation of the Fe/As phases.

2.6 Conclusions and Perspectives

During more than a year of functioning, we obtained nearly complete Fe(II) oxidation and up to 80% As removal during all seasons in the two treatment units (PS and WP supports), despite variations in the Carnoulès AMD hydrochemistry. The rates of biological Fe oxidation were similar to laboratory rates and to those reported for AMD streams worldwide. The As removal yields were greater and more stable than in our previous field pilot and similar to the laboratory bioreactor. The WP bacterial support provided shorter delay before performance recovery. The sludge composition was stable throughout time and similar in the PS and WP systems. The predominance of arsenate phases is a positive outcome in the perspective of long term storage. Hence, the robustness of the treatment regarding seasonal variations of AMD physical-chemistry, environmental and operational conditions suggest great potential for further scale-up and extrapolation of the treatment to other AMD with similar properties.

Further work will focus on additional treatments (sulfate-reducing bioreactor, limestone channel) to improve the quality of the treated mine water. Research is in progress to characterize the bacterial diversity in the units, particularly the genetic potential for As oxidation, which is a key process for As immobilization.

Acknowledgements : The authors acknowledge the financial support of (ADEME) [APR-GESIPOL-2017-COMPAs], the Occitanie region, and BRGM for co-funding of the PhD grant of Camila Diaz-Vanegas, and OSU-OREME for co-funding of the long-term monitoring of Carnoulès AMD physico-chemistry. Thanks to Adam Djibrine and Amandine Malcles for their work during experimental monitoring. Thanks to Jérémy Engevin for bringing his expertise on the design and installation of the devices and to Rémi Freydier, Léa Causse, and Sophie Delpoux for their help in analytical work on the AETE-ISO platform, OSU OREME, Université de Montpellier. The authors would like to thank the editors for their contribution to improve the quality of the manuscript.

2.7 Supporting Information

2.7.1 Calculation

The mass balance equation used was as follows:

$[As(III)]_{diss.Inlet} + [As(V)]_{diss.Inlet} = [As(III)]_{diss.Outlet} + [As(V)]_{diss.Outlet} + [As(III)]_{SPM\ Outlet} + [As(V)]_{SPM\ Outlet} + [As(III)]_{Sludge} + [As(V)]_{Sludge}$

The $[As(III)]_{diss.Inlet}$ was the concentration of As(III) (mg/L) in the dissolved fraction in the inlet water, $[As(III)]_{SPM.Outlet}$ was the concentration of As(III) (mg/L) in SPM in the outlet water, $[As(III)]_{sludge}$ was the concentration of As(III) (mg/L) in the sludge accumulated in the filling material of each tank. The same representation was used for As(V). The $[As(III)]_{Sludge}$ and $[As(V)]_{Sludge}$ (in mg/L) were calculated by the following equation:

$$[As(III)]sludge = \left(\frac{[As(III)]_{SPM.Outlet}}{[As(total)]_{SPM.Outlet}} * ([As(total)]_{diss.Inlet} - [As(total)]_{diss.Outlet})\right)$$

$$[As(V)]sludge = \left(\frac{[As(V)]_{SPM.Outlet}}{[As(total)]_{SPM.Outlet}} * ([As(total)]_{diss.Inlet} - [As(total)]_{diss.Outlet})\right)$$

The rate of As(III) oxidation was calculated according to two methods and averaged. The first one used the decrease of As(III) concentration between inlet and outlet, the second method used the increase of As(V) concentration between inlet and outlet as follows:

$$\text{rate } [As(III)] \text{ decrease } (\text{mol}.L^{-1}.s^{-1}) = \frac{[As(III)]_{diss.Inlet} - [As(III)]_{diss.Outlet} - [As(III)]_{SPM\ .Outlet} - [As(III)]_{Sludge}}{(HRT * 3600)}$$

$$\text{rate } [As(V)] \text{ increase } (\text{mol}.L - 1.s - 1) = \frac{[As(V)]_{diss.Outlet} + [As(V)]_{SPM\ Outlet} + [As(V)]_{Sludge} - [As(V)]_{diss.Inlet}}{(HRT * 3600)}$$

2.7.2 Supplementary Tables

Table SI 1 *Distribution of iron and arsenic between the colloidal phase (>10 kDa or >100 kDa) and the "truly dissolves" phase dissolved (<10 kDa or <100 kDa) expressed in mg/L and in percentage of total (dissolved + particulate) Fe and As.*

Period	Date	Device	Fraction < 0.22 µm (Dissolved fraction)			
			Dissolved [Fe] (mg/L) (% of tot. Fe conc.)		Dissolved [As] (mg/L) (% of tot. As conc.)	
			10 or 100 kDa < Fraction < 0.22 µm (mg/L)	Fraction < 10 or 100 kDa ("truly" dissolved) (mg/L)	10 or 100 kDa < Fraction < 0.22 µm (mg/L)	Fraction < 10 or 100 kDa ("truly" dissolved) (mg/L)
B	12/12/19	PS	7 (2 %) *	347 (98 %)	2 (9 %)	20 (91 %)
		WP	1 (1 %) *	218 (99 %)	1 (8 %)	11 (92 %)
	19/12/19	PS	*	310 (100 %)	1 (6 %)	19 (92 %)
		WP	0.6 (0.2 %) *	299 (100 %)	1 (6 %)	12 (94 %)
E	18/6/20	PS	121 (32 %)	258 (68 %)	22 (68 %)	9 (28 %)
		WP	37 (12 %)	260 (87 %)	9 (39 %)	13 (59 %)

2.7.3 Supplementary Figures

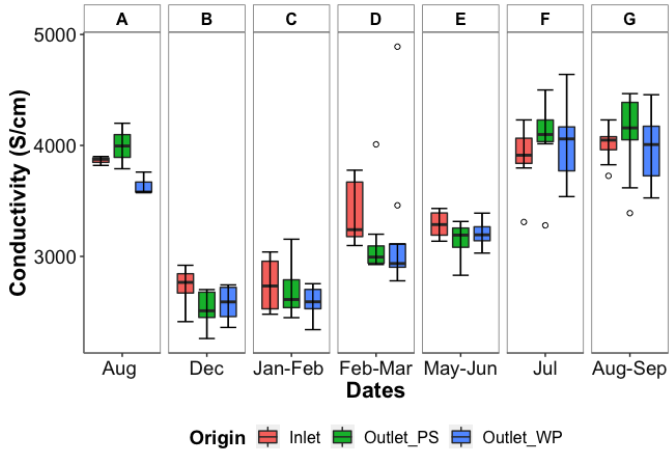

Figure SI 1 . *Boxplot representation of the conductivity measured in the inlet water and in the outlet water from the PS and WP devices during seven periods of monitoring.*

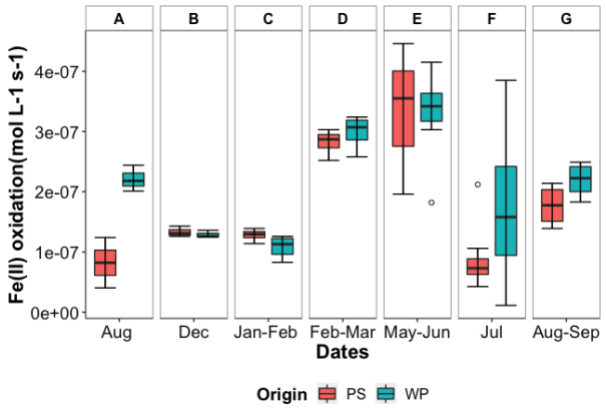

Figure SI. 2 *Iron oxidation rates determined in the PS and WP devices under stationary phases in each period.*

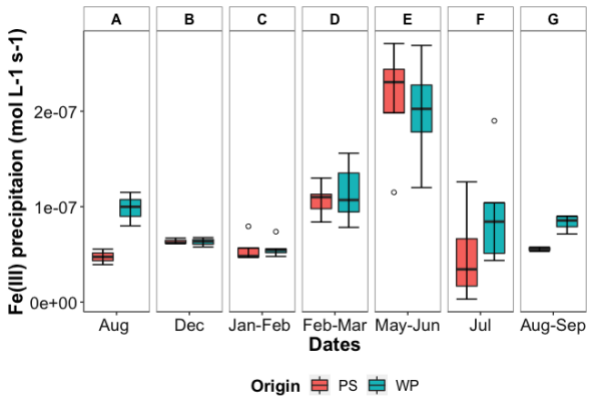

Figure SI 3. *Iron precipitation rates determined in the PS and WP devices under stationary phases in each period.*

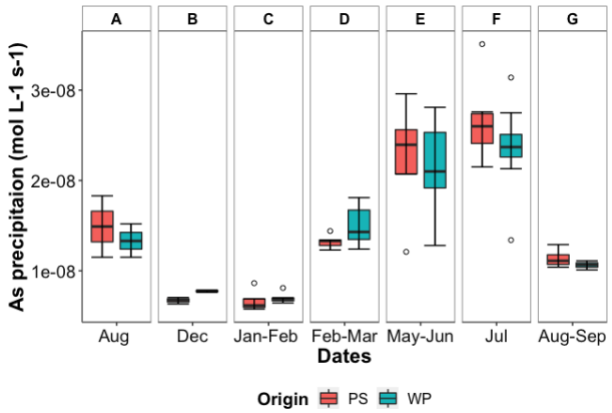

Figure SI 4. Arsenic precipitation rates determined in the PS and WP devices under stationary phases in each period

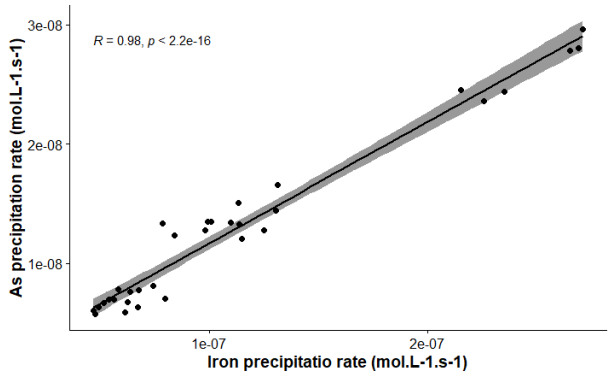

Figure SI 5. *Correlation between arsenic* removal rate and the rate of iron precipitation *during periods with optimal performances (B, C, D and E).*

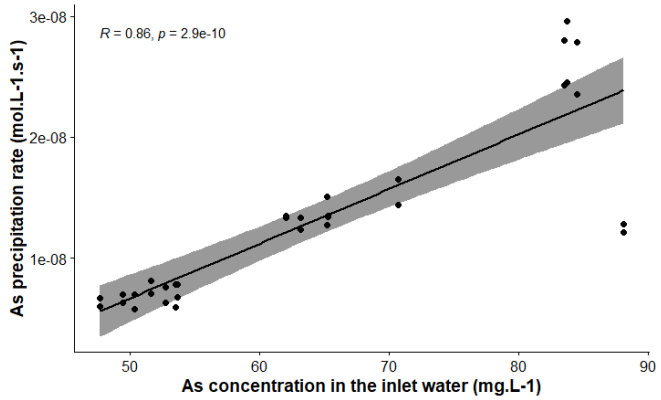

Figure SI 6. *Correlation between arsenic removal rate with arsenic concentration during periods with optimal performances (B, C, D and E)*

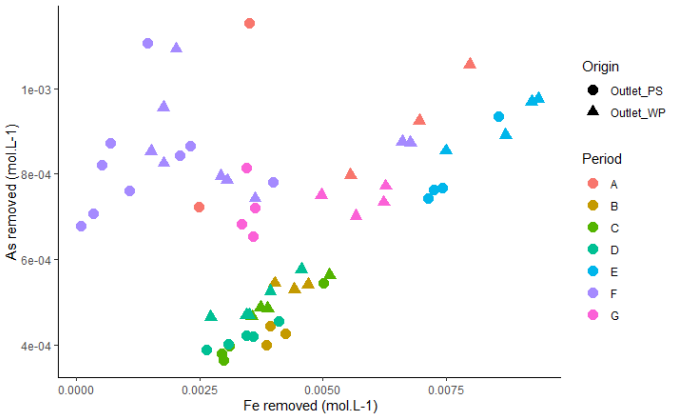

Figure SI 7. *Concentration* **r***emoved from the aqueous fraction with arsenic concentration removed from aqueous fraction during all period (A, B, C, D, E, F and G*

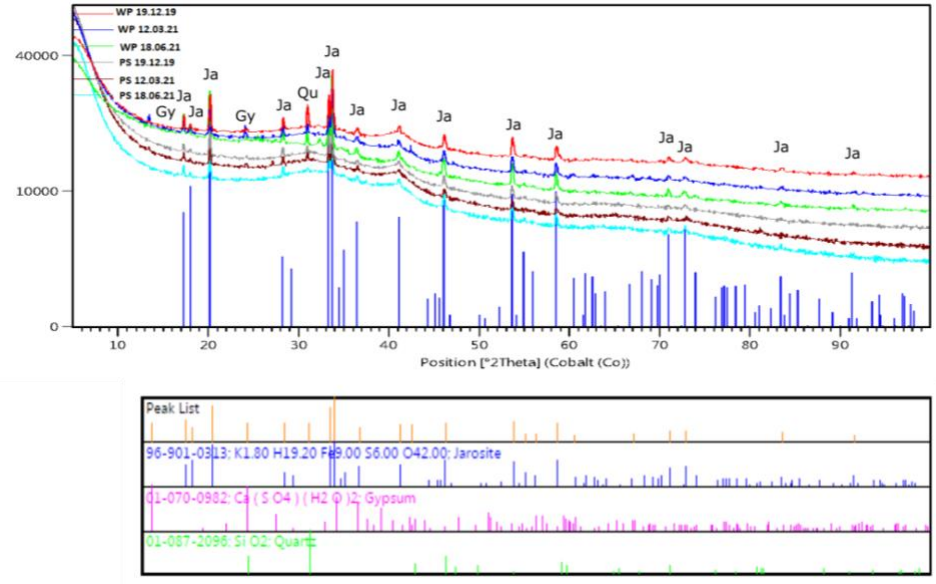

Figure SI 8. *X-ray powder diffraction (XRD) of sludge samples from the PS and WP devices, three samples for the sludge accumulated from the PS support device and three from the WP support device. The dates were 19.Dec 2019, 12.Mar.2020 and 18.Juin.2020.*

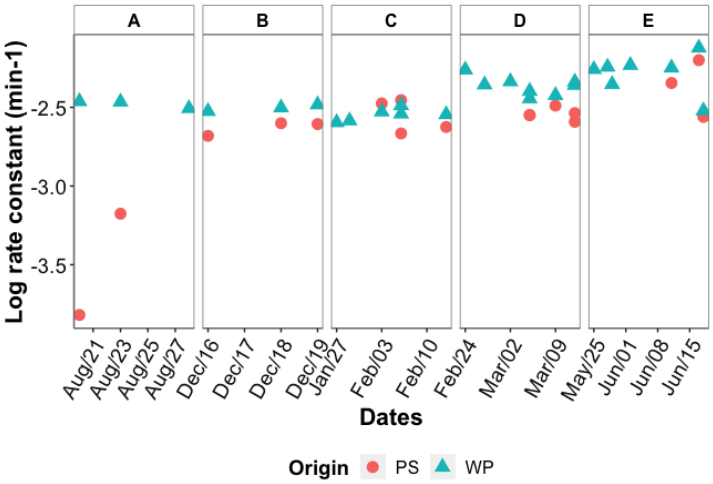

Figure SI 9 *Variation of the first-order kinetic rate constant for the Fe(II) oxidation reaction for PS and WP devices*

Chapitre 3 : Dynamique des communautés bactériennes présentes dans des bioréacteurs d'oxydation dans des conditions de terrain

Introduction

Malgré le grand potentiel de l'utilisation de l'activité des micro-organismes pour traiter une pollution, les processus impliqués et les facteurs qui les contrôlent sont encore mal compris, ce qui rend difficilement prévisible les performances de ces traitements biologiques. Cette incertitude limite l'application et l'optimisation de la biorémédiation (Lovley 2003; Hessler et al. 2020). Grâce aux techniques omiques, l'étude des paramètres qui contrôlent la dynamique, la diversité, le métabolisme et l'activité des micro-organismes est désormais possible (Sharma et al. 2022). Dans ce contexte, la dynamique des communautés bactériennes associées à deux bioréacteurs d'oxydation semi-passifs (l'un rempli d'un support de biomasse de copeaux de bois/pozzolana et l'autre rempli d'un support plastique) a été étudiée pendant un an.

Le chapitre précédent a décrit les performances de traitement du fer et de l'arsenic de ces deux bioréacteurs. Les deux pilotes de bio-oxydation ont permis d'oxyder 92% du fer et d'éliminer 43% du fer et 67% de l'arsenic en moyenne, avec un temps de rétention hydraulique minimal de 9h. Les vitesses moyennes d'oxydation du fer, de précipitation du fer et de précipitation de l'arsenic à l'état stationnaire et dans des conditions de fonctionnement normal du système d'aération étaient statistiquement similaires pour les deux bioréacteurs. Une différence entre les deux systèmes était le délai nécessaire pour le rétablissement des performances stables après une perturbation ou une interruption. En effet, après une interruption de l'alimentation, les dispositifs retrouvent leur performance optimale au maximum dix jours après le redémarrage pour le bioreacteur au garnissage plastique et moins de cinq jours pour le bioreacteur au garnissage bois/pouzzolane. La résilience est une caractéristique importante pour des pilotes fonctionnant sur le terrain, où des perturbations imprévisibles peuvent survenir et nécessiter une adaptation rapide du système.

Afin de mieux appréhender l'influence des paramètres environnementaux et opérationnels sur les performances des bioréacteurs (et leur stabilité), une caractérisation des communautés bactériennes impliquées dans les processus mis en jeu est nécessaire. Ainsi, ce deuxième chapitre présente la caractérisation de la diversité et de l'activité bactérienne dans les deux bioréacteurs et discute le lien entre microbiologie, facteurs environnementaux et performances du traitement aérobie.

L'approche mise en œuvre a pour objectif de distinguer les communautés bactériennes présentes (totales) des communautés actives, via l'étude de l'ADN et de l'ARN environnemental respectivement, ainsi que les communautés sessiles (formant des biofilms sur les supports de biomasse) de celles planctoniques (vivant dans l'eau). La diversité bactérienne à l'intérieur des deux bioréacteurs a été déterminée par le séquençage du gène de l'ARNr 16S. La présence et l'expression du gène *aioA* marqueur de la fonction bactérienne d'oxydation de l'arsenic a été mise en évidence par qPCR ciblant respectivement les extraits d'ADN et d'ARN.

Ce chapitre est présenté sous forme d'un article en préparation pour l'issue spéciale « Microbial Ecotoxicology: from the lab to the field » de la revue « FEMS Microbiology Ecology».

3 Article: Towards an understanding of the factors controlling bacterial diversity in semi-passive Fe-oxidation bioreactors treating arsenic-rich acid mine drainage

Diaz-Vanegas C[1,2], Héry M[1], Desoeuvre A[1], Bruneel O[1], Joulian C[2], Battaglia-Brunet F[2], Casiot C[1]*

[1] *HydroSciences Montpellier, Univ. Montpellier, CNRS, IRD, Montpellier, France*

[2] *French Geological Survey (BRGM), Water, Environment, Process and Analyses Division, Orléans, France*

**Corresponding author*

E-mail address: (Héry Marina) marina.hery@umontpellier.fr

3.1 Abstract

Semi-passive bioreactors based on iron (Fe) and arsenic (As) oxidation and co-precipitation are promising for the sustainable treatment of As-rich acid mine drainages (AMD). However, their performance in the field is still highly variable and unpredictable. We recently monitored during one year two optimized semi-passive iron oxidation bioreactors, filled with distinct bacterial biomass carriers (a mix of wood and pozzolana or plastic). The objective of the present work was to characterize the dynamic of the bacterial communities mediating iron and arsenic removal in these two bioreactors, and to explore the influence of the environmental and operational drivers on their diversity and activity. The diversity of the total and active communities (both suspended and attached to the biomass carriers) were analyzed by 16S rRNA gene metabarcoding. Arsenite-oxidizing bacteria were quantified by qPCR and RT-qPCR targeting *aioA* gene. Bacterial communities were dominated by several iron oxidizing bacteria present in variable proportions. The better resilience to disturbances previously observed for the bioreactor filled with wood and pozzolana was related to a higher bacterial richness. The bioreactor filled with the plastic biomass carrier was characterized by a more variable bacterial diversity although these variations did not significantly impact the global treatment performance. We evidenced for the first time the expression of *aioA* gene in a treatment device, associated with the presence of active *Thiomonas* spp. in the bioreactors. These results confirmed the contribution of biological arsenite oxidation to the arsenic removal process. Shifts in the bacterial communities could be attributed to both operational and physiochemical parameters; including the nature of the biomass carrier, the water pH and oxygen availability. Our results showed that the resilience and functional redundancy of the suspended and attached bacterial communities developed in the two bioreactors conferred robustness and stability to the treatment systems, in terms of Fe and As oxidation and removal.

Keywords biological arsenic oxidation, biological iron oxidation, bioremediation, *aioA* genes

3.2 Introduction

Acid mine drainages (AMD) are undesired products of the weathering of sulfide minerals present in tailings. They contribute to decrease the pH and release metals and metalloids into aquatic environments. Arsenic is associated with more than 200 minerals (Alam and Mcphedran 2019) such as arsenopyrite (FeAsS). Their oxidation releases this toxic metalloid, which is mobilized across the aquatic bodies downstream of the mine tailings (Paikaray 2015). The chronic toxicity of arsenic is a threat to public and environmental health (Huq et al. 2020).

Closed and abandoned mines are the main source of AMD (Rezaie and Anderson 2020). Because the cost of remediation is often covered by limited public funds, the development of cost-effective and low-maintenance treatments is necessary. Autochthonous microbial communities thriving in AMD containing arsenic are the key to treat this pollution. Indeed, bacterially mediated iron and arsenic oxidation, followed by their co-precipitation is a natural process responsible for the partial removal of the arsenic present in AMD (Casiot et al. 2003b; Asta et al. 2010a). Arsenic is usually present in AMD under the arsenite As(III) form. Biological oxidation of As(III) to As(V) contributes to reduce its mobility, due to the higher affinity of As(V) with the Fe-rich solid particles present in tailings and streams (Maillot et al. 2013). Thus, the combined action or iron- and arsenic-oxidizing bacteria contributes to arsenic and iron removal from polluted waters.

The Reigous creek, near the former Carnoulès mine (Southern France), is an exceptional example of an arsenic impacted AMD that has been extensively studied during more than 20 years (Leblanc et al. 1996, 2002; Casiot et al. 2003b; Egal et al. 2010; Volant et al. 2014). Seasonal variations of the physico-chemistry of the AMD waters were evidenced (Egal et al. 2010) and were associated with temporal dynamics of the bacterial diversity (Volant et al. 2014). In this site, natural attenuation mediated by ferrous iron- and arsenite- oxidizing bacteria is responsible for the treatment of about 30% of soluble As, through the formation of biogenic precipitates such as tooleite, schwertmannite and amorphous As(V)- and As(III)-Fe (III) phases (Casiot et al. 2003a; Morin et al. 2003; Egal et al. 2010). However, natural attenuation is not sufficient to reach the threshold limit (0.83 µg/L over the local geochemical background value) allowed by European Water Directive (2000/60/EC) for dissolved As concentration in downstream river water. Furthermore, the accumulation of biogenic precipitates in the creek bed is of concern due to the possible remobilization of As during extreme rainfall events affecting the region (Resongles et al. 2014, 2015).
Previous studies attempted to develop a treatment system for As-rich AMD based on natural attenuation process (Hedrich and Johnson 2012; Macías et al. 2012b; Ahoranta et al. 2016; Fernandez-Rojo et al. 2017, 2018, 2019). Fernandez-Rojo et al. (2017, 2018) obtained nearly 80% As removal in a laboratory-scale continuous flow bioreactor, fed with the Carnoulès AMD. Later, a first attempt made with an *in situ* pilot suffered important performance variations and highlighted the importance to optimize oxygenation and support for bacterial attachment (Fernandez-Rojo et al. 2019). The dynamic of the bacterial communities inside this field pilot was described by Laroche et al. (2018). Arsenate (As(V)) enrichment in the biogenic

precipitates was associated with an increase in the abundance of arsenite-oxidizing bacteria. However, to the best of our knowledge, arsenite oxidase expression, which is a key process in such treatment, has not been evidenced yet in a treatment system. Furthermore, there are still gaps to be filled about the stability of the bacterial diversity and activity facing seasonal and operational fluctuations, and the implications on treatment efficiency and robustness (Fernandez-Rojo et al. 2019). Recently, we obtained a relatively stable As removal efficiency, (67%), in two optimized semi-passive field bioreactors using air injection and porous biomass carriers (Diaz-Vanegas et al. 2022). These semi-passive treatment units, monitored during one year, showed improved and more stable performances compared to previous field study and are promising for the treatment of arsenic-rich AMD. Understanding the dynamic of the bacterial community in such system is of prime importance since Fe oxidation only relies on bacterial activity at acid pH and As oxidation is bacterially catalyzed.

Hence, the present work aims to characterize the bacterial diversity and activity in the two optimized semi-passive iron oxidation bioreactors described by Diaz-Vanegas et al. (2022) under varying on-site operating and seasonal conditions. Two types of biomass carriers (plastic support and a mix of wood chips and pozzolana) were compared. We focused on active bacterial communities through the analysis of environmental RNA and distinguished the communities attached to the supports to thoses in suspension. Bacterial diversity was determined by metabarcoding of the 16S rRNA gene and the presence and the expression of the arsenite oxidase gene quantified by qPCR. Then, we related this microbiological characterization to bioreactors performance and discussed the links between the dynamic of the bacterial communities, the variations of the physico-chemistry of the AMD water and the system treatment stability.

3.3 Materials and methods

3.3.1 Bioreactor setup, operation and sampling

Two bioreactors of 1 m^3 each were installed downstream the Carnoulès tailing dam as described in Diaz-Vanegas et al. (2022). Briefly, the bioreactors were continuously fed with the Reigous' AMD; the flow rate was controlled by pumps. Each bioreactor was equipped with air diffusers to avoid oxygen limitation. The two bioreactors were filled with different biomass carriers. One bioreactor was filled with a plastic biomass carrier ("PS") (Biofill, Type A), the other with a mixture of coarse wood chips and pozzolana ("WP" for Wood-Pozzolana). The two biomass carriers showed different properties: the plastic carrier had higher porosity (96%) but lower specific surface (>160 m^2/m^3) than the wood-pozzolana mixture (porosity: 64% and specific surface estimated to 333 m^2/m^3).

The bioreactors were monitored during 218 days; monitoring covered all the seasons and was divided in seven periods A, B, C, D, E, F and G from July 2019 to September 2020. The periods were defined based on the flow rate and some undesired interruptions due to technical and operational issues. Water circulation was stopped between period A and B due to an electrical

supply problem (September-November), so during three months the bioreactors were operated in batch conditions. During period F and beginning of period G, the accumulation of biogenic precipitates led to the clogging of the air diffusers in both bioreactors. The air diffusers started working properly again after a maintenance later in period G (September), 15 days before the last sampling.

Outlet waters and biogenic precipitates formed inside the reactors were collected periodically for bacterial community characterization. Sample collection began in period B (due to the time required to form the precipitates in sufficient quantity), and it was carried out once per period for each bioreactor. This sampling strategy allows to consider both the bacterial community from the water defined as the suspended community and the one associated with the biogenic precipitates accumulated in the biomass carriers that corresponds to the attached community.

The biogenic precipitates were collected by scrapping the biomass carrier in each bioreactor. The biogenic precipitates from the WP bioreactor were sampled only from the wood chips (due to the difficult access to the pozzolana fallen at the bottom of the tank). Samples were collected in Falcon tubes (50 mL) and leaved some minutes for decantation. The supernatant was discarded and the precipitates were distributed into six cryo-tubes (2 mL). The attached community corresponds to the bacterial communities living in the biogenic precipitates. For each point of sampling (outlet PS and outlet WP), six replicates of outlet water (300 mL each one) were filtered on sterile 0.22 µm cellulose acetate filters. All the solid samples and filters were flash-frozen in dry ice in the field before transport to the laboratory and storage at -80 °C until DNA and RNA extractions. The suspended communities correspond to the bacteria living in the aqueous phase and associated with the suspended particulate matter (SPM) recovered from the filters (0.22 µm).

3.3.2 Geochemical evolution of the inlet and outlet waters and of the biogenic precipitates inside the two bioreactors

The chemical characterization of the inlet water, outlet water and biogenic precipitates of each bioreactor is detailed in our previous study (Diaz-Vanegas et al. 2022). Both bioreactors showed similar Fe oxidation and As removal rates, represented respectively by the kinetic constant value KOFe and the As precipitation rate determined in Diaz-Vanegas et al (2022). The highest performances were obtained during period E (Fe oxidation) and F (As precipitation) as shown in Figure 13. In the biogenic precipitates, more than 60 % of total As was under the As(V) oxidation state during the entire monitoring (Table SI 2).

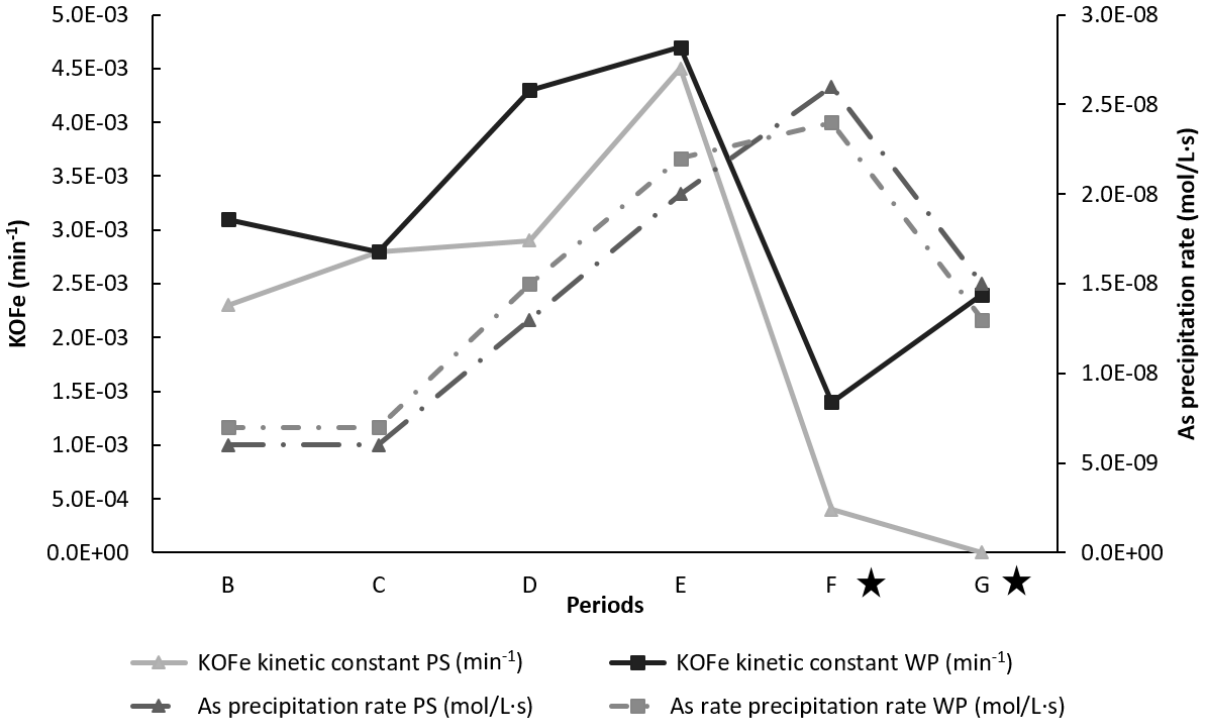

Figure 13. *Evolution of the bioreactor performances (represented by KOFe and As precipitation rate). Solid lines represent the evolution of the kinetic constant value (KOFe) for the WP and PS bioreactors. Dashed lines represent the evolution of the arsenic precipitation rates (mol/L·s) calculated for each pilot. The triangles and the squares represent the data from the PS and WP bioreactor respectively (Diaz-Vanegas et al. 2022). The stars represent the periods with the clogging of the air diffusers. The values used for this graph correspond to the average of the data obtained for each period.*

The physicochemical data for inlet and outlet waters corresponding to the sampling performed for microbiological analyses are summarized in Table 10 and Supplementary Table S2. These data were used for the correlation analyses. The performance indicators used for the correlations include the first-order kinetic constant of Fe oxidation (KOFe) (min^{-1}), Fe precipitation rate (mol/L·s), As precipitation rate (mol/L·s) and percentage of arsenate released in the outlet water (As(V)% outlet).

In the inlet water, arsenic concentration varied between 50 and 100 mg/L and iron concentration between 500 and 1000 mg/L. The AMD was more concentrated in pollutants during the driest and hottest season (periods E, F and G) as described before (Egal et al. 2010). The pH of the AMD varied between 3.7 and 4.8, with the highest values during period B. The AMD showed a temperature between 8 and 22°C with the highest value during period E. The coldest temperature was measured during periods B and C, which also correspond to the periods with the lowest concentration of total iron (449-501 mg/L) and arsenic (49-54 mg/L). The hydraulic retention time (HRT) was slightly different between the two devices, with approximately one hour more in the WP device. Two HRT were tested (~ 9h and ~ 18h), but the difference in the performances (rates of Fe and As oxidation and precipitation) was less than 10%.

Occasional measurements of dissolved oxygen concentration inside the bioreactors showed dysfunction of the air diffusers in period F.

Table 10 *Inlet and outlet water main characteristics*

Date (d.m.y)	Period	T (°C)	pH inlet	As T inlet (mg/L)	Fe (II) inlet (mg/L)	HRT (h)		TOC (mg/L)		DO (mg/L)	
						PS	WP	PS	WP	PS	WP
19.12.19	B	13.9	4.82	53.64	501	18	19	2.3	5.4	NA	NA
06.02.20	C	8.3	4.11	49.5	448.9	18	19	3.0	3.5	10.7	NA
12.03.20	D	14.1	3.87	70.7	665.2	9	10	2.9	3.0	9.1	10.0
18.06.20	E	22.3	3.79	88.1	732.3	18	19	NA	NA	6.1	5.0
27.07.20	F	20.2	4.12	93.1	820.7	9	10	4.0	4.6	0.2	3.1
15.09.20	G	20.5	4.44	91.0	768.6	18	19	4.6	4.1	NA	NA

DO was measured inside the bioreactor

3.3.3 DNA and RNA extraction and cDNA synthesis

The molecular characterization of the total and active bacterial communities, were based on the analyses of environmental DNA and RNA (cDNA) respectively.

For each bioreactor, DNA was extracted from biogenic precipitates and outlet water filters using DNeasy PowerSoil kit and DNeasy PowerWater kit (Qiagen) respectively, according to the manufacturer's recommendations. The RNA extractions were performed from biogenic precipitates and outlet water filters using FastRNA Pro Soil-Direct kit (MP Biomedicals) and RNeasy Power Water Kit (Qiagen) respectively, according to the manufacturer's recommendations. Residual DNA was removed from the extracted RNA with an additional Turbo DNase treatment (Turbo DNA-free kit, Ambion). The absence of DNA was verified by attempting to amplify 16S rRNA gene with 8F (5′-AGAGTTTGATCCTGGCTCAG-3′, Lane 1991) and 1489R (5′-TACCTTGT TACGACTTCA-3′, Weisburg et al. 1991) primers. Reverse transcription was immediately performed using the iScript™ cDNA Synthesis Kit (Biorad). The quality of the cDNA was confirmed by 16S rRNA gene amplification as described above or by *aioA* gene amplification with aoxBM1-2F (5-CCACTTCTGCATCGTGGGNTGGGNT A-3) and aoxBM3-2R (5-TGTCGTTGCCCCAGATGADNCCYTTYT-3) primers (Quéméneur et al. 2008).DNA and RNA extracts were quantified with a fluorometer (Qubit ®, Invitrogen) and stored at -80°C until further analysis.

3.3.4 Sequencing of 16S rRNA gene and bioinformatics

For metabarcoding, the V3 and V4 regions of the bacterial 16S rRNA gene were amplified (341F: 5'-CCTACGGGNGGCWGCAG-3'- 805R: 5'-GACTACHVGGGTATCTAATCC-3'). Libraries of amplicons and illumina MiSeq sequencing were performed by MetaHealth metagenomic-based services (CIRAD, PHIM, Eco&Sols, Montpellier, France).

Illumina sequencing, base calling and demultiplexing were carried out using RTA v1.18.54, MCS 2.6 and bcl2fastq 2.17. Paired Illumina MiSeq reads were assembled with vsearch v2.18.0 (Rognes et al. 2016) using the command fastq_mergepairs and the option

fastq_allowmergestagger. Demultiplexing and primer clipping were performed with cutadapt v3.4 (Martin 2011) forcing a full-length match for sample tags and allowing a 2/3-length partial match for forward and reverse primers. Only reads containing both primers were retained. For each trimmed read, the expected error was estimated with vsearch's command fastq_filter and the option eeout. Each sample was then dereplicated, i.e. strictly identical reads were merged, using vsearch's command derep_fulllength, and converted to FASTA format.
To prepare for clustering, the samples were pooled and processed by another round of dereplication with vsearch. Files containing expected error estimates were also dereplicated to retain only the lowest expected error for each unique sequence. Clustering was performed with swarm v3.1.0 (Mahe et al. 2021), using a local threshold of one difference and the fastidious option. Operational taxonomic unit (OTU) representative sequences were then searched for chimeras with vsearch's command uchime_denovo (Edgar et al. 2011). In parallel, representative sequences were assigned using the stampa pipeline (https://github.com/frederic-mahe/stampa/) and a trimmed version of the reference database SILVA SSURef NR99 v138.1 (Quast et al. 2013).

Clustering results, expected error values, taxonomic assignments and chimera detection results were used to build a raw OTU table. Up to that point, reads that could not be merged, reads without tags or primers, reads shorter than 32 nucleotides and reads with uncalled bases ("N") had been eliminated. To create the "cleaned" OTU table, additional filters were applied to keep only non-chimeric OTUs, OTUs with an expected error per nucleotide below 0.0002, OTUs containing more than three reads or seen in at least two samples. All codes and representative OTU sequences can be found in HTML format (Supplementary File S1) and the raw data are available under the bioproject (https://www.ebi.ac.uk/ena/data/view/XXXXXX).

The OTU table was processed with R 3.5.2 (R Core Team, 2018) for additional filtering steps and statistical analysis with the packages tidyverse 1.3.0 (Wickham 2017).

3.3.5 aioA and 16S rRNA genes quantification

Abundance of the *aioA* gene (encoding the catalytic subunit of the arsenite oxidase) and of the bacterial 16S rRNA genes were quantified by a real-time PCR from the DNA extracts and from the cDNA. For 16S, we used universal primers 341F (5'CCTACGGGAGGCAGCAG-3') and 515R (5'ATTACCGCGGCTGCTGGCA-3'). For *aioA*, we used primers aoxB m4-1F (5'GCCGGCGGGGGNTWYGARRAYA-3') and m2-1R (5'GGAGTTGTAGGCGGGCCK RTTRGDAT-3) (Quéméneur et al. 2008). The quantification was performed with the CFX Real-Time PCR Detection system (Bio-Rad), using SsoAdvanced SYBRR® Green Supermix and each primer at 0.4 µM (16S rRNA gene) or 0.3 µM (*aioA* gene). Calculation of copy numbers was done as described in Cébron et al. (2008). A linear calibration curve ($r^2 > 0.9$) was obtained over 7 orders of magnitude, ranging from 10^2 to 10^8 gene copies of a linearized plasmid.

3.3.6 Biostatistics analysis

All statistical analyses were performed with R version 3. Chao1 and Shannon indices were calculated using the vegan and ggplot2 packages for biological diversity statistics in R (Wickham 2016; Oksanen et al. 2020). Bray Curtis was used as diversity metric to compare the bacterial communities from each bioreactor (R packages phyloseq and dplyr (McMurdie and Holmes 2013; Wickham et al. 2022)).
The analysis of similarity (ANOSYM, 999 permutations) was performed to compare the statistical differences between pre-defined groups. It allowed us to compare the results obtained for the structure of the bacterial communities based on the following criteria: biomass carrier WP versus PS, the different periods of monitoring, the total (DNA) versus the active (RNA) communities, and the suspended versus the attached bacterial communities (R package vegan, Oksanen et al. 2022).

A non-metric multidimensional scaling (NMDS) ordination was used to visualize bacterial community variations among samples, the differences among the structure of the communities are represented by the distance between the points. The Indicators Species Analysis was performed to identify the main species responsible for the differences in bacterial community composition between defined groups (R package indicspecies, De Caceres and Legendre 2009). Significant differences between the different groups were detected with one-way ANOVA (p-value 0.05) followed by Tukey test. The data that did not follow a normal distribution were analyzed by Kruskal-Wallis test. Finally, the correlations between biological and physicochemical variables were performed by the Spearman test, Spearman was used instead of Pearson's correlation due to non-normal distribution of the data (R package heatmaply, Galili et al. 2017).

3.4 Results

3.4.1 General description of the bacterial diversity

Illumina sequencing yielded a total of 5 119 340 sequences of bacterial 16S rRNA gene corresponding to 116 samples. Considering all periods together, based on Chao 1 (richness) and Shannon (evenness and richness) indices, the alpha diversity was higher (Kruskal-Wallis, p-value < 0.001) in the bioreactor filled with the wood and pozzolana (WP) than in the bioreactor with the plastic carrier (PS) (Figure 14.a). For both bioreactors, the alpha diversity of the suspended community sampled from the outlet water was lower than the one of the attached communities sampled from the biogenic precipitates (Kruskal-Wallis, p-value < 0.01) (Figure SI 10). Alpha diversity measured for the overall active and total bacterial communities were similar (Figure SI 12; Kruskal-Wallis, p-value > 0.05).

The results obtained for the beta diversity (reflecting the taxa turnover) did not follow the same trend as the one obtained for the alpha diversity. Indeed, we observed a higher beta diversity associated with the PS bioreactor compared to the WP bioreactor (Mann-Whitney; p-value <0.0001) (Fig 14.b). Also, the suspended community showed higher beta diversity than the

attached communities (Figure SI 10). Finally, the total bacterial community presented higher beta diversity than the active one (Figure SI 11).

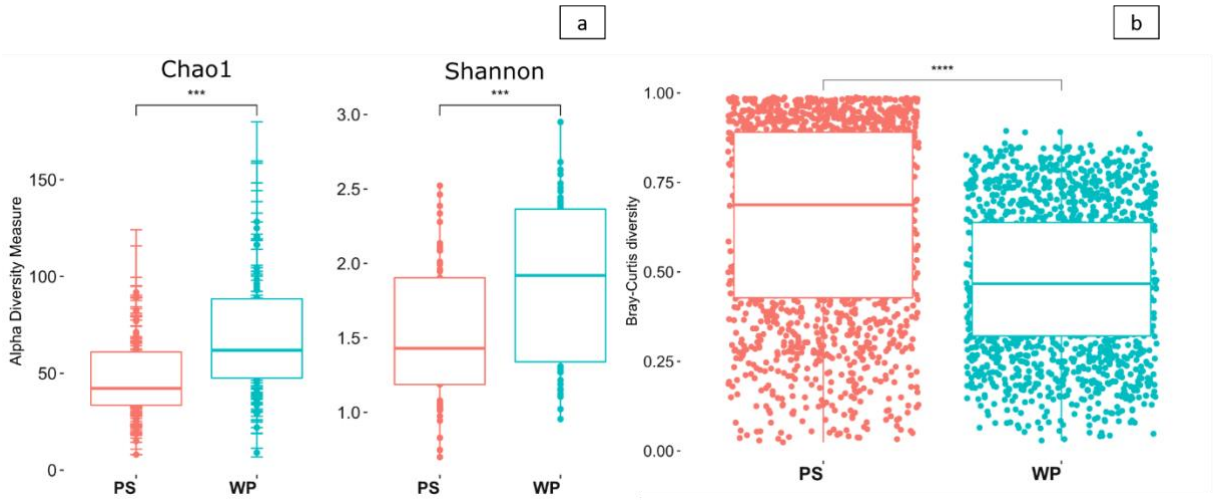

Figure 14. *Indices to measure diversity of the bacterial communities developed in PS and WP bioreactors; alpha diversity: Chao1 and Shannon (a), beta diversity (Bray-Curtis) (b). ("****" =p-value ≤ 0.0001, "***" p-value ≤ 0.001, "**"= p-value ≤ 0.01, "*"= p-value ≤ 0.05, "ns" = p-value > 0.05). These analyses include total and active communities.*

3.4.2 Dynamic of the bacterial community structures in the PS and WP bioreactors

The dynamic of the bacterial communities developed in both bioreactors was represented by non-metric multidimensional scaling (NMDS). In complement, an ANOSIM test was used to determine significant differences in the bacterial community composition of groups of samples. Groups were defined according to the sampling period, the nature of the biomass carrier, the lifestyle (attached versus suspended communities) and the metabolic status (total versus active communities). The most important differences were observed between the different periods of monitoring (represented by the different colors in the NMDS) (ANOSIM test, R 0.4463 p-value 0.001). There were marked variations of the bacterial community structure particularly between the first periods of monitoring (B and C), and the latest ones (D, E, F and G). These variations were more pronounced for the PS bioreactor than for the WP, reflected by the wider ellipse shown in Figure 15, and in agreement with the higher beta diversity measured in PS (Figure 14.b).

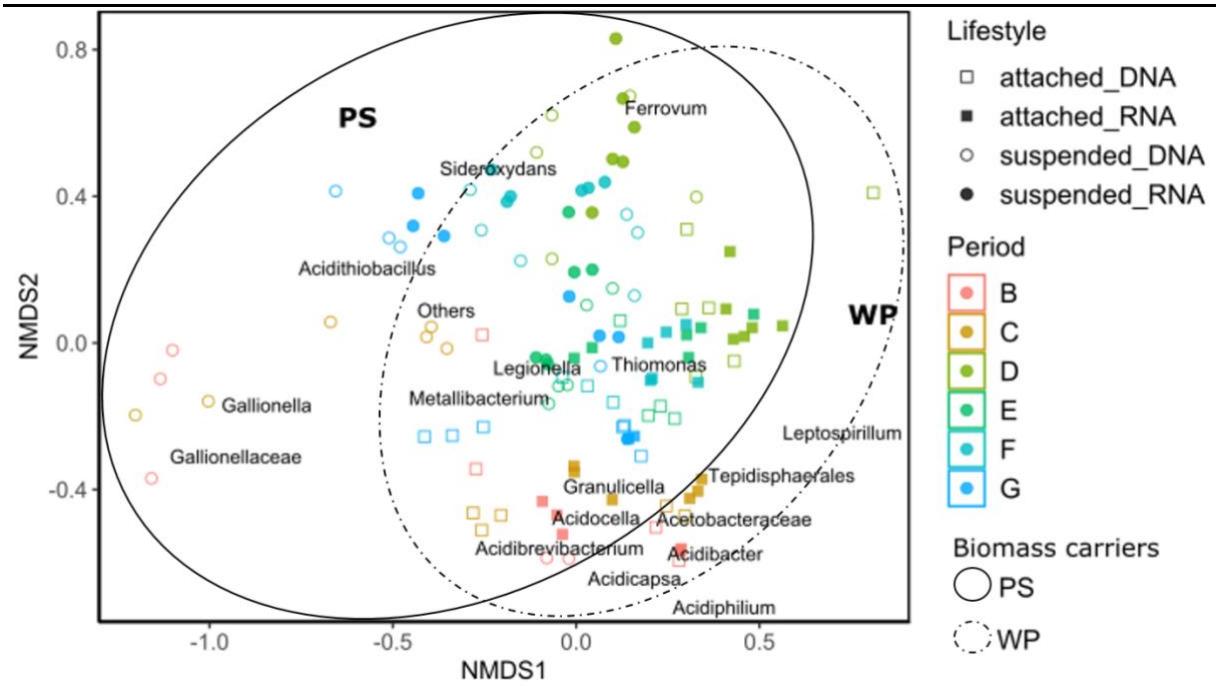

Figure 15. *NMDS with the main taxa (genus level) explaining the communities' differences (p-value ≤ 0.05). The symbols represent the structure of the bacterial communities of each sample. The shape represents the lifestyle (suspended or attached) and the status of the community (total community based on DNA analysis or active community based on RNA analysis). The colors represent the periods of monitoring (B, C, D, E, F and G). The two ellipses differentiate the samples from each bioreactor (dashed line for the WP samples and solid line for the PS samples).*

The influence of the lifestyle and of the biomass carrier was moderate compared to the temporal dynamic. The lifestyle was the second criteria driving the bacterial communities (suspended or attached in the biogenic precipitates) (ANOSIM test, R 0.1935 p-value 0.001) and the third criteria was the biomass carrier (plastic or wood/pozzolana) (ANOSIM test, R 0.1535 p-value 0.001). Finally, active communities were relatively distinct from the total ones during the first stage of the monitoring (period B and C). During the other periods, the structure of the active and the total communities appeared more similar. Overall, the status (total versus metabolically active) of the bacterial communities was the factor explaining the less the differences between the samples (ANOSIM test, R 0.05887 p-value 0.001).

Indicators species analysis revealed the bacterial taxa that contributed the most to the shifts in the bacterial communities. For instance, *Gallionella* and *Gallionellaceae*-related sequences dominated the PS bioreactor during periods B and C. *Acidicapsa*, *Acidiphium*, *Acidibacter*, *Acidibrevibacterium*, *Granulicella* and *Tepidsphareales*-related sequences were representative of samples collected in the WP bioreactor particularly during the first periods B and C. *Acidithiobacillus* was representative of samples collected in the PS bioreactor at the end of the monitoring (periods F and G). *Thiomonas* was representative of the total and the metabolically active bacterial communities in both bioreactors particularly during period E.

3.4.3 Taxonomic composition of the bacterial communities thriving in the two bioreactors

The most abundant phyla identified in the outlet water and the biogenic precipitates sampled in both bioreactors were *Proteobacteria* (62%) and *Nitrospirota* (35%). *Acidobacteria* was the third more abundant phylum, representing only 1% of the total number of sequences. On the whole data set, the dominant genera were the iron-oxidizing (FeOB) bacteria *Leptospirillum*, *Ferrovum, Acidithiobacillus* and an undetermined genus of the *Gallionellaceae* family. *Leptospirillum* was abundant and active from the beginning to the end of the monitoring, mainly in the biogenic precipitates. *Ferrovum* was more abundant and active in the suspended community (outlet water), particularly from the D period of the monitoring.

The dynamic of the FeOB populations was different in the two bioreactors (Figure 16). In the PS bioreactor, the first two periods B and C (December and February) were dominated by *Leptospirillum*, *Gallionella*, and an undetermined genus from *Gallionellaceae* family, while in the WP bioreactor, *Leptospirillum* was the only dominant FeOB. Then the FeOB populations evolved towards a dominance of *Ferrovum* and *Leptospirillum* in both bioreactors. At the end of the monitoring (period F and G) the communities of the PS bioreactor were enriched with *Acidithiobacillus. Gallionella* was mainly present and active during the first stage of the monitoring only in the suspended community of the WP bioreactor, but present in both suspended and attached communities in the PS bioreactor.
The sequences affiliated with *Gallionellaceae* family were dominant in PS bioreactor in the suspended and attached communities during period B and C, but their relative abundance dramatically decreased from period D. In a lesser extent, the same trend was observed for *Acidocella* and *Granulicella*.

Thiomonas was the sixth most dominant genus identified in the metabarcoding data. It was always detected in both the total and active communities, although its distribution showed a different pattern in the two bioreactors. In the WP bioreactor, *Thiomonas* was more abundant in the suspended community during period E (with a similar trend between total and active communities). On the contrary, in the PS bioreactor, *Thiomonas* was more represented in the attached community, with a stable abundance over time.
Acidiphillium was present in both bioreactors, for most of the monitoring period, but was more represented in the attached community than in the suspended community.
Metallibacterium was present in relatively low proportions in both systems (Figure 16), and RNA-based analysis showed that this genus was probably not metabolically active.

Indicator Species Analysis supported our previous observations about the bacterial genera representative of a particular group; in the attached communities (biogenic precipitates) the representative genera were *Acidiphilium, Leptospirillum, Acidibacter, Acidicapsa* for both bioreactors, and *Acidocella, Acidibrevibacterium* and *Granulicella* for WP only. On the contrary, *Ferrovum* and *Sideroxydans* were representative of the suspended community in both bioreactors. *Legionella* and an undetermined genus of *Acidobacteriaceae* family were representative of the suspended community only in the WP bioreactor.

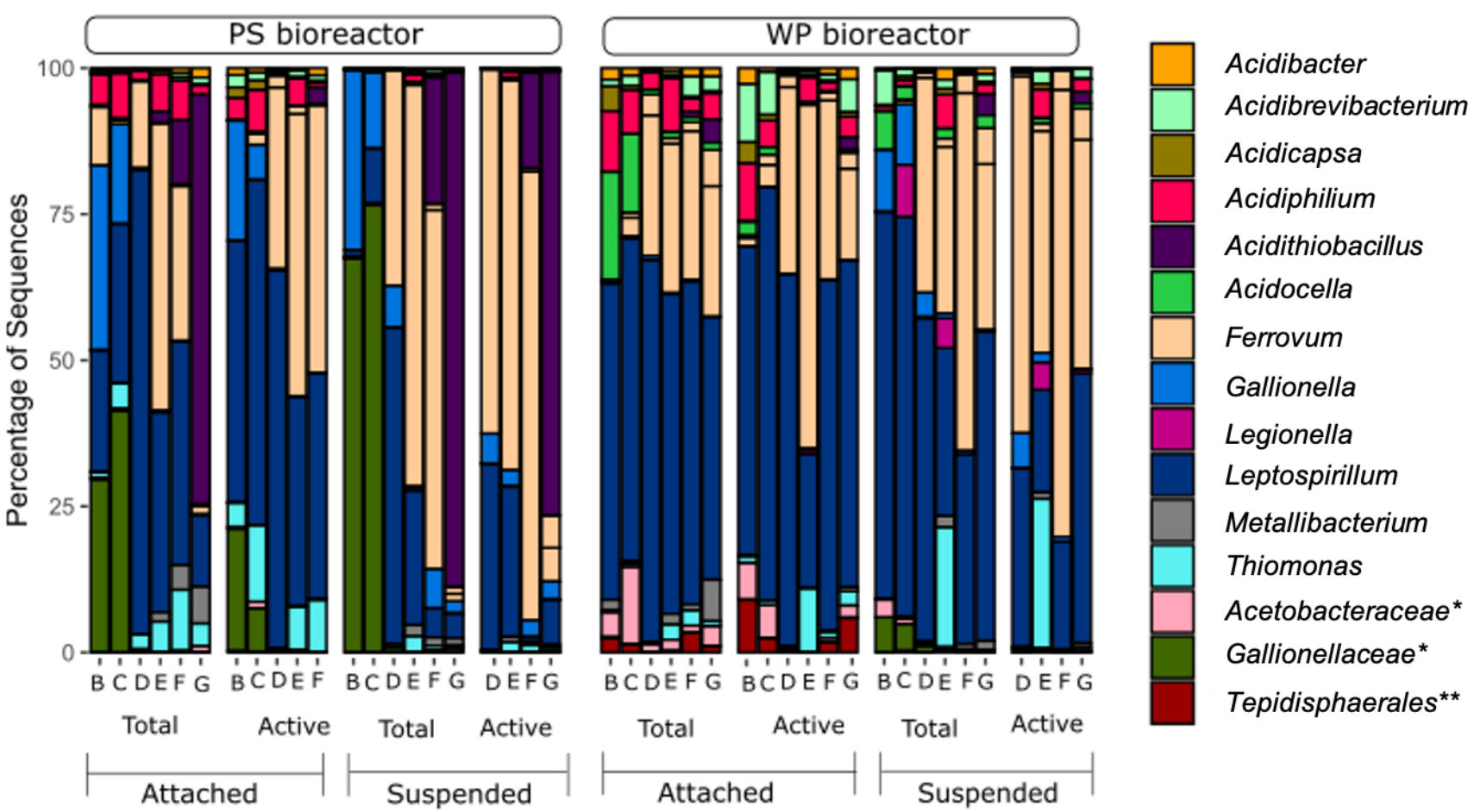

Figure 16. *Evolution of the relative abundances of the main bacterial genera (relative abundance > 0.05 % of total number of sequences) over the monitoring periods. The results are presented for the PS (plastic biomass carrier) and WP (wood and pozzolana as biomass carrier) bioreactors according to the different lifestyle (attached versus suspended) and to the status of the communities (total or active). When genus identification was not possible, classification was made at the family level (∗) or at the order level (∗∗).*

3.4.4 Abundance and expression of 16S rRNA and aioA genes

Based on environmental DNA analysis, the 16S rRNA gene copy number varied between 10^2 to 10^6 copies/mg of biogenic precipitate and between 10^4 to 10^7 copies/mL of water in both bioreactors (Figure 17.a and 17.b). The average bacterial biomass of the biogenic precipitates community was similar between both bioreactors (Figure 17.a). The average biomass of suspended communities in water remained stable between the inlet and the outlet water of the PS and WP bioreactors (Figure 17.b). The biomass varied over time without any clear trend (Figure S.I 3).

Results based on cDNA showed between 10^3 to 10^6 16S rRNA transcripts copies/mg of biogenic precipitate and between 10^3 to 10^5 16S rRNA transcripts copies/mL of water, without difference between the two bioreactors (Figure 17.a and 17.b).

Based on DNA analysis, the number of *aioA* genes in both bioreactors varied between 10^1 to 10^5 copies/mg of biogenic precipitate and between 10^2 to 10^6 copies/mL of water (Fig 5.c and 5.d). The number of genes and the number of transcripts of the arsenite oxidase were similar in both bioreactors (Figure 17.c and 17.d), except for the attached community of WP in which *aioA* transcripts remained below the detection limit (Figure 17.c). The expression of the arsenite oxidase gene (*aioA* transcripts) has been evidenced only in 14 samples over a total of 60 samples, and showed up to 150 transcripts copies/mL of water in the WP bioreactor during period E and up to 421 transcript copies /mg of biogenic precipitate in the PS bioreactor in period C (Figure SI 13). In the other samples, recovery of *aioA* transcripts was below the detection limit. The results suggest that the arsenite-oxidizing activity might be more expressed during period E and C, compared to other periods. However, technical limitations associated with mRNA extraction yield and cDNA synthesis could have interfered with the analysis.

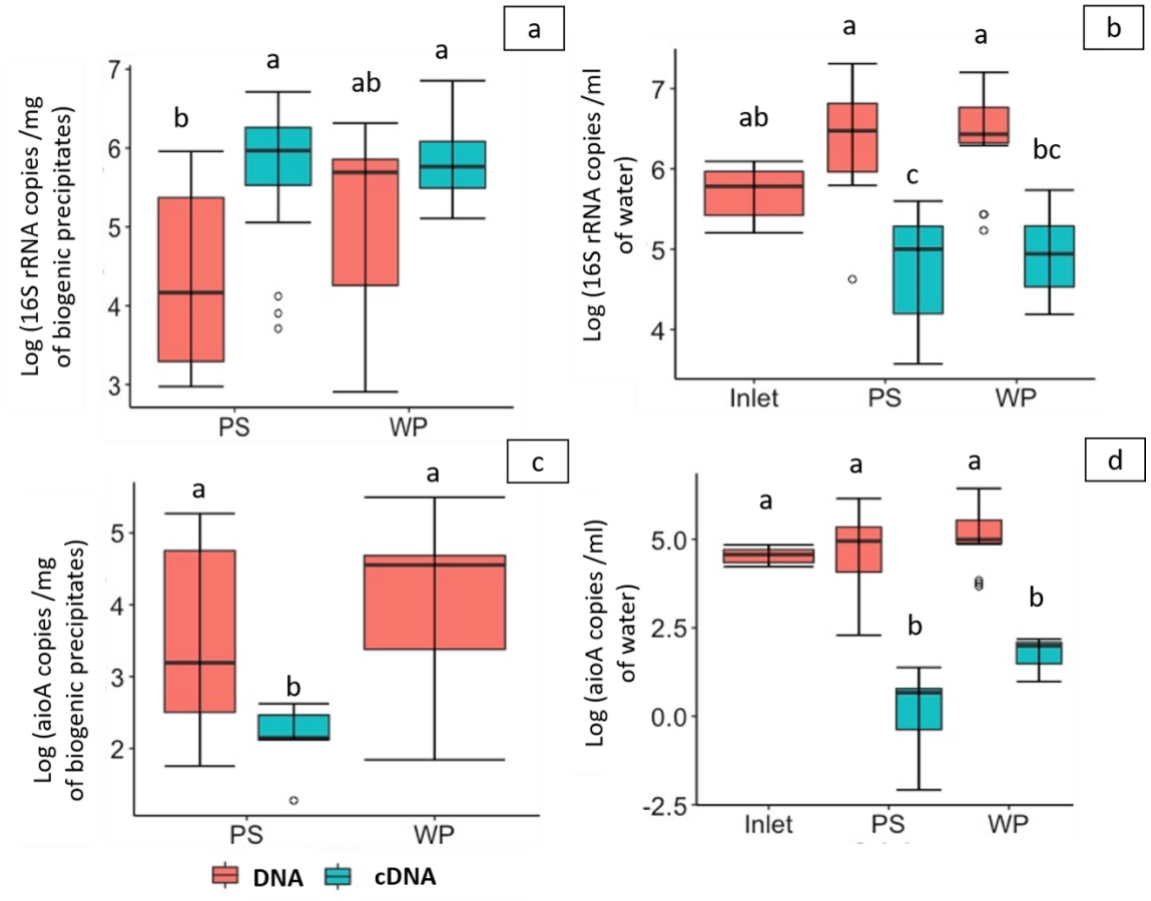

Figure 17. *Abundance of genes and transcripts in the biogenic precipitates' communities and in the water communities inside the two bioreactors (average of all the periods). 16S rRNA genes and transcripts in the attached community (a), and in the suspended community (b), aioA genes and transcripts in the attached community (c) and in the suspended community (d). Analyses were performed on DNA (presence of the genetic potential) and cDNA (gene expression / protein synthesis potential). Values annotated with the same letter are not significantly different (Tukey's multiple range test with p = 0.05). Average values for all periods. The quantification of the aioA transcripts from cDNA in the WP biogenic precipitates was below the detection limit.*

The relative abundance of bacteria carrying *aioA* gene in the bacterial community and its dynamic in the bioreactors were assessed based on *aioA*/16S rRNA genes ratio (Figure 18). In the WP bioreactor, the suspended bacterial communities sampled at period E was the most enriched in arsenite-oxidizing bacteria (0.6 copies of *aioA*/16S rRNA ratio). On the contrary, in the PS bioreactor, the attached communities were the most enriched in arsenite-oxidizing bacteria. The highest enrichment was observed for periods C, D and E (average of 0.35 copies of *aioA* /16S rRNA ratio).

The relative abundance of *aioA* gene varied widely according to the period, the bioreactor and the lifestyle but without any clear trend. For instance, the average of the relative abundances of arsenite oxidase gene was similar in the outlet waters of both bioreactors (0.09 ± 0.15 copies of *aioA* /16S rRNA ratio) and the feed water (Carnoulès AMD) (0.07 ± 0.02 copies of *aioA* /16S rRNA ratio).

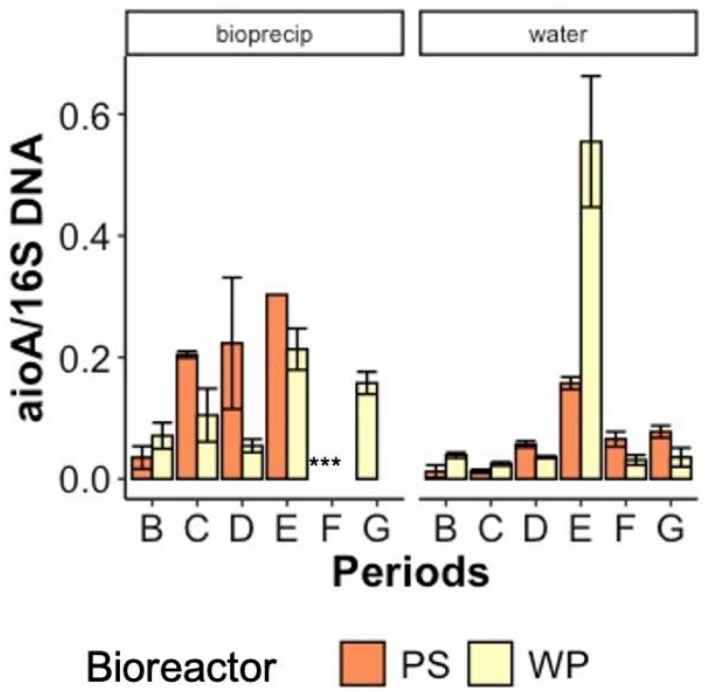

Figure 18. *aioA/16S rRNA genes ratio in the suspended (outlet water) and attached communities (biogenic precipitates) in the two bioreactors. Data are mean values (n= 3). *** the three asterisks correspond to period F (bioreactor PS and WP) and period G (only bioreactor PS), for which data are missing due to technical limitations.*

3.4.5 Links between the bacterial communities and the physicochemical characteristics of the AMD or the treatment performances.

Correlations between the microbiology (abundance of the most dominant bacterial taxa developed in the bioreactors) and the physico-chemistry of the AMD were assessed by calculating Spearman's coefficients (significant when the coefficient was ≥ 0.5 or ≤ -0.5). Correlations were also determined between the microbiology and the variables reflecting the performance of the treatment system (kinetic constant value KOFe), Fe precipitation rate, As precipitation rate, As(V) % in the outlet, pH outlet) or the operating conditions (HRT) (Figure 19).

The relative abundance of sequences related to *Ferrovum*, *Acidithiobacillus* and *Acidobacteriaceae* were positively correlated with dissolved As concentration, temperature and Fe(II) concentration in the inlet water (correlation > 0.5) as shown Figure 19. In a lesser extent, *Thiomonas* also showed a positive correlation with those parameters. On the contrary, taxa *Gallionella* and *Gallionellaceae* showed a negative correlation with those parameters (correlation -0.5). The relative abundance of arsenite-oxidizing bacteria (*aioA*/16S rRNA ratio) was positively correlated with the temperature, the total dissolved As concentration and the percentage of As(III) in the inlet water. The rates of Fe precipitation and As precipitation were strongly positively correlated with the relative abundance of *Ferrovum* (correlation 0.6 and 0.7 respectively). The percentage of As(V) in the outlet water was positively correlated with the relative abundance of arsenite-oxidizing bacteria *Thiomonas* (correlation 0.6) and in lesser

extent with *Acidobacteraceae*-undetermined genus and *Acidiphilium* (correlation 0.5). On the contrary, this parameter was negatively correlated with *Gallionella* and *Gallionellaceae*-undetermined genus (correlation -0.5).
The pH of the outlet water was positively correlated with the abundance of *Gallionella* and *Gallionellaceae*-undetermined genus (correlation 0.5). and negatively correlated with *Ferrovum* (correlation -0.7).

The relative abundance of the arsenite-oxidizing bacteria (*aioA*/16S rRNA genes ratio) was strongly positively correlated with *Thiomonas* (correlation 0.8). Two HRT were evaluated in both bioreactors (~9h and ~18h). There was a positive correlation between the relative abundance of *Acidibrevibacterium*, *Acidiphilium* and *Acidobacteriaceae* relative sequences and HRT. However, no significant correlations between the FeOB and the HRT were evidenced.

	As T inlet (mg/L)	Fe(II) inlet (mg/L)	T (°C) inlet	As(III) % inlet	pH inlet	KOFe (min-1)	Fe rate precipitation (mol/L·s)	As rate precipitation (mol/L·s)	As(V) % outlet	pH oulet	HRT (h)	*aioA*/16S rRNA ratio
Thiomonas	0.2	0.2	0.4	0.3	-0.3	-0.2	-0.1	-0.2	0.6	-0.3	0.3	0.8
Leptospirillum	-0.3	-0.4	-0.3	-0.4	-0.2	0.3	0.1	0.2	-0.2	0.2	-0.3	-0.1
Ferrovum	0.6	0.6	0.5	0.3	-0.5	0.3	0.7	0.6	0.3	-0.7	-0.3	0.4
Gallionella	-0.5	-0.4	-0.5	-0.4	0.1	-0.5	-0.3	-0.4	-0.5	0.5	-0.1	-0.4
**Gallionellaceae*	-0.6	-0.5	-0.6	-0.5	0.2	-0.4	-0.3	-0.4	-0.5	0.6	-0.1	-0.3
Acidithiobacillus	0.6	0.6	0.4	0.6	0.4	-0.2	-0.2	-0.2	0.2	-0.3	0.2	0.6
Sideroxydans	-0.1	-0.1	0.0	-0.2	-0.2	0.1	0.2	0.2	-0.1	-0.1	-0.2	-0.3
Acidicapsa	-0.2	-0.3	0.1	-0.1	-0.1	-0.4	0.0	-0.3	0.3	0.1	0.4	0.1
Acidiphilium	-0.2	-0.2	0.0	0.1	-0.1	-0.1	-0.5	-0.4	0.5	0.1	0.5	0.6
Acidibrevibacterium	0.0	0.0	0.1	0.2	0.3	0.0	-0.4	-0.4	0.4	0.0	0.7	0.0
**Acidobacteriaceae*	0.5	0.5	0.4	0.5	0.1	-0.1	-0.2	-0.2	0.5	-0.2	0.5	0.6
**Acetobacteraceae*	-0.3	-0.4	-0.2	-0.1	0.1	0.2	-0.3	-0.3	0.1	0.2	0.4	-0.1
***Tepisphaerales*	0.0	0.0	0.0	0.1	0.1	0.1	-0.3	-0.2	0.3	0.1	0.4	0.0
aioA/16S ratio	0.6	0.5	0.6	0.7	-0.4	-0.1	0.4	0.1	0.6	-0.3	0.2	1.0

Spearman Correlation
-1.0 -0.5 0.0 0.5 1.0

Figure 19. *Heat map of the Spearman correlation coefficients between relative abundance of the most dominant genera (horizontal axis) and physicochemical, operational parameters or performances indicators (vertical axis). The parameters used are presented in Table 10 and Supplementary Table S2. The first group includes the main parameters of the inlet water (considering all the dataset). The second group includes the performance indicators (considering only the periods with optimal performances B-E). The third group corresponds to the operational parameter HRT (also considering only the periods B-E). Correlation analyses were performed with the abundance of the whole total and active communities (based on DNA and RNA analyses). The last group corresponds to the relative abundance*

of the arsenite-oxidizing bacteria (correlation performed only with the abundance of the total communities (based on DNA analyses).

3.5 Discussion

This study aimed to characterize the dynamics of the total and active bacterial communities thriving in two iron-oxidation bioreactors, filled with different biomass carriers and treating a real As-rich AMD *in situ*. The one-year monitoring covered seasonal variations associated with a variability of environmental conditions (e.g temperature) and changes in the chemistry of the AMD.

3.5.1 Characterization of the total and active bacterial communities

In the two bioreactors, both total and active bacterial communities were dominated by several iron oxidizing bacterial genera (FeOB) (*Leptospirillum*, *Ferrovum*, *Acidiothiobacillus*, an undetermined genus of *Gallionellaceae*, and *Gallionella*). *Ferrovum* was over-represented in the active community (37% and 21% in the whole RNA and DNA data sets respectively). This finding is in line with the probable important role played by this iron oxidizing bacteria in the treatment (Sheng et al. 2016; Wang et al. 2016; Grettenberger et al. 2020). *Leptospirillum* followed the same trend but in a lesser extent (38 and 36% respectively). On the contrary, *Acidithiobacillus*, undetermined genus of *Gallionellaceae* and *Gallionella* were globally more abundant in the total community than in the active one, suggesting a possible limited contribution of these taxa to the treatment process. In particular, *Acidithiobacillus* represented 9 % of the total DNA sequences and only 5 % of the cDNA sequences reinforcing the idea of its possible lower efficiency in remediation systems compared to other FeOB (Heinzel et al. 2009; Laroche et al. 2018). Ebrahimi et al. (2005) observed that the short dominance of *Acidithiobacillus ferroxidans* in attached community was accompanied by a treatment efficiency limited to 90% while a shift towards *Leptospirillum* dominance probably contributed to an increase of the performances up to 98%. The dominance of *Leptospirillum* in the active communities during the first two periods in both bioreactors can be explained by its dominance in the AMD feeding water (data not shown).

Ferrovum was more represented in the suspended community than in the attached one. *Ferrovum* has the capacity to release extracellular polymeric substances (EPS) (Johnson et al. 2014; Plewniak et al. 2020), which could promote its development in the small iron flocs suspended in the outlet water (Florence et al. 2016). *Ferrovum* has been previously associated with “acid streamers”, which are macroscopic biofilms formed by acidophilic microorganisms due to the bacterial release of EPS (Hedrich and Johnson 2012; Kay et al. 2013). EPS could also promote mineral precipitation in the suspended fraction (Florence et al. 2016; Hoffmann et al. 2021).

Thiomonas was the fourth most abundant genus active in similar proportions in both bioreactors (4% of the whole cDNA sequences and 2% of the whole DNA sequences). *Thiomonas* was

present in a relative similar abundance in a laboratory iron oxidation bioreactor treating the Carnoulès AMD (2% of DNA sequences, Fernandez-Rojo et al. 2018). These proportions are higher but of the same order of mangnitude as those found in the Regious Creek sediments (1.1% of DNA sequences, Laroche et al. 2018). The occurrence and role of these arsenite-oxidizing bacteria will be further discussed in a next section of the discussion. Heterotrophic iron reducing bacteria were detected in the bioreactors: genera *Acidibacter* (0.6 % of the total and of the active community), *Acidocella* (1.7% DNA and 0.3% RNA) and *Metallibacterium* (1.3 % DNA and 0.3 % RNA). They have been previously reported in acidic mine waters (Afzal Ghauri et al. 2007; Johnson et al. 2014; Gavrilov et al. 2019) and in iron oxidizing bioreactors (Sheng et al. 2016; Jin et al. 2020). Genus *Acidiphillum* (3% DNA and 2.5% RNA) includes mixotroph species, which can switch between chemoheterotrophy and chemoautotrophy depending on the conditions, which is a great advantage in an oligotrophic environment as the AMD (Hao et al. 2010). Most of these iron reducing bacteria are characterized by a metabolic versatility including iron-reduction, carbon-fixation and sulfur oxidation capacities (Bartsch et al. 2017; Gavrilov et al. 2019). These versatile bacteria were poorly represented in the active community during most of the monitoring. However, their presence requires special attention: operational conditions and especially oxygenation should be carefully controlled to avoid suitable conditions for ferric iron reduction, which would contribute to As remobilization into the aqueous phase (Tufano and Fendorf 2008). Arsenic remobilization has been evidenced from river sediments impacted by the Carnoulès AMD during incubation under anoxic conditions (Héry et al. 2014).

3.5.2 Influence of the biomass carrier on the bacterial diversity

Biomass carriers provide a physical support for bacterial growth, extend their survival rate, enhance oxygen transfer, and sustain biofilm development (Tyagi et al. 2011). Al-Amshawee et al. (2021) reported that the biomass attached to the carriers can be up to 500 times more resistant than suspended bacteria to sudden changes. In the present study, the bacterial community developed on WP biomass carrier was richer (number of OTUs) than the community developed in the PS carrier (Figure 14). Differences between the two types of carriers in term of taxonomic composition of the bacterial communities mainly concerned the first stage of the monitoring. Indeed, during the early-stage, bacterial community developed on the PS biomass carrier was dominated by chemoautotrophs (i.e. *Galionellla* and *Leptospirillum*), while the bacterial community associated with WP carrier was composed by both chemoauthotrophs (i.e. *Leptospirillum*, *Acidiphillum*) and chemoheterotrophs (i.e *Acidobacteriaceae*, *Acidocella*, *Acidiphillum*, *Acidicapsa*, *Acidibacter* and *Acidibrevibacterium*).

Our first assumption to explain these differences was that organic carbon provided by the wood chips could promote the development of heterotrophic bacteria. The wood chips are often used in bioreactors as biofilm support as well as a source of organic carbon or electron donors (Lopez-Ponnada et al. 2017; Zhao et al. 2019). This idea concurs with occasional measurements

of total organic carbon in the biogenic precipitates accumulated in the two bioreactors, indicating a much higher concentrations in the WP (71 ± 47 g/kg) than in the PS (3 ± 0.7 g/kg (dry wt.). However, the difference was minor in the treated waters (outlet water WP: 5 ± 2 mg/L; PS: 3 ± 1 mg/L). Thus, it cannot be excluded that the organic carbon from the WP carrier corresponded to refractory organic matter that cannot be metabolized by the bacteria. Furthermore, no known cellulolytic bacteria were evidenced in the WP bioreactor. Consequently, the metabolic pathways involved on organic carbon cycling in the WP bioreactor would require further investigations.

Our second assumption to explain the differences of bacterial communities thriving on the two types of biomass carriers is related to their surface properties (i.e shape, porosity, surface roughness) and composition. According to Pereira et al. (2000) and Campos-Quevedo et al. (2021) the surface roughness is the most important parameter for bacterial colonization, mainly because the irregularities in the surface promote initial colonization and protect microorganisms from detachment. Thus, crevices, cracks and grooves present in the wood chips could allow more diverse micro-habitats and for consequence a higher alpha diversity.

Gallionella spp. and an undetermined genus of *Gallionellaceae* were the main OTUs responsible for the initial differences among the communities associated to each bioreactor: they were dominant in the PS bioreactor. *Gallionella* produces a variety of exopolymers that could be an advantage for the attachment on the plastic biocarrier (Emerson et al. 2013). Furthermore, the organic carbon rich environment provided by the wood chips may have inhibited the proliferation of *Gallionella*, explaining why these bacteria were poorly represented in the WP bioreactor. According to Fleming et al. (2014), *Gallionella* negatively co-occurred with high concentrations of organic carbon.

Despite these differences observed during the early stages, WP and PS bioreactors showed similar performances for all the periods of the monitoring. This suggests that the bacterial groups that differ between the two supports may not play an important role in the process. The similarities between the communities in the two bioreactors may be related to the fact that after some time, both carriers are covered by the same mineral phases: jarosite, amorphous schwertmannite and amorphous ferric arsenate (Diaz-Vanegas et al. 2022), which replace the wood chips and plastic carriers as support for biomass attachment. Such replacement of biomass carrier by precipitated minerals was described by Ebrahimi et al. (2005). Kinnunen et al. (2004) and Wang et al. (2012) also showed the role of jarosite on the attachment of FeOB in a fuidized-bed reactor and its efficiency to maintain a stable bacterial concentration that enhance iron oxidation and promote Fe(III) precipitation by acting as jarosite seed.

Despite similar overall performances, differences were observed between the two bioreactors in term of microbial ecology (diversity) and system functionality (capacity to recover after operational disturbances). In particular, a higher alpha diversity was evidenced in the WP bioreactor (Figure 14.a). Feng et al. 2017 reported that higher diversity can be associated with improved resilience to disturbances. This agrees with the better ability of the WP bioreactor to recover its performance (in term of Fe oxidation and precipitation, and of As removal) after

operational disturbances (interruptions, changes in the HRT and clogging of the air diffusers) (Diaz-Vanegas et al. 2022).

3.5.3 Arsenic oxidation

The role of *Thiomonas* spp. in arsenic oxidation in Carnoulès ecosystem has been demonstrated (Bruneel et al. 2003; Morin et al. 2003; Casiot et al. 2006). The activity of arsenite oxidase was evidenced *in situ* in the Reigous by a proteomic approach (Hovasse et al. 2016). The detection of *Thiomonas* by CARD FISH and metabarcoding recently suggested that arsenite oxidation occurred in a pilot treating arsenic rich AMD *in situ* and was probably mediated by *Thiomonas* (Laroche et al. 2018). Here, we evidenced for the first time, the expression of the arsenite oxidase gene concomitant with the presence of metabolically active *Thiomonas* in a bioreactor. Furthermore, the relative abundances of *aioA* genes and *Thiomonas* related 16S rRNA sequences (Figure 18) were positively correlated. These result confirmed the contribution of arsenite oxidation (mediated by *Thiomonas* spp.) to the treatment process.

Arsenite oxidase gene (*aioA)* was detected in all the biogenic precipitates and the outlet waters of both bioreactors, confirming the stable presence of arsenite-oxidizing bacteria in these treatment systems as observed in a previous field pilot (Laroche et al. 2018). The relative abundance of arsenite-oxidizing bacteria strongly varied depending on the nature of the samples (biogenic precipitates or water) and the period, with a particular enrichment in the suspended community of the WP bioreactor during period E. In the PS bioreactor, the highest concentrations were observed during period C, D and E. Our results suggest that arsenite-oxidizing bacteria may represent higher proportions of the total community compared to what was described in other systems. For instance, samples from geothermal areas have showed a relative abundance of *aioA* ranging from 0.1 to 19.5% (Sonthiphand et al. 2021). In groundwater systems of an old tin mine, the relative abundance of *aioA* gene ranged from 0.85 to 37.13%. In these waters, the highest As concentration was 10 µg/L. High arsenic concentrations (50 to 100 mg/L) mainly in the As(III) form in the Reigous AMD might explain the elevated concentration of As-oxidizing populations quantified in the Reigous AMD (inlet water) that fed the PS and WP bioreactors. However, the operational conditions applied in the bioreactors did not evidence any enrichment in As-oxidizing populations inside the treatment units (Figure 17.d).

The highest abundances of *aioA* genes and *aioA* transcripts were observed during period E, where an increase of *Thiomonas* related sequences was also noticed (Figure 17). Period E was characterized by an increase of temperature by more than 5°C, an increase of the total Fe concentration (~ 100 mg/L), and total As concentration (~ 15 mg/L) (Table 10 and Diaz-Vanegas et al. 2022). Similarly, Tardy et al. (2018) showed in batch experiment that high temperature stimulated arsenite oxidation associated with an increase of both the abundance of *aioA* genes and of *Thiomonas* spp. Quemeneur et al. (2010) found high *aioA* gene densities associated with high concentration of As in surface water.

In the present study, arsenite-oxidizing bacteria distribution was different in the two bioreactors: they were more represented in the attached community in the PS bioreactor, and in the suspended one in the WP bioreactor. In opposition to the common idea that the formation of a carrier-attached biofilm enhances bacterial activity, Michel (2007) showed that As(III) oxidation activity of some *Thiomonas* strains was higher for the planktonic cells (suspended) than for the sessile ones (attached). This is in agreement with our results, for the WP bioreactor, but contradictory with the results obtained for the PS bioreactor. Consequently, arsenite oxidation by *Thiomonas* in the studied bioreactors did not seem to be conditioned by their lifestyle (attached or suspended). It is also possible that the *Thiomonas* strains coming from the Reigous AMD developed in the PS and WP bioreactors were able to switch from attached to suspended mode as reported by Farasin et al. (2017).

Arsenic oxidation activity led to the enrichment into As(V) in the biogenic precipitates (80 ± 11 %) and in the outlet water (41 ± 26 %, compared with 25 ± 5 % in the inlet water) (Diaz-Vanegas et al. 2022). Because of the higher affinity of As(V) for iron minerals (Paikaray 2015), As removal under its oxidized form is more efficient and stable. Thus, of bacterially mediated As oxidation occurring in these field bioreactors contributes to As removal efficiency.

3.5.4 Geochemical and environmental factors influencing bacterial diversity and activity

In AMD affected environments, bacterial diversity is under the control of geochemical and environmental parameters (Méndez-García et al. 2014, 2015; Volant et al. 2014). As supported by Spearman correlations, pH, dissolved Fe(II) and As concentrations as well as water temperature were drivers determining the dynamic of FeOB and As(III) oxidizers populations thriving in the iron oxidizing bioreactors. pH is considered as one of the main variables shaping microbial communities in the AMD emplacements. This important influence of pH is mainly due to its relationships with other geochemical variables such as minerals solubility, which basically controls the dissolved As and Fe concentration present in the AMD (Jones et al. 2015; Méndez-García et al. 2015).

In the present study, *Gallionella* and *Gallionellaceae*-related sequences showed a positive correlation with pH of both inlet and outlet waters. The decrease of their relative abundance in the PS bioreactor coincided with the decrease of the pH. From period D, the bacterial communities inside the bioreactors were enriched with *Ferrovum* that is known for its capacity to grow in more acidic conditions than *Gallionella* (Ziegler et al. 2013). Accordingly, *Ferrovum* showed a negative correlation with pH. All these findings are consistent with previous studies showing that *Gallionella* is favored at pH > 3 while *Ferrovum*, are favored at pH < 3 (Heinzel et al. 2009; Jones et al. 2015; Sheng et al. 2017).

In AMD, dissolved ferrous iron (Fe(II)) is one of the main energy source for bacteria; thus, its concentration is another important factor determining geochemical niches of FeOB (Jones et al. 2015). Here, *Gallionella* and *Gallionellaceae*-related sequences were negatively correlated with Fe(II) concentration as described elsewhere (Fleming et al. 2014). The abundance of

Ferrovum increased during period D and E in both bioreactors concomitantly to the increase of the Fe(II) concentration in the inlet water. Assignment of *Ferrovum* to high iron concentration was also reported by Jones et al 2015.

In the PS bioreactor, *Acidithiobacillus* abundance increased when the highest Fe(II) concentration (712-1049 mg/L) was measured in the inlet water (periods F and G). This is in contradiction with other studies (Jones et al. (2015) that reported *Acidithiobacillus* spp. restricted to lower Fe(II) concentration (< 224 mg/L). Our results suggest that another factor should be responsible of the dynamic of *Acidithiobacillus* in the PS bioreactor at the end of the monitoring. During periods F and G, oxygenation was not optimal due to the clogging of the aeration system. Such oxygen limitation could be detrimental to *Ferrovum* and *Leptospirillum* (Ziegler et al. 2013; Johnson et al. 2014). Conversely, the capacity of *Acidithiobacillus* to live in microaerophilic conditions has been widely described (Dave et al. 2008). Thus, the dynamic of *Acidithiobacillus* in the bioreactors may be attributed to the synergy of the lack of oxygenation, the different biomass carrier used or another undetermined factor.

Active oxygenation could actually also be considered a relevant factor in the dynamics of other taxa such as *Gallionella* and *Gallionellacea* undetermined genus. Different genera of *Gallionellacea* family are microaerophilic (i.e *Gallionella* and *Sideroxydans*) (Fabisch et al. 2013; Mühling et al. 2016). Thus, their abundance during period B and C in the PS bioreactor could be promoted by the batch conditions between the period A and B, during the interruption of bioreactors operation (when the water circulation and aeration were stopped).

In addition to pH, Fe(II) concentration and oxygen, other parameters that influence bacterial diversity in the bioreactors were dissolved arsenic concentration and water temperature, as previously observed by Laroche et al (2018) and Tardy et al. (2018). Indeed, as discussed in a previous section, the present study supports the positive influence of temperature on the raise of the relative abundance of *Thiomonas* spp / arsenite-oxidizing bacterial populations. In contrast, *Gallionella* and *Gallionellaceae*-related sequences were negatively correlated with arsenic concentration and temperature of the inlet water, also observed by Fleming et al. (2014). Another interesting result was the positive correlation between *Ferrovum* abundance and temperature and arsenic concentration in the inlet water (as shown Figure 7). To our knowledge, such correlations have not been described before. They revealed the adaptation of *Ferrovum* to high arsenic concentrations, which makes it a good candidate for the bioremediation of highly arsenic-rich effluents.
On the contrary, *Gallionella* and *Gallionellaceae*-related sequences were negatively correlated with arsenic concentration suggesting their possible poor adaptability for the treatment of As rich AMD.

3.5.5 Links between treatment performance and microbiology

To date, there have been no other studies exploring the links between the active bacterial community dynamics and the performances of an iron-oxidizing bioreactor treating high-As AMD under field conditions.

The integrated analysis of performance indicators (As and Fe precipitation rates and Fe(II) oxidation kinetic constant KOFe) and microbiological variables provides insights about the relationships between total and active bacterial diversity and treatment efficiency during periods of optimal operation (B-E). The abundance of total and active *Leptospirillum* and *Ferrovum* were positively correlated with performance indicators. Both genera are well known for their highly efficient iron oxidation activity (Chen et al. 2020; Johnson et al. 2014). Although they do not directly contribute to As transformation, the maintenance of their activity even at high As concentration (50 – 100 mg/L) is an important point to consider for the treatment of high-As AMD.

Slight differences were observed in the composition of the bacterial communities developed in the two bioreactors, particularly in the beginning and at the end of the monitoring, as well as some differences in the distribution of key bacteria like *Thiomonas* spp. (both total and active) among the suspended and attached community.

Despite these differences, the general performances in terms of As and Fe oxidation and removal were similar in both bioreactors. The global stability of the system performances (including both the temporal stability and the capacity to recover the performances after disturbances) may rely on functional redundancy of the bacterial communities developed in both bioreactors. Functional redundancy is based on different taxonomic groups sharing similar functions, which allow the performance of a system to be maintained even when the community structure changes (Allison and Martiny 2008). Thus, the robustness of the treatment system may rely both on the resilience capacity and the functional redundancy of the bacterial communities. This is in line with the uncoupling between the resilience in function and the resilience in bacterial diversity described by Mills et al. (2003) .

3.6 Conclusion

The use of high-porosity biomass carriers and optimized operating conditions including aeration allowed the development of active bacterial communities that mediated more stable Fe- and As-removal performances compared to the previous field-pilot (filled with sand as biomass carrier, Fernandez-Rojo et al. 2019).

The nature of the biomass carrier (plastic or mix wood/pozzolana) influenced the bacterial community structure during the first stages of the bacterial colonization; then communities with similar taxonomic composition were established in both bioreactors. The bioreactor filled with wood and pozzolana (WP) showed a faster recovery of its performances after interruptions that may be attributed to a higher bacterial richness. This ecological and low-cost filling material could therefore be preferred for future up-scaling.

The bioreactors were dominated by diverse FeOB, whose dynamic was under the influence of pH, dissolved Fe and As concentration and temperature. The over-representation of *Ferrovum* in the active community, together with the positive correlation between its abundance and the

highest treatment performances, confirmed its central role in the treatment efficiency. Furthermore, *Ferrovum* appeared particularly well adapted for the treatment of arsenic rich effluents. *Leptospirillum* was another permanent member of the active community throughout the monitoring, which suggests its contribution to the stable performances.

Arsenic removal was accompanied by arsenate enrichment in the biogenic precipitates. The contribution of *Thiomonas* spp. to arsenic removal through As(III) oxidation was supported by its constant presence in the metabolically active communities thriving in both bioreactors. Furthermore, the expression of the arsenite oxidase gene (*aioA*) was evidenced for the first time in the treatment bioreactors under field-conditions. More effort is required to optimize the quantification of *aioA* expression to better identify the factors regulating the expression of this key function.

We demonstrated that the studied bioreactors promoted the development of stable and active bacterial populations responsible for the removal of arsenic mainly under its oxidized form (As(V)), which is clear advantage for future application in bioremediation. The resilience of bacterial communities to operational disruptions and variability of the chemistry of the AMD of on-site treatment is an essential point in the perspective of a large-scale AMD treatment.

3.7 Supplementary Information

Table SI 2. *Chemical characterization of inlet and outlet waters and performance indicators for the sampling dates where microbioligical analyses were performed*

Date (dd.mm.yy)	Period	Flow rate	HRT (h)		pH inlet	Temp.	As T inlet	Fe (II) inlet	As(III) inlet	KOFe (min -1)		Fe rate prec. (mol/L*s)		As removal ratio (min -1)		As(V) outlet %		TOC outlet (mg/L)	
		(L/h)	PS	WP		(°C)	mg/L	mg/L	%	PS	WP	PS	WP	PS	WP	PS	WP	PS	WP
19.12.19	B	15	17.5	19.3	4.82	13.9	53.64	501	73	2.50 E-03	3.30 E-03	6.20 E-08	5.80 E-08	3.60 E-04	2.10 E-04	9.7	34.5	2.32	5.44
06.02.20	C	15	17.5	19.3	4.11	8.3	49.5	448.9	71	2.20 E-03	2.90 E-03	4.90 E-08	5.40 E-08	3.80 E-04	2.26 E-04	38.4	40.3	3.03	3.54
12.03.20	D	30	8.8	9.7	3.87	14.1	70.7	665.2	71	2.90 E-03	4.60 E-03	1.30 E-07	1.30 E-07	9.80 E-04	6.70 E-04	20.2	13.9	2.89	3.01
18.06.20	E	15	17.5	19.3	3.79	22.3	88.1	732.3	80	2.75 E-03	3.00 E-03	1.20 E-07	1.25 E-07	3.30 E-04	2.10 E-04	61.2	96.5	NA	NA
27.07.20	F	30	8.8	9.7	4.12	20.2	93.1	820.7	78	3.54 E-04	1.50 E-03	3.20 E-09	1.04 E-07	8.60 E-04	6.90 E-04	27.9	19.5	4.02	4.61
15.09.20	G	15	17.5	19.3	4.44	20.5	91.0	768.6	82	1.20 E-03	2.30 E-03	5.80 E-08	7.10 E-08	3.90 E-04	3.30 E-04	78.9	87.5	4.56	4.13

Date (d.m.y)	Period	Total As (wt%)		Total Fe (wt%)		As/Fe (mol/mol)		%As V (wt%)	
		PS	WP	PS	WP	PS	WP	PS	WP
19.12.19	B	10.7	4.9	37	22	0.39	0.30	81	88
06.02.20	C	NA	NA	NA	NA	NA	NA	NA	NA
12.03.20	D	9.1	5.7	36	28	0.34	0.27	69	53
18.06.20	E	8.6	8.3	36	32	0.32	0.35	77	78
27.07.20	F	8.3	5.0	31	25	0.36	0.26	83	83
15.09.20	G	12.2	8.4	33	25	0.49	0.45	92	94

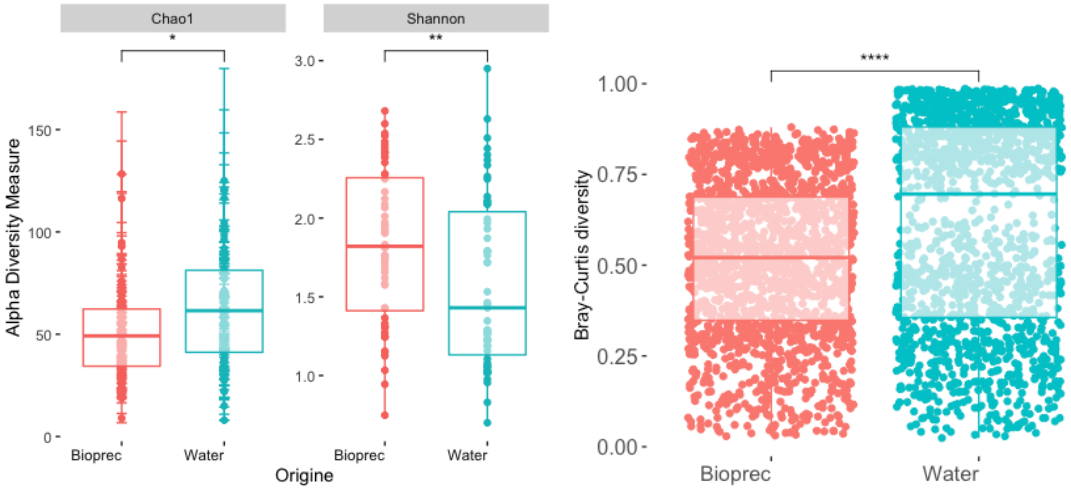

Figure SI 10. *Indices of alpha and beta diversity obtained from the different types of samples (biogenic precipitates and water).*

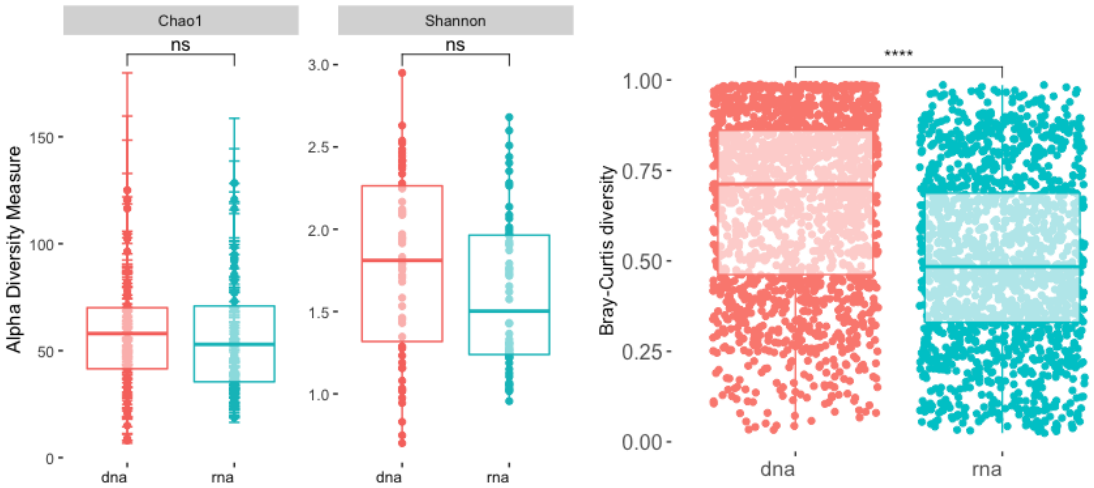

Figure SI 11. *Indices of alpha and beta diversity obtained from the DNA and RNA extracts.*

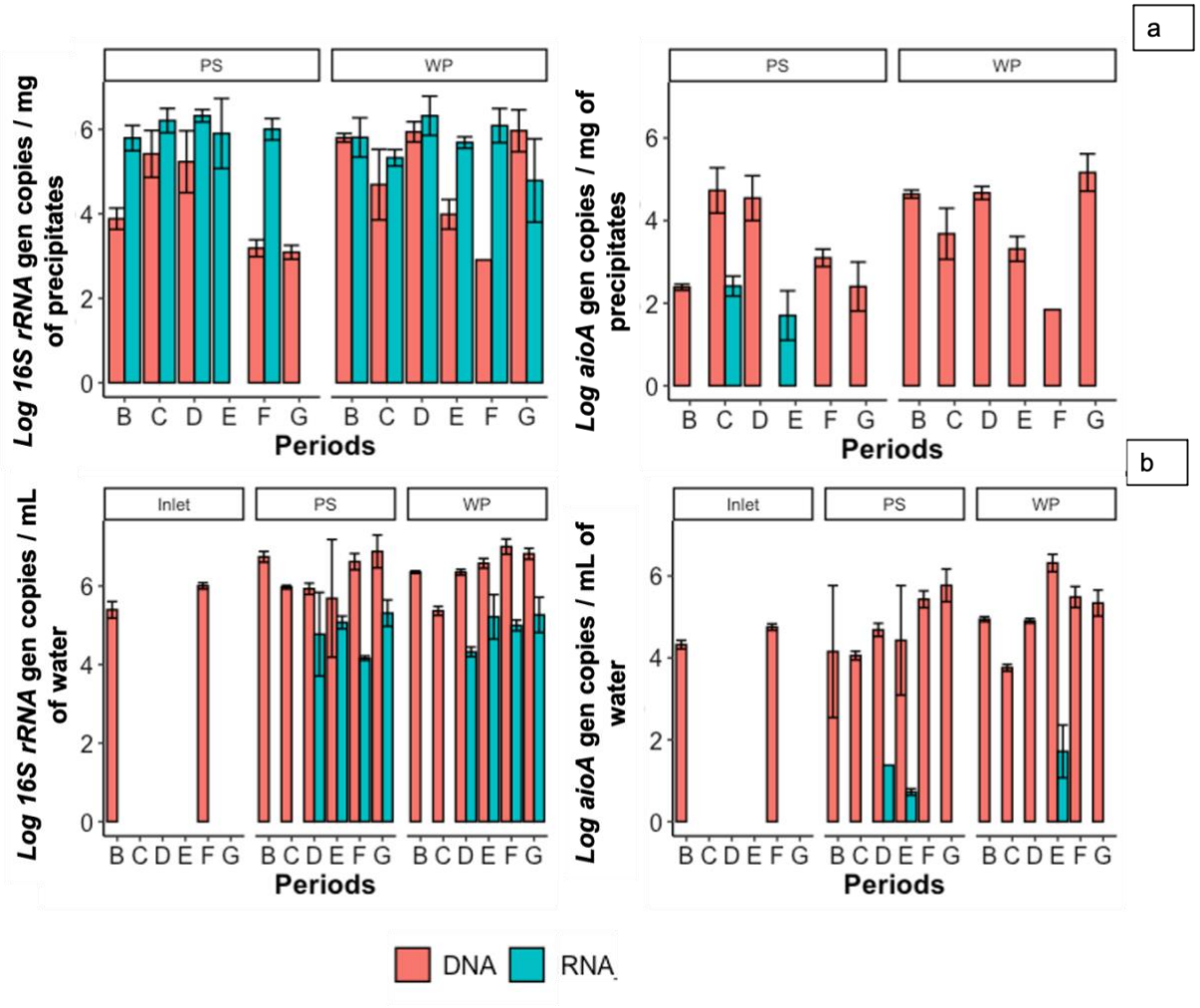

Figure SI 12. *Log Gen #copies / mg of biogenic precipitates along the periods of monitoring (a). Log Gen #copies / mL of water (b).*

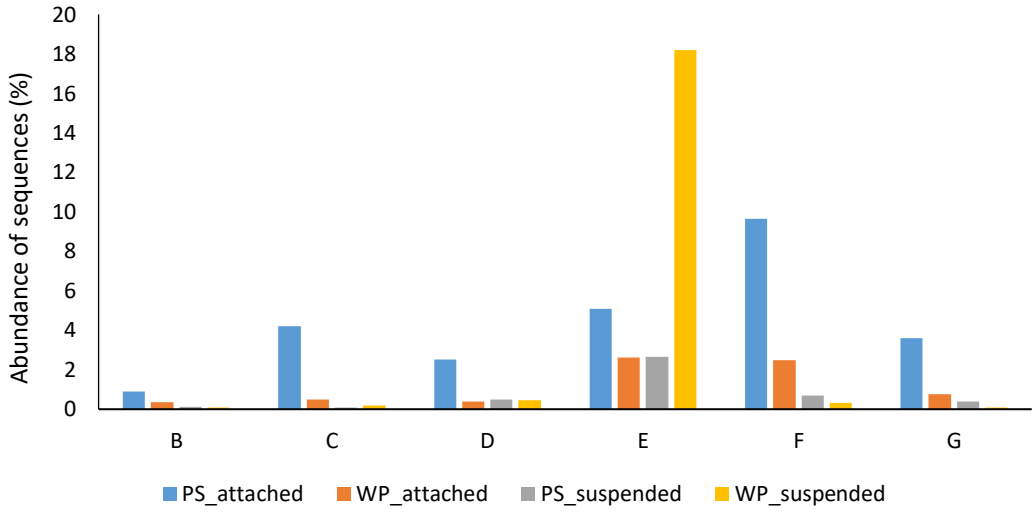

Figure SI 13. *Relative abundance of Thiomonas spp related 16S rRNA gene sequences during the monitoring*

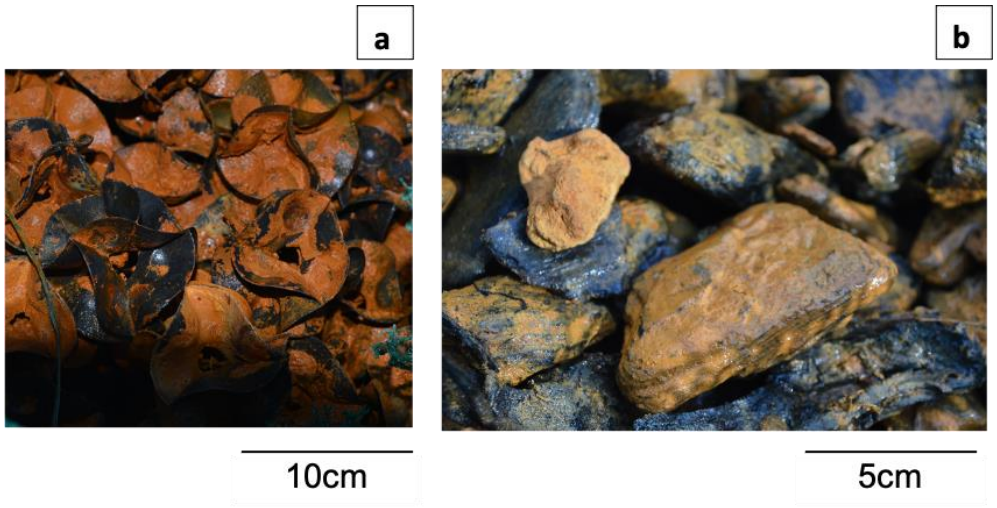

Figure SI 14. *Photos of the biomass carriers of each bioreactor showing with the orange biogenic precipitates. Biogenic precipitates on the plastic carrier PS (a), biogenic precipitates on the mix wood and pozzolana WP (b).*

Chapitre 4 : Traitement d'un DMA arsénié au sein d'un bioréacteur de sulfato-réduction à l'échelle du pilote de terrain

Introduction

Les deux chapitres précédents se sont concentrés sur un système de remédiation basé sur l'oxydation biologique du fer, où l'arsenic est éliminé par un processus de co-précipitation. Malgré l'intérêt de cette approche ne nécessitant aucun ajout de réactif, le procédé d'oxydation a montré certaines limites pour le traitement du DMA de Carnoulès, notamment un traitement insuffisante de l'arsenic, libérant un effluent avec une concentration minimale de 10 mg/L d'As, ainsi que le traitement limitée des cations métalliques Zn^{2+}, Cd^{2+} ou Pb^{2+}. Un traitement alternatif ou complémentaire est donc nécessaire pour répondre aux seuils règlementaires fixés par la directive-cadre sur l'eau (DCE) relatifs aux eaux de surface.

Une des stratégies potentielles pour compléter le traitement d'oxydation est un système basé sur la réduction des sulfates. La réduction des sulfates produit des sulfures capables de précipiter les metalloïdes et les métaux comme l'As, le Zn, le Pb et le Fe (Johnson and Hallberg 2005). L'activité des bactéries sulfato-réductrices (BSR) constitue l'élément clé de la performance de ces systèmes (Neculita et al. 2007). Lors de la réduction de sulfates, le pH de l'effluent augmente, ce qui constitue un avantage de ce type de traitement. Une des conditions nécessaires dans ce processus est l'ajout de sources de carbone ou de l'hydrogène comme donneurs d'électrons, car la concentration en carbone organique dans le DMA est généralement faible (< 10 mg/L) (Kolmert and Johnson 2001). Jusqu'à présent, les processus de biorémediation des DMA riches en As utilisant des bactéries sulfato-réductrices ont été étudiés dans des conditions contrôlées à l'échelle du laboratoire. L'applicabilité de ces systèmes à des DMA arséniés réels dans des expériences à l'échelle du pilote de terrain n'a pas encore été évaluée.

Dans ce contexte, un bioréacteur de sulfato-réduction a été installé sur le terrain pour traiter le DMA de Carnoulès. Les résultats du suivi physico-chimique et microbiologique de ce bioréacteur pendant près d'un an sont présentés dans ce chapitre. Le couplage d'un bioréacteur d'oxydation en aval du bioréacteur de sulfato-réduction a également été évalué durant les trois derniers mois dans le cadre de ce suivi. Les objectifs de ce chapitre sont d'une part d'étudier les rendements de traitement des métaux et métalloides, et la dynamique des communautés bactériennes associées au bioréacteur de sulfato-réduction, sous différentes conditions (diminution de temps de séjour, conditions climatiques et variation saisonnière de la chimie du DMA). Il s'agit notamment de mieux comprendre comment la dynamique des communautés bactériennes, en réponse aux variations, contribue finalement à la robustesse du bioréacteur. D'autre part, l'objectif est d'évaluer la faisabilité du couplage entre un bioréacteur de sulfato-réduction et un bioréacteur d'oxydation et la diversité des communautés bactériennes se développant dans ce dernier bioréacteur.

La caractérisation physico-chimique et microbiologique de l'influent et de l'effluent du bioréacteur de sulfato-réduction et du bioréacteur d'oxydation couplé a été réalisée au cours de différentes phases de fonctionnement, et la caractérisation des boues a été réalisée à la fin de l'expérience. La caractérisation microbiologique comprend la diversité et la composition taxonomique des communautés bactériennes ; elle a été évaluée par le séquençage du gène de

l'ARNr 16S. La présence et la quantification de gènes fonctionnels d'intérêt ont été déterminées par qPCR. Nous avons ensuite relié cette caractérisation microbiologique aux performances des bioréacteurs et discuté des liens potentiels entre ces paramètres.

Les résultats des recherches relatives à ce chapitre sont présentés sous la forme d'un article en préparation.

4 Article in preparation: Field trial of a sulfate-reducing bioreactor treating the arsenic-rich acid mine drainage from the Carnoulès mine

4.1 Abstract

Sulfate-reducing (SR) bioreactors have showed great potential to treat As-rich AMD under laboratory conditions, but their performances in the field are not well documented so far. Two of the general aims of the present work are: 1) to determine the robustness of the SR bioreactor under field conditions s during one year at the Carnoulès mine, France where AMD exhibits 21-100 mg/L As, 500-900 mg/L Fe and 12-20 mg/L Zn, and 2) to evaluate the efficiency and bacterial community structure of an iron oxidation bioreactor (FeOB) connected downstream the SR bioreactor during the last 120 days of functioning. Physico-chemical and microbiological characterization was performed at different stages of operation, for the inlet water, for water collected at mid-height of the SR column bioreactor (mid-point) and for the outlet water collected from the SR and FeOB bioreactors. Chemical and microbial characterization of biogenic precipitates was performed in both bioreactors at the end of the monitoring. The continuously fed SR bioreactor reached up to 99% of As and Zn removal within a hydraulic retention time (HRT) of 10 hours. Releasing an effluent with less than 1 mg/L of As or Zn, regardless of the conditions, including residence time, temperature and AMD chemistry. The Fe concentration in the effluent varied between 10 and 200 mg/L. An important achievement was the reduction of the SR bioreactor residence time from 29 days to 5 days. It was also observed an efficient consumption of the organic substrate, leading to (1) low organic carbon content in the effluent (less than 20 mg/L), and (2) high efficiency sulfate reduction H_2S by using the complete oxidation of glycerol. These results could be related to the significant diversification evidenced among the sulfate-reducing bacterial community. Regarding the efficiency of the FeOB connected at the outlet of the SR bioreactor, it precipitated partially the residual Fe concentration but did not provide significant additional As removal, despite the detection of iron-oxidizing- and arsenite-oxidising bacteria in the precipitates and outlet water. A longer monitoring time would be required to reach stable conditions and better evaluate the added value of the SR and FeOB bioreactors connected in series.

Keywords Sulfate-reducing bacteria, As-rich acid mine drainage, bioremediation, field bioreactor

4.2 Introduction

Mining activities are a major source of arsenic (As) pollution of water and soil worldwide. Arsenic has a high affinity with sulfide minerals ores and it is therefore released into water with production of acid mine drainage (AMD) (Luo et al. 2020). Sulfate-reducing (SR)

bioreactors have been used as a suitable and sustainable solution to treat different kinds of AMD (Sánchez-Andrea et al. 2014). Some of these bioreactors are already operating in the field at large scale (Skousen et al. 2017), even in passive conditions (Sheoran et al. 2010; Sato et al. 2018; Vasquez et al. 2021). The main advantages of the passive SR treatments are the following: once installed, they do not need continuous addition of reagents, they require infrequent and low cost maintenance (Johnson and Hallberg 2005; Rötting et al. 2008a). The passive SR bioreactors are often filled with a reactive mixture that combines different types of electron donors to promote a long-term operation. Most of them contain organic low-cost raw materials such as wastes from agricultural industry (Sheoran et al. 2010; Zhang and Wang 2016).

To the best of our knowledge, there is not passive SR bioreactor treating highly contaminated AMD, especially with low pH and high concentration of As. Passive SR bioreactors are generally not suitable for the selective precipitation of valuable elements (Ňancucheo et al. 2012). Indeed, the use of complex electron donor sources does not allow the control of sulfate reduction rates and therefore selective precipitation. However, semi-passive bioreactors are well suited to balance efficiency, investments and maintenance costs. Ňancucheo and Johnson (2012) showed for the first time the feasibility to use glycerol as the main electron donor in an SR bioreactor under acid conditions to promote the selective precipitation of zinc (Zn) and copper (Cu). Nowadays several studies are based on the use of glycerol due to the cost-efficiency of this substrate (Zhang and Wang 2016; Campos-Quevedo et al. 2021a; Hernández et al. 2022). During the reduction process, the pH of the effluent increases due to the consumption of protons, this increase of pH being also an interesting advantage of a SR treatment. One of the key conditions for an efficient process is to guaranty anoxic or low oxygen conditions to avoid the inhibition of sulfate-reducing bacteria (SRB) metabolism by oxygen (Barton and Fauque 2009).

The Carnoulès AMD has been described as one of the most As-contaminated AMDs worldwide (50-100 mg/L). During 15 years, iron oxidation has been the main strategy studied to remove the Fe and As from this AMD (Fernandez-Rojo et al. 2017, 2019), because it is based on a natural attenuation process observed *in situ* (Casiot et al. 2003a; Elbaz-Poulichet et al. 2006; Egal et al. 2010). However, due to incomplete As removal (As concentration being decreased at best down to 10 mg/L, Diaz-Vanegas et al. 2022), and limitation to remove cations such as Zn^{2+}, Cd^{2+} or Pb^{2+}, it is necessary to find a complementary or alternative treatment to reach the regulatory thresholds for these elements (Zn: 7.8 µg/L, Pb: 1.2 µg/L and Cd: 0.08-0.25 µg/L by European Water Directive for surface water). One promising option could be to use a SR bioreactor. Sulfate reduction produces sulfides, and the remediation process relies on the precipitation of metals- and metalloids-sulfides: mainly As-, Zn- and Fe- sulfides in the case of the Carnoulès AMD. The Equations 19 and 20 represent the incomplete and complete oxidation of glycerol by sulfate, respectively, followed by the precipitation of As, Zn and Fe presented in the Equations 21, 22 and 23 respectively.

$$0.75\ SO_4^{2-} + C_3H_8O_3 + 1.5\ H^+ \rightarrow 0.75\ H_2S + C_2H_4O_2 + CO_2 + 2\ H_2O \quad \textit{Equation 19}$$

$$7\ SO_4^{2-} + 4\ C_3H_8O_3 + 14\ H^+ \rightarrow 7\ H_2S + 12\ CO_2 + 16\ H_2O \quad \textit{Equation 20}$$

$$2\ H_3AsO_3 + 3H_2S \rightarrow As_2S_3 \downarrow + 6\ H_2O \quad \textit{Equation 21}$$

$$Zn^{2+} + S^{2-} \rightarrow ZnS \quad \textit{Equation 22}$$

$$Fe^{2+} + S^{2-} \rightarrow FeS \quad \textit{Equation 23}$$

Previous trials under laboratory conditions treating the Carnoulès AMD showed promising results (Le Pape et al. 2017; Battaglia-Brunet et al. 2021). These trials including batch and continuously fed bioreactors used glycerol as main electron donor. Agar and yeast extract were also supplied to promote the bacterial growth and colonization, but their use has to be limited in order to minimize the treatment costs at larger scale. The trials in batch conditions with real AMD showed the feasibility of total arsenic removal by precipitation of amorphous orpiment (am-As_2S_3) and realgar (AsS) (Le Pape et al. 2017). Then the continuously fed SR bioreactor reached up to 99% of As and Zn removal within a hydraulic retention time (HRT) of 10 hours. In the continuous fed SR bioreactor, iron remained in solution (Battaglia-Brunet et al. 2021). This is an advantage in the perspective of limiting the risk of clogging of the SR bioreactor by Fe precipitates and thus extending the life span of the bioreactor; this selective precipitation is possible by limiting glycerol supply. A side advantage of this limitation is the lower operating cost (Ňancucheo et al. 2012). The Fe released in the effluent would be treated in a second stage, which consists of an aerobic bioreactor based on iron-oxidation followed by Fe and As co-precipitation.

Despite the promising results obtained from these first laboratory trials (Le Pape et al. 2017; Battaglia-Brunet et al. 2021), there are still some knowledge gaps that need to be filled in order to apply this approach to a full-scale treatment. The main gaps rely on the long-term stability of the performances, the resilience of the microbial SRB community toward seasonal variations of meteorologic conditions (especially water and air temperature) and changes in AMD physico-chemistry. A better understanding of the interactions between the microbiology and geochemical processes occurring inside the SR bioreactor would help us to overcome these gaps and improve the efficiency of the process.

In the present study we evaluate the performance of a field-scale SR bioreactor treating the Carnoulès AMD. The bioreactor was implemented during 375 days and was fed with a mixture of glycerol and natural AMD. On day 259, an iron oxidation bioreactor was installed downstream the SR bioreactor. This stage corresponded to the first test of such coupling of bioreactors in field conditions.

In this context, the present study had four aims: (i) to determine the robustness of the SR bioreactor under field conditions, (ii) to test the impact of decreasing HRT on the performance of the treatment (HRT being a key parameter for the future dimensioning of large-scale

treatment plants), (iii) to evaluate the relationship between the microbial communities and operating conditions (HRT) or environmental parameters (i.e temperature and AMD chemistry), and (iv) to evaluate the efficiency and bacterial community structure of an iron oxidation bioreactor (FeOB) connected downstream the SR bioreactor.

4.3 Methodology

4.3.1 Sulfate-reducing bioreactor approach

During the summer 2020, a sulfate-reducing (SR) bioreactor was installed on the Carnoulès, working under up-flow conditions. The bioreactor was inoculated with a sulfate-reducing consortium of bacteria enriched from the Reigous creek sediments (Battaglia-Brunet et al. 2021). In fact, three bioreactors were successively set up in the laboratory to gradually increase the volume of the SR bioreactor: the first one was a 300 mL column, which was used to inoculate a 5 L column, which in turn was used to inoculate the 25 L bioreactor. The preliminary phases (300 mL) were developed in a previous project (Le Pape et al. 2017; Battaglia-Brunet et al. 2021). The 300 mL column was operated with an entirely nutrient-enriched agar-filled pozzolana (3-5 mm), kept oxygen-free under nitrogen flow (sealed column). In parallel, a new 300 mL column was set up in the laboratory and maintained continuously in order to keep the sulfate-reducing bacteria active and to have a reserve of inoculum available to reseed the SR reactor if needed. The 5 L bioreactor (65 cm high; 9.2 cm diameter) was less controlled in terms of oxygen absence: it was filled with 90% simple pozzolana (3-5 mm) + 10% agar pozzolana. It had a useful volume of 2.1 L. It operated for 3 months at 38 days average of HRT, before being used to inoculate the 25 L reactor.

The bioreactor monitored in the present study (Figure 20) has a total capacity of 50 L, only half of the capacity was used, corresponding to a working volume of 14.5 L. It was filled with 25 kg of pozzolana, 17 % of the pozzolana (size 3-5 mm) coming from the 5 L bioreactor used to up-scale the process, and 83 % of clean pozzolana (size 6-12 mm). The bioreactor had two sampling ports, one at 31 cm from the bottom (midpoint) and the other at 62 cm from the bottom (the outlet port, as shown Figure 20). The pozzolana bed top surface was covered with 2 cm of compost as a barrier to oxygen diffusion. This bioreactor was operated for 4 months in the laboratory, with an HRT of 58 days for the first 130 days. Then, the HRT was reduced to 14.5 days (1 liter per day). An increase in the pH of the effluent was always observed during the laboratory phase showing maintenance of BSR activity. Then the bioreactor was transported from the laboratory to the field.

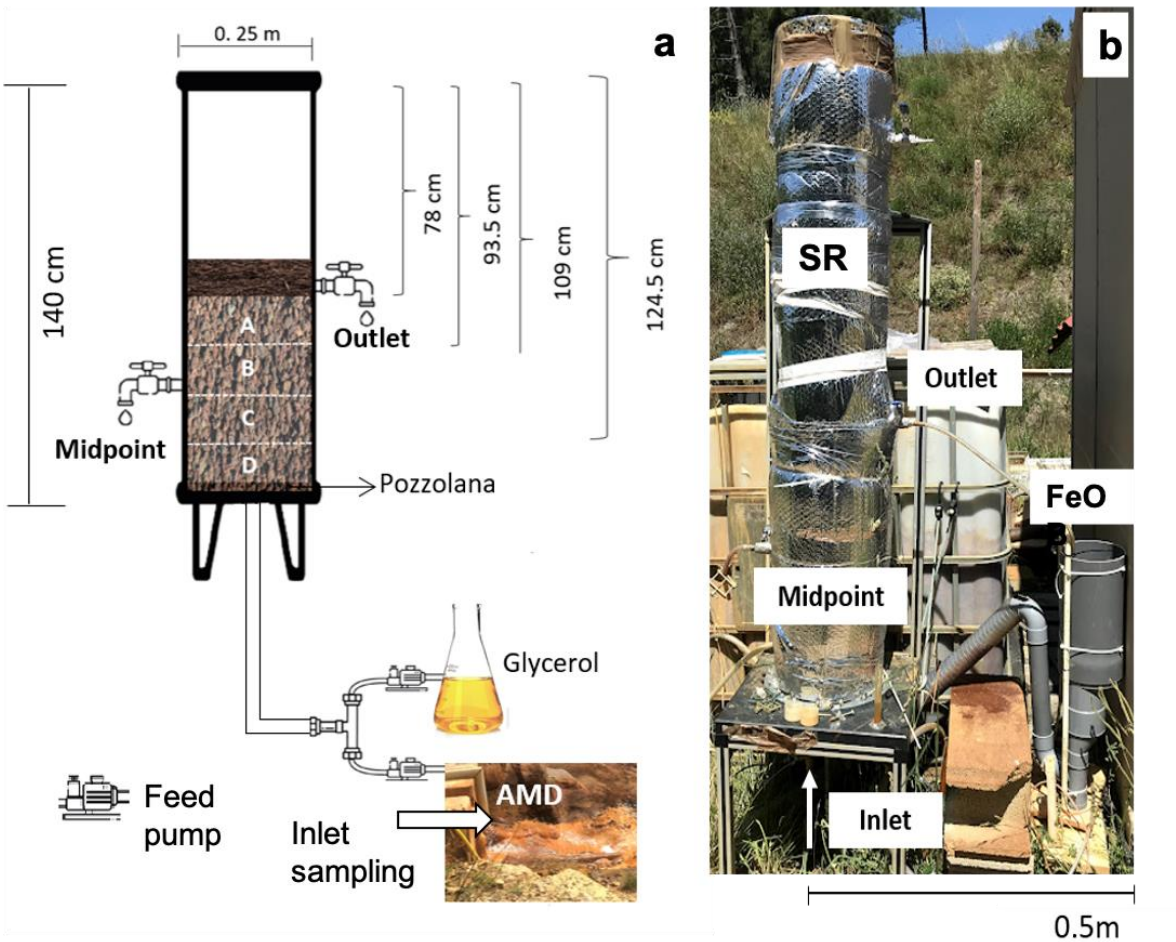

Figure 20. *SR bioreactor filled with pozzolana (a). Pictures of the SR bioreactor field-pilot with bio-oxidation module coupling (FeOB), during the functioning (b).*

4.3.2 Operation and monitoring

Under field conditions, the bioreactor was up-flow fed, using peristaltic pumps, with a mixture of AMD and glycerol (0.5 g/L). During the first month, this mixture was supplemented with yeast extract (1 g/L). Yeast extract was used to promote the bacterial biomass production during the first stage of adaptation to the field conditions. Yeast extract played several roles: electron donor, carbon source, nitrogen source, and reducing agent. After one month of operation on site, the supply of yeast extract was stopped, and glycerol was then the only external nutrient. The stability of the SR bioreactor was controlled initially by pH measurement at least twice a week and sampling at least once a week for sulfur, iron, arsenic and zinc concentrations determination.

During the first 124 days of functioning, the bioreactor was fed continuously. At the end of the fall season, the temperature started decreasing and the sanitary situation (COVID-19) restricted the weekly monitoring of the bioreactor. The system was then switched to fed-batch conditions. The main purpose was to maintain the microbial community alive in "dormancy" inside the bioreactor. A fresh layer of 10 cm of compost was added at the top of the pozzolana bed to prevent oxygen diffusion, and the bioreactor was fed (from the bottom) once each two weeks

with 1 L of AMD supplemented with glycerol and yeast extract (0.5 g/L and 1 g/L respectively). Temperature and pH were measured at the influent, in the midpoint effluent and at the outlet. Then at day 224, when outside temperature remained higher than 12°C, at day 224, the bioreactor was again continuously fed. The bioreactor continuously worked for almost 5 months (March to July 2021). During this phase, HRT was progressively decreased from 29 days to 5 days. The bioreactor worked for a total of 373 days, including 86 days under fed-batch conditions.

Table 11 describes the different experimental phases with corresponding operating conditions including theoretical HRT in the SR bioreactor. Weekly measurement of the flow rate allowed to estimate the HRT. The decision to increase the inlet flow was based on the stability of the pH in the midpoint of the bioreactor. For most of the changes in the inlet flow rate, the waiting time was at least 3 times the theoretical HRT, before increasing the inlet flow rate.

Table 11 *Conditions of functioning during the successive experimental stages including duration, HRT, concentration of glycerol, dates of biological and chemical sampling and periods of the coupling of SR bioreactor with bio-oxidation module.*

Period	Day	Yeast Extract (1 L/h)	Working conditions	Target HRT (d)	Biological sampling	Coupling with FeOB*
I	0 - 29	+	Continuous	14.5		-
II	29 - 55	-	Continuous	14.5	Day 43	-
III	55 - 78	-	Continuous	9.7	Day 68	-
IV	78 - 110	-	Continuous	14.5	Day 110	-
V	110 - 115	-	Continuous	13.2		-
VI	115 - 124	-	Continuous	14.5	Day 124	-
VII	124 - 224	+	Fed Batch	-		-
VIII	224 - 239	-	Continuous	29	Day 239	-
IX	239 - 279	-	Continuous	14.5	Day 273	-
X	279 - 296	-	Continuous	11.6		Yes
XI	296 - 313	-	Continuous	7.6	Day 302	Yes
XII	313 - 344	-	Continuous	5.5		Yes
XIII	344 - 373	-	Continuous	4.7	Day 348, 365 and 373	Yes

*FeOB: Iron oxidation bioreactor

4.3.3 Coupling

During the last four experimental periods (from day 279 to day 373), the SR bioreactor was coupled to a Fe oxidation bioreactor (FeOB) dedicated to the oxidation and precipitation of the residual iron (Table 11). This FeOB bioreactor consisted in a PVC reactor with a total volume of 3.2 L, internal diameter 14 cm, and a useful volume of 2 L (Figure 21). It was filled with 800 g of wood chips, which is used as biomass carrier to enhance the bacterial colonization. The FeOB bioreactor was supplied with oxygen by an air pump at 0.5 L/min, and equipped with a steel bubbler to promote gas exchange and improve oxygenation.

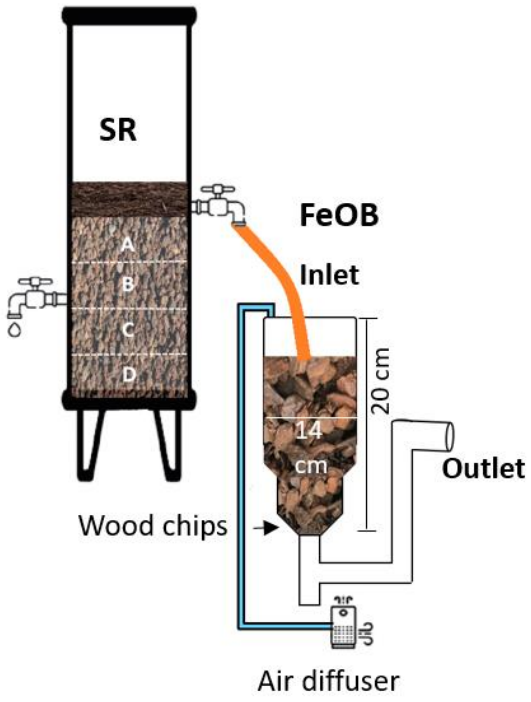

Figure 21. *Characteristics of FeOB bioreactor installed downstream the SR bioreactor.*

4.3.4 Water physico-chemical characterization

Water samples were collected once per week at four points: 1) inlet AMD, 2) midpoint of SR bioreactor, 3) outlet port of the SR bioreactor and 4) outlet port of the FeOB bioreactor. The water samples were preserved and characterized according to the routine procedures described in Fernandez-Rojo et al. (2017). They were split in two sub samples for *in situ* and lab measurements. The *in situ* physicochemical measurements were conducted using a Hach HQ40D portable multi-meter (i.e. temperature, pH, redox potential and electrical conductivity). Then, 100mL of the second subsample was filtered using 0.22 µm cellulose filters. Afterwards, the filtered sample was immediately distributed in different aliquots; one aliquot was diluted in 1% HNO_3 solution (Suprapur quality) for major and trace element analysis and another aliquot was diluted in 0.05 % (w:w) phenanthrolium chloride solution and 10 g/L hydroxylamine hydrochloride solution for Fe(II) concentration determination. The samples were stored at 4°C and treated according to the appropriate protocols for specific chemical analysis.

The Fe(II) concentration was quantified by colorimetry using the ortho-phenanthroline method by absorbance at 510 nm with a JENWAY 6320D spectrophotometer (detection limit = 88 µg/L, accuracy = ±5%). Major and trace elements, including total Fe, As, Zn and S concentrations, were determined by inductively coupled plasma-mass spectrometry (ICP-MS; Thermo X7 Series) at the AETE-ISO platform, University of Montpellier (France). An external calibration with internal standard correction procedure and international certified reference waters (CNRC SLRS-5, NIST SRM 1643e) was used for quality control.

Occasional measurements of sulfates, total organic carbon (TOC) and acetate were made. The sulfate (SO_4^{2-}) concentration was measured by turbidimetry (Method EPA 9038), which is a method based on precipitation of sulfate ions with barium chloride and analysis by spectrophotometry at 420 nm. These analyses showed that almost 100% of the total sulfur (S) present in the inlet, midpoint and outlet port was in the form of sulfate (1215 ± 332, 1020 ± 131 and 1015 ± 83 mg/L respectively). For that reason, the rate of sulfate reduction was calculated based on the difference between the total dissolved sulfur (S) present in the inlet water, and determined by ICP-MS, and the sulfur present in the outlet water. This difference was considered as the sulfate that was reduced then precipitated inside the bioreactor at a specific sampling time. The TOC was analyzed by a catalytic oxidation at 720°C and infrared measurement of CO_2 (Shimadzu TOC-L Analyzer), while acetate was quantified by ion chromatography (Dionex) (standard NF ISO 10304).

4.3.5 Precipitates characterizations

The SR bioreactor was stopped on July 27th 2021, after 373 days of functioning. The midpoint and bottom entry ports were opened to drain the liquid. Once emptied, the precipitates were recovered from four levels: section D the bottom (0–15.5 cm), section C middle (15.5–31 cm), section B middle-top (31–46.5 cm) and section A at the top of the bioreactor (46.5–62 cm). Samples were collected from each level and mixed to form a composite sample that was divided into sub-samples for the different analysis. The FeOB was stopped the same day as the SR bioreactor, all the liquid was drained. The biogenic precipitates were collected by scrapping the wood chips of the bioreactor. Also, a big composite sample was prepared and divided in sub-samples for analysis.

The sludge's analysis included mass balance, microbiological and chemical characterization. Samples were collected and stored in glass jars closed under N_2 flow to minimize the oxidation. They were stored at 4 ◦C until further analysis.

To recover and separate the precipitates from the pozzolana for chemical analysis and mass balance, the following protocol was applied. Firstly, a flask of 500 mL was filled with pozzolana covered of sludge, one flask was filled for each section (A, B, C, D) from the SR bioreactor. MilliQ water was added (750 mL) to each flask (corresponding to each section), and the four flasks were agitated for 30 minutes at 200 rpm. Then, the samples were sieved using 1 mm diameter sieve, the liquid phase of each flask was recovered in Falcon tubes (50 mL) and centrifuged for 12 minutes at 4400 x g (Sorwall ST40, Thermo Scientific). The supernatant was discarded and the pellet was recovered, frozen and lyophilized. Total Fe, As, Zn and S concentrations in the lyophilized precipitates were determined by ICP-MS after acid digestion (Fernandez-Rojo et al. 2017).

Secondly, with the purpose to analyze the dryness of the sludge, the rest of the solid material (pozzolana + precipitates attached to the pozzolana) was sieved using 1 mm diameter sieve. This helped to remove the pozzolana that was washed and weighed. Then the precipitates were dried for 48 h at 40°C, and the dry precipitates were again weighed.

A leaching test was performed (by the external laboratory WESSLING, France) by an internal method with the precipitates recovered from the bottom section (section D) of the SR bioreactor to evaluate the mobilization of soluble substances from the precipitates in contact with water. The solid samples were sieved from the 4mm sieve. Leaching with water was performed on a subsample (20 g) of the precipitates with a solid to liquid ratio of 1:10. Leachate was filtrated at 0.45 µm and analyzed for dissolved metals (Cr, Ni, Cu, Zn, As, Se, Cd, Ba, Pb, Mo and Sb) concentrations by ICP-MS following the NF EN ISO 17294-2 standard.

4.3.6 Biological analyses

During the year of monitoring, nine sampling campaigns were performed for microbial characterization. Three replicates of effluents (300 mL each one) were sampled at the midpoint of the SR bioreactor, influent and outlet of the FeOB bioreactor. They were filtered on sterile 0.22 µm cellulose acetate filters. The filters were transported in an ice box; once back in the laboratory they were stored at – 80°C until microbial DNA extraction. DNA was extracted from the frozen filters using the DNeasy PowerWater kit (Qiagen). For the characterization of the bacterial communities from the sludge, the precipitates were sampled as mentioned in the previous section (above). The precipitates sampled for the microbiological analysis of the SR bioreactor included the poozolana while the precipitates from the FeOB was separated from the wood carrier. One sample of each section A, B, C, D of SR bioreactor and one sub-sample of whole FeOB precipitates were stored each one in an Eppendorf tube, they were flash-frozen in dry ice on site, transported to the laboratory and stored at -80°C until DNA extraction. Then DNA was extracted using the DNeasy PowerSoil kit (Qiagen).

The extractions from the filters and precipitates were performed according to the manufacturer's recommendations. The concentration of DNA extracts was measured with a fluorometer (Qubit ®, Invitrogen) and the DNA was stored at -80°C until further analysis. For metabarcoding, DNA extracts were sent to the ADNid Company (Montpellier, France), which performed the PCR amplification of bacterial 16S rRNA gene V3-V4 region (341F: 5'-CCTACGGGNGGCWGCAG-3'- 785R: 5'-GACTACHVGGGTATCTAATCC-3'), amplicon libraries construction, Illumina sequencing, verified and validated the quality of the sequences. Bioinformatic analyses were conducted on Illumina sequence reads using the FROGS (Find Rapidly OTUs with Galaxy Solution) pipeline implemented into the Genotoul platform of the Galaxy server (Toulouse, France) (Escudié et al. 2018). Fastq paired reads were merged with Vsearch software, and clustering into OTU (Operational Taxonomic Unit) with Swarm and an aggregation distance clustering of 1. Chimera and OTU with a proportion less than 0.0005% of all sequences were removed. Taxonomic affiliation was performed using BLAST and the Silva 138.1 database for 16S rRNA gene sequences. During the analysis, the default parameters of the server were set. Then Operational Taxonomic Units (OTU) clustering (98.2% identity threshold) and subsampling for even sample size (rarefaction to 1000 reads per sample) were applied, and finally filters to eliminate "unknown phylum" and "Cyanobacteria phylum" were eliminated using filters available in Phyloseq (Rstudio).

4.3.7 Functional genes copies quantification

The abundance of *aioA, dsrA a*nd 16S rRNA genes copies were quantified by a real-time PCR from the DNA extracts, using the following primers: for 16S rRNA gene, we used universal primers 341F (5'CCTACGGGAGGCAGCAG-3') and 515R (5'ATTACCGCGGCTGCTGGCA-3'); for *aioA* gene, we used primers aoxB m4-1F (5'GCCGGCGGGGGNTWYGARRAYA-3') and m2-1R (5'GGAGTTGTAGGCGGGCCKRTTRGDAT-3) (Quéméneur et al. 2008). Finally, for the *dsrA* gene primers dsr1F+ (5'ACSCACTGGAAGCACGGCGG-3') and dsr-R (5'GTGGMRCCGTGCAKRTTGG-3) (Schippers and Neretin 2006).
Gene copies quantification were performed with a CFX Real-Time PCR Detection system (Bio-Rad), using SsoAdvanced SYBRR® Green Supermix. Calculation of copy numbers was done as described in Cébron et al. (2008). A linear calibration curve ($r^2 > 0.9$) was obtained over 7 orders of magnitude, ranging from 10^2 to 10^8 gene copies of a linearized plasmid.

4.3.8 Biostatistics analysis

Statistical analyses were performed with R version 3 mainly. Chao1 and Shannon indices were calculated using the phyloseq package (McMurdie and Holmes 2013). Bray Curtis dissimilatory matrix was used as diversity metric to compare the bacterial communities present in the AMD inlet, and those developed in the SR bioreactor and in the FeOB bioreactor. These included the suspended communities recovered from the inlet water, midpoint effluent of the SR bioreactor and outlet effluent of the FeOB bioreactor, and the attached communities present in the precipitates of both bioreactors at the end of the operation. Analysis of similarity (ANOSYM, 999 permutations) was performed to compare the statistical difference between pre-defined groups. It allowed us to compare the composition of the bacterial communities based on the following criteria: the different sampling points (inlet, midpoint SR bioreactor or outlet port FeOB bioreactor), the different periods of monitoring (stages I to XIII), the suspended (recovered from water) versus the sessile (recovered from the sludge) bacterial communities. Then, indicator species analysis was performed to identify the representative species associated to a group. Spearman coefficients were calculated to establish the correlations between the OTU abundance (R package indicspecies, De Caceres and Legendre 2009), physico-chemical parameters and bioreactors performances.

A non-metric multidimensional scaling (NMDS) ordination approach was used to visualize bacterial community variation among samples. The difference among the structure and composition of the communities is represented by the distance between the points. Significant differences of parameters among the treatments were detected with one-way ANOVA (p-value 0.05) followed by Tukey test.

4.4 Results

4.4.1 Water sample characterization

The total S, As, Fe and Zn concentrations in the Carnoulès AMD (inlet) varied seasonally, and showed during the summer twice the concentrations observed during the winter (Figures 22, 23 and 25).

4.4.1.1 pH evolution

The pH of the inlet AMD water ranged between 2.8 and 5 along the SR operation (Figure 22). The pH increased to 4.3 - 7.3 at the midpoint port and until 2.8 - 7.8 at the outlet port. The highest pH increase (about 2 units) was observed between inlet and midpoint while a further ~0.3 units increase was observed between midpoint and outlet SR. Such pH increases reflected occurrence of biological sulfate-reduction. After the suppression of the yeast extract (end of stage I), the pH at midpoint and outlet were significantly affected (decrease of ~ two or even four pH units). However, after the fed-batch period, the midpoint and outlet pH remained higher than ~ 5.5, providing a pH increase of about 2-3 units compared to the Inlet, despite the stop of yeast extract supply. This suggested a recovery of the sulfate reduction activity. The pH increase (about ~ 2 units) was maintained during the successive periods of HRT decrease (periods VIII to XIII), although a slight decrease of 0.2 to 0.5 units was observed at midpoint and outlet respectively, throughout these periods, suggesting a slight decrease of sulfate-reduction activity. The coupling with FeOB after day 267 first induced an additional pH increase of about one unit compared to outlet SR, probably because of degassing dissolved CO_2, this gas being produced by glycerol biodegradation in the SR bioreactor. After day 351, the FeOB induced a decrease of pH of the effluent, which finally reached pH ~ 3 after 100 days of functioning.

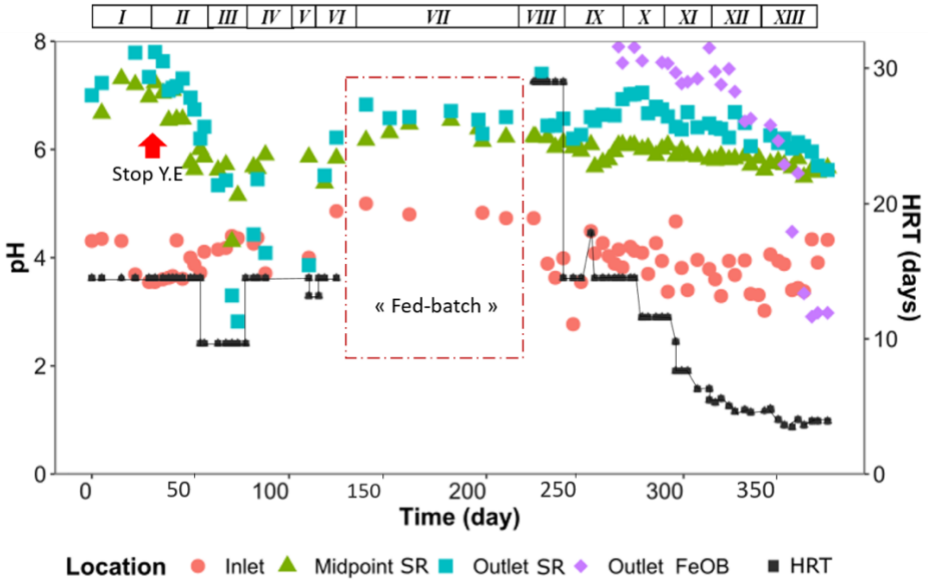

Figure 22. *Variations of the pH measured in the inlet water, midpoint port, outlet port of the SR bioreactor and outler port of the iron-oxidation bioreactor. The modification of the HRT along the monitoring was represented by black squares and black line. The values of HRT correspond to the real*

values measured in the field. The red arrow indicates the stopping of yeast extract feeding and the red box to dashed line represents the fed-batch period.

4.4.1.2 S monitoring

Dissolved sulfur (S) concentration in the inlet AMD water varied from 670 to 1080 mg/L throughout the whole experiment duration. It decreased between inlet and midpoint, with variable decrease throughout time, reflecting a highly inconsistent sulfate-reducing activity, from 80% of sulfate removal during period I to 17% during period XIII and reaching less than 1% during period VI (Figure 23). The suppression of yeast extract induced a dramatic decrease of sulfate-reduction. However, it restarted after the fed-batch period, reaching up to 73% removal at day 270. This demonstrated that the reduction of sulfate could proceed without continuous yeast extract supplementation. From day 270 to day 380, the sulfur concentration at midpoint and outlet SR increased concomitantly to the decrease of HRT and to the increase of inlet sulfur concentration, which did not clearly identify the main controlling factor. During the whole operatig period, similar S concentrations were measured at midpoint and outlet SR, showing that most sulfate-reducing activity was localized within the two first layers (D and C) of the SR bioreactor (Figure 20). The rate of sulfate reduction before the fed-batch period ranged between 0 and 0.6 mM/day. After the fed-batch period, the rates ranged between 0.1 and 1 mM/day; they increased with the decrease of HRT (Figure 24).

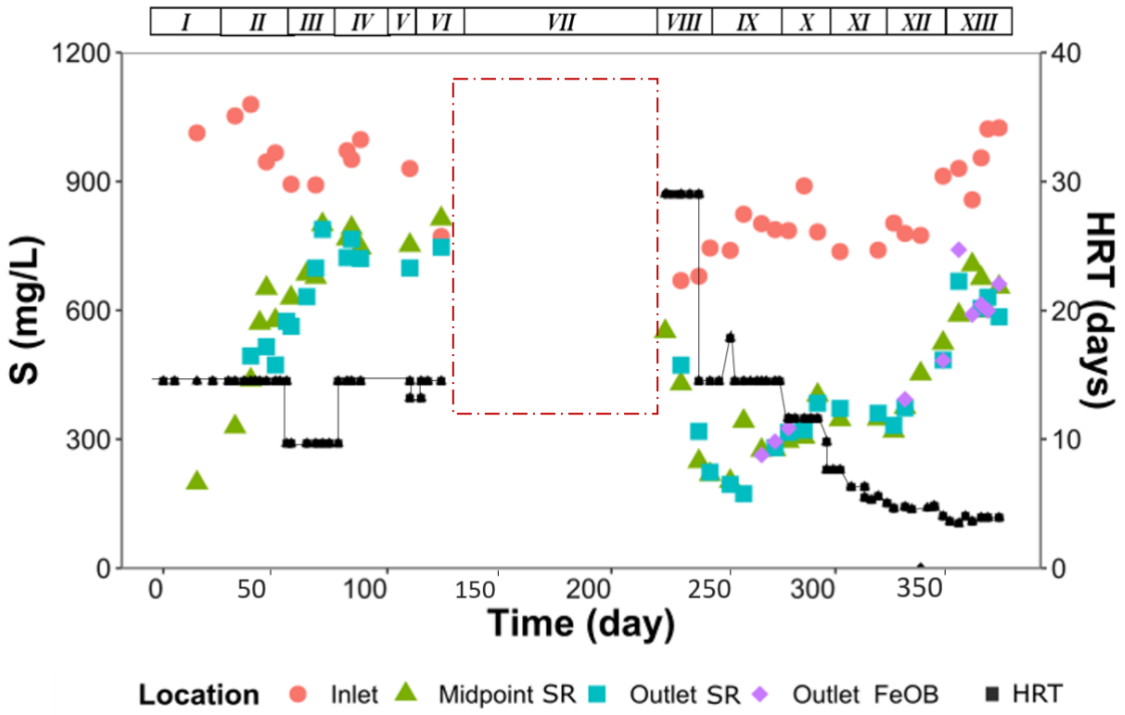

Figure 23. *Variations of the sulfur (mg/L) measured in the inlet water, midpoint port, outlet port of the SR bioreactor and outlet port of the iron-oxidation bioreactor. The modification of the HRT along the monitoring was represented by black squares and black line.*

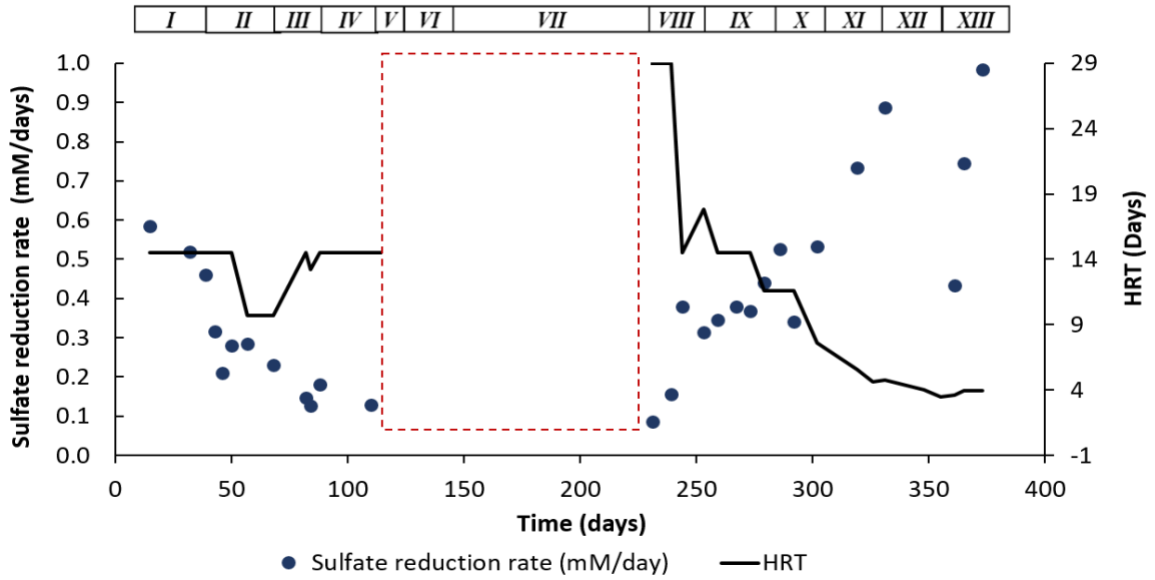

Figure 24. *Evolution of the sulfate reduction rate and HRT at the midpoint port of the SR bioreactor along the functioning (370 days). The red box to dashed line represents the fed-batch period.*

4.4.1.3 Fe evolution

Dissolved Fe concentration in the inlet AMD water varied from ~ 500 mg/L to ~ 1000 mg/L throughout the whole experiment duration (Figure 25). Fe removal varied strongly between periods I to VI. It was up to 99% during period I. Then after the yeast extract supply was stopped, it dropped from 91% (period II) down to 33% (period VI), releasing an effluent with a concentration up to 500 mg/L of Fe (as shown Figure 25). After the batch mode, between period VIII and period X, Fe removal yield increased from 64% to 92% and the outlet Fe concentration reached less than 17 mg/L at day 279, despite the decrease of HRT by a factor of three. After day 350 (periods XI and XII), the outlet Fe concentration increased up to 300 mg/L, showing a loss of Fe precipitation efficiency. This loss of efficiency occurred while HRT did not change significantly, but it was concomitant to the increase of inlet Fe concentration.
During more than 70% of the time (80 days) of the coupling operation, the residual iron feeding the FeOB bioreactor was less than 50 mg/L. Only after day 350, the FeOB bioreactor received more than 100 mg/L and almost 300 mg/L during the last week. During the first 80 days of operation, the FeOB bioreactor removed all residual Fe (outlet Fe < 1 mg/l) until day 350, and then removed between 50 and 90%. Up to 99% of untreated Fe released from the outlet port of both bioreactors (SR and FeOB) corresponded to ferrous iron (data not shown).

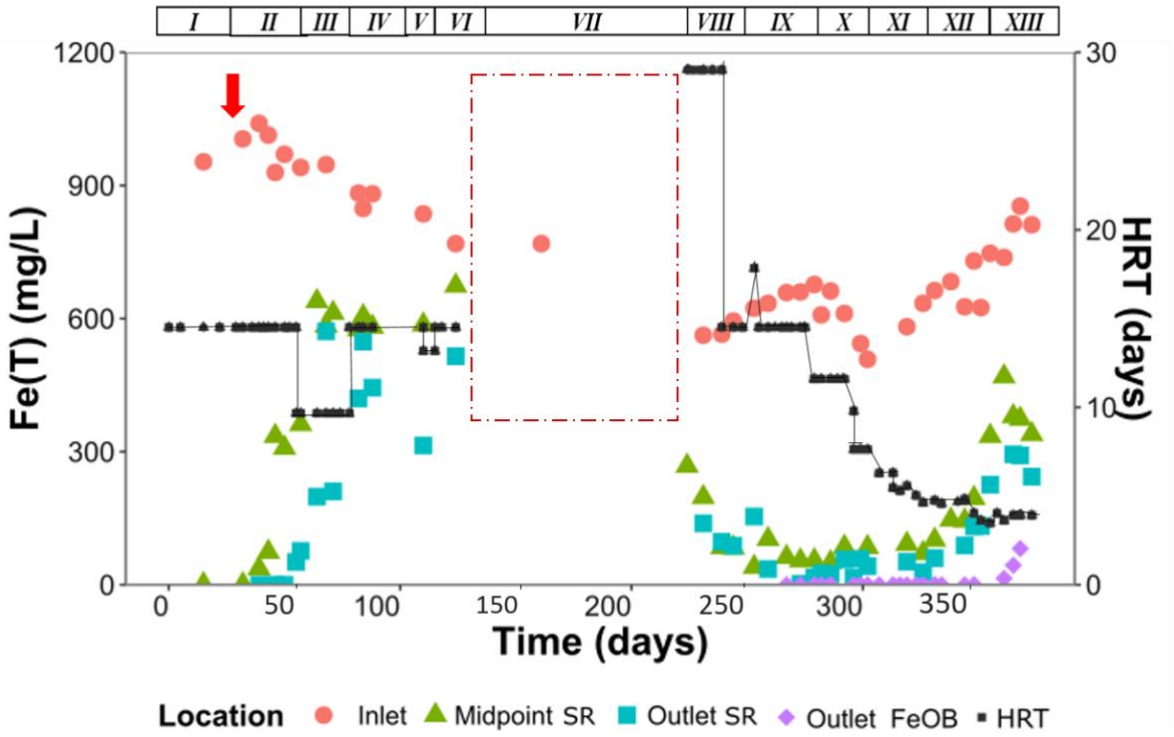

Figure 25. *Variations of the total iron (mg/L) measured in the inlet water, midpoint port and outlet port of the SR bioreactor. The modification of the HRT along the monitoring was represented by black squares and black line.*

4.4.1.4 As and Zn removal

The As concentration in the inlet AMD averaged 68 ± 21 mg/L, with the highest concentration during period I (Figure 26.a). As removal was stable all along the monitoring between, 99.1% and 99.9%, the removal being achieved in the bottom half of the bioreactor. The As concentration in the effluent of the SR bioreactor was between 0.02 and 0.8 mg/L.

Zn concentration in the inlet water varied between 12 and 20 mg/L (Figure 26.b). Zn removal reached up to 99.9% and it was relatively stable along the monitoring. Most of the removal was achieved in the bottom half of the bioreactor. However, in some occasions the top half of the bioreactor also contributed to remove the residual Zn (Figure 26.b). For instance, there was a diminution of the Zn removal in the bottom of the bioreactor during period III. During this period, at the midpoint port, Zn concentration reached 4 mg/L. This diminution coincided with the reduction of the HRT from 14.5 to 9 days. During the entire monitoring, Zn concentration at the outlet water was between 0.01 to 0.4 mg/L.

The oxidation bioreactor functioning after day 250 showed limited additional As or Zn removal (Figure 26). Regarding the As removal, the influent of the FeOB bioreactor contained less than 400 µg/L of As and the effluent showed a range of As concentration between 140 and 10 µg/L (Figure SI 15).

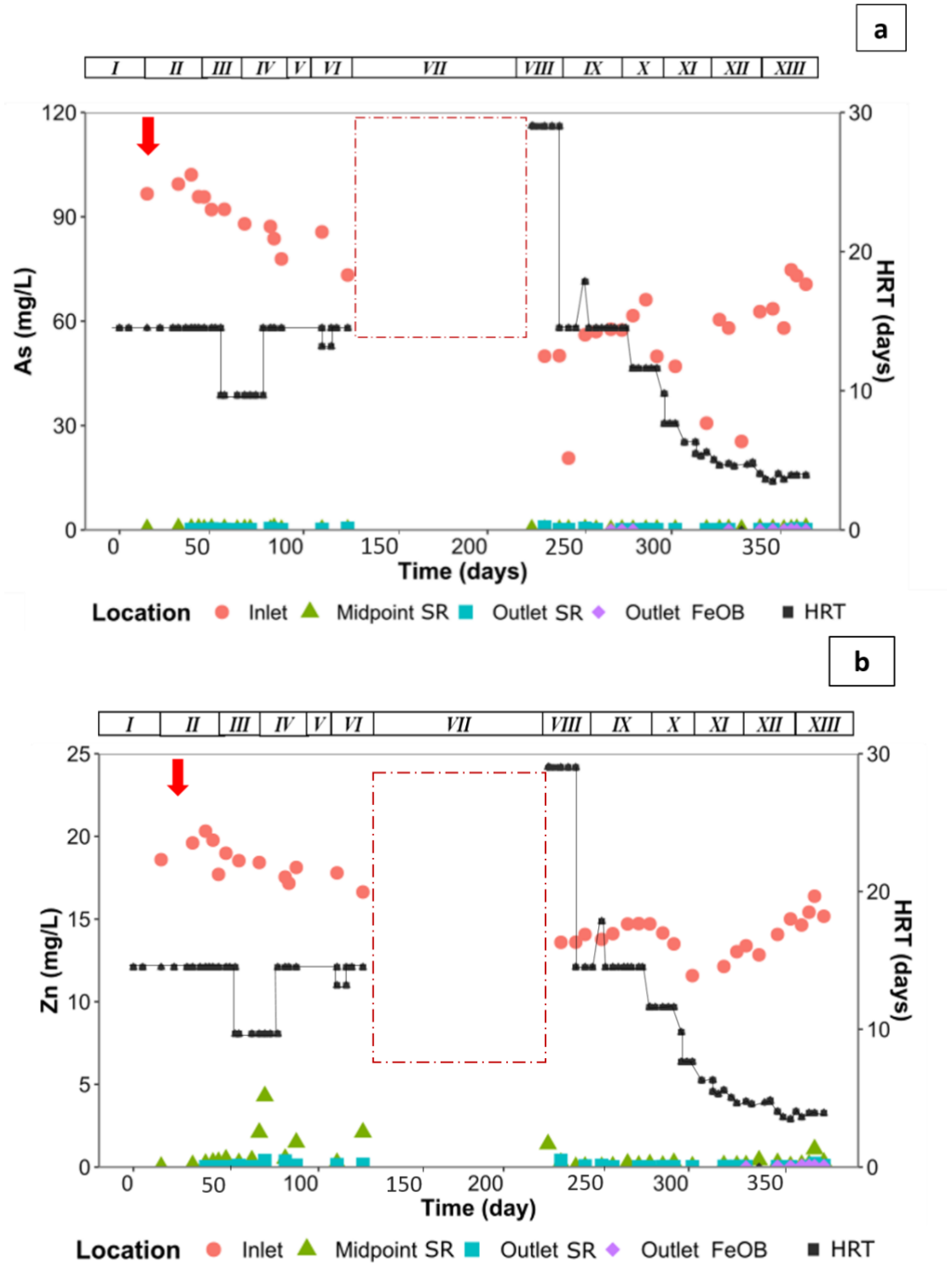

Figure 26. *Variations of total arsenic concentration (a) and total dissolved zinc concentration (b) measured in the inlet water, midpoint port and outlet port of the SR bioreactor. The red arrow indicates the stopping of yeast extract feeding and the red box to dashed line represents the fed-batch period.*

4.4.1.5 Organic substances

Sporadic measures of TOC between period III and period XIII showed an average of 18 ± 11 mg/L in the outlet effluent while the TOC measures in the inlet water after the mix of AMD

and glycerol was 225.2 ± 28.4 mg/L. This showed that glycerol was almost entirely consumed in the SR bioreactor and that its oxidation probably followed the full oxidation pathway. Average acetate concentrations in the midpoint effluent and outlet port measured in stage XII and XIII were 0.6 ± 0.4 mg/L and 0.3 ± 0.3 mg/L respectively, which confirmed the latter statement.

4.4.2 Precipitates characterization

A total of 2.3 kg of dry precipitates (without pozzolana) was recovered from the SR bioreactor after almost one year of operation. Fourty percent of these precipitates were accumulated in the bottom of the bioreactor (D section). The physical properties (color and smell) of the precipitates accumulated in the four sections of the SR bioreactor were different (Figure 27). The bottom (C and D) of the bioreactor showed the darkest sludge, with precipitates well bonded to the pozzolana, and a strong smell of hydrogen sulfide (H_2S). Some of those precipitates showed yellow-gold formations (Figure 27.c). The top section (A) of the bioreactor was covered with a brown layer that corresponded mainly to a mixture of precipitates and a layer of compost (Figure 27.a).

Arsenic and Zn were mainly precipitated in the first bottom section of the bioreactor (section D, Table 12). Iron precipitated all along the bioreactor, but a higher Fe accumulation was observed in the three bottom sections (B, C, D) than in the top section (A). XRD characterization did not reveal any crystallized mineral. Despite the high As and Zn concentrations measured in the precipitates of the bottom of the bioreactor (section D) (48700 mg/kg dry weight for As and 14200 mg/kg dw for Zn), the leachable fraction was only 0.75 mg/kg dry weight for As and 19 mg/kg dw for Zn (Table 13).

Table 12 *Characterization of the precipitates accumulated in four sections inside the SRB bioreactor.*

Section	Pozzolana + precipitates mass (kg)	Precipitates mass (kg)	Moisture precipitates (%)	Dry precipitates (kg)	Fe (mg/kg)	Zn (mg/kg)	As (mg/kg)
A	6.0	2.1	70	0.6	67800	200	100
B	4.8	1.1	66	0.4	125300	300	500
C	8.5	1.7	70	0.5	124900	400	1100
D	12.1	2.8	72	0.8	246100	14200	48700
Total	31.5	7.8		2.3			

All the concentrations were measured by dry weight (dw).

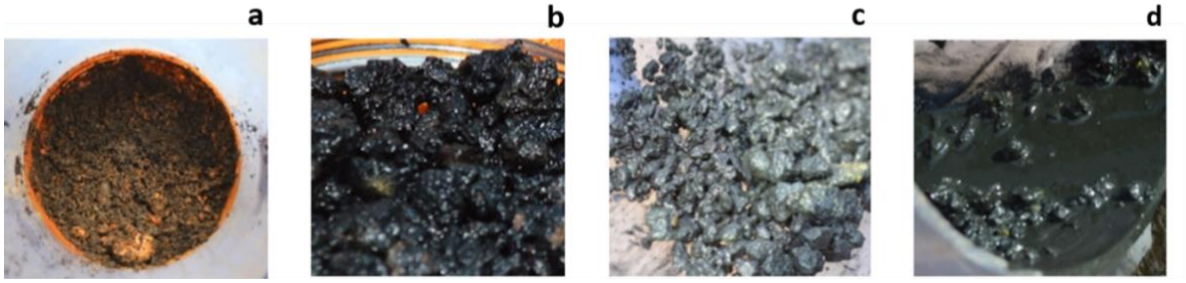

Figure 27. *Precipitates accumulated in the different sections of the SR bioreactor. Top view of the bioreactor presenting ochre color (a); biogenic precipitates and pozzolana sampled from the section C (b); black biogenic precipitate with some yellow-gold formations attached to the pozzolana (c); solid and liquid wastes at the bottom of the reactor (d).*

Table 13 *Characterization of precipitates sampled at the bottom of the SR bioreactor (section D) including dry matter and solubilized fraction during leaching test.*

Solubilized fraction (mg/kg dw)		**Class 1[1] (mg/kg dw)**	
TOC	86.0	TOC	1000
Arsenic (As)	0.75	Arsenic (As)	25
Zinc (Zn)	19	Zinc (Zn)	200
Sulfates (SO_4^{2-})	7300	Sulfates (SO_4^{2-})	--
pH	4.5	pH	4<pH>13

[1] Classification of the European Council Directive 1999/31/EC of April 26. 1999 on the landfill of waste; class 1: reserved for special industrial.

4.4.3 Dynamics of the bacterial communities

A total of 340 OTUS were obtained (genus level) with a similarity higher than 98.2%. The six most abundant phyla were *Patescibacteria*, *Desulfobacterota*, *Proteobacteria*, *Bacteroidota*, *Firmicutes* and *Spirochaetota*. According to the Shannon index that represents the richness and equitability of the community, the alpha diversity in the inlet water and FeOB bioreactor's effluent were higher than the alpha diversity in the midpoint of the SR bioreactor. The attached communities of the FeOB showed a higher alpha diversity than the attached communities in the SR bioreactor (Figure 28.a). Globally, the attached communities showed a higher alpha diversity than the suspended communities. There was no significant difference in the alpha diversity measured for the attached communities sampled from the four sections inside the SR bioreactor. However, according to the Shannon index there is a downward trend descending along the bioreactor (as shown in Figure 28.b).

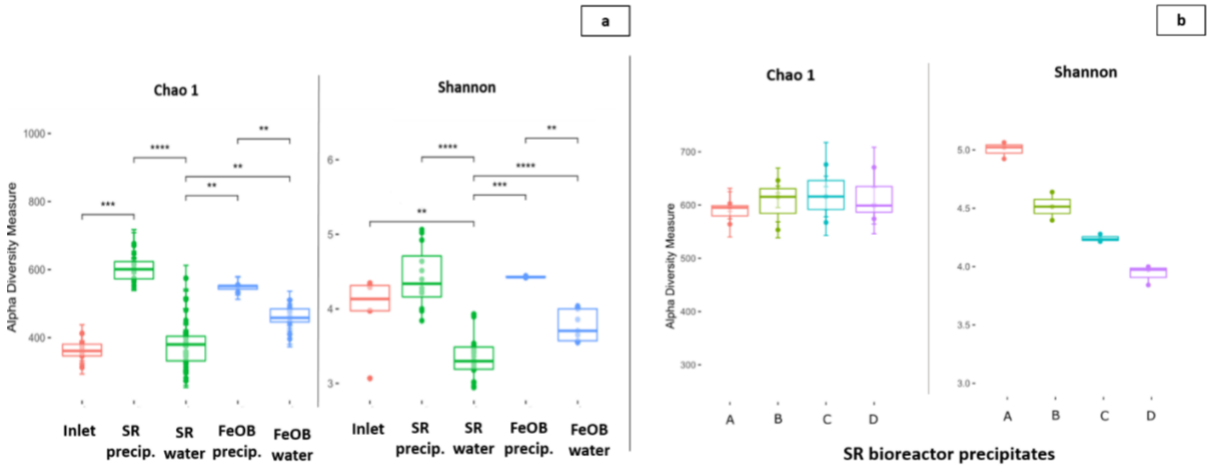

Figure 28. *Alpha diversity indices (Chao1 and Shannon) of the bacterial communities developed in each sampling point; inlet water, attached and suspended communities of the SR bioreactor and attached and suspended communities of the FeOB bioreactor (a); precipitates accumulated in the four sections of the SR bioreactor (b). ("****" =p-value ≤0.0001, "***" p-value ≤0.001, "**"= p-value ≤ 0.01, "*"= p-value ≤ 0.05. Only significant differences are shown in the figure (p-value > 0.05, not significant).precip. corresponds to the abbreviation of precipitates.*

Then beta diversity, representing the turnover of the bacterial community along the functioning. The highest beta diversity was observed in the suspended community of the SR bioreactor while the lowest diversity was associated with the fixed community of the FeOB

bioreactor. There was no significant difference of beta diversity between the different layers of precipitates accumulated inside the SR bioreactor (Figure 29.b).

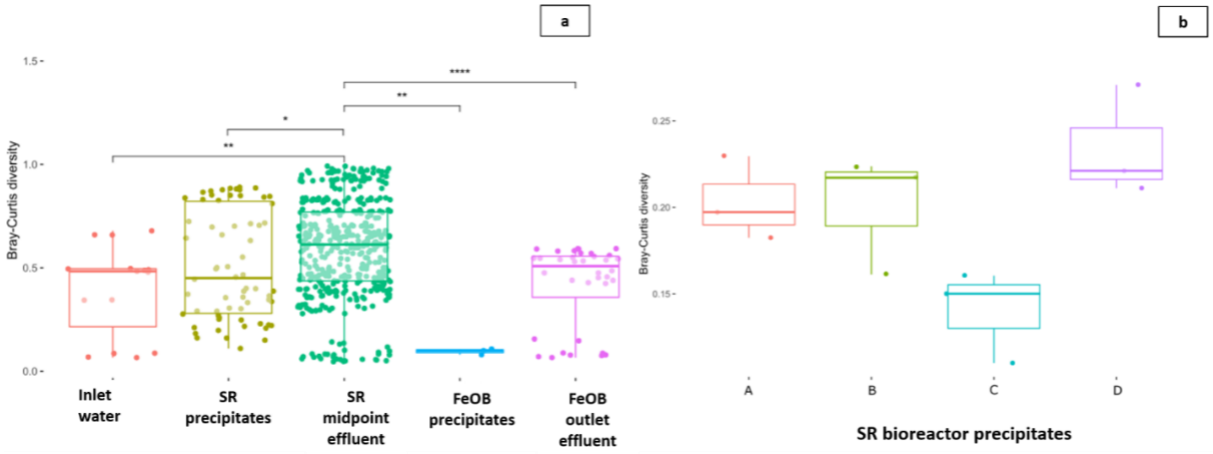

Figure 29. *Indices to measure beta diversity (Bray-Curtis, p-value<0.05) of the bacterial communities developed in the inlet water, the attached and suspended communities of the SR bioreactor and the attached and suspended communities of the FeOB bioreactor (a). Bray-Curtis indices from the 4 sections of the precipitates accumulated in the SRB bioreactor (b). ("****" =p-value ≤0.0001, "***" p-value ≤0.001, "**"= p-value ≤0.01, "*"= p-value ≤0.05). Only significant differences are shown in the figure (p-value > 0.05, not significant).*

The 16S rRNA gene metabarcoding from different sampling campaigns allowed to study the bacterial community composition during the SR bioreactor functioning and during its coupling with the FeOB bioreactor (Figure 30). The observations described below were also reinforced by the Indicator Species Analysis, which listed the genera that are statistically relevant of a particular group of data (Table 14).

In the inlet water, the most dominant taxa were *Parcubacteria*-related sequences (36 ± 9%), *Gallionella* (28 ± 2%), *Sideroxydans* (13 ± 1%) and *Elusidimicrobia*-related sequences (5 ± 1%). *Gallionella* and *Sideroxydans* correspond to iron-oxidizing bacteria. A slight difference was observed in the inlet water during periods II and IX, the difference relies in the relative abundance of *Parcubacteri*a-related sequences and *Gallionellacea*-related sequences, the first one dominated during period II while the second one during period IX.

The top 5 of the most dominant taxa present in the midpoint port of the SR bioreactor were *Desulfatirhabdium* (14 ± 9%), *Microbacter* (11 ± 7%), *Desulfovibrio* (9 ± 5%), *Spirochaetaceae*-related sequences (10 ± 4%) and *Parcubacteria*-related sequences (17 ± 13%). The bacterial community identified in the suspended community included different groups like fermentative bacteria such as *Microbacter* and *Treponema*, and iron-oxidizing bacteria such as *Gallionella* and *Ferritrophicum*. However, this community was mainly dominated by sulfate-reducing bacteria, which represented 20 to 50% of the total sequences identified along the monitoring. Several genera of sulfate-reducing bacteria were identified along the monitoring, *i.e Desulfovirga, Desulfurispora, Desulfobacterium, Desulfurivibrio, Desulfobulbus, Desulfatirhabdium* and *Desulfosporosinus*. At the beginning of the functioning (until day 110) sulfate-reducing populations were dominated by genera *Desulfurispora* (16 ±

5%) *and Desulfovirga* (11 ± 5%). Then from period VI (Day 124), which was just before the dormancy stage at day 239, the diversity shifts occurred. The bacterial community was enriched mainly with the sulfate-reducing bacteria *Desulfatirhabdium* (13 ± 1%), *Desulfovibrio* (12 ± 0.6%) and *Desulfosporosinus* (13 ± 1%). Finally at the end of the monitoring during period XIII (Day 348, 365 and 373) the community was dominated by *Desulfatirhabdium* (21 ± 4%) *and Desulfovibrio* (9 ± 3%) while *Desulfosporosinus* (2 ± 1%) was less represented. The abundance of the other metabolic groups presented in the suspended community of the SR bioreactor also evolved. For instance, the fermentative bacteria *Microbacter* were present along the monitoring with the highest relative abundance in the beginning during period II (27 ± 0.1%) and the lowest at the end during period XIII (4 ± 1).

Regarding the communities present in the sludge, there was a clear difference in the attached communities developed in each section of the SR bioreactor. For example, *Gallionella* was dominant in the top of the SR bioreactor including section A and B with an average of 31 ± 3 % and 14 ± 2% respectively. Other genera well represented in the top layers were *Ferritrophicum* and undetermined sequences of the *Desulfobulbaceae* family. *Desulfarihabdium* was dominant in the bottom three layers B, C and D with 24 ± 3%, 28 ± 1% and 32 ± 6% respectively. Other genera such as *Pelosinus, Microbacter* and *Desulfosporosinus* were also present in these 3 bottom sections. However, only a few taxa were present in similar abundance in the four sections such as *Spirochaetaceae*-related sequences.

Finally, the five most abundant taxa present in the FeOB bioreactor were *Parcubacteri*a-related sequences (38 ± 5%), *Gallionella* (11 ± 8%), *Ferritrophicum* (7 ± 7%) *Desulfatirhabdium* (7 ± 2%), and the unknown bacteria (7 ± 5%).
The suspended community in the coupled FeOB was dominated by *Parcubacteria*-related sequences (36 ± 4%), then iron-oxidizing bacteria such *Gallionella* (11 ± 9%), *Ferritrophicum* (9 ± 8%) and *Sideroxydans* (1 ± 0.8%), and some sulfate-reducing bacteria such as *Desulfatirhabdium* (8 ± 2%). The attached community was dominated also by iron-oxidizing bacteria such *Gallionella* (9 ± 1%), *Sideroxydans* (2 ± 0.4%*)* and *Ferritrophicum* (2 ± 0.3%), the arsenite-oxidizing bacteria *Thiomonas* (4 ± 1%), but also by sulfate-reducing bacteria such as *Desulfatirhabdium* (6 ± 1%). The most dominant taxa corresponded to *Parcubacteria*-related sequences (43 ± 2%). the community evolved throughout time. For instance, the composition of the bacterial community in the first sampling was similar to the composition of the top of the SR bioreactor community, while samples from the later sampling events (Day 365 and Day 373) were less similar. The relative abundance of the genus *Ferritrophicum*, that includes iron-oxidizing bacteria, and the arsenite-oxidizing genus *Thiomonas*, increased along the functioning. Both were represented in the attached and suspended communities.

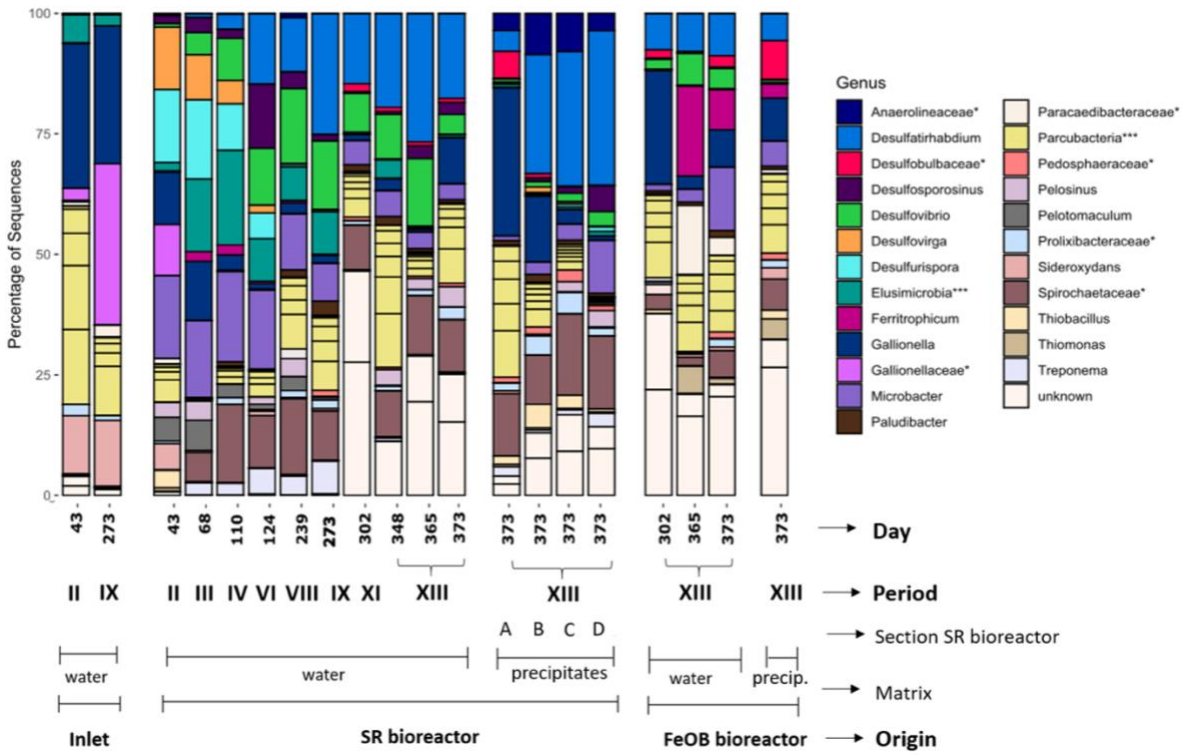

Figure 30. *Evolution of the taxonomic composition of the bacterial communities present at the midpoint of the SR bioreactor (10 samplings campaigns), at the inlet water (two sampling campaigns), at the outlet water of the FeOB bioreactor (three sampling campaigns), the four sections of the precipitates accumulated in the SR bioreactor and the precipitates of the FeOB bioreactor. Composition at the genus level, when genus identification was not possible, grouping of several OTUs was made at the family level (∗), at the order level (∗∗) and at the class level (∗∗∗). Only taxa with relative abundance > 0.5% were retained in the group of samples. Each box of each bar represent an OTU.*

Table 14 *Bacterial taxa representative (p-value < 0.05) of the different samples according to Indicator Species Analysis.*

Taxa	Inlet water	SR effluent	SR precip. A	SR precip. B	SR precip. C	SR precip. D	FeOB effluent	FeOB precip.
Desulfatirhabdium		X		X	X	X		
Gallionella	X		X					
*Spirochaetaceae**		X	X	X	X	X		
Microbacter						X		
Desulfovibrio		X						
*Elusimicrobia****	X	X						
*Parcubacteria****	X		X				X	X
*Gallionellaceae**	X							
Desulfosporosinus		X				X		
Sideroxydans	X							
Ferritrophicum							X	
Treponema		X	X			X		

Pelosinus	X			X	X		
*Prolixibacteraceae**			X	X			
*Paracaedibacteraceae**						X	
*Anaerolineaceae**			X	X			
*Desulfobulbaceae**		X					X
*Pedosphaeraceae**		X	X	X	X		X
Thiomonas						X	X

When genus identification was not possible, classification was made at the family level (∗), at the order level (∗∗) and at the class level (∗∗∗), precip. corresponds to the abbreviation of precipitates

The dynamic and diversity of the *bacterial communities* developed in the three sampling locations (inlet, midpoint SR bioreactor and outlet FeOB bioreactor) was represented by non-metric multidimensional scaling (*NMDS*). There was a clear distinction between the bacterial communities from the inlet AMD and those from the two other sampling locations (Figure 31). This difference was less pronounced between the midpoint SR and outlet FeOB. Also, the temporality was an important factor in the distribution of the communities; the bacterial community of the midpoint SR bioreactor was stabilized after 273 days of functioning as shown by the proximity of the squares during the last 5 samplings campaigns from Day 273 to Day 373 (between Period IX-XIII).

There was also a difference between the attached and suspended communities in each bioreactor (Figure 31). Differences were observed also within the attached communities among the different sections inside the SR bioreactor.

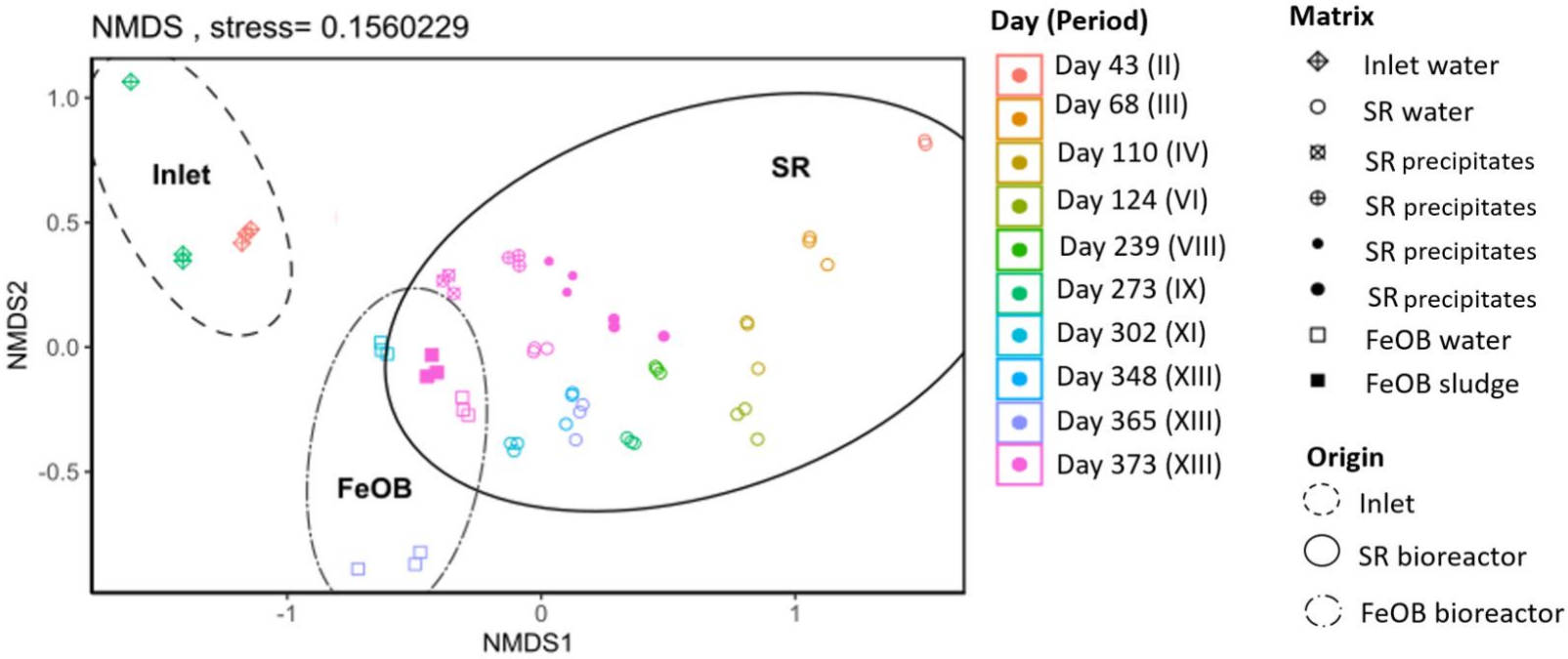

Figure 31. *NMDS representing the structure of the bacterial communities of each sample. The shape distinguished the combination of the origin (FeOB or SR bioreactor) and type of sample (water or sludge). The colors represent the days of monitoring. The ellipses represent the three sampling locations inlet water, FeOB bioreactor and SR bioreactor.*

4.4.4 Quantification of 16S rRNA and aioA gene

The quantification of 16S rRNA gene copies/mL of water or 16S rRNA gene copies/mg of precipitates was used as indicator of bacterial biomass abundance.
In water from the midpoint of SR bioreactor, the abundance was between 1 x 10^7 and 4 x 10^7 copies/mL (Figure 32). The highest concentration was reached 49 days after the change from batch conditions (day 124 to day 224) to continuous feeding. At day 365, the biomass of the suspended community significantly decreased and remained similar until the end of the functioning.

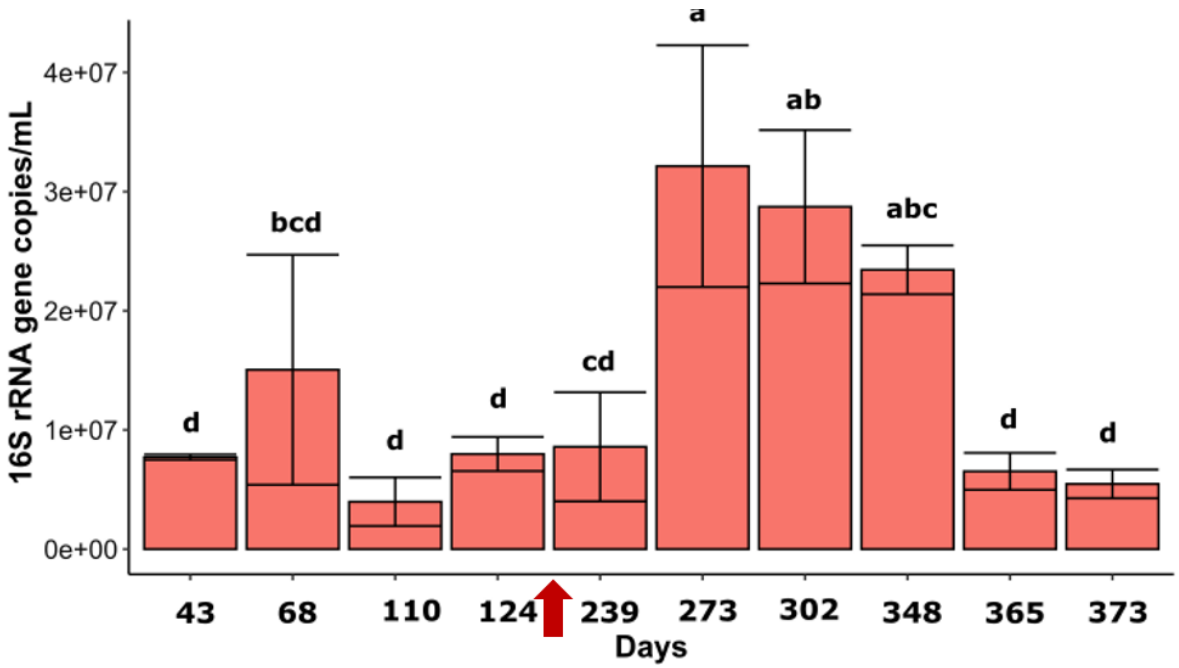

Figure 32. *Abundance of copies of 16S rRNA gene/mL in water from the midpoint of the SR bioreactor. Different letter in the figures indicate significant differences according to Kruskal-Wallis test ($p < 0.05$). The red arrow indicate the fed-batch period.*

In the precipitates from the four sections of the SR bioreactor, the range of bacterial biomass of the attached community including the four sections was between 1.1 x 10^4 and 8 x 10^6 16S rRNA gene copies/mg of precipitates (Figure 33). The top of the bioreactor (section A) showed the highest biomass concentration while the other three sections showed a similar biomass concentration (8.5 ± 4.5 x 10^4 16S rRNA gene copies/mg of sludge).

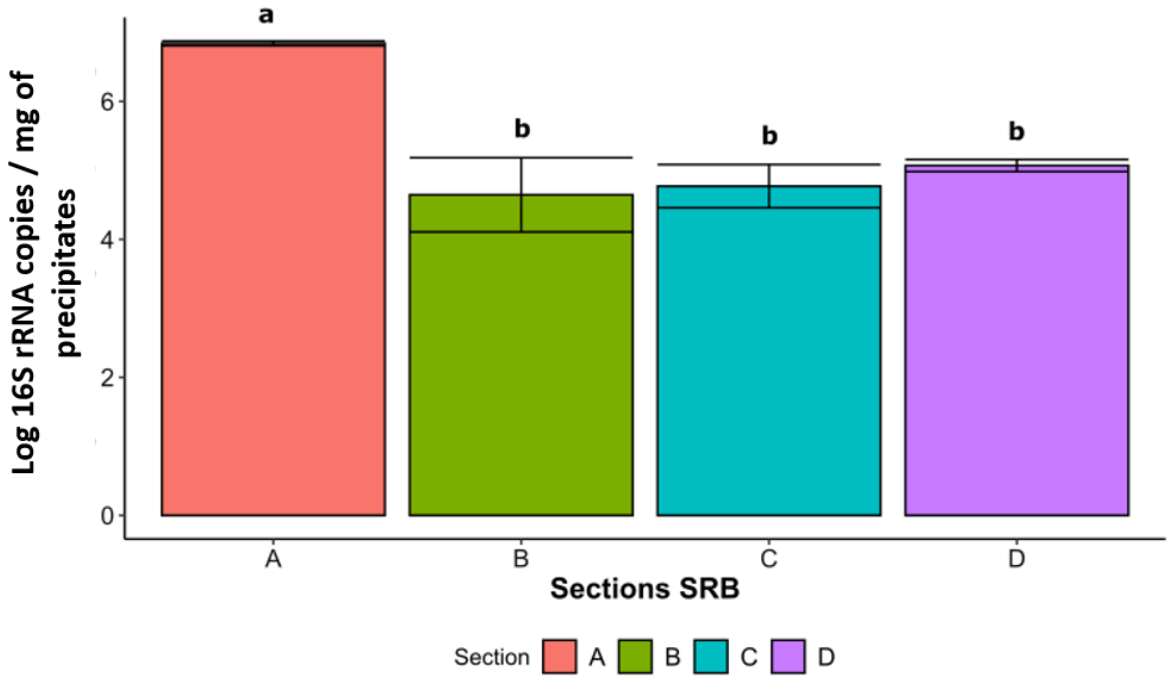

Figure 33. *Abundance of copies of 16S rRNA gene and present in the precipitates of the four sections of the SR bioreactor, from the top to the bottom A, B, C and D. Log 16S rRNA gene copies/mg of sludge. Different letter in the figures indicate significant differences according to Kruskal-Wallis test ($p < 0.05$) (expressed in wet weight).*

aioA gene (marker gene for arsenite-oxidising bacteria) was quantified in the different samples (Figure 34). The concentration of the *aioA* gene of the bacterial community was between 1.5 x 10^2 and 3.7 x 10^5 *aioA* gene copies/mL in the inlet water, between 3.5 x 10^4 and 8.2 x 10^5 *aioA* gene copies/mL in the midpoint port of the SR bioreactor and between 1.8 x 10^5 and 3.9 x 10^6 *aioA* gene copies/mL in the FeOB outlet. Regarding the attached communities, it ranged between 3.2 x 10^2 and 4.6 x 10^5 *aioA* gene copies/mg of precipitates in the SR bioreactor and between 8.7 x 10^5 and 1.7 x 10^6 *aioA* gene copies/mg of precipitates in the FeOB.

The abundance of functional gene copies was normalized with the 16S rRNA gene copies. The relative abundance of *aio*A gene copies was higher for the inlet AMD and for the effluent of the FeOB bioreactor than for the midpoint effluent of the SR bioreactor (Figure 35.a). The trend was similar for attached community recovered from the precipitates, the relative abundance of *aio*A genes was higher in the FeOB bioreactor than in the SR bioreactor (Figure 35.b).

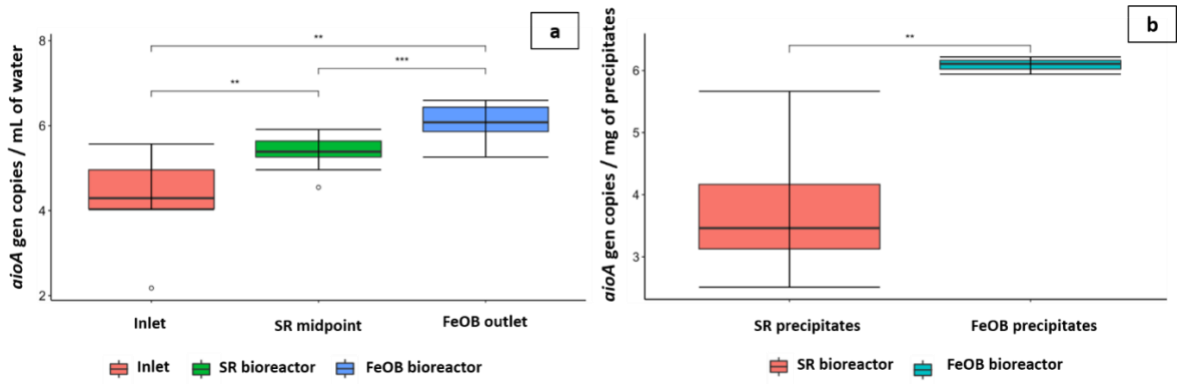

Figure 34. *Average of arsenite oxidase gene (aioA) gene copies/mL of water in the water in Carnoulès AMD (inlet), SR bioreactor and FeOB bioreactor including all dates monitored (a) Average of arsenite oxidase (aioA) gene copies/mg of precipitates at the end of the monitoring including four sections of the SR bioreactor (b). Asterisks represent significant differences ("**** =p-value ≤ 0.0001, "***" p-value ≤ 0.001, "**"= p-value ≤ 0.01, "*"= p-value ≤ 0.05, "ns" = p-value > 0.05). Only significant differences are shown in the figure (p-value > 0.05, not significant).*

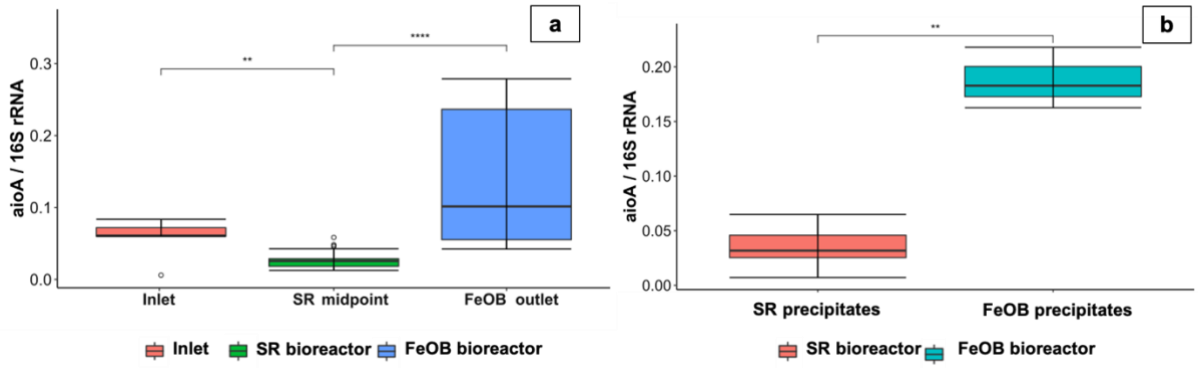

Figure 35. *Average of the relative abundance of the arsenite oxidase (aioA) gene copies detected in the treated water from the midpoint of the SR bioreactor. The aioA/16S rRNA ratio represented the relative abundance of the aioA in the midpoint water of the SR bioreactor and outlet water of the FeOB (a). Average of the relative abundance detected in the precipitates recovered after one year of operating in the SR and FeOB bioreactors (b).*

The use of *dsr* gene as a marker of sulfate-reducing bacteria failed (raw results presented in Anexxe 1. Quantification of the *dsr* gen) due to the low specificity of the *dsrA* primers. Additional efforts are needed to use the quantification of the *dsr* gene as a reliable indicator of sulfate-reducing bacteria. This low specificity was also observed in previous studies such as Burns et al. (2012), Drennan et al. (2016) and Vasquez et al. (2018), in those studies the quantification of *dsr* genes finally could not be related with the bioreactor's performances.

4.4.5 Interactions between geochemical parameters and bacterial community composition

According to redundancy analysis (RDA), the pH and temperature of the midpoint effluent, the As concentration in the inlet water (also Fe and Zn concentration) and HRT are the main

parameters that influence the composition and diversity of the bacterial communities in the SR bioreactor (Figure 36).

The sulfate-reducing genera *Desulfovirga* and *Desulfurispora* were correlated with the pH of the midpoint effluent and As concentration. *Desulfosporosinus*, *Microbacter*, *Treponema* and *Elusimicrobia*-related sequences were positively correlated with longer HRT and negatively correlated with the temperature. On the contrary, *Desulfatirhabdium* was positively correlated with the temperature and negatively correlated with HRT.

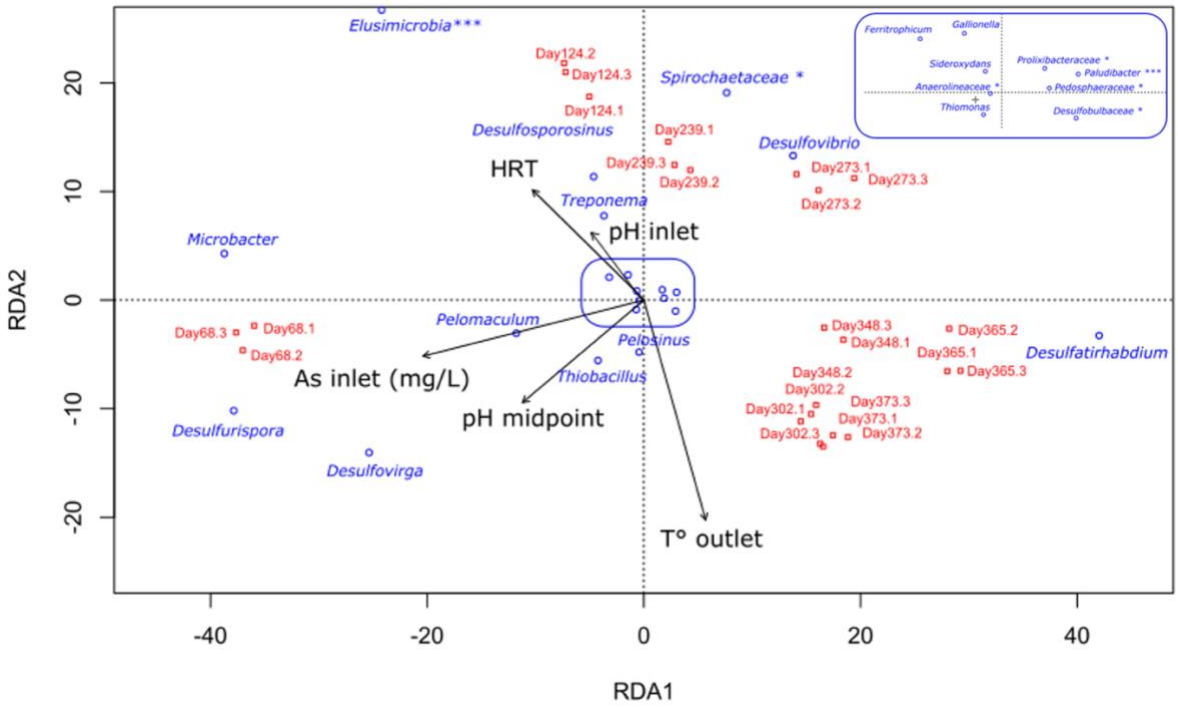

Figure 36. *Redundancy analysis (RDA) representing the interactions among the physic-chemical variables i.e pH midpoint effluent, temperature midpoint effluent, HRT and the abundance of the most abundant taxa identified in the water of the midpoint port of the SR bioreactor (only the taxa with a relative abundance ≥ 1%). The square in the center represented the taxa that were overlapped (Gallionella, Sideroxydans, Ferritrophicum, Thiomonas, Paludibacter***, Prolixibacteraceae*, Pedosphaeraceae* Desulfobulbaceae* and Anaerolineaceae*). When genus identification was not possible, classification was made at the family level (*), at the order level (**) and at the class level (***)*

Correlations between biological variables such as bacterial biomass (16S rRNA gene copies /mL), and abundance of the most abundant taxa identified in the midpoint effluent of the SR bioreactor (only the taxa with a relative abundance ≥ 1%) and sulfate reduction rate were explored (supplemental Figure SI 16). The only positive correlation observed with the rates of SO_4^{-2} reduction (mM/day) was with the genus of sulfate-reducing genus *Desulfatirhabdium* (Spearman correlation coefficient 0.6). However, the sulfate-reductio rate was negatively correlated with the abundance of the sulfate-reducing genus *Desulfosporosinus* (Spearman correlation coefficient -0.5), and with most of the other taxa such as *Ferritrophicum*, *Desulfurispora*, *Desulfovirga*, *Microbacter*, *Pelotomaculum*, *Anaerolineaceae*, *Treponema*, *Elusimicrobia*-related sequences and *Sideoroxydans*. (Spearman correlation coefficient < -0.5). No significantly correlation was found between the suspended bacterial biomass and the rate of sulfate reduction during the whole monitoring (Spearman correlation coefficient 0.28).

However, the highest sulfate reduction rates were observed when the highest suspended biomass concentrations were detected as shown Figure 32 (between day 300 and day 350).

4.5 Discussion

4.5.1 Performances of the sulfate-reducing bioreactor

Despite the variability of sulfate reduction yield (%) in the SR bioreactor, the system remained stable toward As and Zn removal, presenting nearly 100% efficiency. The yellow-gold precipitates evidenced in the bottom of the bioreactor (Figure 27) could correspond to amorphous orpiment (As_2S_3), which was detected in the lab-scale trials performed with the Carnoulès AMD (Le Pape et al. 2017, Battaglia-Brunet et al. 2021), as well as with synthetic As-rich solutions (Battaglia-Brunet et al. 2012).

Arsenic and zinc removal was stable all along the monitoring, despite the gradual decrease of the HRT from 29 days to 4 days, the seasonal variation in the AMD chemistry and the changes in the feed conditions (batch or continuous). Most of the As and Zn removal occurred in the bottom half of the bioreactor (sections C and D, Figure 20), while the removal in the second half of the bioreactor was moderate and variable.
Fe removal was widely variable, and depended on the concentration of reduced sulfate and consequently on the concentration of sulfides available for Fe precipitation in the bottom of the bioreactor. As predicted by the solubility products of As, Zn and Fe sulfides according to pH, As sulfide precipitated at the lowest pH, followed by Zn (at pH near 4.5). Finally, Fe was the last element to precipitate when pH increased and reached values around 5. This sequence was already observed with Carnoulès AMD in batch experiments (Le Pape et al. 2017), and explains the phenomena observed in the present study, i.e. a higher dependency of Fe removal to the sulfate-reducing activity, and the large spreading of Fe precipitates along the bioreactor levels, contrary to As and Zn that were mainly precipitated closer to the feed entry of the SR bioreactor (section D).

4.5.2 Parameters controlling the sulfate reduction

Due to the similarity between the concentrations of total sulfur in the midpoint and the outlet port, it was assumed that most of the reduction of sulfate occurred in the bottom of the SR bioreactor. This observation concurs with the yields of As, Zn and Fe removal calculated at the midpoint water and also with the elevated concentration of these elements in the precipitates accumulated in the bottom of the bioreactor (section D).
The amount of reduced sulfate was variable during the functioning. Parameters such as the HRT, the pH and the structure of the bacterial communities are factors widely mentioned as controlling the efficiency of this kind of bioreactors. For instance, Vasquez et al. (2018) observed that the HRT had a strong influence on the microbial activity and finally impacted the performance of a SR bioreactor treating AMD. In the present study, the HRT ranged between 4 and 29 days during the functioning of the SR bioreactor. The precipitation of metal sulfides required at least 3 to 5 days (Neculita et al. 2007). A HRT lower than 1 day can wash

out biomass, increase input of dissolved oxygen and limit the time for the SRB to neutralize the acidity of the AMD, which finally lead to a decrease of metal removal efficiency (Neculita et al. 2007; Vasquez et al. 2018). However, a long HRT is not a viable solution for a full-scale treatment.

Our study confirmed that HRT affected outlet pH and bacterial community composition (Figure 17). During the 375 days of monitoring, five different HRT were tested and the results evidenced a control of the outlet pH by the HRT (Figure 22). A diminution in the HRT was associated with a diminution of the outlet pH, and this effect was particularly pronounced at the beginning of the monitoring (before the fed-batch period). The main trend observed was an effluent with a higher pH when a longer HRT was applied. During the whole operation, the midpoint and outlet pH were not correlated to inlet pH, suggesting that the sulfate-reducing activity was not dependent on the pH of the AMD.

In the present study, the performances in terms of sulfate reduction rates were not influenced by the HRT in the same way during all the experiment. In particular, a strong change was observed between the first periods and after the fed-batch period. During period II and period V the same HRT of 14.5 days was fixed, and the sulfate reduction rate were 0.4 ± 0.2 mM/day and 0.05 ± 0.1 mM/day respectively. Despite the same HRT was applied during these two periods the ranges of sulfate reduction rates were different. Moreover, we obtained a rate of 0.12 ± 0.05 mM/days was obtained with an HRT of 29 days (period VI), compared to a rate of 0.9 ± 0.2 mM/day with an HRT of 4 days (period XIII). The increase of the rates of sulfate-reducing activity associated with the diminution of the HRT suggested the adaptation of the bacterial community to the increase of the inlet flow after the fed-batch period. This is a promising result for the treatment with an HRT of four days.

Based on the RDA analysis, the HRT was identified as an important driver for the composition of the suspended bacterial community, which was characterized in the midpoint effluent of the SR bioreactor. Passive SR bioreactors tested under field conditions dealing with Fe rich AMD are reported to work with an HRT of 2 days, but most of them being composed by a combination of treatment units (Sato et al. 2018; Vasquez et al. 2021). To our knowledge, there is no SR bioreactors tested under field conditions treating As-rich AMD, as the ones reported in the literature are still working under laboratory conditions. Furthermore, most of those studies were still performed with synthetic AMD and As concentration between 0.5 to 20 mg/L, and HRT between 9 to 48 hours (Luo et al. 2008; Altun et al. 2014; Sahinkaya et al. 2015). For that reason, the present study is an important improvement in the application of the sulfate-reducing bioremediation in the treatment of As-rich AMD.

We assumed that the bacterial biomass inside the bioreactor would increase during the fed-batch period, but without being reflected by the suspended biomass in the midpoint effluent during the first sampling (239 day) due to the long HRT (29 days) that corresponded to a low glycerol feeding flow. At day 273, the decrease of HRT to 14.5 days (period IX) may have contributed to stimulate the growth of biomass in the system and may explain the peak of suspended biomass found in the midpoint effluent. After this peak, the bacterial biomass of the suspended community decreased along the functioning. This decrease occurred during the

continuous diminution of the HRT and might reflect the exceeding of an optimal feeding flow-rate for bacterial growth, stimulated by the glycerol flow but inhibited by arsenic, acidity and ferric iron brought by the influent.

Thus, the increase of the SR bioreactor performances in terms of rates of sulfate reduction since period X was not accompanied by an increase of the suspended bacterial biomass. This result reinforced the idea of the main role of the attached community in the reduction of sulfate, this attached community forming a biofilm over the pozzolana and precipitates (Song et al. 2012; Lefticariu et al. 2015; Campos-Quevedo et al. 2021a). An increase of the bacterial biomass attached to the precipitates along the bioreactor functioning might have occurred. The bacterial community sampled at the midpoint port was roughly representative of the composition of the community inside the SR bioreactor, whereas some differences exist as shown by the final characterization of both suspended and attached communities. Thus, the characterization of the suspended bacterial community sampled at the midpoint is not enough to assess the changes in the structure and the biomass of the attached community.

So, the increase of the sulfate reduction rate after the fed-batch period may be explained by an increase of biomass of the whole attached community, including SRB biomass, and enrichment of the SRB community during this fed-batch period. This period probably gave the time to the SRB community to grow, SRB being characterized by a relatively slow growing rate (Sahinkaya et al. 2019). As a consequence, the fed-batch period seemed to enhance the activity and/or abundance of the sulfate-reducing bacterial community and its adaptability to the field conditions and operational changes.

4.5.3 Shifts in the composition of the bacterial communities during operation

During the functioning of the SR bioreactor, an enrichment of the strictly anaerobic populations of sulfate-reducing bacteria occurred, principally *Desulfatirhabdium* and *Desulfovibrio*. *Desulfosporosinus* was also present but in less proportion that remained relatively stable along the monitoring with only one rise during period VI (13 ± 2 %). These three genera were often dominant in passive pilot-scale bioreactors installed in different mine sites geographically distant (Rezadehbashi and Baldwin 2018). *Desulfosporosinus* was the dominant sulfate reducer in the consortium enriched from Carnoulès site and previously studied (Le Pape et al. 2017; Battaglia-Brunet et al. 2021). It was used to inoculate the semi-passive SR bioreactor working on site. In the bioreactor on site, *Desulfosporosinus* was found in similar proportion both in the attached and the suspended communities. In the attached community, *Desulfosporosinus* was more abundant in the precipitates recovered at the bottom of the SR bioreactor (layer D). Despite the dominance of *Desulfosporosinus* in the consortium used to inoculate the SR bioreactor, its relative abundance remained limited along the functioning. It ranged only between 0.2 and 15% in the suspended community and between 0.2 and 9% in the attached community in the three bottom sections of the bioreactor (B, C and D).

Desulfatirhabdium was the most abundant genus in both the attached and suspended communities. The rise in its relative abundance (25 ± 1%) coincided with the period of high

sulfate reduction rates (period IX). This relation was supported by the positive correlation (Pearson coefficient 0.6) between this genus abundance and sulfate reduction rate. Furthermore, the abundance of *Desulfatirhabdium* was also negatively associated with acetate concentration in the effluent. This is in line with previous study showing that this genus was able to oxidize completely the glycerol and even able to degrade the acetate (Campos-Quevedo et al. 2021a), which is a product of the incomplete glycerol oxidation (Equation 19).

Desulfovibrio was predominant in the suspended community and the variability of its abundance showed a similar trend as *Desulfatirhabdium*, the highest abundance of *Desulfovibrio* occurring at period IX (14 ± 1) and the lowest (2 ± 1%) in the beginning of the monitoring. This genus is well described in sulfate-reducing bioreactor working at pH 4.0–4.5 (Sánchez-Andrea et al. 2012). *Desulfovibrio* species oxidize only incompletely glycerol, releasing acetate as end-product of the oxidation (Rabus et al. 2013; Zhou et al. 2022). However, as concentrations of acetate at the outlet port of the SR bioreactor were low, we supposed that the acetate released by *Desulfovibrio* could be used by acetotrophic bacteria including the acetotrophic and sulfate-reducing *Desulfatirhabdium genus* (Sánchez-Andrea et al. 2014; Campos-Quevedo et al. 2021a). These metabolic interactions may have contributed to the dominance and cohabitation of these two genera in the bacterial community.

In addition to sulfate reducers, fermentative microorganisms were present, but in smaller proportions. The main genera associated with fermentative bacteria developed in the SR bioreactor were *Micobacterium, Treponema, Clostridium, Ruminiclostridium, Sedimentibacter* and *Sporotomaculum*. Most of them were identified in either the attached or suspended communities. Those genera obtain energy from the fermentation of organic matter and provide simple carbon sources and hydrogen to the SRB (Campos-Quevedo et al. 2021b). In our case, these trophic interactions were not primarily relevant as the glycerol is already a simple electron donor. However, acetogenic species belonging to *Treponema* and *Clostridium genera* could contribute to produce the acetate that, as mentioned before, can be used by acetotrophic sulfate-reducing bacteria (Hernández et al. 2022).

Association between *Desulfovibrio* and *Clostridium* is widely described in the literature. *Desulfovibrio* is a sulfate-reducing bacterium that can be inhibited by the mixture of metals such as Zn, Fe and Co. In the SR bioreactor, *Clostridium* was potentially able to release H_2 that promoted sulfate reduction by *Desulfovibrio*. The resulting release of sulfide might contribute to decrease the initial concentration of those metals, which provides the optimal conditions for *Desulfovibrio* activity (Alexandrino et al. 2014).

Based on the high rates of sulfate reduction and low concentration of acetate in the outlet port of the SR bioreactor, we supposed that a total oxidation of glycerol occurred along the functioning. The consortium inoculated in the SR bioreactor as mentioned before contained, as mentioned before, *Desulfosporosinus* as the main SRB (Battaglia-Brunet et al. 2021). *Desulfosporosinus* includes acidophilic species of sulfate-reducing bacteria that perform an incomplete oxidization of organic substrates to acetate (Alazard et al. 2010; Sánchez-Andrea et al. 2014). Thus, result obtained during this on-site experiment highlights the role of the

diversification of the microbial community during on site feeding with AMD in the performance of the SR bioreactor. In the previous laboratory experiences, the bacterial community composition during the continuous feeding was similar to the consortium enriched and inoculated directly in the bioreactor. The diversification of the community in this field trial could have allowed the development of bacteria capable of complete oxidation of glycerol. In fact, in the present study the bacterial diversification observed *in situ* allowed the development of *Desulfatirhabdium*, an acetotrophic sulfate-reducing bacteria. The presence of acetotrophic sulfate-reducing bacteria in the SR bioreactor could contribute to its remarkable performances and possible durability. As a fact, incomplete glycerol implies higher glycerol consumption to treat metals and metalloids. On the other hand, incomplete oxidation promotes acetate accumulation. This accumulation of acetate can be toxic for the acidophilic bacteria even at µM concentrations (González et al. 2019). So, the incomplete glycerol oxidation and release of acetate would induce a negative effect on the microbial community and consequently in the performances.

Another shift observed in the bacterial communities that contributed to increase SR bioreactor performances was linked to the fed-batch period. As mentioned before, this fed-batch period could have played the role of acclimation period for the bacterial communities, during which the bacterial biomass increased but also the population for SRB were enriched in quantity and diversity, as shown by Figure 30. This enrichment in SRB would explain rapid adaptability of the community to changes in the HRT and environmental temperature maintaining the performances of the bioreactor.
In the present study, the main drivers of the suspended bacterial community identified by the RDA analysis were HRT, pH, temperature and As concentration (as shown in Figure 36), all tendencies previously mentioned in the literature (Vasquez et al. 2016).

Concerning the bacterial community developed in the FeOB bioreactor, its composition in the first sampling was similar to that at the top of the SR bioreactor, resulting from the inoculation of the FeOB by the SR bioreactor effluent. The presence of Fe-oxidizing bacteria at this stage can be related to the development of an oxidizing zone in the top layer of the SR bioreactor, because of the oxygen diffusion.
Ferritrophicum and *Gallionella* were identified in the attached and suspended communities retrieved from aqueous and solid samples of the FeOB bioreactor. Particularly, there was an increase of *Ferritrophicum* abundance along the functioning of the aerobic bioreactor. These iron-oxidizing bacteria were brought by the AMD used to feed the SR bioreactor. They were probably in dormancy under the anaerobic conditions of the SR bioreactor and became active again when the optimal conditions were promoted in the FeOB bioreactor. They are known to survive under microaerophilic conditions which give them an advantage over other FeOB under SR bioreactor conditions (Emerson et al. 2013; Fabisch et al. 2013).

Evolution of the FeOB bacterial community could be related to the oxygen availability, and to the late increase of Fe concentration and decrease of pH. The relative abundance of the genus *Ferritrophicum*, that includes iron-oxidizing bacteria, and *Thiomonas* arsenite-oxidizing bacteria, increased along the functioning. As a fact, this bioreactor never reached stable

conditions, and further studies will be needed to better characterize the active bacterial community and correlate the corresponding data with bioreactor efficiency.

The arsenite oxidation potential of the bacterial communities present in the inlet AMD, SR bioreactor and FeOB bioreactor was evaluated. Relative abundance of *aioA* genes was significantly higher in the FeOB bioreactor and inlet AMD than in the SR bioreactor, as expected. The low redox conditions in the SR bioreactor probably reduced the populations of arsenic-oxidizing bacteria, compared to the optimal conditions present in the inlet AMD and FeOB. However, results underline the potential of the FeOB to perform both Fe(II) and As(III) oxidation, contributing to efficient As removal from the treated AMD.

4.5.4 Performances of the iron oxidation bioreactor coupled to the sulfate reduction bioreactor

The coupling of the FeOB bioreactor to the outlet port of the SR bioreactor was operated during 114 days. The objective of this aerobic step was the removal of residual Fe and As from the SR bioreactor effluent. Maintaining an incomplete Fe removal in the SR bioreactor would reduce the risks of clogging by Fe precipitates and also reduce the amount of organic substrate (i.e glycerol) needed for the sulfate reduction.
The pH of the influent feeding the coupled FeOB bioreactor ranged from 5.5 to 7. This range of pH was expected to promote rapid abiotic Fe oxidation (Kirby et al. 1999). However, it cannot be ruled out a possible contribution of biological iron oxidation due to the presence of neutrophilic iron-oxidizing bacteria such as *Ferritrophicum* and *Gallionella*. The high pH values of the FeOB influent were linked with the high yields of sulfate reduction in the SR bioreactor after the fed-batch period, the SR bioreactor promoted the precipitation of at least 50% of the Fe present in the Carnoulès AMD. For consequence, the FeOB was fed with a variable concentration of Fe, between 10 mg/L and 300 mg/L. More than 80% of the iron released in the outlet of the FeOB corresponded to ferrous iron, which suggests that the kinetics of iron oxidation was the main limitation of the Fe removal in the FeOB bioreactor.

Thus, a longer monitoring of the coupling stage (SRB bioreactor + FeOB bioreactor) with a Fe concentration higher than 100 mg/L in the influent of the FeOB bioreactor would be required to reach stable conditions and better evaluate the efficiency of the FeOB step for Fe oxidation and precipitation. As already observed in iron oxidation bioreactors dealing with As-rich AMD, this stage requires between 5 and 10 days of adaption before reaching stable performances (Diaz-Vanegas et al. 2022). Considering that the ferric iron precipitation releases protons, this precipitation would contribute to decrease the pH inside the systems (Nordstrom et al. 2015), which is expected to enhance the biological oxidation rate.

Despite the limitations of the coupling's evaluation, the obtained results gave us important clues to be considered for the up-scaling of an entire treatment process (including sulfate reduction and iron oxidation phases). For the up-scaling an additional step should be installed to treat the residual Fe and increase the pH downstream of the FeOB bioreactor.

4.6 Conclusion

The main advances of this field trial are the demonstrations of adaptability of the bacterial consortium to *in situ* temperature variations, seasonal variations in water chemistry and operating conditions. The diversification of sulfate-reducing community seemed to positively influence the bioreactors performances. In fact, the diversity of the bacterial community in this field trial was higher that the diversity observed in the previous laboratory trials, and this high diversification promoted the complete degradation of the electron donor (i.e glycerol) improving the treatment performance. The durability of the bioreactor efficiency was demonstrated in terms of stable and total As and Zn removal despite the reduction of the residence time from 29 to 4 days.
The stage of iron oxidation after the sulfate-reducing step contributes to decrease the residual Fe and As present in the effluent of the SR bioreactor. Regardless of the types of Fe oxidation performed in the FeOB bioreactor (abiotic or biotic), the effluent showed As concentration down to 10 µg/l, mainly promoted by the sorption of co-precipitation of the As with the Fe(III) hydroxides/hydroxysulfates (Paikaray 2015).

Regarding the iron removal, the efficiency of the aerobic stage depends on the Fe concentration in the influent. When the effluent of the SR bioreactor presents a Fe concentration lower than 100 mg/L, the iron oxidation stage is efficient and enough to completely treat Fe. However, when the Fe concentration in the effluent of the SR bioreactor is higher than 100 mg/L, an additional phase for the treatment will be required to remove the residual iron and acid consumption downstream of the FeOB bioreactor.

Future research should focus on the optimization of the organic substrate input to reduce costs, in order to identify the minimum quantity of glycerol necessary to achieve efficient removal of As and Zn by the coupled SR /FeOB bioreactors. Next operational steps will include the up-scaling of the SR bioreactor in a pilot with proportions closer to a full-scale treatment plant (in a pond). Furthermore, it will be required to design a system to increase the final pH downstream the FeOB step (lime drain or DAS) for the periods with high Fe concentration in the AMD.

4.7 Supplementary Information

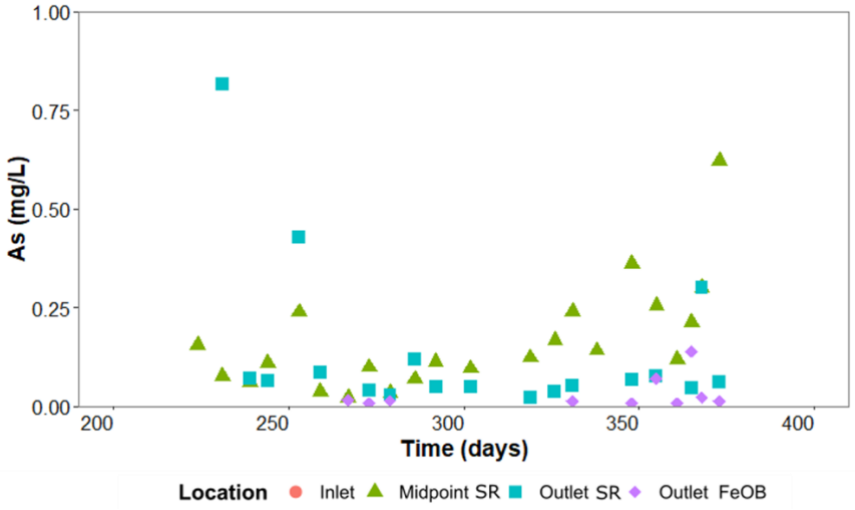

Figure SI 15. *As concentration (mg/L) in the midpoint and outler water of the SR bioreactor and outler waater of the FeOB bioreactor. Zoom of the Figure 27.*

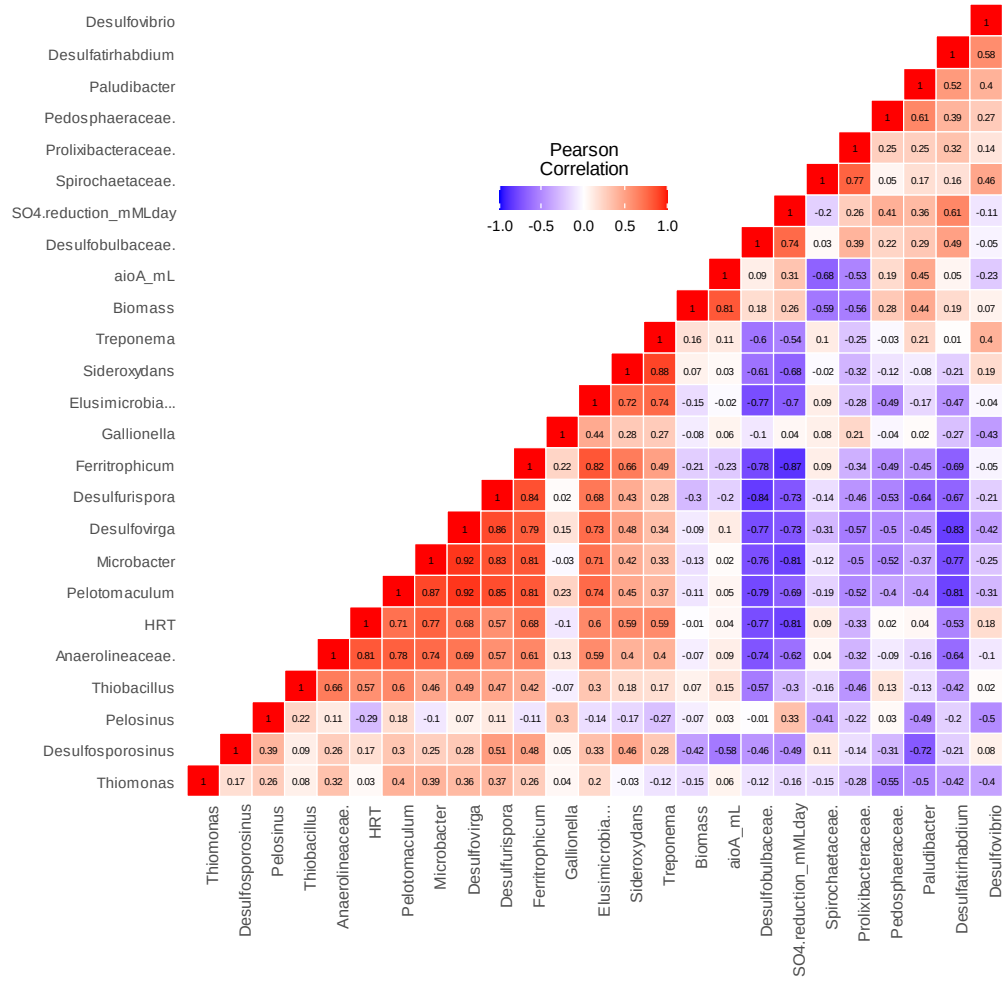

Figure SI 16. *Heat map of the Spearman correlation coefficients between relative abundance of the most dominant genera (horizontal axis), biomass (16S rRNA gen copies/ mL of water), arsenite oxidazing potential (aioA gen copies/mL) and HRT or Rate of sulfate reduction (mM/day).*

Conclusion Générale et Perspectives

Principaux résultats du travail de thèse

L'objectif principal de cette thèse était de faire progresser les connaissances sur les conditions d'exploitation optimale des processus naturels d'oxydo-réduction biologique conduisant à la précipitation du fer, de l'arsenic et du zinc dans les Drainages Miniers Acides (DMA) riches en As. Il s'agissait également de mieux comprendre le rôle des facteurs environnementaux, opérationnels, et ceux associés à la physico-chimie du DMA, dans le contrôle des performances, ainsi que les liens étroits avec la dynamique des communautés bactériennes et l'expression de gènes fonctionnels clés. Les deux grands processus étudiés sont complémentaires : 1) la bio-oxydation du fer (Fe) et de l'arsenic (As) conduisant à leur co-précipitation partielle et 2) la sulfato-réduction, permettant d'éliminer le Zn sous forme de sulfures, celui-ci ne pouvant être éliminé par l'étape aérobie, ainsi que l'As et une partie du Fe. L'objectif, à terme, de ces recherches, est de contribuer à la mise en œuvre de systèmes de bioremédiation sur des bases théoriques plutôt qu'empiriques, comme c'est le cas actuellement. Concernant le cas particulier du site atelier de Carnoulès sur lequel les dispositifs ont été étudiés, l'objectif était de tester ces systèmes de bioremédiation à une échelle supérieure à celle étudiée auparavant et *in situ*, avec à terme, la perspective d'un traitement adapté à ce site.
L'aspect le plus novateur par rapport aux travaux antérieurs a été de tester *in situ* et sur le long terme les deux approches complémentaires, permettant la prise en compte de la variabilité saisonnière (changements de température et de physico-chimie du DMA). Cet essai sur le terrain a permis de recueillir des informations importantes sur la faisabilité et les limites de ces deux approches de biorémediation au niveau fondamental et opérationnel. Les deux processus (bio-oxydation et sulfato-réduction) ont été testés séparément et combinés.

Les principaux résultats de la thèse sont synthétisés ci-dessous. :

Traitement basé sur un bioréacteur d'oxydation

Les bioréacteurs d'oxydation du fer et de l'arsenic ont fonctionné pendant un an et ont permis d'oxyder la quasi-totalité du fer (92 ± 6%) et une grande partie de l'arsenic (79 ± 10% d'As(V) dans les précipités formés) et d'éliminer 43 ± 11% de Fe et 67 ± 10% de l'As, pour un temps de séjour de 9 h. Ces résultats ont confirmé que l'aération forcée combinée avec des supports de biomasse à haute porosité (i.e. support plastique ou pouzzolane/copeaux de bois) sont des facteurs clés pour augmenter les performances et leur stabilité dans le temps par rapport au pilote de terrain entièrement passif (sans aération forcée) rempli d'un lit de sable, testé précédemment (Fernandez-Rojo et al. 2019).
Les bioréacteurs d'oxydation (PS et WP) ont produit des boues contenant 8% d'arsenic, principalement sous forme d'arséniates ferrique amorphes (AFA), schwertmannite amorphe et jarosite, facilement décantables, comme l'indique la faible proportion d'As particulaire dans l'effluent (8% de l'arsenic total) malgré l'absence d'un bassin de décantation dédié. Grâce à l'optimisation des conditions opératoires (support de biomasse, aération forcée et temps de

séjour stabilisé), nous avons réussi à quantifier la limite du bioprocédé en termes de concentration en As minimale atteignable dans l'effluent, de l'ordre de 10 mg/L, cette limite étant liée à la solubilité élevée des phases minérales de Fe-As au pH acide de l'effluent (pH 2,8 ± 0,3) généré par la précipitation du fer. Même si cela correspond à une amélioration de la qualité de l'eau du Reigous d'un facteur 10 pour sa concentration en As, cette valeur est bien au-dessus du seuil établi par la DCE pour les eaux de surface (valeur NQE (Directive Européenne cadre sur l'Eau, 2000/60/CE) = 0,83 µg/L + valeur du fond géochimique local), et également au-dessus du seuil établi par l'arrêté préfectoral défini site par site, qui est en général au maximum de 100 µg/L. Notons que cette valeur limite est liée à la composition du DMA de Carnoulès, très riche en As, générant des phases minérales également très riches ; il n'existe pas d'expérience comparable de traitement par oxydation biologique dans la littérature pour des DMA possédant une concentration en As aussi élevée, ce qui limite toute comparaison de l'efficacité du système développé avec des procédés similaires.

Dans tous les cas, un traitement complémentaire est nécessaire du fait de l'acidité de l'effluent traité (pH 2,8), des concentrations élevées en sulfate (2417 ± 486 mg/L), en zinc (15 ± 3 mg/L) et en plomb (0,3 ± 0,2 mg/L). Un traitement passif tel que le Substrat Alcalin Dispersé (Rotting et al. 2008a), permettant de neutraliser le pH, précipiter le fer et adsorber les métaux et l'As restants, pourrait être envisagé plutôt qu'un traitement physico-chimique classique par ajout d'une base et d'un floculant (Ahoranta et al. 2016).
Concernant la dynamique des communautés bactériennes dans le système, les techniques moléculaires basées sur l'ARN, visant les gènes exprimés, ont montré que les bactéries responsables de l'oxydation du Fe et de l'As sont restées actives tout au long du fonctionnement des bioréacteurs d'oxydation. Particulerment, *Ferrovum* a montré un rôle central dans l'efficacité du traitement, ce genre semblait particulièrement bien adapté au traitement des effluents riches en arsenic. *Leptospirillum* était un membre permanent de la communauté active tout au long du suivi, ce qui suggère sa contribution aux performances stables.
Il a été constaté que la résilience et la redondance fonctionnelle des communautés bactériennes sessile et planctonique développées dans les bioréacteurs ont conféré au traitement une grande robustesse vis-à-vis des variations des conditions environnementales et opératoires et une stabilité des performances. Ces propriétés écologiques étaient liées à la diversité de la communauté associée à chaque support de biomasse.

Bioréacteur basé sur la sulfato-réduction

Le bioréacteur de sulfato-réduction a permis d'éliminer en moyenne 99,7 ± 0,2% de l'As et 97,8 ± 3 du Zn avec un temps de séjour minimal de 4 jours. Il a également piégé entre 33 et 99,9% du fer (55 ± 12% en moyenne). Le substrat organique a été consommé en grande partie (94 ± 2%), conduisant à une concentration en carbone organique dans l'effluent inférieure à 20 mg/L et à un rendement de oxydation du glycérol en CO_2 proche de 100%.
L'augmentation d'échelle visée dans la présente thèse par rapport aux travaux précédents (Battaglia-Brunet et al. 2021) a donc été réalisée avec succès, passant d'un bioréacteur de 300

mL au laboratoire à 25 L sur site. Le suivi des performances au cours des différentes étapes de diminution du temps de séjour de 29 à 4 jours a démontré le maintien de rendements de traitement de l'As et Zn optimaux. Un résultat marquant concerne la corrélation positive observée entre la température, la vitesse de réduction des sulfates, et l'abondance de *Desulfatirhabdium*. Cette bactérie sulfato-réductrice est caractérisée par sa capacité à oxyder totalement le glycérol en CO_2 (Campos-Quevedo et al. 2021), ce qui représente un avantage en termes de rendement de sulfato-réduction.

La période de fonctionnement en fed-batch, imposée par les conditions sanitaires, semble avoir renforcé les performances globales ultérieures de la communauté microbienne installée dans le bioréacteur. Elle a permis un meilleur maintien de l'activité de sulfato-réduction (estimée à 0,6 ± 0,3 mM/jour), en réponse à une diminution du temps de séjour au cours des étapes ultérieures, en comparaison avec la période antérieure à la phase de fed-batch. Enfin, la modification du temps de séjour, le pH et la période de fonctionnement du bioréacteur (associée à une évolution de différents paramètres tels que la température et la physico-chimie du DMA) sont les principaux facteurs qui influencent le plus la structure de la communauté BSR, ce phénomène ayant été décrit dans des études précédentes portant sur ce type de bioprocédé (Vasquez et al. 2018).

Couplage d'un bioréacteur de réduction des sulfates et d'un bioréacteur d'oxydation

L'efficacité du couplage du bioréacteur d'oxydation biologique en traitement de finition après le bioréacteur de sulfato-réduction n'a pu être évaluée que sur une semaine. Pendant cette période, la concentration en fer dans l'effluent du BSR alimentant le bioréacteur d'oxydation était supérieur à 100 mg/L, permettant une évaluation de ses performances. Cette étape d'oxydation biologique en aval de l'étape de sulfato-réduction a contribué à diminuer l'As résiduel (de 140 ± 170 µg/l à 10 µg/l), mais la concentration élevée du Fe(II) en sortie du pilote montre que la vitesse d'oxydation limitée n'as pas permis un abattement total du fer. La durée de l'essai de couplage est toutefois insuffisante pour juger de l'efficacité du bioréacteur d'oxydation couplé sur le long terme et de l'intérêt d'un tel couplage.

Malgré ces limitations, les communautés sessile et planctonique présentes dans le bioréacteur d'oxydation du fer en aval du bioréacteur de sulfato-réduction ont été caractérisées. La communauté planctonique était principalement dominée par des bactéries appartenant aux groupes des SRB et des FeOB, les genres dominants de FeOB étant *Gallionella* et *Ferrirophicum,* contrairement aux réacteurs d'oxydation biologique découplés, dans lesquels *Leptospirillum* et *Ferrovum* dominaient. Ceci suggère que les genres *Gallionella* et *Ferrirophicum* sont plus tolérants que le reste de la communauté FeOB aux conditions anaérobies imposées par le bioréacteur de sulfato-réduction. Le genre As-oxydant *Thiomonas* était également présent dans la communauté sessile (4%) et planctonique (en moyenne 3%) du bioréacteur d'oxydation couplé, malgré des concentrations en As bien inférieures et des concentrations en carbone organique bien supérieures à celles de l'alimentation du réacteur découplé. Sa présence suggère un potentiel d'oxydation de l'As dans ce bioréacteur.

Conclusions

Grace à la quantité de données collectées, la diversification des analyses effectuées et l'approche interdisciplinaire mise en œuvre, ce travail de thèse a permis d'avancer tant sur le plan opérationnel que sur le plan fondamental dans le développement d'un système de traitement biologique applicable aux DMAs riches en As, basé sur des processus naturels réalisés par des microorganismes autochtones. A ce jour, la conception d'installations de traitement de DMA utilisant des micro-organismes reste basée principalement sur des connaissances empiriques. Ce travail de thèse a permis d'améliorer la compréhension du fonctionnement de ces systèmes, les actions et rétroactions entre les facteurs physico-chimiques, les conditions opératoires et les paramètres biologiques. En cela, l'utilisation des techniques moléculaires comme les "omiques" joue un rôle clé. A travers cette étude, nous avons montré qu'elles pouvaient permettre de faire le lien entre la composition/la dynamique des communautés bactériennes colonisant les systèmes de traitement et certains facteurs environnementaux contrôlant leur diversité et leur activité. Compte tenu du rôle central des communautés bactériennes dans les processus en jeu, ces connaissances sont cruciales pour mieux comprendre les dysfonctionnements éventuels et anticiper les performances des systèmes de bioremédiation. Ceci est particulièrement vrai pour les systèmes *in situ* passifs ou semi-passifs à faible maintenance confrontés à des variations saisonnières et à d'éventuels dysfonctionnements liés à des perturbations des conditions opératoires.

Le bioréacteur d'oxydation du fer et le bioréacteur de réduction des sulfates ont montré individuellement une efficacité notable, malgré certaines limitations, et une robustesse remarquable vis-à-vis des aléas, par conséquent ils s'avèrent adaptés aux conditions *in situ*. Cette adaptabilité peut être largement attribuée à la résilience et la redondance fonctionnelle des communautés bactériennes responsables de chacun des traitements (Allison and Martiny 2008). Ces deux propriétés écologiques sont attribuées à la diversité en termes de richesse en espèces ou au remplacement des espèces (Girvan et al. 2005; Feng et al. 2017). Cette robustesse suggère un potentiel intéressant pour une exploitation à une échelle supérieure et l'extrapolation des traitements étudiés à d'autres DMA présentant des propriétés similaires.

Perspectives

Recherches à developper sur la bioremédiation des drainages de mine

Le travail expérimental réalisé dans le cadre de cette thèse constitue une étape essentielle vers l'élaboration d'un modèle de transport réactif permettant de représenter le fonctionnement de ces systèmes de traitement. Cette phase de modélisation permettrait de tester la sensibilité du modèle aux différents facteurs, de prédire l'efficacité de ces systèmes dans différentes conditions et d'extrapoler à des DMA de composition proche. L'intégration dans les modèles de variables relatives à la communauté bactérienne de ces systèmes (e.g cinétiques bactériennes de transformation des éléments, quantité de biomasse active Fe- ou As-oxydante ou SO_4-reductrice) pourrait permettre d'améliorer leur adaptabilité.

En ce qui concerne le bioréacteur de sulfato-réduction, une prochaine étape devrait être l'optimisation de la concentration en glycérol. L'objectif est de définir la quantité minimale nécessaire dans le but de réduire les coûts. Une conduite optimale du process devrait viser une quantité de glycérol fournie nécessaire et suffisante pour la précipitation de l'As et du Zn mais pas pour celle du fer, ce dernier pouvant être éliminé par un bioréacteur d'oxydation couplé ou/et un réacteur de neutralisation physico-chimique. D'autre part, une diminution du temps de séjour à moins de quatre jours pourrait être envisagée. En effet, dans l'expérience menée, tout l'As et le Zn étaient précipités à mi-hauteur du bioréacteur, ce qui correspond à la partie inférieure de la colonne, proche de l'alimentation. Ceci suggère que le temps de séjour pourrait encore être réduit de moitié.

Malgré les progrès réalisés dans la caractérisation de la diversité et de la composition des communautés présentes dans le bioréacteur de sulfato-reduction, il est important de progresser dans l'identification des populations actives, en particulier celles responsables de l'activité sulfato réductrice (quantification des gènes *dsr*). Ce travail a été abordé dans le cadre de cette thèse n'a pas abouti à des résultats exploitables pour des raisons pratiques (temps et budget contraints ayant été des obstacles à l'optimisation des méthodes).
En ce qui concerne le bioréacteur aérobie, la question de la durabilité sur le long terme du support de biomasse à base de bois et de pouzzolane se pose. L'impact des produits de dégradation du bois sur le fonctionnement de la communauté autotrophe des bactéries Fe-oxydantes et les performances associées devraient être abordés. Un point qui reste à approfondir et qui constituait l'un des objectifs de cette thèse, est l'identification des facteurs susceptibles de réguler l'expression de l'activité arsénite oxydante dans un système de traitement fonctionnant en conditions de terrain. Malgré l'observation de l'expression du gène et de sa corrélation avec la présence de *Thiomonas* dans les communautés actives, un effort méthodologique supplémentaire serait nécessaire pour optimiser la quantification de l'expression d'*aioA*, cette quantification aiderait à identifier les facteurs qui régulent cette expression. Toutefois, un contrôle strict des conditions opératoires et une variation de ces conditions sur une gamme suffisamment large serait nécessaire, ce qui reste complexe à mettre en œuvre lors d'expériences de terrain à grande échelle.

Enfin, la présente thèse s'est concentrée sur les communautés bactériennes, négligeant ainsi une part importante de la diversité représentée par les archaea et par les eucaryotes, qui sont présents dans les DMA et ont des fonctions écologiques importantes. Particulièrement, dans le DMA de Carnoulès les communautés d'archées ont été caractérisés (Bruneel et al. 2008) ainsi que les communautés eucaryotes (Volant 2012), certaines espèces jouant un rôle dans le cycle biogéochimique de l'arsenic, du fer, du soufre, du carbone et de l'azote (Volant et al. 2012). Notamment, certaines espèces ont une activité potentielle d'oxydation de l'arsenite ou encore sont impliquées dans la méthanogénèse (Andres and Bertin 2016). Certains de ces microorganismes ont montré un grand potentiel pour le traitement actif de DMA riches en arsenic (Gonzalez-Contreras et al. 2012a). Or, leur rôle dans les procédés de bioremédiation des eaux minières reste encore mal connu. Il serait donc intéressant de cibler ces communautés dans les travaux de recherche futurs.

Vers la mise en place d'une stratégie de bioremédiation en plusieurs étapes adaptée au DMA de la mine de Carnoulès

La présente thèse a permis d'obtenir des résultats prometteurs, cependant le procédé de traitement n'est pas encore prêt à être directement mis en œuvre à l'échelle industrielle. Ainsi, la prochaine étape devrait être la mise en place d'un démonstrateur avec des proportions plus proches de l'étape de traitement à grande échelle.

Si l'idée est de conserver le même ordre dans les étapes anaérobie puis aérobie lors de la mise en œuvre d'un traitement à plus grande échelle, une étape supplémentaire devrait être considérée pour éliminer le Fe résiduel et augmenter le pH en aval du bioréacteur FeOB.

A noter que le choix de l'ordre des étapes BSR et FeOB était basé sur le fait qu'il apparaissait impossible de proposer l'ordre inverse du fait de concentrations élevées en Fe(III) (~ 300 mg/L) subsistant dans l'effluent du réacteur FeOB non couplé et du fait du pH acide (~ 2,6). Cependant, la proportion élevée de Fe(II) dans l'effluent du bioréacteur FeOB couplé suggère que la diminution de la quantité de fer oxydé dans le bioreacteur pourrait réduire la concentration de Fe(III) dissous libéré dans l'effluent. Ceci compte tenu de la toxicité du fer ferrique sur les bactéries sulfato-réductrices qui a été rapportée (Zhang et al. 2009). Or les communautés sulfato-réductrices du bioreacteur de sulfato-reduction ont finalement résisté à des concentrations en fer ferriques représentant jusqu'à 6% du fer total dans l'eau d'alimentation, soit environ 30 mg/L. Cette résistance est soutenue par des études récentes qui indiquent que le fer ferrique n'a pas eu d'effet toxique sur la réduction des sulfates pour des teneurs en Fe(III) de l'ordre de 50 mg/L, en raison de la résistance de certaines populations de BSR (Yang et al. 2021). Ces aptitudes pourraient permettent d'envisager le traitement par oxydation biologique comme une étape préliminaire avant l'étape de réduction des sulfates pour éliminer une partie du fer et de l'arsenic. Un avantage de cette configuration serait de limiter le risque de colmatage du dispositif BSR et de réduire la consommation de glycérol. La faisabilité de cette approche a été démontrée par quelques études (Hedrich et Johnson 2014 ; Hayashi et al. 2020). Une autre approche évoquée dans la littérature a porté sur le couplage d'un bioréacteur de sulfato-réduction en aval d'un traitement physico-chimique passif par un substrat alcalin dispersé (DAS) (Vasquez et al. 2021). Toutefois, ces couplages ont été appliqués à des DMA moins chargés en fer et en arsenic. La faisabilité reste donc à démontrer dans le cas du DMA de Carnoulès.

En complément de ces perspectives d'amélioration portant sur le traitement à proprement parler, la gestion des boues produites reste un point à considérer. Une étude de stabilité dans les conditions de stockage long terme envisagées serait à prévoir, afin d'évaluer le risque de relargage de l'arsenic et de rechercher des solutions pour maîtriser ce risque. L'évaluation de la valorisation potentielle des boues riches en zinc du BSR pourrait également être considérée (possibilité de tester des méthodes d'hydrométallurgie pour séparer les sulfures).

Enfin, afin de vérifier que ces stratégies de remédiation sont écologiquement durables et pertinentes, dans un contexte de changement climatique, par rapport aux méthodes classiques, il serait intéressant d'effectuer une comparaison avec une stratégie de remédiation physico-chimique telle que le chaulage, à l'aide des techniques d'analyse du cycle de vie (ACV).

Bibliographie

Afzal Ghauri M, Okibe N, Barrie Johnson D (2007) Attachment of acidophilic bacteria to solid surfaces: The significance of species and strain variations. Hydrometallurgy 85:72–80. https://doi.org/10.1016/j.hydromet.2006.03.016

Ahoranta S, Hulkkonen H, Salminen T, Kuula P, Puhakka J, Lakaniemi (2020) Formation and use of biogenic jarosite carrier for high-rate iron oxidising biofilms. Res Microbiol 171:243–251. https://doi.org/10.1016/j.resmic.2020.06.004

Ahoranta SH, Kokko ME, Papirio S, Ozkaya B, Puhakka J (2016) Arsenic removal from acidic solutions with biogenic ferric precipitates. J Hazard Mater. https://doi.org/10.1016/j.jhazmat.2015.12.012

Al-Amshawee S, Yunus MYBM, Lynam JG, Lee WH, Dai F, Dakhil IH (2021) Roughness 762 and wettability of biofilm carriers: A systematic review. Environ Technol Innov 763 21:101233. https://doi.org/10.1016/j.eti.2020.101233

Alam R, Mcphedran K (2019) Applications of biological sulfate reduction for remediation of arsenic. A review. Chemosphere 222:932–944. https://doi.org/10.1016/j.chemosphere. 2019.01.194

Alazard D, Joseph M, Battaglia-Brunet F, Cayol JL, Ollivier B (2010) Desulfosporosinus acidiphilus sp. nov.: A moderately acidophilic sulfate-reducing bacterium isolated from acid mining drainage sediments. Extremophiles 14:305–312. https://doi.org/10.1007/ s00792-010-0309-4

Alexandrino M, Costa R, Canário AVM, Costa MC (2014) *Clostridia* initiate heavy metal bioremoval in mixed sulfidogenic cultures. Environ Sci Technol 48:3378–3385. https://doi.org/10.1021/es4052044

Allison S, Martiny J (2008) Resistance, resilience, and redundancy in microbial communities. PNAS 105:1 www.pnas.org/cgi/doi/10.1073/pnas.0801925105

Altun M, Sahinkaya E, Durukan I, Bektas S, Komnitsas K (2014) Arsenic removal in a sulfidogenic fixed-bed column bioreactor. J Hazard Mater 269:31–37. https://doi.org/10.1016/j.jhazmat.2013.11.047

Anand V, Kaur J, Srivastava S, Bist V, Singh P, Srivastava S (2022) Arsenotrophy: A pragmatic approach for arsenic bioremediation. J Environ Chem Eng 10:107528. https://doi.org/10.1016/j.jece.2022. 107528

Andres J, Bertin PN (2016) The microbial genomics of arsenic. FEMS Microbiol Rev 40:299–322. https://doi.org/10.1093/femsre/fuv050

Asere TG, Stevens CV, Du Laing G (2019) Use of (modified) natural adsorbents for arsenic remediation: A review. Sci Total Environ 676:706–720. https://doi.org/10.1016/ j.scitotenv.2019.04.237

Asta MP, Ayora C, Acero P, Cama J (2010a) Field rates for natural attenuation of arsenic in Tinto Santa Rosa acid mine drainage (SW Spain). J Hazard Mater 177:1102–1111. https://doi.org/10.1016/j.jhazmat.2010.01.034

Asta MP, Ayora C, Román-Ross G, Cama J, Acero P, Gault A, Charnock J, Bardelli F (2010b) Natural attenuation of arsenic in the Tinto Santa Rosa acid stream (Iberian Pyritic Belt, SW Spain): The role of iron precipitates. Chem Geol 271:1–12. https://doi.org/10.1016/j.chemgeo.2009.12.005

Asta MP, Cama J, Martínez M, Giménez J (2009) Arsenic removal by goethite and jarosite in acidic conditions and its environmental implications. J Hazard Mater 171:965–972. https://doi.org/10.1016/j.jhazmat.2009.06.097

Asta MP, Kirk Nordstrom D, Blaine McCleskey R (2012) Simultaneous oxidation of arsenic and antimony at low and circumneutral pH, with and without microbial catalysis. Appl

Geochem 27:281–291. https://doi.org/10.1016/j.apgeochem.2011.09.002

Ayangbenro AS, Olanrewaju OS, Babalola O(2018) Sulfate-reducing bacteria as an effective tool for sustainable acid mine bioremediation. Front Microbiol 9:1–10. https://doi.org/10.3389/fmicb.2018.01986

Aytar P, Kay CM, Mutlu MB, Cabuk A, Johson DB (2015) Diversity of acidophilic prokaryotes at two acid mine drainage sites in Turkey. Environ Sci Pollut Res 22:5995–6003. https://doi.org/10.1007/s11356-014-3789-4

Azubuike CC, Chikere CB, Okpokwasili GC (2016) Bioremediation techniques–classification based on site of application: principles, advantages, limitations and prospects. World J Microbiol Biotechnol 32:1–18. https://doi.org/10.1007/s11274-016-2137-x

Barton LL, Fauque GD (2009) Chapter 2 Biochemistry, physiology and biotechnology of sulfate-reducing bacteria, 1st edn. Elsevier Inc.

Bartsch S, Gensch A, Stephan S, Doetsch A, Gescher J (2017) Metallibacterium scheffleri: Genomic data reveal a versatile metabolism. FEMS Microbiol Ecol 93:1–10. https://doi.org/10.1093/femsec/fix011

Battaglia-Brunet F, Casiot C, Fernandez-Rojo L, Hery M, Le Pape P, Tris H, Morin G, Touzé S, Joulian C (2021) Laboratory-scale bio-treatment of real arsenic-rich acid mine drainage. Water Air Soil Pollut 232. https://doi.org/10.1007/s11270-021-05276-z

Battaglia-Brunet F, Clarens M, D'Hugues P, Foucher S, Morin D (2002a) Monitoring of a pyrite-oxidising bacterial population using DNA single-strand conformation polymorphism and microscopic techniques. Appl Microbiol Biotechnol 60:206–211. https://doi.org/10.1007/s00253-002-1095-4

Battaglia-brunet F, Crouzet C, Morin D, Joulian C (2012) Precipitation of arsenic sulphide from acidic water in a fixed-film bioreactor. 46: 3923-3933. https://doi.org/10.1016/j.watres.2012.04.035

Battaglia-Brunet F, Dictor M-CC, Garrido F, Crouzet C, Morin D, Dekeyser K, Clarens M, Baranger P (2002) An arsenic(III)-oxidizing bacterial population: Selection, characterization, and performance in reactors. J Appl Microbiol 93:656–667. https://doi.org/10.1046/j.1365-2672.2002.01726.x

Battaglia-Brunet F, Joulian C, Garrido F, Dictor MC, Morin D, Coupland K, Johnson DB, Hallberg K, Baranger P (2006) Oxidation of arsenite by *Thiomonas* strains and characterization of *Thiomonas arsenivorans* sp. nov. Antonie van Leeuwenhoek, Int J Gen Mol Microbiol 89:99–108. https://doi.org/10.1007/s10482-005-9013-2

Ben Ali HE, Neculita CM, Molson JW, Maqsoud A, Zagury G (2019) Performance of passive systems for mine drainage treatment at low temperature and high salinity: A review. Miner Eng 134:325–344. https://doi.org/10.1016/j.mineng.2019.02.010

Bertin PN, Heinrich-Salmeron A, Pelletier E, Goylhen-Chollet F, Arsène-Ploetze F, Gallien E, Lauga B, Casiot C, Calteau A, et al (2011) Metabolic diversity among main microorganisms inside an arsenic-rich ecosystem revealed by meta-and proteo-genomics. ISME J 5:1735–1747. https://doi.org/10.1038/ismej.2011.51

Bigham JM, Schwertmann U, Traina SJ, Winland RR, Wolf M (1996) Schwertmannite and the chemical modeling of iron in acid sulfate waters. Geochim Cosmochim Acta 60:2111–2121. https://doi.org/10.1016/0016-7037(96)00091-9

Brown JF, Jones DS, Mills DB, Macalady L, Burgos W (2011) Application of a depositional facies model to an acid mine drainage site. Appl Environ Microbiol 77:545–554. https://doi.org/10.1128/AEM.01550-10

Bruneel O, Duran R, Casiot C, Elbaz-Poulichet F, Personné JC (2006) Diversity of microorganisms in Fe-As-rich acid mine drainage waters of Carnoulès, France. Appl Environ Microbiol 72:551–556

Bruneel O, Pascault N, Egal M, Bancon-Montigny C, Goñi-Urriza MS, Elbaz-Poulichet F, Personné JC, Duran R (2008) Archaeal diversity in a Fe-As rich acid mine drainage at Carnoulès (France). Extremophiles 12:563–571

Bruneel O, Personné JC, Casiot C, Leblanc M, Elbaz-Poulichet F, Mahler BJ, Le Flèche A, Grimont (2003) Mediation of arsenic oxidation by Thiomonas sp. in acid-mine drainage (Carnoulès, France). J Appl Microbiol 95:492–499. https://doi.org/10.1046/j.1365-2672.2003.02004.x

Brusseau ML, Chorover J (2019) Chemical processes affecting contaminant transport and fate, 3rd edn. Elsevier Inc.

Burns AS, Pugh CW, Segid YT, Behum PT, Lefticariu L, Bender K (2012) Performance and microbial community dynamics of a sulfate-reducing bioreactor treating coal generated acid mine drainage. Biodegradation 23:415–429. https://doi.org/10.1007/s10532-011-9520-y

Burton ED, Bush RT, Johnston SG, Watling KM, Hocking RK, Sullivan LA, Parker G (2009) Sorption of arsenic(V) and arsenic(III) to schwertmannite. Environ Sci Technol 43:9202–9207. https://doi.org/10.1021/es902461x

Burton ED, Karimian N, Johnston SG, Schoepfer V, Choppala G, Lamb D (2021) Arsenic-imposed effects on schwertmannite and jarosite formation in acid mine drainage and coupled impacts on arsenic mobility. ACS Earth Sp Chem 5:1418–1435. https://doi.org/10.1021/acsearthspacechem.1c00047

Campos-Quevedo N, Moreno-Perlin T, Razo-Flores E, Stams A, Celis L, Sanchez-Andrea I (2021a) Acetotrophic sulfate-reducing consortia develop active biofilms on zeolite and glass beads in batch cultures at initial pH 3. Appl Microbiol Biotechnol 105:5213–5227. https://doi.org/10.1007/s00253-021-11365-0

Campos-Quevedo NG, Sánchez-Andrea I, López-Lozano NE, Stams A, Celis L (2021b) In search of sulfate-reducing consortia able to degrade acetate under acidic conditions. J Chem Technol Biotechnol 96:1228–1236. https://doi.org/10.1002/jctb.6635

Carlson L, Bigham JM, Schwertmann U, Kyek A, Wagner, F (2002) Scavenging of As from acid mine drainage by schwertmannite and ferrihydrite: A comparison with synthetic analogues. Environ Sci Technol 36:1712–1719. https://doi.org/10.1021/es0110271

Casiot C, Leblanc M, Bruneel O, Personné JC, Koffi K, Elbaz-Poulichet (2003a) Geochemical processes controlling the formation of As-rich waters within a tailings impoundment (Carnoulès, France). Aquat Geochemistry 9:273–290. https://doi.org/10.1023/B:AQUA.0000028985.07557.39

Casiot C, Morin G, Juillot F, Bruneel O, Personé JC, Leblanc M, Duquesne K, Bonnefoy V, Elbaz-Poulichet F (2003b) Bacterial immobilization and oxidation of arsenic in acid mine drainage (Carnoulès creek, France). Water Res 37:2929–2936. https://doi.org/10.1016/S0043-1354(03)00080-0

Casiot C, Pedron V, Bruneel O, Duran R, Personné JC, Grapin G, Drakidès C, Elbaz-Poulichet F (2006) A new bacterial strain mediating As oxidation in the Fe-rich biofilm naturally growing in a groundwater Fe treatment pilot unit. Chemosphere 64:492–496. https://doi.org/10.1016/j.chemosphere.2005.11.072

Cébron A, Norini MP, Beguiristain T, Leyval C (2008) Real-Time PCR quantification of PAH-ring hydroxylating dioxygenase (PAH-RHDα) genes from Gram positive and Gram negative bacteria in soil and sediment samples. J Microbiol Methods 73:148–159. https://doi.org/10.1016/j.mimet.2008.01.009

Chai L, Tang J, Liao Y, Yang Z, Liang L, Li Q, Wang H, Yang W (2016a) Biosynthesis of schwertmannite by *Acidithiobacillus ferrooxidans* and its application in arsenic immobilization in the contaminated soil. J Soils Sediments 16:2430–2438.

https://doi.org/10.1007/s11368-016-1449-7

Chai L, Yue M, Yang J, Wang Q, Li Q, Liu H (2016b) Formation of tooeleite and the role of direct removal of As(III) from high-arsenic acid wastewater. J Hazard Mater 320:620–627. https://doi.org/10.1016/j.jhazmat.2016.07.069

Challan Belval S, Garnier F, Michel C, Chautard S, Breeze, Garrido F (2009) Enhancing pozzolana colonization by As(III)-oxidizing bacteria for bioremediation purposes. Appl Microbiol Biotechnol 84:565–573. https://doi.org/10.1007/s00253-009-2077-6

Chen L, Li J, Chen YT, Huang L, Hua Z, Hu M, Shu W (2013) Shifts in microbial community composition and function in the acidification of a lead/zinc mine tailings. Environ Microbiol 15:2431–2444. https://doi.org/10.1111/1462-2920.12114

Coudert L, Bondu R, Rakotonimaro T V, Guittonny M, Neculita CM (2020) Treatment of As-rich mine effluents and produced residues stability: Current knowledge and research priorities for gold mining. J Hazard Mater 386:121920. https://doi.org/10.1016/j.jhazmat.2019.121920

Dave SR, Gupta KH, Tipre DR (2008) Characterization of arsenic resistant and arsenopyrite oxidizing *Acidithiobacillus ferrooxidan*s from Hutti gold leachate and effluents. Bioresour Technol 99:7514–7520. https://doi.org/10.1016/j.biortech.2008.02.019

De Caceres M, and Legendre P. (2009). Associations between species and groups of sites: 797 indices and statistical inference. Ecology 90: 3566–3574. doi: 10.1890/ 08-1823.1

Debiec K, Krzysztoforski J, Uhrynowski W, Sklodowska A, Drewniak K (2017) Kinetics of arsenite oxidation by Sinorhizobium sp. M14 under changing environmental conditions. Int Biodeterior Biodegrad 119:476–485. https://doi.org/10.1016/j.ibiod.2016.10.049

Desoeuvre A, Casiot C, Héry M (2015) Diversity and distribution of arsenic-related genes along a pollution gradient in a river affected by acid mine drainage. Microb Ecol 71:672–685. https://doi.org/10.1007/s00248-015-0710-8

Diaz-Vanegas C, Casiot C, Lin C, De Windt L, Héry M, Desoeuvre A, Bruneel O, Battaglia-Brunet F, Jacob J (2022) Performance of semi - passive systems for the biological treatment of high - As acid mine drainage : Results from a year of monitoring at the Carnoulès mine (Southern France). Mine Water Environ. https://doi.org/10.1007/s10230-022-00885-4

Dixit S, Hering JG (2003) Comparison of arsenic(V) and arsenic(III) sorption onto iron oxide minerals: Implications for arsenic mobility. Environ Sci Technol 37:4182–4189. https://doi.org/10.1021/es030309t

Drahota P, Filippi M (2009) Secondary arsenic minerals in the environment: A review. Environ Int 35:1243–1255. https://doi.org/10.1016/j.envint.2009.07.004

Drennan DM, Almstrand R, Lee I, Landkamer L, Figueroa L, Sharp J (2016) Organoheterotrophic bacterial abundance associates with zinc removal in lignocellulose-based sulfate-reducing systems. Environ Sci Technol 50:378–387. https://doi.org/10.1021/acs.est.5b04268

Drewniak L, Sklodowska A (2013) Arsenic-transforming microbes and their role in biomining processes. Environ Sci Pollut Res 20:7728–7739. https://doi.org/10.1007/s11356-012-1449-0

Druschel GK, Baker BJ, Gihring TM, Banfield JF (2004) Acid mine drainage biogeochemistry at Iron Mountain, California. Geochem Trans 5:13–32. https://doi.org/10.1063/1.1769131

Duquesne K, Lebrun S, Casiot C, et al (2003) Immobilization of arsenite and ferric iron by *Acidithiobacillus ferrooxidans* and its relevance to acid mine drainage. 69:6165–6173. https://doi.org/10.1128/AEM.69.10.6165

Dzionek A, Wojcieszyńska D, Guzik U (2016) Natural carriers in bioremediation: A review. Electron J Biotechnol 23:28–36. https://doi.org/10.1016/j.ejbt.2016.07.003

Ebrahimi S, Fernández Morales FJ, Kleerebezem R, Heijnen J, van Loosdrecht M (2005) High-rate acidophilic ferrous iron oxidation in a biofilm airlift reactor and the role of the carrier material. Biotechnol Bioeng 90:462–472. https://doi.org/10.1002/bit.20448

Edgar RC, Haas BJ, Clemente JC, Quince C, Knight R (2011) UCHIME improves sensitivity and speed of chimera detection. Bioinformatics 27:2194–2200. https://doi.org/10.1093/bioinformatics/btr381

Edwards KJ, Schrenk MO, Hamers R, Banfield JF (1998) Microbial oxidation of pyrite; experiments using microorganisms from an extreme acidic environment. Am Mineral 83:1444–1453. https://doi.org/10.2138/am-1997-11-1233

Egal M, Casiot C, Morin G, Parmentier M, Bruneel O, Lebrun S, Elbaz-Poulichet (2009) Kinetic control on the formation of tooeleite, schwertmannite and jarosite by *Acidithiobacillus ferrooxidans* strains in an As(III)-rich acid mine water. Chem Geol 265:432–441. https://doi.org/10.1016/j.chemgeo.2009. 05.008

Egal M, Casiot C, Morin G, Elbaz-Poulichet F, Cordier MA, Bruneel O (2010) An updated insight into the natural attenuation of As concentrations in Reigous Creek (southern France). Appl Geochem 25:1949–1957. https://doi.org/10.1016/j.apgeochem.2010.10.012

Elbaz-Poulichet F, Bruneel O, Casiot C (2006) The Carnoules mine. Generation of As-rich acid mine drainage, natural attenuation processes and solutions for passive in-situ remediation. Difpolmine (Diffuse pollut from mining activities). Montpellier, France. hal-00184269

Emerson D, Field EK, Chertkov O, Davenport KW, Goodwin L, Munk C, Nolan, Woyke T (2013) Comparative genomics of freshwater Fe-oxidizing bacteria: Implications for physiology, ecology, and systematics. Front Microbiol 4:1–17. https://doi.org/10.3389/fmicb.2013.00254

Emett MT, Khoe GH (2001) Photochemical oxidation of arsenic by oxygen and iron in acidic solutions. Water Res 35:649–656. https://doi.org/10.1016/S0043-1354(00)00294-3

España J, Pamo E, Santofimia E, Aduvire O (2016) Geochemistry and mineralogy of AMD in the Iberian Pyrite Belt (Spain). ImwaDe

España JS, Pamo EL, Pastor ES, Andrés JR, Rubí JA (2005a) The natural attenuation of two acidic effluents in Tharsis and La Zarza-Perrunal mines (Iberian Pyrite Belt, Huelva, Spain). Environ Geol 49:253–266. https://doi.org/10.1007/s00254-005-0083-2

España JS, Pamo EL, Santofimia E, Reyes J, Martin JA (2005b) Acid mine drainage in the Iberian Pyrite Belt (Odiel river watershed, Huelva, SW Spain): Geochemistry, mineralogy and environmental implications. Appl Geochem 20:1320–1356. https://doi.org/10.1016/j.apgeochem.2005.01.011

Fabisch M, Beulig F, Akob DM, Küsel K (2013) Surprising abundance of Gallionella-related iron oxidizers in creek sediments at pH 4.4 or at high heavy metal concentrations. Front Microbiol 4:1–12. https://doi.org/10.3389/fmicb.2013.00390

Fabisch M, Freyer G, Johnson CA, Buchel G, Akob DM, Neu TR, Kusel K (2016) Dominance of "*Gallionella capsiferriformans*" and heavy metal association with Gallionella-like stalks in metal-rich pH 6 mine water discharge. Geobiology 14:68–90. https://doi.org/10.1111/gbi.12162

Falagán C, Foesel B, Johnson B (2017) *Acidicapsa ferrireducens* sp. nov., *Acidicapsa acidiphila* sp. nov., and *Granulicella acidiphila* sp. nov.: novel acidobacteria isolated from metal-rich acidic waters. Extremophiles 21:459–469. https://doi.org/10.1007/s00792-017-0916-4

Fan J hui, Liu X yu, Gu Q yuan, Zhang M, Hu X (2019) Effect of hydraulic retention time and pH on oxidation of ferrous iron in simulated ferruginous acid mine drainage treatment with inoculation of iron-oxidizing bacteria. Water Sci Eng 12:213–220. https://doi.org/

10.1016/j.wse.2019.09.003

Farasin J, Koechler S, Varet H, Deschamps J, Dillies MA, Proux C, Erhardt M, Huber A, Jagla B, Briandet R, Coppée JY, Arsène-Ploetze F (2017) Comparison of biofilm formation and motility processes in arsenic-resistant Thiomonas spp. strains revealed divergent response to arsenite. Microb Biotechnol 10:789–803. https://doi.org/10.1111/1751-7915.12556

Feng K, Zhang Z, Cai W, Liu W, Xu M, Yin H, Wang A, He Z, Deng Y (2017) Biodiversity and species competition regulate the resilience of microbial biofilm community. Mol Ecol 26:6170–6182. https://doi.org/10.1111/mec.14356

Fernandez-Rojo L, Casiot C, Laroche E, Tardy V, Bruneel O, Delpoux S, Desoeuvre A, Grapin G, Savignac J, Boisson, J Morin, G, Battaglia-Brunet F, Joulian C, Héry M (2019) A field-pilot for passive bioremediation of As-rich acid mine drainage. J Environ Manage 232:910–918. https://doi.org/10.1016/j.jenvman.2018.11.116

Fernandez-Rojo L, Casiot C, Tardy V, Laroche E, Le Pape P, Morin G, Joulian C, Battaglia-Brunet F, Braungardt C, Desoeuvre A, Delpoux S, Boisson J, Héry M (2018) Hydraulic retention time affects bacterial community structure in an As-rich acid mine drainage (AMD) biotreatment process. Appl Microbiol Biotechnol 102:9803–9813. https://doi.org/10.1007/s00253-018-9290-0

Fernandez-Rojo L, Héry M, Le Pape P, Desoeuvre A, Torres E, Tardy V, Resongles E, Laroche E, Delpoux S, Joulian C, Battaglia-Brunet F, Boisson J, Grapin G, Morin G, Casiot C (2017) Biological attenuation of arsenic and iron in a continuous flow bioreactor treating acid mine drainage (AMD). Water Res 123:594–606. https://doi.org/10.1016/j.watres.2017.06.059

Filippi M, Drahota P, Machovič V, Böhmová V, Mihaljevič M (2015) Arsenic mineralogy and mobility in the arsenic-rich historical mine waste dump. Sci Total Environ 536:713–728. https://doi.org/10.1016/ j.scitotenv.2015.07.113

Fleming EJ, Cetinić I, Chan CS, King DW, Emerson D (2014) Ecological succession among iron-oxidizing bacteria. ISME J 8:804–815. https://doi.org/10.1038/ismej.2013.197

Florence K, Sapsford DJ, Johnson DB, Kay CM, Wolkersdorfer C (2016) Iron-mineral accretion from acid mine drainage and its application in passive treatment. Environ Technol (United Kingdom) 37:1428–1440. https://doi.org/10.1080/09593330.2015.1118558

Fukushi K, Sasaki M, Sato T, Yanase N, Amano H, Ikeda H (2003) A natural attenuation of arsenic in drainage from an abandoned arsenic mine dump. Appl Geochem 18:1267–1278. https://doi.org/10.1016/ S0883-2927(03)00011-8

Galili T, O'Callaghan A, Sidi J, Sievert C (2017) heatmaply: an R package for creating interactive cluster heatmaps for online publishing, Bioinformatics, 34:1600-1602 https://doi.org/10.1093/bioinformatics/btx657

Garcia-Ochoa F, Gomez E, Santos VE, Merchuk JC (2010) Oxygen uptake rate in microbial processes: An overview. Biochem Eng J 49:289–307. https://doi.org/10.1016/ j.bej.2010.01.011

Garcia-Rios M, De Windt L, Luquot L, Casiot C (2020) Modeling of microbial kinetics and mass transfer in bioreactors simulating the natural attenuation of arsenic and iron in acid mine drainage. J Hazard Mater 405:124133. https://doi.org/10.1016/j.jhazmat.2020.124133

García-Sánchez A, Alonso-Rojo P, Santos-Francés F (2010) Distribution and mobility of arsenic in soils of a mining area (Western Spain). Sci Total Environ 408:4194–4201. https://doi.org/10.1016/j.scitotenv.2010.05.032

Gavrilov SN, Korzhenkov AA, Kublanov IV, Bargiela R, Zamana LV, Popova AA,

Toshchakov SV, Golyshin PN, Golyshin OV (2019) Microbial communities of polymetallic deposits' acidic ecosystems of continental climatic zone with high temperature contrasts. Front Microbiol 10:. https://doi.org/10.3389/fmicb.2019.01573

Geets J, Borremans B, Diels L, Springael D, Vangronsveld J, van der Lelie D, Vanbroekhoven K (2006) DsrB gene-based DGGE for community and diversity surveys of sulfate-reducing bacteria. J. Microbiol. Methods 66:194–205

Geoderis (2019) Etude sanitaire et environnementale sur les anciennes exploitations minières de La-Croix-de-Pallières et de Saint-Sébastien-d'Aigrefeuille (30) Rapport de synthèse

Gibert O, de Pablo J, Cortina JL, Ayora C (2002) Treatment of acid mine drainage by sulphate-reducing bacteria using permeable reactive barriers: A review from laboratory to full-scale experiments. Rev Environ Sci Biotechnol 1:327–333. https://doi.org/10.1023/A:1023227616422

Giloteaux L, Duran R, Casiot C, Brueneel O, Elbaz-Poulichet F, Goñi-Urriza M (2013) Three-year survey of sulfate-reducing bacteria community structure in Carnoulès acid mine drainage (France), highly contaminated by arsenic. FEMS Microbiol Ecol 83:724–737. https://doi.org/10.1111/1574-6941.12028

Girvan M, Campbell C, Killham K, Prosser JI, Glover LA (2005) Bacterial diversity promotes community stability and functional resilience. Environ Microbiol -

Gonzalez-Contreras P, Weijma J, Buisman CJN (2012a) Bioscorodite crystallization in an airlift reactor for arsenic removal. Cryst Growth Des 12:2699–2706. https://doi.org/10.1021/cg300319s

Gonzalez-Contreras P, Weijma J, Buisman CJN (2012b) Kinetics of ferrous iron oxidation by batch and continuous cultures of thermoacidophilic Archaea at extremely low pH of 1.1-1.3. Appl Microbiol Biotechnol 93:1295–1303. https://doi.org/10.1007/s00253-011-3460-7

Gonzalez-Contreras P, Weijma J, Van Der Weijden R, Buisman CJN (2010) Biogenic scorodite crystallization by *Acidianus sulfidivorans* for arsenic removal. Environ Sci Technol 44:675–680. https://doi.org/10.1021/es902063t

Gonzalez Contreras PA (2012) Biological crystallization of scorodite for arsenic removal

González D, Liu Y, Villa Gomez D, et al (2019) Performance of a sulfidogenic bioreactor inoculated with indigenous acidic communities for treating an extremely acidic mine water. Miner Eng 131:370–375. https://doi.org/10.1016/j.mineng.2018.11.011

Grettenberger CL, Havig JR, Hamilton TL (2020) Metabolic diversity and co-occurrence of multiple *Ferrovum* species at an acid mine drainage site. BMC Microbiol 20:1–14. https://doi.org/10.1186/s12866-020-01768-w

Grishin SI, Bigham JM, Tuovinen OH (1988) Characterization of jarosite formed upon bacterial oxidation of ferrous sulfate in a packed-bed reactor. Appl Environ Microbiol 54:3101–3106. https://doi.org/10.1128/aem.54.12.3101-3106.1988

Habe H, Sato Y, Aoyagi T, et al (2020) Design, application, and microbiome of sulfate-reducing bioreactors for treatment of mining-influenced water. Appl Microbiol Biotechnol 104:6893–6903. https://doi.org/10.1007/s00253-020-10737-2

Hallberg KB (2010) New perspectives in acid mine drainage microbiology. Hydrometallurgy 104:448–453. https://doi.org/10.1016/j.hydromet.2009.12.013

Halter D, Goulhen-Chollet F, Gallien S, et al (2012) In situ proteo-metabolomics reveals metabolite secretion by the acid mine drainage bio-indicator, Euglena mutabilis. ISME J 6:1391–1402. https://doi.org/10.1038/ismej.2011.198

Hao C, Wang L, Gao Y, Zhang L, Dong H (2010) Microbial diversity in acid mine drainage of Xiang Mountain sulfide mine, Anhui Province, China. Extremophiles 14:465–474. https://doi.org/10.1007/s00792-010-0324-5

Hedrich S, Johnson DB (2014) Remediation and selective recovery of metals from acidic mine waters using novel modular bioreactors. Environ Sci Technol 48:12206–12212. https://doi.org/10.1021/es5030367

Hedrich S, Johnson DB (2013) Acidithiobacillus ferridurans sp. nov., an acidophilic iron-, sulfur- and hydrogen-metabolizing chemolithotrophic gammaproteobacterium. Int J Syst Evol Microbiol 63:4018–4025. https://doi.org/10.1099/ijs.0.049759-0

Hedrich S, Johnson DB (2012) A modular continuous flow reactor system for the selective bio-oxidation of iron and precipitation of schwertmannite from mine-impacted waters. Bioresour Technol 106:44–49. https://doi.org/10.1016/j.biortech.2011.11.130

Hedrich S, Schlömann M, Barrie Johnson D (2011) The iron-oxidizing proteobacteria. Microbiology 157:1551–1564. https://doi.org/10.1099/mic.0.045344-0

Heinzel E, Janneck E, Glombitza F, Schlömann M, Seifert J (2009) Population dynamics of Iron-oxidizing communities in pilot plants for the treatment of acid mine waters. Environ Sci Technol 43: 6138–6144. doi: 10.1021/es900067d

Heinzel E, Hedrich S, Janneck E, Glombitza F, Seifert J, Schlomann M (2009) Bacterial diversity in a mine water treatment plant. Appl Environ Microbiol 75:858–861. https://doi.org/10.1128/AEM.01045-08

Hernández P, Recio G, Canales C, Schwarz A, Villa-Gomez D, Southam G, Nancucheo I (2022) Evaluation of operating conditions on sulfate reduction from acidic wastewater in a fixed-bed bioreactor. Miner Eng 177:. https://doi.org/10.1016/j.mineng.2021.107370

Héry M, Casiot C, Resongles E, Gallice Z, Bruneel O, Desoeuvre A, Delpoux S (2014) Release of arsenite, arsenate and methyl-arsenic species from streambed sediment affected by acid mine drainage: A microcosm study. Environ. Chem. 11:514–524

Hessler T, Harrison STL, Huddy RJ (2020) Linking performance and microbial ecology in a biological sulphate reducing reactor system with biomass retention developed for the treatment of acid rock drainage. Hydrometallurgy 197:. https://doi.org/10.1016/j.hydromet.2020.105471

Hoffmann TD, Reeksting BJ, Gebhard S (2021) Bacteria-induced mineral precipitation: A mechanistic review. Microbiol (United Kingdom) 167:. https://doi.org/10.1099/mic.0.001049

Hogsden KL, Harding JS (2012) Anthropogenic and natural sources of acidity and metals and their influence on the structure of stream food webs. Environ Pollut 162:466–474. https://doi.org/10.1016/j.envpol.2011.10.024

Holt E, Koivusalo H, Korkealaakso J, Weding L (2018) Filtration Systems for Stormwate r Quantity and Quality Management: Guideline for Finnish Implementation

Hovasse A, Bruneel O, Casiot C, Desoeuvre A, Farasin J, Héry M, Van Dorssealaer A, Carapito C, Arsene-Ploetze (2016) Spatio-temporal detection of the Thiomonas population and the Thiomonas arsenite oxidase involved in natural arsenite attenuation processes in the Carnoulès acid mine drainage. Front Cell Dev Biol 4:. https://doi.org/10.3389/fcell.2016.00003

Hudson-Edwards KA, Santini JM (2013) Arsenic-microbe-mineral interactions in mining-affected environments. Minerals 3:337–351. https://doi.org/10.3390/min3040337

Huq ME, Fahad S, Shao Z, Sarven MS, Khan IA, Alam M, Saeed M, Ullah H, Adnan M, Saud S, Cheng Q, Shaukait A, Wahid F, Zahim M, Raza MA, Saeed B, Riaz M, Khlan WU (2020) Arsenic in a groundwater environment in Bangladesh: Occurrence and mobilization. J Environ Manage 262:110318. https://doi.org/10.1016/j.jenvman.2020.110318

Igarashi T, Herrera PS, Uchiyama H, Miyamae H, Iyatomi N, Hashimoto K, Baltazar Tabelin C (2020) The two-step neutralization ferrite-formation process for sustainable acid mine

drainage treatment: Removal of copper, zinc and arsenic, and the influence of coexisting ions on ferritization. Sci Total Environ 715:136877. https://doi.org/10.1016/j.scitotenv.2020.136877

Jackson K, Koch I, Reimer KJ (2013) Mechanisms of dissolved arsenic removal by biochemical reactors: A bench- and field-scale study. Appl Geochemistry 29:174–181. https://doi.org/10.1016/j.apgeochem.2012.11.012

Jin D, Wang X, Liu Liang J, Zhou L (2020) A novel approach for treating acid mine drainage through forming schwertmannite driven by a mixed culture of *Acidiphilium multivorum* and *Acidithiobacillus ferrooxidans* prior to lime neutralization. J Hazard Mater 400:123108. https://doi.org/10.1016/j.jhazmat.2020.123108

Johnson DB, Hallberg KB (2003) The microbiology of acidic mine waters. Res Microbiol 154:466–473. https://doi.org/10.1016/S0923-2508(03)00114-1

Johnson DB, Hallberg KB (2005) Acid mine drainage remediation options: A review. Sci Total Environ 338:3–14. https://doi.org/10.1016/j.scitotenv.2004.09.002

Johnson DB, Hallberg KB, Hedrich S (2014) Uncovering a microbial enigma: isolation and characterization of the streamer-generating, iron-oxidizing, acidophilic bacterium "*Ferrovum myxofaciens*." Appl Environ Microbiol 80:672–680. https://doi.org/10.1128/AEM.03230-13

Johnson DB, Kanao T, Hedrich S (2012) Redox transformations of iron at extremely low pH: Fundamental and applied aspects. Front Microbiol 3:1–13. https://doi.org/10.3389/fmicb.2012.00096

Johnston SG, Burton ED, Keene AF, Planer-Friedrich B, Voegelin A, Blackford M, Lumpkin GR (2012) Arsenic mobilization and iron transformations during sulfidization of As(V)-bearing jarosite. Chem Geol 334:9–24. https://doi.org/ 10.1016/j.chemgeo.2012.09.045

Jones DS, Kohl C, Grettenberger C, Larson L, Burgos W, Macalady J (2015) Geochemical niches of iron-oxidizing acidophiles in acidic coal mine drainage. Appl Environ Microbiol 81:1242–1250. https://doi.org/10.1128/AEM.02919-14

Kabiraj A, Biswas R, Halder U, Bandopadhyay R (2022) Bacterial arsenic metabolism and its role in arsenic bioremediation. Curr Microbiol 79:1–15. https://doi.org/10.1007/s00284-022-02810-y

Kanel SR, Greneche JM, Choi H (2006) Arsenic(V) removal from groundwater using nano scale zero-valent iron as a colloidal reactive barrier material. Environ Sci Technol 40:2045–2050. https://doi.org/10.1021/es0520924

Kay CM, Rowe OF, Rocchetti L, Coupland K, Hallberg K, Johnson B (2013) Evolution of microbial "Streamer" growths in an acidic, metal-contaminated stream draining an abandoned underground copper mine. Life 3:189–210. https://doi.org/10.3390/life3010189

Kendall MR, Madden AS, Elwood Madden ME, Hu Q (2013) Effects of arsenic incorporation on jarosite dissolution rates and reaction products. Geochim Cosmochim Acta 112:192–207. https://doi.org/10.1016/j.gca.2013.02.019

Kinnunen PHM, Puhakka JA (2004) High-rate ferric sulfate generation by a L*eptospirillium ferriphilum* dominated biofilm and the role of jarosite in biomass retainment in a fluidized-bed reactor. Biotechnol Bioeng 85:697–705. https://doi.org/10.1002/bit.20005

Kirby CS, Thomas HM, Southam G, Donald R (1999) Relative contributions of abiotic and biological factors in Fe(II) oxidation in mine drainage. Appl Geochemistry 14:511–530. https://doi.org/10.1016/S0883-2927(98)00071-7

Kolmert A, Johnson DB (2001) Remediation of acidic waste waters using immobilised acidophilic sulfate-reducing bacteria. Chem Technol Biotechnol 46:836–843. https://doi.org/10.1002/jctb.453

Lane DJ (1991) 16S/23S rRNA Sequencing. In: Stackebrandt, E. and Goodfellow, M., Eds., Nucleic Acid Techniques in Bacterial Systematic, John Wiley and Sons, New York, 115-175

Laperche V, Bodénan F, Dictor M, Baranger P (2003) Guide méthodologique de l'arsenic, appliqué à la gestion des sites et sols pollués. Brgm/Rp-52066-Fr 0–93

Laroche E, Casiot C, Fernandez-Rojo L, A, Tardy V, Bruneel O, Battaglia-Brunet F, Joulian C, Héry M (2018) Dynamics of bacterial communities mediating the treatment of an As-rich acid mine drainage in a field pilot. Front Microbiol 9:1–13. https://doi.org/10.3389/fmicb.2018.03169

Le Pape P, Battaglia-Brunet F, Parmentier M, Joulian C, Gassaud C, Fernandez-Rojo, Guigner JM, Ikogou M, Stetten L, Olivi L, Casiot C, Morin G (2017) Complete removal of arsenic and zinc from a heavily contaminated acid mine drainage via an indigenous SRB consortium. J Hazard Mater 321:764–772. https://doi.org/10.1016/j.jhazmat.2016.09.060

Leblanc M, Achard B, Ben Othman D, Luck JM (1996) Accumulation of arsenic from acidic mine waters by ferruginus bacterial accretions (stromatolites). Appl Geochemistry 11:541–554

Leblanc M, Casiot C, Elbaz-Poulichet F, Personnè C (2002) Arsenic removal by oxidizing bacteria in a heavily arsenic-contaminated acid mine drainage system (Carnoulès, France). Geol Soc Spec Publ 198:267–274. https://doi.org/10.1144/GSL.SP.2002.198.01.17

Lefticariu L, Walters ER, Pugh CW, Bender KS (2015) Sulfate reducing bioreactor dependence on organic substrates for remediation of coal-generated acid mine drainage: Field experiments. Appl Geochemistry 63:70–82. https://doi.org/10.1016/j.apgeochem. 2015.08.002

Levenspiel O (Oregon SU) (1999) Chemical Reaction Engineering, Third edit. John Wiley & Sons, New York, NY

Li H, Zeng XC, He Z, Chen X, Guoji E, Han Y, Wang Y (2016a) Long-term performance of rapid oxidation of arsenite in simulated groundwater using a population of arsenite-oxidizing microorganisms in a bioreactor. Water Res 101:393–401. https://doi.org/10.1016/j.watres.2016.05.058

Li J, Wang Q, Oremland R, Kulp T, Rensing C, Wang G (2016b) Microbial Antimony Biogeochemistry: Enzymes, Regulation, and Related Metabolic Pathways. Appl Environ Microbiol 82:5482–5495

Li Q, Zhang M, Yang J, Liu Q, Liao Q, Liu H, Wang Q (2020) Formation and stability of biogenic tooeleite during Fe(II) oxidation by Acidithiobacillus ferrooxidans. Mater Sci Eng C 111:110755. https://doi.org/10.1016/j.msec.2020.110755

Liu J, Deng S, Zhao F, Cheng H, Frost R (2015) Spectroscopic characterization and solubility investigation on the effects of As(V) on mineral structure tooeleite (Fe6(AsO3) 4SO4(OH)4·H2O). Spectrochim Acta - Part A Mol Biomol Spectrosc 134:428–433. https://doi.org/ 10.1016/j.saa.2014.06.111

Lizama A. K, Fletcher TD, Sun G (2011) Removal processes for arsenic in constructed wetlands. Chemosphere 84:1032–1043. https://doi.org/10.1016/j.chemosphere. 2011.04.022

Lopez-Ponnada E V., Lynn TJ, Peterson M, Ergas SJ, Mihelcic JR (2017) Application of denitrifying wood chip bioreactors for management of residential non-point sources of nitrogen. J Biol Eng 11:1–14. https://doi.org/10.1186/s13036-017-0057-4

Lovley DR (2003) Cleaning up with genomics: Applying molecular biology to bioremediation. Nat. Rev. Microbiol. 1:35–44

Luo C, Routh J, Dario M, Sarkar S, Wei L, Luo D, Liu Y (2020) Distribution and mobilization of heavy metals at an acid mine drainage affected region in South China, a post-

remediation study. Sci Total Environ 724:138122. https://doi.org/10.1016/j.scitotenv.2020.138122

Luo Q, Tsukamoto TK, Zamzow KL, Miller GC (2008) Arsenic, selenium, and sulfate removal using an ethanol-enhanced sulfate-reducing bioreactor. Mine Water Environ 27:100–108. https://doi.org/10.1007/s10230-008-0032-x

Macías F, Caraballo MA, Nieto JM, Rotting T, Ayora C (2012a) Natural pretreatment and passive remediation of highly polluted acid mine drainage. J Environ Manage 104:93–100. https://doi.org/10.1016/j.jenvman.2012.03.027

Macías F, Caraballo MA, Rötting TS, Pérez-López R, Nieto JM, Ayora C (2012b) From highly polluted Zn-rich acid mine drainage to non-metallic waters: Implementation of a multi-step alkaline passive treatment system to remediate metal pollution. Sci Total Environ 433:323–330. https://doi.org/10.1016/j.scitotenv.2012.06.084

Mahé F, Czech L, Stamatakis A, Quince C, de Vargas C, Dunthorn M, Rognes T (2021) Swarm v3: towards tera-scale amplicon clustering. Bioinformatics 38:267–269. https://doi.org/10.1093/bioinformatics/btab493

Mahto KU, Das S (2022) Bacterial biofilm and extracellular polymeric substances in the moving bed biofilm reactor for wastewater treatment: A review. Bioresour Technol 345:126476. https://doi.org/10.1016/j.biortech.2021.126476

Maillot F, Morin G, Juillot F, Bruneel O, Casiot C, Ona-Nguema G, Wang Y, Lebrun S, Qubry E, Vlaic G, Brozn GE (2013) Structure and reactivity of As(III)- and As(V)-rich schwertmannites and amorphous ferric arsenate sulfate from the Carnoulès acid mine drainage, France: Comparison with biotic and abiotic model compounds and implications for As remediation. Geochim Cosmochim Acta 104:310–329. https://doi.org/10.1016/ j.gca.2012.11.016

Majzlan J, Dachs E, Benisek A, Bender Koch C, Bolanz R, Göttlicher J, Steininger R (2016) Thermodynamic properties of tooeleite, Fe63+(As3+O3)4(SO4)(OH)4·4H2O. Chemie der Erde 76:419–428. https://doi.org/ 10.1016/j.chemer.2016.05.001

Majzlan J, Lalinská B, Chovan M, Jurkovicˇ L, Milovska´ S, Go¨ttlicher J (2007) The formation, structure, and ageing of As-rich hydrous ferric oxide at the abandoned Sb deposit Pezinok (Slovakia). Geochim Cosmochim Acta 71:4206–4220. https://doi.org/10.1016/j.gca.2007.06.053

Majzlan J, Plášil J, Škoda R, Gescher J, Kögler F, Rusznyak A, Küsel K, Neu T, Mangold S, Rothe J (2014) Arsenic-rich acid mine water with extreme arsenic concentration: Mineralogy, geochemistry, microbiology, and environmental implications. Environ Sci Technol 48:13685–13693. https://doi.org/10.1021/es5024916

Martin M (2013) Cutadapt removes adapter sequences from high-throughput sequencing reads. EMBnet.journal 7:2803–2809

McMurdie PJ, Holmes S (2013) phyloseq: an R package for reproducible interactive analysis and graphics of microbiome census data. PloS One 8, e61217

Méndez-García C, Mesa V, Sprenger RR, Richter M, Suaréz M, Solano J, Bargiela R,Golyshina O V, Manteca A, Ramos JL, Gallego JR, Llorente I, Martins dos Santos V AP, Jensen ON, Pelaez AI, Sanchez J, Ferrer M (2014) Microbial stratification in low pH oxic and suboxic macroscopic growths along an acid mine drainage. ISME J 8:1259–1274. https://doi.org/10.1038/ismej.2013.242

Méndez-García C, Peláez AI, Mesa V, Sánchez J, Golyshina OV, Ferrer M (2015) Microbial diversity and metabolic networks in acid mine drainage habitats. Front Microbiol 6:1–17. https://doi.org/10.3389/ fmicb.2015.00475

Michel C, Jean M, Coulon S, Dictor M.-C Delorme F, Morin D, Garrido F (2007) Biofilms of As(III)-oxidising bacteria: Formation and activity studies for bioremediation process

development. Appl Microbiol Biotechnol 77:457–467. https://doi.org/10.1007/s00253-007-1169-4

Migaszewski ZM, Gałuszka A, Dołęgowska S (2018) Arsenic in the Wiśniówka acid mine drainage area (south-central Poland) – Mineralogy, hydrogeochemistry, remediation. Chem Geol 493:491–503. https://doi.org/10.1016/j.chemgeo.2018.06.027

Migaszewski ZM, Gałuszka A, Dołęgowska S (2019) Extreme enrichment of arsenic and rare earth elements in acid mine drainage: Case study of Wiśniówka mining area (south-central Poland). Environ Pollut 244:898–906. https://doi.org/10.1016/j.envpol.2018.10.106

Mills A, Herman J, Hornberger G, Ford R (2003) Functional redundancy promotes functional stability in diverse microbial bioreactor communities. SAE Int

Moeng K (2019) Community perceptions on the health risks of acid mine drainage: the environmental justice struggles of communities near mining fields. Environ Dev Sustain 21:2619–2640. https://doi.org/10.1007/s10668-018-0149-4

Mohan D, Pittman CU (2007) Arsenic removal from water/wastewater using adsorbents-A critical review. J Hazard Mater 142:1–53. https://doi.org/10.1016/j.jhazmat.2007.01.006

Mondal P, Majumder CB, Mohanty B (2006) Laboratory based approaches for arsenic remediation from contaminated water: Recent developments. J Hazard Mater 137:464–479. https://doi.org/10.1016/j.jhazmat.2006.02.023

Morin G, Juillot F, Casiot C, Bruneel O, Personné JC, Elbaz-Poulichet F, Leblanc M, Ildefonse P, Calas G (2003) Bacterial formation of tooeleite and Mixed Arsenic(III) or Arsenic(V) - Iron(III) gels in the carnoulès acid mine drainage, France. A XANES, XRD, and SEM study. Environ Sci Technol 37:1705–1712. https://doi.org/ 10.1021/es025688p

Morodi TJ, Mpofu C (2018) Environmental decision making on acid mine drainage issues in South Africa: An argument for the precautionary principle. Sci Eng Ethics 24:1181–1199. https://doi.org/10.1007/s11948-017-9933-z

Mühling M, Ullrich SR, Poehlein A, Voitel M, Drechsel A, Erler B, Tischler J, González C, Holmes D, Schlömann1 M (2016) Comparative genomic analysis of acidophilic iron oxidizing bacteria from a pilot plant for the microbial remediation of AMD water: insights into strategies for speciation and metabolic adaptation to life at low pH and under low nutrient concentration. Min Meets Water - Conflicts Solut 1022–1026

Mühling M, Poehlein A, Stuhr A, Voitel M, Daniel R, Schlömann1 M (2016) Reconstruction of the metabolic potential of acidophilic sideroxydans strains from the metagenome of an microaerophilic enrichment culture of acidophilic iron-oxidizing bacteria from a pilot plant for the treatment of acid mine drainage reveals metabolic . Front Microbiol 7:1–16. https://doi.org/10.3389/ fmicb.2016.02082

Müller AL, Kjeldsen KU, Rattei T, Pester M, Loy A (2015) Phylogenetic and environmental diversity of DsrAB-type dissimilatory (bi)sulfite reductases. ISME J 9:1152–1165. https://doi.org/ 10.1038/ismej.2014.208

Nancucheo I, Bitencourt JAP, Sahoo PK, Oliveira Alves, Siqueira JO, Oliveira G (2017) Recent Developments for Remediating Acidic Mine Waters Using Sulfidogenic Bacteria. Biomed Res Int 2017:. https://doi.org/10.1155/2017/7256582

Ňancucheo I, Hedrich S, Johnson DB (2012) New microbiological strategies that enable the selective recovery and recycling of metals from acid mine drainage and mine process waters. Mineral Mag 76:2683–2692. https://doi.org/10.1180/minmag.2012.076.7.04

Ňancucheo I, Johnson DB (2012) Selective removal of transition metals from acidic mine waters by novel consortia of acidophilic sulfidogenic bacteria. Microb Biotechnol 5:34–44. https://doi.org/10.1111/j.1751-7915.2011.00285.x

Nazari B, Jorjani E, Hani H, Manafi Z, Riahi A (2014) Formation of jarosite and its effect on important ions for Acidithiobacillus ferrooxidans bacteria. Trans Nonferrous Met Soc

China (English Ed 24:1152–1160. https://doi.org/10.1016/S1003-6326(14)63174-5

Neculita C-M, Zagury GJ, Bussière B (2007) Passive treatment of acid mine drainage in bioreactors using sulfate-reducing bacteria. J Environ Qual 36:1–16. https://doi.org/ 10.2134/jeq2006.0066

Neculita, C.M., Zagury, G.J., Bussiere, B., 2021. Passive treatment of acid mine drainage at the reclamation stage. In: Bussi`ere, B., Guittonny, M. (Eds.), Hard rock mine reclamation: from prediction to management of acid mine drainage. CRC Press, pp. 271–296. https://doi.org/10.1201/9781315166698/-11

Neiva AMR, de Carvalho PCS, Antunes IMHR, et al (2016) Spatial variability of soils and stream sediments and the remediation effects in a portuguese uranium mine area. Chemie der Erde 76:501–518. https://doi.org/10.1016/j.chemer.2016.08.003

Newman DK, Beveridge TJ, Morel FMM (1997a) Precipitation of arsenic trisulfide by Desulfotomaculum auripigmentum. Appl Environ Microbiol 63:2022–2028. https://doi.org/10.1128/aem.63.5.2022-2028.1997

Newman DK, Kennedy EK, Coates JD, et al (1997b) Dissimilatory arsenate and sulfate reduction in *Desulfotomaculum auripigmentum* sp. nov. Arch Microbiol 168:380–388. https://doi.org/10.1007/s002030050512

Nordstrom DK, Alpers CN (1991) Geochemistry of acid mine waters. In: reviews in economic geology

Nordstrom DK, Blowes DW, Ptacek CJ (2015) Hydrogeochemistry and microbiology of mine drainage: An update. Appl Geochemistry 57:3–16. https://doi.org/10.1016/j.apgeochem. 2015.02.008

Oksanen J, Blanchet FG, Friendly M, Kindt R, Legendre P, McGlinn D, Minchin PR, O'Hara RB, Simpson GL, Solymos P, Henry M, Stevens H, Szoecs E, Wagner H (2018) vegan: community ecology package, R pack- age version 2.5-3

Oremland RS, Hoeft SE, Santini JM, et al (2002) Anaerobic oxidation of arsenite in Mono Lake water and by a facultative, arsenite-oxidizing chemoautotroph, strain MLHE-1. Society 68:4795–4802

Osborne TH, Jamieson HE, Hudson-Edwards KA, et al (2010) Microbial oxidation of arsenite in a subarctic environment: Diversity of arsenite oxidase genes and identification of a psychrotolerant arsenite oxidiser. BMC Microbiol 10:. https://doi.org/10.1186/1471-2180-10-205

Paikaray S (2015) Arsenic geochemistry of acid mine drainage. Mine Water Environ 34:181–196. https://doi.org/10.1007/s10230-014-0286-4

Paktunc D, Bruggeman K (2010) Solubility of nanocrystalline scorodite and amorphous ferric arsenate: Implications for stabilization of arsenic in mine wastes. Appl Geochem 25:674–683. https://doi.org/10.1016/j.apgeochem.2010.01.021

Park I, Tabelin CB, Jeon S, Li X, Seno K, Ito M, Hiroyoshi N (2019) A review of recent strategies for acid mine drainage prevention and mine tailings recycling. Chemosphere 219:588–606. https://doi.org/ 10.1016/j.chemosphere.2018.11.053

Park JH, Han YS, Ahn JS (2016) Comparison of arsenic co-precipitation and adsorption by iron minerals and the mechanism of arsenic natural attenuation in a mine stream. Water Res 106:295–303. https://doi.org/10.1016/j.watres.2016.10.006

Pesic B, Oliver DJ, Wichlacz P (1989) An electrochemical method of measuring the oxidation rate of ferrous to ferric iron with oxygen in the presence of *Thiobacillus ferrooxidans*. Biotechnol Bioeng 33:428–439. https://doi.org/10.1002/bit.260330408

Pereira MA, Alves MM, Azeredo J, Mota M, Oliveira R (2000) Influence of physico-chemical properties of porous microcarriers on the adhesion of an anaerobic consortium. J Ind Microbiol Biotechnol 24:181–186. https://doi.org/10.1038/sj.jim.2900799

Planer-Friedrich B, London J, Mccleskey RB, Nordstrom DK, Wallschläger D (2007) Thioarsenates in geothermal waters of yellowstone National Park: Determination, preservation, and geochemical importance. Environ Sci Technol 41:5245–5251. https://doi.org/10.1021/es070273v

Plewniak F, Koechler S, Le Paslier D, D, Héry M, Bruneel O, Bertin P (2020) In situ metabolic activities of uncultivated Ferrovum sp. CARN8 evidenced by metatranscriptomic analysis. Res Microbiol 171:37–43. https://doi.org/10.1016/j.resmic.2019.09.008

Quast C, Pruesse E, Yilmaz P, Gerken J, Schweer T, Yarza P, Peplies J, Glockner F (2013) The SILVA ribosomal RNA gene database project: Improved data processing and web-based tools. Nucleic Acids Res 41:590–596. https://doi.org/10.1093/nar/gks121

Quemeneur M, Cébron A, Billard P, Battaglia-Brunet F, Garrido F, Leyval C, Joulian C (2010) Population structure and abundance of arsenite-oxidizing bacteria along an arsenic pollution gradient in waters of the upper isle river basin, France. Appl Environ Microbiol 76:4566–4570. https://doi.org/10.1128/ AEM.03104-09

Quéméneur M, Heinrich-Salmeron A, Muller D, Lièvremont D, Jauzein M, Bertin P, Garrido F, Joulian C (2008) Diversity surveys and evolutionary relationships of aoxB genes in aerobic arsenite-oxidizing bacteria. Appl Environ Microbiol 74:4567–4573. https://doi.org/10.1128/AEM.02851-07

Quiceno-Vallejo MF, Escobar MC, Vásquez Y (2020) Impact of mine drainage on the microbial community of the soil. Rev la Acad Colomb Ciencias Exactas, Fis y Nat 44:241–256. https://doi.org/10.18257/raccefyn.940

Rabus R, Hansen TA, Widdel F (2013) Dissimilatory sulfate- and sulfur-reducing prokaryotes. In: Rosenberg, E., DeLong, E.F., Lory, S., Stackebrandt, E., Thompson, F. (eds) The Prokaryotes. Springer, Berlin, Heidelberg. https://doi.org/10.1007/978-3-642-30141-4_70

Rambabu K, Banat F, Pham QM, Ho SH, Ren NQ, Loke Show P (2020) Biological remediation of acid mine drainage: Review of past trends and current outlook. Environ Sci Ecotechno 2:100024. https://doi.org/10.1016/j.ese.2020.100024

Resongles E, Casiot C, Freydier R, Dezileau L, Viers J, Elbaz-Poulichet (2014) Persisting impact ofhistorical mining activity to metal (Pb, Zn, Cd, Tl, Hg) and metalloid (As, Sb) enrichment in sediments of the Gardon River, Southern France. Sci Total Environ 481:509–521. https://doi.org/10.1016/j.scitotenv.2014.02.078

Resongles E, Casiot C, Freydier R, Le Gall M, Elbaz-Poulichet F (2015) Variation ofdissolved and particulate metal(loid) (As, Cd, Pb, Sb, Tl, Zn) concentrations under varying discharge during a Mediterranean flood in a former mining watershed, the Gardon River (France). J Geochemical Exploration 158: 132-142. https://doi.org/10.1016/j.gexplo.2015.07.010

Rezadehbashi M, Baldwin SA (2018) Core sulphate-reducing microorganisms in metal-removing semi-passive biochemical reactors and the co-occurrence of methanogens. Microorganisms 6:. https://doi.org/10.3390/microorganisms6010016

Rezaie B, Anderson A (2020) Sustainable resolutions for environmental threat of the acid mine drainage. Sci Total Environ 717:137211. https://doi.org/10.1016/j.scitotenv.2020.137211

Rognes T, Flouri T, Nichols B, Quince C, Mahé F (2016) VSEARCH: a versatile open source tool for metagenomics. PeerJ 18;4:e2584. doi: 10.7717/peerj.2584

Romero FM, Prol-Ledesma RM, Canet C (2010) Acid drainage at the inactive Santa Lucia mine, western Cuba: Natural attenuation of arsenic, barium and lead, and geochemical behavior of rare earth elements. Appl Geochemistry 25:716–727. https://doi.org/10.1016/j.apgeochem.2010.02.00

Rotting T, Ayora C, Carrera J (2008a) Improved passive treatment of high Zn and Mn

concentrations using caustic magnesia (MgO): particle size effects. Environ Sci Technol 42:9370–9377

Rötting TS, Thomas RC, Ayora C, Carrera J (2008b) Passive treatment of acid mine drainage with high metal concentrations using dispersed alkaline substrate. J Environ Qual 37:1741–1751. https://doi.org/10.2134/jeq2007.0517

Sahinkaya E, Gunes FM, Ucar D, Kaksonen AH (2011) Sulfidogenic fluidized bed treatment of real acid mine drainage water. Bioresour Technol 102:683–689. https://doi.org/10.1016/j.biortech.2010.08.042

Sahinkaya E, Isler E, Yurtsever A, Coban I (2019) Sulfidogenic treatment of acid mine drainage using anaerobic membrane bioreactor. J Water Process Eng 31:

Sahinkaya E, Yurtsever A, Toker Y, et al (2015) Biotreatment of As-containing simulated acid mine drainage using laboratory scale sulfate reducing upflow anaerobic sludge blanket reactor. Miner Eng 75:133–139. https://doi.org/10.1016/j.mineng.2014.08.012

Sánchez-Andrea I, Rodríguez N, Amils R, Sanz JL (2011) Microbial diversity in anaerobic sediments at Río Tinto, a naturally acidic environment with a high heavy metal content. Appl Environ Microbiol 77:6085–6093. https://doi.org/10.1128/AEM.00654-11

Sánchez-Andrea I, Sanz JL, Bijmans MFM, Stams AJM (2014) Sulfate reduction at low pH to remediate acid mine drainage. J Hazard Mater 269:98–109. https://doi.org/10.1016/j.jhazmat.2013.12.032

Sánchez-Andrea I, Triana D, Sanz JL (2012) Bioremediation of acid mine drainage coupled with domestic wastewater treatment. Water Sci Technol 66:2425–2431. https://doi.org/10.2166/wst.2012.477

Sánchez-España J, Yusta I, Diez-Ercilla M (2011) Schwertmannite and hydrobasaluminite: A re-evaluation of their solubility and control on the iron and aluminium concentration in acidic pit lakes. Appl Geochemistry 26:1752–1774. https://doi.org/10.1016/j.apgeochem.2011.06.020

Sánchez España J, López Pamo E, Santofimia Pastor E (2007) The oxidation of ferrous iron in acidic mine effluents from the Iberian Pyrite Belt (Odiel Basin, Huelva, Spain): Field and laboratory rates. J Geochemical Explor 92:120–132. https://doi.org/10.1016/j.gexplo.2006.08.010

Sarmiento AM, Caraballo MA, Sanchez-Rodas D, Nieto JM, Parviainen A (2012) Dissolved and particulate metals and arsenic species mobility along a stream affected by Acid Mine Drainage in the Iberian Pyrite Belt (SW Spain). Appl Geochemistry. https://doi.org/10.1016/ j.apgeochem.2012.07.012

Sato Y, Hamai T, Hori T, Aoyagi T, Inaba T, Hayashi K, Kobayashi M, Sakata, T, Habe H (2018) Year-round performance of a passive sulfate-reducing bioreactor that uses rice bran as an organic carbon source to treat acid mine drainage. Mine Water Environ 37:586–594. https://doi.org/10.1007/s10230-017-0489-6

Schippers A, Neretin L (2006) Quantification of microbial communities in near-surface and deeply buried marine sediments on the Peru continental margin using real-time PCR. Environ Microbiol 8:1251–1260. https://doi.org/doi:10.1111/j.1462-2920.2006.01019.x

Sharma P, Pratap Singh S, Iqbal H, Wang Tong Y (2022) Omics approaches in bioremediation of environmental contaminants: An integrated approach for environmental safety and sustainability. Environ Res 211:. https://doi.org/https://doi.org/10.1016/j.envres.2022.113102

Sheng Y, Bibby K, Grettenberger C, Kaley B, Macalady J, Wang G, Burgos W (2016) Geochemical and temporal influences on the enrichment of acidophilic iron-oxidizing bacterial communities. Appl Environ Microbiol 82:3611–3621. https://doi.org/10.1128/AEM.00917-16

Sheng Y, Kaley B, Bibby K, Grettenberger C, Macalady J, Wang G, Burgos W (2017) Bioreactors for low-pH iron(II) oxidation remove considerable amounts of total iron. RSC Adv 7:35962–35972. https://doi.org/10.1039/ c7ra03717a

Sheoran AS, Sheoran V (2006) Heavy metal removal mechanism of acid mine drainage in wetlands: A critical review. Miner Eng 19:105–116. https://doi.org/10.1016/ j.mineng.2005.08.006

Sheoran AS, Sheoran V, Choudhary RP (2010) Bioremediation of acid-rock drainage by sulphate-reducing prokaryotes: A review. Miner Eng 23:1073–1100. https://doi.org/ 10.1016/j.mineng.2010.07.001

Shi M, Min X, Ke Y, Lin Z, Yang Z, Wang S, Peng N, Yan X, Luo S, Wu J, Wei Y (2021) Recent progress in understanding the mechanism of heavy metals retention by iron (oxyhydr)oxides. Sci Total Environ 752:141930. https://doi.org/10.1016/j.scitotenv .2020.141930

Skousen J, Zipper CE, Rose A, Ziemkiewicz PF, Nairn R, McDonald LM, Kleinmann RL (2017) Review of Passive Systems for Acid Mine Drainage Treatment. Mine Water Environ 36:133–153. https://doi.org/10.1007/s10230-016-0417-1

Song H, Yim GJ, Ji SW, Neculita CN, Hwang T (2012) Pilot-scale passive bioreactors for the treatment of acid mine drainage: Efficiency of mushroom compost vs. mixed substrates for metal removal. J Environ Manage 111:150–158. https://doi.org/10.1016/j .jenvman.2012.06.043

Sonthiphand P, Rattanaroongrot P, Mek-Yong K, Kusonmano K, Rangsiwutisak C, Uthaipaisanwong P, Chotpantarat S, Termsaithong T (2021) Microbial community structure in aquifers associated with arsenic: analysis of 16S rRNA and arsenite oxidase genes. PeerJ 9:1–29. https://doi.org/10.7717/peerj.10653

Srichandan H, Mohapatra RK, Parhi PK, Mishra S (2019) Bioleaching approach for extraction of metal values from secondary solid wastes: A critical review. Hydrometallurgy 189:105122. https://doi.org/10.1016/j.hydromet.2019.105122

Stauder S, Raue B, Sacher F (2005) Thioarsenates in sulfidic waters. Environ Sci Technol 39:5933–5939. https://doi.org/10.1021/es048034k

Tal Galili, Alan O'Callaghan, Jonathan Sidi, Carson Sievert; (2017) heatmaply: an R package for creating interactive cluster heatmaps for online publishing, Bioinformatics, btx657, https://doi,org/10,1093/bioinformatics/btx657

Tardy V, Casiot C, Fernandez-Rojo L, Resongles E, Desoeuvre A, Joulian C, Battaglia-Brunet, Héry M (2018) Temperature and nutrients as drivers of microbially mediated arsenic oxidation and removal from acid mine drainage. Appl Microbiol Biotechnol 102:2413–2424. https://doi.org/10.1007/s00253-017-8716-4

Tsai SL, Singh S, Chen W (2009) Arsenic metabolism by microbes in nature and the impact on arsenic remediation. Curr Opin Biotechnol 20:659–667. https://doi.org/10.1016/j.copbio.2009.09.013

Tsukamoto TK, Killion HA, Miller GC (2004) Column experiments for microbiological treatment of acid mine drainage: Low-temperature, low-pH and matrix investigations. Water Res 38:1405–1418. https://doi.org/10.1016/j.watres.2003.12.012

Tufano KJ, Fendorf S (2008) Confounding impacts of iron reduction on arsenic retention. Environ Sci Technol 42:4777–4783. https://doi.org/10.1021/es702625e

Tyagi M, da Fonseca MMR, de Carvalho CCCR (2011) Bioaugmentation and biostimulation strategies to improve the effectiveness of bioremediation processes. Biodegradation 22:231–241. https://doi.org/10.1007/s10532-010-9394-4

Valdés J, Pedroso I, Quatrini R, Dobson RJ, Tettelin Hm Blake RI, Eisen JA, Holmes DS (2008) Acidithiobacillus ferrooxidans metabolism: From genome sequence to industrial

applications. BMC Genomics 9:1–24. https://doi.org/10.1186/1471-2164-9-597

Vardanyan A, Vardanyan N, Khachatryan A, Zhan R, Sand W (2019) Adhesion to mineral surfaces by cells of leptospirillum, acidithiobacillus and sulfobacillus from armenian sulfide ores. Minerals 9:1–13. https://doi.org/10.3390/min9020069

Vasquez Y, Escobar MC, Neculita CM, et al (2016) Biochemical passive reactors for treatment of acid mine drainage: Effect of hydraulic retention time on changes in efficiency, composition of reactive mixture, and microbial activity. Chemosphere 153:244–253. https://doi.org/10.1016/j.chemosphere.2016.03.052

Vasquez Y, Escobar MC, Saenz JS, Quiceno-Vallejo MF, Neculita CM, Arbeli Z, Roldan F (2018) Effect of hydraulic retention time on microbial community in biochemical passive reactors during treatment of acid mine drainage. Bioresour Technol. https://doi.org/10.1016/j.biortech.2017.09.144

Vasquez Y, Neculita CM, Caicedo G, Cubillos K, Franco J, Vasquez M, Hernandez A, Roldan F (2021) Passive multi-unit field-pilot for acid mine drainage remediation: Performance and environmental assessment of post-treatment solid waste. Chemosphere 133051. https://doi.org/10.1016/j.chemosphere.2021.133051

Villegas-Plazas M, Sanabria J, Junca H (2019) A composite taxonomical and functional framework of microbiomes under acid mine drainage bioremediation systems. J Environ Manage 251:109581. https://doi.org/10.1016/j.jenvman.2019.109581

Volant A (2012) Etude des communautes microbiennes (bactéries, archaea et eucaryotes) et de leurs variations spatiotemporelles dans la mine de Carnoulès fortement contaminée en arsenic

Volant A, Bruneel O, Desoeuvre A, Héry M, Casiot C, Bru N, Delpoux S, Fahy A, Javerliat F, Bouchez O, Bertin P, Elbaz-Poulichet F, Lauga B (2014) Diversity and spatiotemporal dynamics of bacterial communities: Physicochemical and other drivers along an acid mine drainage. FEMS Microbiol Ecol 90:247–263. https://doi.org/10.1111/1574-6941.12394

Volant A, Desoeuvre A, Casiot C, Lauga B, Delpoux S, Morin G, Personné JC, Héry, Elbaz-Poulichet F, Bertin P, Bruneel O (2012) Archaeal diversity: temporal variation in the arsenic-rich creek sediments of Carnoule`s mine, France. Extremophiles 16:645–657

Volant A, Héry M, Desoeuvre A, Casiot C, Morin D, Bertin PN, Bruneel O (2016) Spatial distribution of eukaryotic communities using high-throughput sequencing along a pollution gradient in the arsenic-rich creek sediments of Carnoulès mine, France. Microb Ecol 72:608–620. https://doi.org/10.1007/s00248-016-0826-5

Wakao N, Koyatsu H, Komai Y, Koyatsu H, Komai Y, Shimokawara H, Sakurai Y, Shiota H (1988) Microbial oxidation of arsenite and occurrence of arsenite-oxidizing bacteria in acid mine water from a sulfur-pyrite mine. Geomicrobiol J 6:11–24. https://doi.org/10.1080/01490458809377818

Wang H, Bigham JM, Tuovinen OH (2006) Formation of schwertmannite and its transformation to jarosite in the presence of acidophilic iron-oxidizing microorganisms. Mater Sci Eng C 26:588–592. https://doi.org/10.1016/j.msec.2005.04.009

Wang H, Zeng Y, Guo C, Bao Y, Lu G, Reinferlder JR, Dang Z (2018) Bacterial, archaeal, and fungal community responses to acid mine drainage-laden pollution in a rice paddy soil ecosystem. Sci Total Environ 616–617:107–116. https://doi.org/10.1016/j.scitotenv.2017.10.224

Wang M, Zhou L (2012) Simultaneous oxidation and precipitation of iron using jarosite immobilized Acidithiobacillus ferrooxidans and its relevance to acid mine drainage. Hydrometallurgy 125–126:152–156. https://doi.org/10.1016/j.hydromet.2012.06.003

Wang N, Fang D, Zheng G, Liang J, Zhou L (2019a) A novel approach coupling ferrous iron bio-oxidation and ferric iron chemo-reduction to promote biomineralization in simulated

acidic mine drainage. RSC Adv 9:5083–5090. https://doi.org/10.1039/c8ra09887e

Wang S, Wang X, Zhang C, Zhang C, Li F, Guo G (2016) Bioremediation of oil sludge contaminated soil by landfarming with added cotton stalks. Int Biodeterior Biodegrad 106:150–156. https://doi.org/10.1016/j.ibiod.2015.10.014

Wang Y, Song Y, Wang H, Sun Y, Tsang YF, Pan X (2019b) Effective stabilization of arsenic in contaminated soils with biogenic manganese oxide (BMO) materials. Environ Pollut 113481. https://doi.org/10.1016/j.envpol.2019.113481

Weidner E, Ciesielczyk F (2019) Removal of hazardous oxyanions from the environment using metal-oxide-based materials. Materials (Basel) 16:. https://doi.org/10.3390/ma12060927

Weisburg WG, Barns SM, Pelletier DA, Lane DJ (1991) 16S ribosomal DNA amplification for phylogenetic study. J Bacteriol. 173(2):697-703. doi: 10.1128/jb.173.2.697-703.1991.

Whitehead PG, Hall G, Neal C, Prior H (2005) Chemical behaviour of the Wheal Jane bioremediation system. Sci Total Environ 338:41–51. https://doi.org/10.1016/j.scitotenv.2004.09.004

Wickham H (2017) tidyverse: Easily Install and Load the 'Tidyverse'. R package version 1.2.1. https://CRAN.R-project.org/package=tidyverse

Wickham H, François R, Henry L, Müller K (2022) dplyr: A Grammar of Data Manipulation, R package version 1,0,9, https://CRAN,R-project,org/package=dplyr

Williams M (2001) Arsenic in mine waters: An international study: RN - Environ. Geol., v. 40, p. 267-278. Environ Geol 40:2001

Xie X, Xiao S, He Z, Liu J, Qiu G (2007) Microbial populations in acid mineral bioleaching systems of Tong Shankou Copper Mine, China. J Appl Microbiol 103:1227–1238. https://doi.org/10.1111/j.1365-2672.2007.03382.x

Xu Y, Li H, Zeng XC (2021) A novel biofilm bioreactor derived from a consortium of acidophilic arsenite-oxidizing bacteria for the cleaning up of arsenite from acid mine drainage. Ecotoxicology 30:1437–1445. https://doi.org/10.1007/s10646-020-02283-4

Xu YN, Chen Y (2020) Advances in heavy metal removal by sulfate-reducing bacteria. Water Sci Technol 81:1797–1827. https://doi.org/10.2166/wst.2020.227

Yang Y, Mu Y, Zeng XC, Wu Weiwei, Yuan J, Liu Y, Guoji E, Luo F, Chen X, Li H, Wang J (2017) Functional genes and thermophilic microorganisms responsible for arsenite oxidation from the shallow sediment of an untraversed hot spring outlet. Ecotoxicology 26:490–501. https://doi.org/10.1007/s10646-017-1779-2

Yang Z, Zhu DZ, Yu T, Shypanski A, Zhang G, Zhou Y (2021) Effect of ferric iron and nitrate on hydrogen sulfide control in lab-scale reactors. Environ Sci Water Res Technol 7:1806–1818. https://doi.org/10.1039/d1ew00460c

Yuan Z, Zhang G, Ma X, Yu L, Wang X, Wang S, Jia Y (2021) A combined abiotic oxidation-precipitation process for rapid As removal from high-As(III)-Mn(II) acid mine drainage and low As-leaching solid products. J Hazard Mater 401: 123360. https://doi.org/10.1016/j.jhazmat.2020.123360

Zargar K, Hoeft S, Oremland R, Saltikov CW (2010) Identification of a novel arsenite oxidase gene, arxA, in the haloalkaliphilic, arsenite-oxidizing bacterium Alkalilimnicola ehrlichii strain MLHE-1. J Bacteriol 192:3755–3762. https://doi.org/10.1128/JB.00244-10

Zhang M, Wang H (2016) Preparation of immobilized sulfate reducing bacteria (SRB) granules for effective bioremediation of acid mine drainage and bacterial community analysis. Miner Eng 92:63–71. https://doi.org/10.1016/j.mineng.2016.02.008

Zhao Y, Liu D, Huang W, Yang Y, Ji M, Duc Nghiem L, Thang QT, Tran NH (2019) Insights into biofilm carriers for biological wastewater treatment processes: Current state-of-the-art, challenges, and opportunities. Bioresour Technol 288:121619. https://doi.org/10.1016/j.biortech.2019.121619

Zhou X, Fernández-Palacios E, Dorado AD, Gamisans X, Gabriel D (2022) Assessing main process mechanism and rates of sulfate reduction by granular biomass fed with glycerol under sulfidogenic conditions. Chemosphere 286:. https://doi.org/10.1016/j.chemosphere.2021.131649

Zhu J, Zhang P, Yuan S, Tong M (2020) Arsenic oxidation and immobilization in acid mine drainage in karst areas. Sci Total Environ 727:138629. https://doi.org/10.1016/j.scitotenv.2020.138629

Ziegler S, Dolch K, Geiger K, Krause S, Asskamp M, Eusterhues K, Kriews M, Wilhems-Dick, Goettlicher J, Mazlan J, Gescher J (2013) Oxygen-dependent niche formation of a pyrite-dependent acidophilic consortium built by archaea and bacteria. ISME J 7:1725–1737. https://doi.org/10.1038/ismej.2013.64

Ziemkiewicz PF, Skousen J, Lovett R (1994) Open limestone channels for treating acid mine dranaige: a new look at an old idea. Green Land 24: 36-41.

Annexes :

Anexxe 1. Quantification of the *dsr* gen

The results of sulfate reduction genetic potential (*dsrA* gene copies/mL of water) during the year of monitoring were between 3.5 x 10^7 and x 1.22 x 10^9 *dsrA* gene copies/ mL of water, showing concentrations higher than the quantification of the gen 16S rRNA (10^7 16S rRNA gene copies/mL of water). These results may be due to the 2 amplified bands observed in the final products of qPCR, which reflect the low specificity of the primers used.

The relative abundance of the *dsrA* gene measured in the effluent at the midpoint of the SR bioreactor was variable along the monitoring (Figure A.1.1). With the lowest values during the first sampling, then the sulfate reduction potential stayed stable until day 239, which correspond to the second period after the feed-batch period (day 273). The highest potential was measured at day 273 (period IX), then after this peak the sulfate reduction potential started decreasing, reaching again de lowest concentration at the end of the functioning day 373 (period XIII). But since period IX the relative abundance of the sulfate reduction potential decreased and increased without a clear trend.

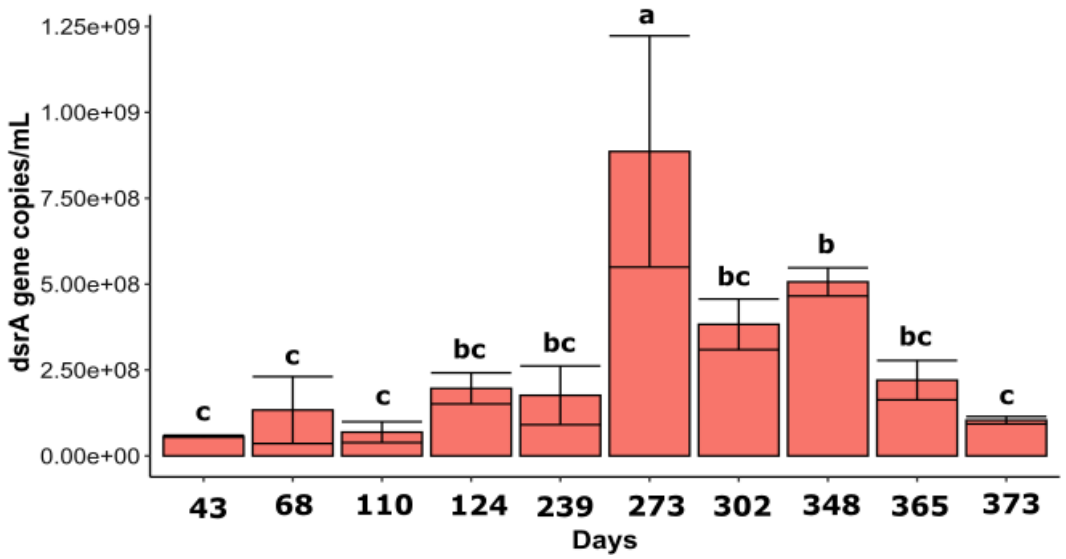

Figure A.1 1. *Abundance of copies of 16S rRNA and dsrA genes in the midpoint water of the SR bioreactor. 16S rRNA gene copies/mL of water (a) and sulfate reductase (dsrA) gene copies/mL of water (b). Different letter in the figures indicate significant differences according to Kruskal-Wallis test ($p < 0.05$).*

The sulfate reduction potential was observed in the sessile bacterial communities developed in the four section A, B, C and D. Due to the low confidence in their quantitative estimation, the evaluation of the *dsr* was only considered as indicator of the presence of sulfate-reducing genetic potential (Figure A.1 2). In the sludge the highest sulfate reduction potential was measured in the top (section A) and the bottom (section D) of the bioreactor, with a slight difference with the middle sections (B and C).

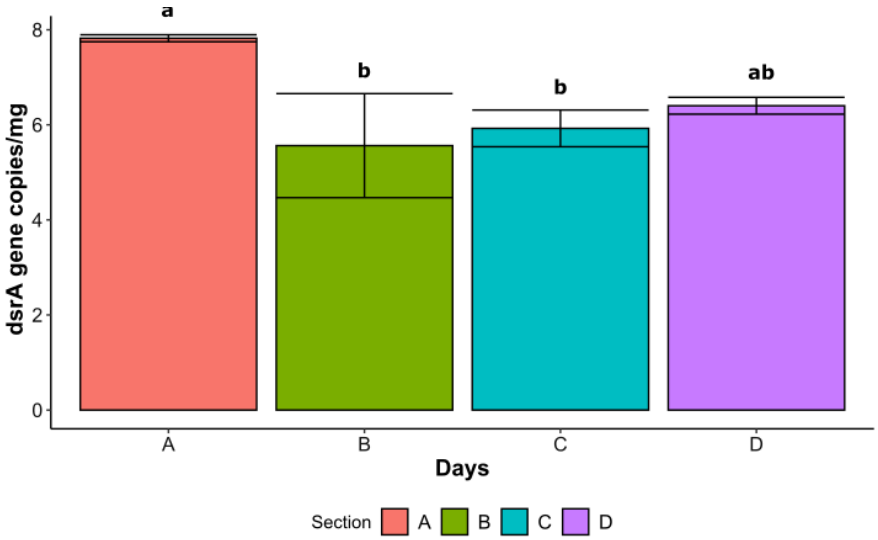

Figure A.1 2. *Abundance of copies of 16S rRNA and dsrA gen present in the sludge of the four sections of the SR bioreactor, from the top to the bottom A, B, C and D. Log 16S rRNA gene copies/mg of sludge (a). Sulfate reductase (dsrA) gene copies/mg of sludge in the 4 sections of the BSR (D). Different letter in the figures indicate significant differences according to Kruskal-Wallis test ($p < 0.05$) (expressed in wet weight).*

The same trend was observed with the sulfate reduction gene abundance (*dsrA*) an enrichment was observed in the BSR that after was mobilized to the FeOB bioreactor. There was not a significant difference among the d*srA* abundance present in the treated water and sludge from both bioreactors.

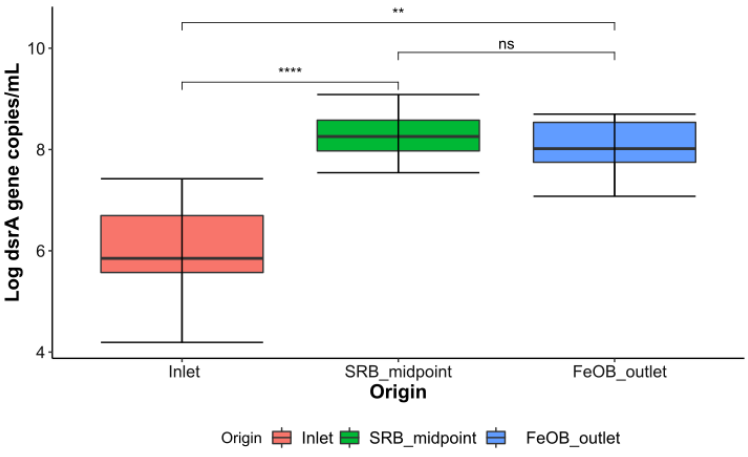

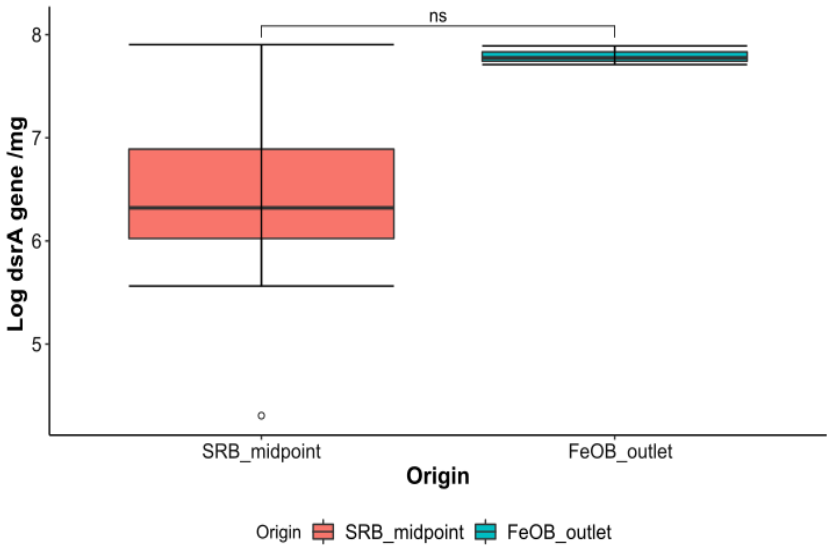

Figure A.1 3. *Quantification of dsrA genes in the water and sludge in Carnoules AMD (inlet), SR bioreactor and FeOB bioreactor. Sulfate reductase (dsrA) gene copies/mL water sampled in the midpoint of the SR bioreactor, inlet and effluent of the FeOB bioreactor (a). Sulfate reductase (*dsrA*) gene copies/mg of sludge at the end of the monitoring for the SR and FeOB bioreactors (b). Asterisks represent significant differences ("**** =p-value ≤ 0.0001, "***" p-value ≤ 0.001, "**"= p-value ≤ 0.01, "*"= p-value ≤ 0.05, "ns" = p-value > 0.05).*